Risk-based Flood Protection Decisions in the context of Climatic Variability and Change

Balqis Mohamed Rehan

Wolfson College

Thesis submitted for the degree of Doctor of Philosophy,

University of Oxford,

Environmental Change Institute

Trinity Term 2016

Acknowledgements

In the name of God the Most Gracious and Most Merciful. First of all, I would like to express my gratitude to the Almighty for His ever constant love and blessings.

My special thanks goes to Professor Alistair Borthwick who gave me the initial support to pursue my study in the University of Oxford. My sincere gratitude also goes to Professor Jim Hall who then willing to extend his support for me to continue my DPhil in the University of Oxford and continue to provide invaluable guidance and advices throughout my DPhil endeavour. I can never thank enough for his tremendous support. I wish all the very best for him and his family.

Special appreciation also goes to the late Professor Radin Umar Radin Sohadi, once a Vice Chancellor of the University of Putra Malaysia (UPM), who gave a much needed approval for me to pursue my study in the University of Oxford, despite a last-minute issue on my eligibility due to the changes of the research topic. Not forgetting my sponsors, especially the Malaysian Ministry of Higher Education, UPM, the University of Oxford, the Wolfson College and the Environmental Change Institute (ECI) that have provided financial assistance during the DPhil studentship. I also like to thank the Head of Department of the Civil Engineering Faculty, UPM and the academic and non-academic staff that have helped me through the process of completing my DPhil. I must also acknowledge the kindness and support given by the ECI's staff and members in answering my queries related to the DPhil research and study life in Oxford. Also to my Malaysian friends who have inspired me to complete the DPhil, I am truly blessed for having them together in this journey.

This journey would not have been possible without the support of my family. To my parents, thank you for willing to provide advices and endless support. To my three beautiful children who always make my day with your joyful nature; I am truly blessed to have you around. Last but no means least, my special thanks goes to you my dear husband for your sacrifices, care and endless support. I would have never made this far without you.

"The sun and the moon move by precise calculation. And the stars and trees prostrate. And the sky He raised and imposed the balance. That you not transgress within the balance. And establish weight in justice and do not make deficient the balance. And the earth He laid out for the creatures. Therein is fruit and palm trees having sheaths. And grain having husks and scented plants. So which of the blessings of your Lord would you deny?"

Translations from the noble Quran, Chapter 'The Most Gracious', verses 5-13

Abstract

Risk-based Flood Protection Decisions

in the context of Climatic Variability and Change

Balqis Mohamed Rehan, Wolfson College, University of Oxford

Submitted for the degree of Doctor of Philosophy

Trinity Term 2016

Flood events have caused detrimental impacts to humans' lives and anthropogenic climate change is anticipated to exacerbate the impact. It has been recognized that a long-term planning through risk-based optimization of flood defence will lead to a cost-effective solution for managing flood risk, but the prevailing assumption of stationarity may lead to an erroneous solution. In attempt to investigate the potential impact of the uncertain underlying statistical characteristics of extreme flow series to flood protection decisions, this research explores risk-based flood protection decisions in the context of climatic variability and change. In particular, the implications of persistence series and nonstationarity were investigated through hypothetical and real case studies. Monte Carlo simulation approach was adopted to capture the uncertainty due to the natural variability. For persistence model, AR(1) was integrated with the GEV model to simulate extreme flow series with persistence. To test the effects of nonstationary, GEV models with a linear location parameter and time as covariate were adopted. Rational decision makers' behaviours were simulated through a designed decision analysis framework. One of the main findings from the research is that the traditional stationary assumption should remain the basic assumption due to insignificant difference of the decisions' economic performance. However, exploration of the nonstationarity assumption enabled identification of options that are robust to climate uncertainties. It is also found that optimized protection of combined measures of flood defence and property-level protection may provide a cost-effective solution for local flood protection. Overall, the simulation and case studies enlighten practitioners and decision makers with new evidence, and may guide to practical enhancement of long term flood risk management decision making.

Table of contents

List of Figures

List of Tables

List of Acronyms

AD	Above Datum
AIC	Akaike Information Criterion
AM	Annual Maxima
AR	Autoregressive
ARMA	Autoregressive and Moving Average
BCR	Benefit-Cost Ratio
BIC	Bayesian Information Criterion
CBA	Cost-Benefit Analysis
CDF	Cumulative Density Function
CEH	Centre for Ecology and Hydrology
CES-AES	Conveyance Estimation System and Afflux Estimation System
CM	Climate Model
CORINE	Coordination of Information on the Environment
DEFRA	Department of Environment, Food and Rural Affairs
DTM/DEM	Digital Terrain Model/Digital Elevation Model
EA	Environment Agency
EEA	European Environmental Agency
ENSO	El-Nino Southern Oscillation
FEMA	Federal Emergency Management Agency
FRM	Flood Risk Management
GEV	Generalized Extreme Value
GIS	Geographic Information Systems
GML	Generalized Maximum Likelihood
GP	Generalized Pareto
GWP	Global Water Partnership
IBCR	Incremental Benefit-Cost Ratio
IID	Independent and Identically Distributed
IPCC	Intergovernmental Panel on Climate Change
L-CV	Coefficient of L-variation
LP3	Log-Pearson Type 3
MCM	Multi-coloured Manual
MCMC	Monte Carlo Markov Chain
ML	Maximum Likelihood

NAO	North Atlantic Oscillation
NPV	Net Present Value
NSE	Nonstationary Model Choice
PDF	Probability Density Function
PDO	Pacific Decadal Oscillation
PLP	Property-level Protection
POP	Perfect Information
POT	Peak Over Threshold
PRO	Proactive (strategy)
PV	Present Value
RCT	Reactive (strategy)
RMSE	Root Mean Square Error
SD	Standard Deviation
SE	Stationary Model Choice
SPRC	Source, Pathway, Receptors and Consequences
SST	Sea Surface Temperature
TPVC	Total Present Value Cost
UK	United Kingdom
UKCIP	UK Climate Impacts Programme
USACE	United States Army Corps of Engineers
USGS	United States Geological Survey
WMO	World Meteorological Organization

Chapter 1 Introduction

1.1 Floods and the impacts

The European Union flood directive (2007) had described floods as 'a covering by water of land not normally covered by water'. Floods can be broadly categorized based on the flood generating systems, either because of meteorological, hydrological or human aggregation flood events (Arnell, 1996;WMO/GWP, 2008). Floods can also be classified in relation to a particular source of flooding, for example pluvial (rainfall), fluvial (river), surface water (rainfall and drainage system), groundwater or dam break flooding (hydraulic structures) (Schanze, 2006). The classification based on sources of flooding is usually used to facilitate management plans in efforts to reduce the undesirable consequences of flooding.

Historically, flood events have caused significant impact on human life. Severe damages to properties and infrastructures, environmental damage and even loss of lives have been experienced in many countries due to the extreme events. Floods in Europe alone have caused approximately 1126 deaths and at least 52 billion Euro insured economic losses between 1998 and 2009 (European Commision, 2012). Asian regions also faced disastrous flood consequences, all too often as a result of the monsoon season with many displaced and losses mounting (e.g. Irandoust and Biswas, Jan, 2012). Compared to other natural disasters, floods have caused more damages over the last 100 years with approximately 359 Billion US dollar economic losses estimated from 1900 to 2013 (Konrad Adenaur Stiftung, 2013).

Floods are natural phenomenon that cannot be prevented, but human activities and climate change might increase the undesirable consequences from flood events (European Union, 2007). Flood risk management is therefore crucial in efforts to reduce the risk of future floods. A key area in flood risk management is the development of a long-term and systematic assessment of alternative strategies aimed for a sustainable and economically effective intervention. The shift from traditional fixed and standard design approach to the more holistic risk-based approach has been well accepted.

However, flood risk management still remains a challenge especially due to the possible effects of climate change and human intervention that may results in different outcomes from the ones estimated during the planning stage. Focusing on fluvial flood risk, the next section will look into observed changes of some of the flood generating drivers, in particular the hydro-meteorological drivers to understanding more on the possibilities of changes in future flood risk,

1.2 Observational changes of the extreme floods climatic drivers

One of the main concerns in fluvial flood risk management is the changes in climatic and non-climatic drivers that may affect the intensity and frequency of the hydrological variable. It is widely known that the global warming would intensify the hydrological cycle (IPCC, 2007). The parallel increase of warming and extreme precipitation can be explained based on physical reasoning: A warmer climate can intensifies the evaporation rate and causes the water holding capacity (i.e. the moisture content) in the atmosphere to increase (Kundzewicz, Hirabayashi and Kanae, 2010). Effectively, intensity of precipitation would increase. Based on observations, significant warming has been recorded since 1950 at most global land areas (IPCC, 2012, pg. 54), leading to concerns over the increase in precipitation that may exacerbate the risk of flooding.

As precipitation is one of the dominant climatic drivers of fluvial flooding (Hannaford and Hall, 2012), it is worthwhile to review the changing pattern in precipitation around the globe. An examination of tropical precipitation events revealed that during warm periods, heavy rain events increased and during cold periods, the events decreased (Allan and Soden, 2008). In snow-dominated regions, it has been observed that snowfall regime has shifted to rainfall regime over the years (IPCC, 2012; e.g. Kapnick and Hall, 2012). Trend detection of extreme precipitation from year 1900 to 2005 shows a predominantly increase trend in regions across the globe as compared to those with decreasing trend (IPCC, 2012). The heterogeneity of trend in extreme precipitation across the globe is expected as interactions between physical atmospheric variables are complex.

Other climatic drivers that may significantly affect the variability of the hydrological variables are the ocean-atmospheric circulation systems. Several studies have been undertaken in the previous

decades to relate the variations in the ocean-atmospheric systems with observations of the hydrological extremes (Khaliq et al., 2006). For example, the Pacific Decadal Oscillation (PDO) has been found to influence snowpack and winter surface climate over the western United States of America (Pizaro and Lall, 2000). The El Nino (La Nina) phase of El-Nino-Southern Oscillation (ENSO) that occurs every 2-7 years has been observed to have a positive link with the anomalous warm (cold) sea surface temperature (SST) in the eastern tropical pacific, accompanied by increased (decreased) convection and cloudiness (Khaliq et al., 2006). It is found that the ENSO variations determined 30-60% annual precipitation variance globally (Dai and Wigley, 2000). Some observed changes of the large circulation patterns have already been linked to the climate change (IPCC, 2007). The effects of climate change to hydrological extremes through the large-scale oscillations further suggests a possible link between the climate change and flood risk. Changes in non-climatic drivers may also contribute to significant changes in the hydrological cycle. For example, impervious pavements or roads from extensive urban developments might increase the intensity of surface runoff. High intensity of surface runoff caused by the impervious terrain and increase in precipitation would consequently affects the river discharge.

Acknowledging the river discharge as an integral result of changes in the hydrological processes and non-climatic flood drivers, the changes in the drivers may contribute to significant changes in the magnitudes and frequency of the extreme flows and potentially cause more damaging consequences (Linde et al., 2010). To understand the possibility of increasing magnitude and frequency of extreme flows, Section 1.3 presents some of the studies on detection of changes in observed river flows. Further, studies in relation to attribution of changes in flow discharges to flood generating drivers and projection and prediction of changes of extreme flows are also reviewed.

1.3 Changes in flow series

In understanding the changes in river flows and attributing the changes to meteorological drivers, trend analyses are often adopted. There are generally two distinct approaches associated with the trend analyses: either by applying a data-driven statistical trend tests to the observed flows and the

meteorological variables of interests, or by using a relatively more complex hydrological model-based approach before the trend analysis is applied (e.g. Hundecha and Merz, 2012). The direct data-driven trend test is favoured due to its ease of application whilst being able to indicate the possible behaviour of the underlying process. It relates the trend behaviour of the observed flows with the meteorological variable of interests. Nonetheless, it fails to capture the physical components of the generating process. Hundecha and Merz (2012) in describing the two distinct approaches highlights that the model-based approach also adopts the statistical trend tests to attribute the changes, but has the advantage of incorporating spatial elements within an ensemble hydrological model, such as catchment state and characteristics of flood-triggering precipitation event. However, the application of model-based study requires the ability to work with complex models and so is time consuming.

Table 1.1 compiles the outcomes of statistical trend tests of seasonal and yearly flow series of various continents that have been published in the IPCC report (2007). It can be seen that some continents are experiencing an increasing trend whilst some have a decreasing trend, reflecting the heterogeneity of the hydrological cycle due to the complex interaction of the physical system. In a much recent study by Stahl, Hisdal et al. (2010), statistical trend analyses were applied to near-natural historical flow records (i.e. flow records without discernible human influence) across 441 small catchments of 15 European countries. The study found that the annual pattern of river flows over 1964-2004 study period generally conform with the observation-based assessment of global rainfall changes, with increasing precipitation in higher latitudes and decreasing trends in the lower latitudes of Europe. Nevertheless, a comprehensive report by the European cooperation in science and technology (Madsen et al., 2013) reveals that trend analyses for 21 European countries indicate that whilst there is some evidence of a general increase in extreme precipitation, there are no clear indications of significant increasing trends at regional or national level of extreme flows.

Table 1.1: Excerpts of trends studies and reference(s) from the IPCC (2007) report

Region	Study area	Data set	Key conclusions	Reference (s)
Rusia	European Russia and western Siberia	80 major basins, records from 60 to 110 years	Increase in winter, summer, and autumn runoff since mid -1970s; decrease in spring flows	Georgiyevsky et al. (1995, 1996, 1997); Shiklomanov and Georgiyevsky (2001)
North America	European former Soviet Union	196 small basins, records up to 60 years	Increase in winter, summer, and autumn runoff since mid-1970s; decrease in spring flows	Georgiyevsky et al. (1996)
	United States	206 catchments	26 catchments with significant trends: half increasing and half decreasing	Lins and Slack (1999)
	California	Major river basins	Increasing concentration of streamflow in winter as a result of reduction in snow	Dettinger and Cayan (1995); Gleick and Chalecki (1999)
	Mississippi basin	Flood flows in major basins	Large and significant increases in flood magnitudes at many gauges	Olsen et al. (1999)
	West-central Canada	Churchill-Nelson river basin	Snowmelt peaks earlier; decreasing runoff in south of region, increase in north	Westmacott and Burn (1997)
South America	Colombia	Major river basins	Decrease since 1970s	Marengo (1995)
	Northwest Amazon	Major river basins	Increase since 1970s	Marengo et al. (1998)
	SE South America	Major river basins	Increase since 1960s	Genta et al. (1998)

Hundecha and Merz (2012) uses weather generator to simulate input variables of hydrological models (Kilsby et al., 2007) by which the flow series is subsequently generated. Upon examining change signals of precipitation and temperature and the relative importance of the two variables in the change pattern in flow series, they found that seasonal maximum daily precipitation significantly contribute to trend in seasonal extreme flows for 1951 to 2003 observations for most investigated catchments.

There are speculations that trends detected from past observations may prevail into the future (Stedinger and Griffis, 2011), especially when the trend detection is based on long observational records. If the trend is assumed to continue unabated into the future, the potential increase of

extreme flow magnitude might significantly affect flood risk management decisions performance. However, the prediction of future trend is always been treated as a purely statistical issue and is not included in flood risk management decision-making process (Rosner, Vogel and Kirshen, 2014). Trends are a form of deterministic model that allow general physical explanations, but are unable to present the randomness of flow discharge for probabilistic analysis. Efforts to include the information from trend tests into flood risk management decision problem furthermore have just recently emerged and the applicability has not been fully tested (e.g. Rosner, Vogel and Kirshen, 2014).

The conventional approach for managing flood risk has always been applying the flood frequency analysis to observations in order to capture the probabilistic information of the dataset (Maidment, 1993). Hence, any deterministic trend if detected is neglected in flood risk management decision making. The dominant role flood frequency analysis plays in flood risk reduction efforts have places greater emphasis in prediction of changes in magnitude and frequency of extreme flows as compared to the trend detection.

Over the years, there have been increasing efforts to project changes in flood frequency and magnitude of extreme flows, predominantly due to the rise of adoptability of regional and global climate models. The approach typically involves extraction of meteorological variables from the downscaling of climate models forced by a predefined greenhouse gasses emission scenarios that are then used to drive hydrological models to simulate river discharges. For calibration purposes, a 30-year baseline period (e.g. 1961-1990) is usually used. Generally, the baseline period serves as a basis to generate a 30-year future flow series (e.g. 2070-2099). The potential increase or decrease of frequency of extreme flows is then investigated by comparing the magnitudes of flow from the probability of occurrence of a standard baseline period and projected flows period (Kay and Jones, 2012b).

A number of studies have demonstrated climate model-based projection of extreme flows. Some of the studies gathered are as follows. Dankers and Feyen (2009) applied the approach using two types of climate models and two different emission scenarios. The changes in extreme flows of 100-year

return period are analysed for the European region. For local or river basin scale (12 km spatial resolution), they found that the simulated responses are significantly different between the climate models or emission scenarios used. At the same time, considerable decrease in flood hazard is projected in north-eastern Europe for continental scale assessment (50 km resolution) regardless the climate models or scenarios, whilst in the rest of Europe a very mixed pattern of increases and decreases or little change was projected. Bell, Kay et al. (2012) has independently analysed projected changes for the Thames Basin at 1 km resolution using an ensemble of 11 RCM outputs under A1B emission scenario. Their study shows that the potential changes in flood frequency between the baseline and projected period vary between 10 to 50% increase at different locations within the basin for 20-year return period.

Projected changes of extreme flows based on climate-models have led authorities to published guidelines for flood managers in adapting to possible future change. For example, based on modelling studies using coupled UKCP02 and hydrological model, Defra in 2006 suggested a safety margin of 20% to be added to the conventional-based design flow to account for the expected changes of 2085 (Prosdocimi, Kjeldsen and Svensson, 2014). An impact study by Joint DEFRA and EA in the UK (Reynard et al., 2009) using projections by UKCP09 and hydrological models had also led the EA to published guidelines to flood managers to incorporate change factors in the conventional design flow over a consecutive years of project life in adapting to potential future change (Environment Agency, 2011).

There are also concerns over the possibility of persistence in flow series owing to the atmospheric circulation systems. The physical reasons of persistence have been linked to the presence of decadal and inter-decadal oscillations from the ocean-atmospheric interactions (Khaliq et al., 2006;Chen and Grasby, 2009;Huntingford et al., 2014). In the UK, a strongly positive signal of the North Atlantic Oscillation (NAO) had been found in the 1990s that can be linked to a cluster of winter flood events during the time. Contrastingly, negative NAO index was found in the early 1960s corresponded to very few flood events (Huntingford et al., 2014). The clustering of floods representing ‘flood rich’ and ‘flood poor’ periods (Lane, 2009), although uncertain, is a possible

response to the NAO (Huntingford et al., 2014). Thus, persistence can generally be reflected by increasing tendency for wet years to tend to follow wet years and for dry years to tend to follow dry years (Matalas and Olsen, 2000;Hirsch, 2011).

Although the potential changes in future extreme flows due to anthropogenic climate change is well-anticipated, it is difficult to discern whether the variability that characterised the changes is due to external forces such as climate change, or due to natural variability (Kundzewicz et al., 2013). Section 1.4 looks further into some of the causes of temporal and spatial uncertainties behind predictions of extreme flows and the implication it brings to flood risk decision making.

1.4 Uncertainty in predicting future extreme flows

The natural variability due to the dynamic movement of water within air, land and water bodies of the hydrological cycle has been limited to the entire chaotic behaviour of the climate system (Ward, 2000;Hallegatte et al., 2012). The hydrological processes operate differently in different places and time according to the climatic regime (e.g. Huntingford et al., 2014) and the physical characteristics of the catchment (e.g. groundwater storage, soil type) (Arnell, 1996;Stahl et al., 2010). As a result, the intensity, duration timing and phase of precipitation are highly variable temporally and spatially, which explains the heterogeneity found in the precipitation and streamflow patterns around the world (refer Table 1.1). Non-climatic agents, such as catchment-scale engineering projects and significant land-use changes may also significantly influence the behaviour of the extremes of catchments. The complex physical interactions of flood generating drivers at catchment to local scale contribute to difficulty in attributing changes of extreme flows to flood drivers. There is also a possibility that the multiple agents of change may eventually compensate the effects to the temporal behaviour of extreme flows (Kundzewicz, 2012), limiting the effects from natural variability alone.

The temporal uncertainty is one of the main challenges in effort to understand the behaviour of possible future changes in extreme flows. For example, in the UK many catchments have moderate historical records of extremes with near-natural historical extreme flows of 40 years historical

records (Hannaford and Marsh, 2008). Lack of reliable and sufficient records that drives the statistical trend tests may lead to detection of short-term trends (Kundzewicz, Hirabayashi and Kanae, 2010). The short-term trends may actually influence by the oscillated climatic variation (Reed and Robson, 1999) rather than a climate induced long-term trend. The potential problems faced by studies of time series with impacts of oscillations on trend analyses are conceptually illustrated in Figure 1.1 (Chen and Grasby, 2009). A relatively short record can return a greater gradient of estimated trend or even an opposite direction of trend as compared to the true trend. Furthermore, it is difficult to distinguish between upward trend, step change and fluctuations. A data series that shows a significant trend often shows significant step change and vice versa (Centre for Ecology and Hydrology, 1999). Hence, a short time series is less credible in predicting whether the fitted trend will continue unabated (Stedinger and Griffis, 2011).

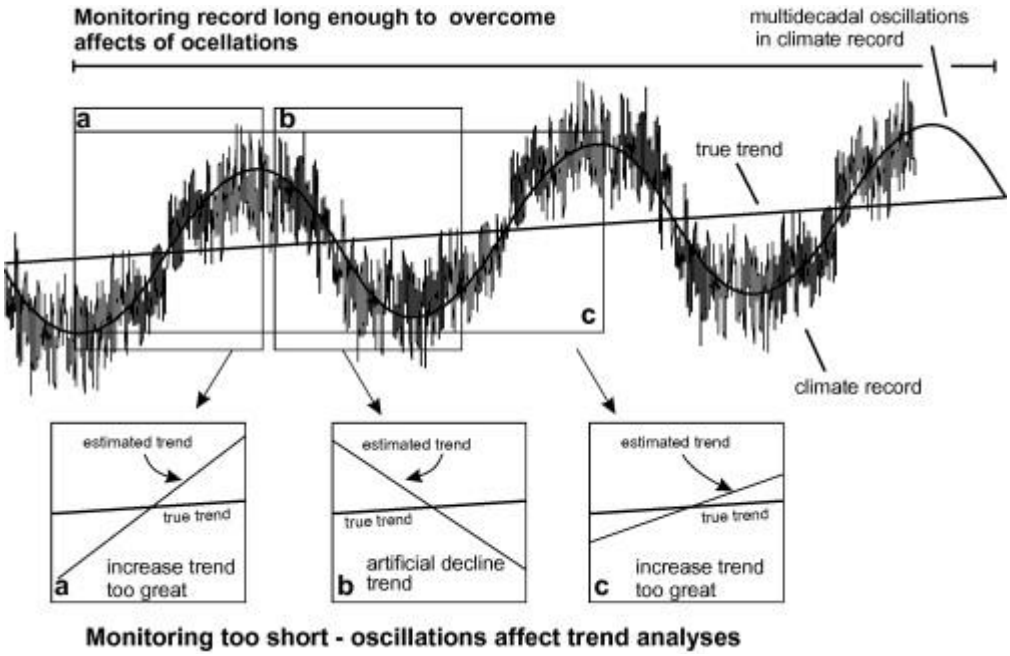

Figure 1.1: A summary showing impacts of oscillations on trend analyses. Main diagram shows a conceptual long-term climate record with a prominent multi-year cyclical component along with a linear increase trends with time. Inset box (a) shows that if climate monitoring captures ½ wavelength starting at the trough and ending at the peak of a cycle, then the estimated trend will be significantly greater than the true trend. In contrast, (b) shows that a ½ cycle record starting at a peak and ending in the trough of a cycle will give a negative trend, even though the true trend is positive. In (c), even one and half cycle length record will give too great an increase due to the record starting at the low point of a cycle (Chen and Grasby, 2009).

Predictions based on ensemble climate models are prone to be misleading due to the temporal uncertainty. Most studies are based on frequency analysis assuming non-changing envelope of probability distribution in a certain time window, typically 30 years, representing current and future climate conditions (Madsen et al., 2013). The estimates are bound to reflect the characteristics of the specific period (Gethering, 2013). The 1961-1990 used in UKCP09 future scenarios is notably 'flood poor' (Bell et al., 2012) whilst different baseline period would exhibit a different properties. The short record would lead to bias in estimates and may fail to capture the true underlying distribution, suggesting cautious interpretation of the predicted future changes. Furthermore, results are hard to verify leading to no conclusion and general proof as to how the changes in the climate can affects flood behaviour (Kundzewicz, Hirabayashi and Kanae, 2010).

It is therefore not surprising that despite an increasing confidence that climate models provide credible estimates of climate variables, only *limited* to *medium* evidence exists to assess climate-driven observed change in the magnitude and frequency of flooding (IPCC, 2012). This leads to *low agreement* on the evidence, hence overall *low confidence* on the influence of climate change to the magnitude and frequency of flooding (IPCC, 2012). Recent studies presented in Kundzewicz, Kanae et al. (2013) also brings to a similar conclusion. Despite the temporal and spatial uncertainty, attempts to predict the future extreme flows based on climate forcing are necessary to provide additional insights, especially when the traditional data-driven flood frequency analysis is also determined by the quality and quantity of hydrometric data.

1.5 The effects of uncertain future to flood risk management

The devastating effects of flood events emphasise the importance of effective management of flood impacts. The chapter has highlighted that despite global warming, physical reasoning and observed increased trends of extreme hydrological events, prediction of future extreme flows still remains a huge challenge. Furthermore, the 'change' pattern could be of various forms making it harder for flood managers to predict the future extreme flows (Merz et al., 2012). In the context of flood risk management decision making, the changes might well be captured in forms that are compatible for flood frequency analysis (Madsen et al., 2013). This would mean that 'no change' in extreme flows

is represented by stationary statistical properties while ‘change’ in extreme flows can be represented by nonstationarity in the statistical properties. The statistical representations are essential in undertaking a risk-based assessment of alternative flood protection measures.

The risk-based optimization methodology itself has long been practiced and becoming widely accepted (e.g. Tung, 2005; Tung and Yen, 2005; Jonkman et al., 2009a; Rosner, Vogel and Kirshen, 2014). Decisions are made by weighing up the probability and consequences of extreme events with flood protection costs. However, in the face of uncertain future associated with the range of future possibilities, any assumptions on the future conditions would inevitably lead to bias. Consequently, understanding the consequences of conflicting predictions to decisions long-term performances is extremely important, not only to assist appropriate planning but also in identifying practical yet a robust approach in flood risk management decision making.

In the recent years, a growing debate about the implication of flood design under stationary assumptions of extreme flows given expected future changes has emerged (e.g. Milly et al., 2008). Whilst progress has been made regarding applying nonstationary models on real streamflow data (e.g. Salas and Obeysekera, 2014; Prosdocimi, Kjeldsen and Svensson, 2014), quantitative analysis of persistent and nonstationary conditions with respect to flood risk management decisions performance is still in its infancy (e.g. O'Connell and O'Donnell, 2014). Furthermore, methodology that aims for robust flood risk management decision making in the context of uncertain probabilistic representation of extreme flows is still developing (e.g. Harvey, Hall and Peppe, 2012; Ward et al., 2014;Rosner, Vogel and Kirshen, 2014). To date, no studies have attempted to provide a rigorous flood risk management decision analysis accounting for the combined effects of persistent or nonstationary conditions of extreme flows, the complexities of flood risk systems and the influence of distinct management strategies or alternative protection measures.

1.6 Research questions

The need to adapt to flood risk to reduce the serious impact of flooding and the importance of prioritising investment allocation in the face of uncertain future provide ample motivation for

further research into identifying appropriate approaches for flood risk management decision making. Whilst there are studies that seeks to identify a robust solution for fluvial flood risk management under future uncertainty, research dealing with integrating the fluvial flood hazard, specifically persistence and nonstationarity, and flood vulnerability into the risk-based decision analysis for uncertainty and sensitivity analyses has received limited attention. Therefore, the overarching aim of this research is to model and explore the performance of **risk-based flood protection decisions in the context of climatic variability and change.** In order to identify the research objectives for the study, a number of interesting research questions are first identified to guide the literature review:

1. What are the main criteria for a robust decision in flood risk management considering different plausible future states?
2. How would persistence and nonstationarity in extreme flow series and distribution, in addition to the conventional independent and identically distribution (IID) assumption, affect the performances of long-term flood risk mitigation decisions?
3. What are the important components of flood risk assessment and how can they be modelled for a systematic simulation-based decision analysis?
4. What are the appropriate ways to integrate identified flood risk components with their inherent complexity into a practical risk-based options appraisal in aiming to evaluate the outcomes of different assumptions of future state?
5. How would the different perspectives of change in flood risk management decision making and the potential future states affect the relative outcomes and behaviour of flood risk management economic performances, and subsequent recommendations?

In order to address the research questions, identify specific objectives for the thesis and facilitate methodological development to accomplish the aim, chapter 2 and chapter 3 are dedicated for the literature review. The contents of the chapters are provided in Section 1.8.

1.7 Research objectives and general methodological approach

Based on the literature review, there is a growing interest in understanding how robustness of decision making and decisions can be achieved, but studies that have demonstrated assessment concerning the influence of persistence and nonstationarity to alternative decisions economic performance are sparse. Such study is important to enable long-term performances of such investment decisions to be analysed within the context of different perspective of change and different possible hazard variability. It is also found that whilst considerable research have been devoted to modelling flood damage and assessment of flood risk, less attention has been paid to model them in the context of a risk-based optimization of flood protection. Rigorous modelling of the key components for the risk-based decisions are often undertaken separately with different objectives rather than having a consistent similar decision variable across all components (i.e. the probability of hazard, potential damage and intervention cost). For example, the lack of attention to developing a more flexible and adaptable damage model limits the usability of such model to fixed protection plans.

Seeking to explore local risk-reduction protection plans using engineering measures, a wide range of potential measures can be incorporated into the risk-based decision making, such as flood proofing and channel modification. The inclusion of such options within a comprehensive risk-based appraisal and simulation-based decision analysis is rarely undertaken hence limiting the ability to understand comparative long-term economic consequences of the options in the context of uncertain future. Such comparison may offer added information for a better decisions in local risk-reduction planning.

A number of important research objectives have been identified in accomplishing the aim of the thesis:

1. To establish a risk-based optimization methodology with explicit treatment of the modelling components for a robust decision analysis framework.
2. To quantify uncertainty propagation and sensitivity of the economic performance of alternative time-dependence strategies with partial information under persistent scenarios

3. To capture and analyse uncertainty propagation and sensitivity of the economic performance of decisions with partial information under nonstationary scenarios.
4. To develop a systematic micro-scale vulnerability assessment framework for damage modelling concerning community-based intervention portfolios.
5. To compare the economic performance of decisions with respect to stationary and nonstationary conditions and a number of alternative flood risk management portfolios, through a risk-based cost-benefit analysis that integrates a probability distribution and realistic damage and cost models associated with the community-based portfolios.

Chapter 4, 5, 6 and 7 provide the development of methodologies, application, results and analysis to satisfy the research objectives. Basically the methodological approach in this theses is simulation and case studies. More elaboration on the methodological approaches and the contents of the remaining chapters are presented in Section 1.8.

1.8 Thesis structure

The thesis comprises 8 chapters. Chapter 2 focuses on reviewing literature on long-term planning for fluvial flood risk reduction. A broad overview of flood risk management is presented. Potential structural interventions, with emphasise on local protection, are also addressed. Chapter 2 further reviews long-term planning tools, specifically the cost-benefit analysis and optimization methodologies. The perspective of robustness for long-term planning of flood management is also addressed therein.

Chapter 3 discusses on the components of risk assessment in more detail. The aspect of fluvial flood hazard is focused on persistent and nonstationary characteristics of extreme flows additional to the conventional stationary assumption in flood frequency analysis. The chapter discusses the emerging perspective of nonstationarity and highlights the gaps from the literature. The ways in which flood vulnerability can be modelled are also reviewed with the focus on micro-scale assessment to address the challenges to model flood vulnerability and flood damage given the different physical interventions.

The development of methodology, application and analysis are pursued in chapter 4 to chapter 7, where each chapter comes with an individual set of refined objectives. Simulations and case studies of a real location is adopted for the exploration. As it is essential that a sufficient dataset of extreme flows is used for a reliable representation of the probability distribution models, a sufficiently long gauged time series of flow discharges from Thames at Kingston gauging station is used for the baseline distribution for simulations of stationary conditions, whilst the future flows from the same gauging station is also used for simulations of nonstationary conditions.

In chapter 4, a decision analysis framework incorporating the risk-based optimization methodology is designed. Scenarios of persistent flows are adopted to test the economic performance of two mutually exclusive time-dependent strategies for flood risk reduction. In particular, decision makers' behaviour in deciding upon an optimal flood protection is simulated. The main focus of the chapter is to provide insights on the uncertainty and sensitivity of the economic performance of decisions conditional to the strategies adopted and the climate scenarios.

Adopting the developed framework of decision analysis from Chapter 4, Chapter 5 proceeds on evaluating the uncertainty and sensitivity of the economic performances of decisions based on scenarios of nonstationary underlying distribution additional to the conventional stationary distribution. The future flows projected from climate models and historical observations were used in the study and the outcomes of the decisions' performance are compared. The chapter seeks to understand the relative implication of stationary and nonstationary predictions in flood risk management decision making under a range of possible future underlying conditions.

Chapter 6 proposes flood damage modelling techniques for a number of community-based flood protections accounting micro-scale assessment. Furthermore, the modelling are demonstrated using spatial information of a real location, and the resulting outcomes of flood vulnerability are analysed. The selected community-based protection measures are partly motivated by the case study location, whereby there has been an on-going work by the EA in managing flood risk involving the area. The developed methodological approach emphasises flexibility to ensure its adaptability when it comes to evaluating against a range of flood events and alternatives flood protection designs.

The damage modelling from Chapter 6 is taken forward into Chapter 7 to demonstrate the practicality of the risk-based optimization methodology under stationary and nonstationary conditions for a number of selected community-based portfolios comprise of the selected flood protection measures. Attention is given to the involvement of property-level protection and combined protection of property and embankment protections. Cost models of the related protection options within each portfolio are therefore developed for the cost-benefit analysis. Owing to the complexity of the damage modelling and cost estimation of the real case study, the application of the risk-based portfolios appraisal only focuses on capturing the sensitivity of the economic performances of the different portfolios under stationary and nonstationary conditions, but not the uncertainty range as aimed in Chapters 4 and 5.

The thesis is finally summarised and concluded in Chapter 8. Recommendations for future works and limitations identified are also included.

Chapter 2 Literature Review: Flood risk management

We review the literature on flood risk management decision making to help understand the concept and challenges surrounding the process. We also highlight key literatures that will be used in our model development. Literature about flood risk management decision making is enormous and only those seemingly essential to this thesis are discussed herein. This includes the principles of modern flood risk management and necessary tools for flood risk management options appraisal. This Chapter reviews flood risk management decision making starting from the background of flood risk management in Section 2.1 and followed by the intervention planning for flood risk management in Section 2.2. Section 2.3 continues to describe on the cost-benefit analysis. Robustness in long-term planning of flood risk management is discussed in Section 2.4. Lastly, Section 2.4 provides a summary of the chapter.

2.1 Flood risk management

Flood risk management is defined as 'the holistic and continuous societal analysis, assessment and reduction of flood risk' by Schanze (2006) and 'the process of data and information gathering, risk assessment, appraisal of options, and making, implementing and reviewing decisions to reduce, control, accept or redistribute risks of flooding' by Hall et al. (2003a). These definitions highlight the involvement of a complex appraisal process and a variety of options salient to managing flood risk. Indirectly, they also emphasise thorough assessment of risks and options appraisal before decisions are to be made.

Flood design has shifted from a historical event-based approach to a return period based approach and currently the risk-based approach (Rasekh, Afshar and Afshar, 2010). The historical event-based design was based on its ability to withstand the previous catastrophic disaster. This approach was too simplistic and prone to be costly and impractical. Probabilistic estimates of the return period design make use of past observations to yield a more realistic design. Most often, the approach

focuses on a fixed value of exceedance probability and does not account for the individuality of a project related to the specific flood risk system (i.e. the interrelated aspect of economic, social and environment of the flood prone area). For example, a frequently used design sets a fix protection target of a 100-year return period flood event whilst some countries have differing protection designs of 10 to 10000-year return period (Kundzewicz, 2012, p. 18). The allowable exceedance probability is translated to a specific water level corresponds to the associated discharge loading. The results would then be used to establish the primary physical characteristics of such defence protection, followed by the incorporation of safety factors (Hall and Penning-Rowsell, 2011). Focusing on a specific severity of flood loading that a particular flood defence is expected to withstand may lead to unnecessary spending and it often neglects the analysis of corresponding flood consequences that may or may not be severe to the most vulnerable community. Furthermore, owing to the potential nonstationarity due to climate-related changes in flood drivers, the concept of return period has already being questioned (e.g. Serinaldi and Kilsby, 2015) (more discussion in Section 3.2 in Chapter 3).

The risk-based approach of modern flood risk management explicitly takes into account both the flood loadings and the potential impacts in the assessment. It also considers existing uncertainty and the trade-off between initial investment and the expected economic consequences of failure for a range of loads and their damaging impacts. This is a tremendous shift, where the implementation of the risk-based approach requires a rigorous analysis of a flood risk system. Over the last decade, the risk-based approach has become possible with the advances in science and the falling cost of computation (Harvey, Hall and Peppe, 2012).

The term ‘flood risk’, however, is used in published documents with rather distinct meanings. It indicates either a common language or the technical terminology of risk analysis whereby the connotations may be dictated based on the needs and interests of particular stakeholders or decision makers (Hall, 2014). Commonly in technical assessment, the risk-based concept is well known as the product of a range of flood probability and the damaging consequences (De Wrachien, Mambretti and Schultz, 2011; Merz et al., 2010a). Quantification of flood risk requires

consideration of a full range of flood events including those exceeding the design standard. The inclusion of the range of possible events allows a full picture of the expected losses concerning all possible damaging flood events to be captured in the ultimate quantified risks.

The shift from traditional responses to flood risks to modern flood risk management has established salient principles. These principles stress applying a whole-system approaches for flood risk management. The concept was first highlighted in Sayers, Hall and Meadowcroft (2002) and Hall et al. (2003a) and had since been emphasised in Merz et al. (2010a), Hall (2014) and Sayers et al. (2013). The whole-system of flood risk propagation is important for a 'complete' assessment in managing flood risk, although not equal detail (Sayers et al., 2013). Some of the characteristics of the modern flood risk management that encompasses these principles have been discussed briefly above and some prominent issues are highlighted below (adapted from Hall (2014)):

1) *Inclusion of a full range of flood events and the expected consequences*.

- The risk assessment in the modern flood risk management addresses a full range of flood events concerning the targeted sources of flood hazard. Accounting the full possibilities and consequences of events allows a risk-informed judgement to be made. Limiting assessment to a fixed design standard can misguide users into poor investment and planning choices. Complete safety against flood events is a delusion, whilst efforts to manage flood risk recognize the possible damaging consequences of residual risks. Acceptance of residual risks, which is the portion of risk that remains when the design probability is exceeded (Di Baldassarre, 2012, p. 89), requires identification of flood receptors that are most vulnerable to flooding.

2) Integrated systems approach

- It is recognized that structural protection should be complemented by non-structural measures in managing flood risk, which means development of portfolios of measures by assembling 'hard' and 'soft' measures. There is in fact increasing awareness that traditional flood defence should be complemented or replaced by other measures. An integrated protection system planned for future decades should therefore be embedded in flood risk

management and thoroughly assessed for their effectiveness. It is important to recognize that flood consequences are significantly influenced by the existence (or non-existence) and conditions of the defence system. Therefore, assessment of risks may include the performance of defences and their effective contribution in reducing flood risks.

3) Risk-informed decision making

- An essential part of flood risk management is the decision making, where judgement is made based on the information of risks associated with each proposed options, along with any other costs and benefits. A proportionate response to risk is sought to ensure that investment put forward is based on the most cost-effective solution for the given case. Hence, transparency in the process of estimating flood risks and accessibility of the results are crucial.

A flood risk system that reflects the element at risks, vulnerability to flooding can be conceptualised as a geographical area within a boundary of interest comprising biophysical (such as soil, water, ground elevation and physical elements on the flood prone area), economical and societal components (Mens et al., 2011). The existence of the many components within the system places a great emphasis on the adoption of the systems-based risk assessment framework (Sayers et al., 2013). The framework describes the flooding state into layers of causal linkages representing the physical processes of flood risk propagation. The concept of flood propagation is intuitive where flood is considered to be triggered by exceedance of flood hazard above a current protection level, which then continues to make its way to communities and assets in the flood prone area, through which damaging impacts occur. Segmenting the physical processes of flood propagation from its source to consequences provides a way of relating magnitudes of flood impacts to magnitudes of flood hazard. The segmentation reflects the well-established concept of SPRC (Source, Pathway, Receptors and Consequences), which is in fact implicitly embedded within the systems-based framework. Whilst SPRC highlights the state of the segments associated with a flood event (Kundzewicz, 2012), the systems-based assessment emphasises the existence of complexity to model each segment (Sayers, 2014).

The definition behind SPRC, as given in Messner et al. (2007) and Merz et al. (2010a), is as follows: 'Source' refers to the hydrological variable by which the flood hazard originated. The routes of flood waters take to reach flood receptors are referred as 'Pathways' and the entity that may be harmed due to the hazard that may propagate across the 'Pathways' is called 'Receptors'. 'Consequences' is the impact of flooding such as economic, social or environmental damage. Whilst the definition may not be as relevant for technical assessment as opposed to theoretical discussion, a clear definition can assist a common understanding between flood risk managers and stakeholders participating in the decision-making process.

Taken from Merz et al. (2010a), 'hazard' may be denoted as 'a chance phenomenon capable of causing harm'. For fluvial flood risk management, flood hazard is usually represented in hydrological term as extreme flow discharge. It is also commonly referred to as extreme flood water level that causes inundation to assets in flood damage modelling studies (Apel et al., 2009; de Kok and Grossmann, 2010). The possible consequences of flooding often referred to as the flood vulnerability. The definition of 'vulnerability' is somewhat ambiguous because it often represented as one of the composite elements contributing to flood risks. More discussion related to vulnerability assessment is presented in Section 3.3 in Chapter 3.

Although the risk-based approach is well-accepted in the scientific literature, the practical application has been proven to be challenging (Rasekh, Afshar and Afshar, 2010). For instance, there exists a set of relevant variables associated with each state of a flood event that influences the overall estimation of flood risks. It is imperative to reflect upon these variables prior to undertaking flood risk assessment and identify how the variables might be incorporated into a systematic flood risk assessment. The following highlights some of the challenges related to characterising these variables (adapted from Hall, 2015):

1) Loading is naturally variable.
   River flows that generate fluvial flood hazard are naturally variable that require statistics. It is vital to address the potential risks from low-frequency events as that also contribute to the overall risk of flooding (Hall and Penning-Rowsell, 2011). Observations are the main

source for statistical inference, yet with the scarcity of observations and potential change in climate related risk, extrapolation is uncertain.

2) Combinations of load and response are important.
   The severity of flood impacts not only depends on the magnitude of flooding, but also the performance of existing defences. It is also influenced by the characteristics of the pathway and the preparedness of the community in the flood prone area. The more sources of flooding considered, the more complex it is to determine the probability of the combinations.

3) Spatial interactions are important.
   Flood propagation involves spatial elements that would influence the severity of flood impacts. Depending upon the domain and scale of the flood risk management, the spatial interaction may be reflected by an upstream protection and downstream increase of flood severity, or by the extent of fluvial flood from the river and the relative elevation of flood Receptors from the river. The natural propagation of flood is complex and to some extent may limit the ability for a complete assessment of flood risk.

4) Complex and uncertain responses must be accommodated.
   The physical processes of flood propagation are known to be complex. Relevant measurements of response to flood impacts and the historical direct and indirect flood impacts are also scarce; hence the ability to validate assessment of flood risk is difficult if not impossible. Furthermore, human behaviour that responds to flooding is also unpredictable. Therefore, models of responses to flood risk can be complex and highly uncertain.

5) Dynamic behaviour of variables over a range of timescales.
   The state of the environment and climate, the socio-economic development of population and human interventions in the flooding system may imply significant changes to flood risk (Sayers, Hall and Meadowcroft, 2002).

The above challenges reflect that modelling of a flood risk system requires identification of the important variables that may influence the flood risk of the area of interests. The precision of

information required in characterising the variables is greatly determined by the spatial scope of flood risk management decisions (Hall et al., 2003b). For example, at a local scale decision making is related to alternative options appraisal. In this case, the design components should be resolved in appropriate detail (Hall, 2014). A national scale decision, on the other hand, deals with prioritisation of expenditure for which should be based upon realistic datasets that can be aggregated on a national scale. There is, however, a great concern over possible discrepancies and exaggeration of national scale evaluation (Penning-Rowsell, 2014). Flood impacts are acutely experienced on the local level (Keskitalo, 2013;IPCC, 2012) and impact at a larger geographical scale is a result of an aggregation of a location-specific damages (Jongman et al., 2012). Attention to flood risk system at the local scale is therefore crucial, not only for the purpose of options appraisal but also to improve accuracy of information for national policy decision making.

2.2 Intervention planning for managing flood risk

Flood risk management should be built upon clear objectives of the main purposes of intervention. The objectives will determine the way in which one would respond to potential future flood risk. During the planning stage, one or more of the following objectives may be sought; prevention, protection and/or preparedness. Preventive actions typically imply that construction of properties and infrastructure on flood prone area are avoided. Protection of existing properties and infrastructure on flood prone area against severe flood consequences, on the other hand, can be obtained by protecting the most vulnerable elements at risks with structural and non-structural measures, such as construction of flood defences or flood proofing, whilst preparedness towards the potential consequences of flood risks involves understanding of the potential impact of flood event. This might require effective communication that may stimulate awareness of the community and stakeholders, for example, through providing flood maps and public engagement.

In efforts to reduce flood risk, flood risk management has long focuses on combination of these objectives. This thesis, however, focuses only on flood protection with the aim to quantify flood risk reduction related to structural and non-structural long-term interventions. There is no single universally effective response in all cases (Hall, 2014) yet a combination of structural and non-

structural measures potentially offers effective protection in reducing adverse flood impact. Structural measures are often thought of as the best measures for flood risk reduction (Klijn et al., 2009). A stand-alone solution of non-structural measures would likely to lead to severe damages during low probability flood events (Hamill, 2011), yet structural measures alone could not protect against all flood events. Generally, non-structural measures may modify the susceptibility of elements at risks from floods (Merz et al., 2010a), whilst structural measures may delay and reduce the extent of flood propagation (Mays, 2011). Without developing structural measures, non-structural measures are deemed to be less effective (Heidari, 2009).

As structural measures offer significant protection to areas that are prone to extreme flood risk, appropriate 'hard' measures for the areas should be identified during the planning stage. Engineering-related measures for reducing flood risk can be distinguished into three spatial scope of intervention; a catchment-wide, a community-based or a property-level types of protection (Environment Agency, April, 2010). Though property-level protection can be a stand-alone solution, it can also be integrated as part of the community-based protection measures. Similarly, community-based measures can also be one of the measures to be considered for a catchment-wide flood protection. Besides the spatial scope of intervention, the selection of appropriate measures to be considered in reducing flood risk is also highly determined by stakeholders' preference and evidence of performances of the measures. This is indirectly discussed in the subsequent paragraphs.

The catchment-wide flood protection is concerned with protecting several large communities at risk within the catchment area. Examples of interventions that would likely reduce flood risks for the elements at risk in the catchment area are allocations of water reservoir, retention ponds, or construction of channel diversions. Water reservoirs and retention ponds are likely to reduce the amount of runoff into the main channel, while channel diversion increases the conveyance capacity for the channel. Because the thesis is interested in detail analysis of flood risk management decisions performance in the context of stationary and nonstationary flood frequency within a local

intervention scope, the discussion with regard to catchment-wide flood protection is deemed unnecessary.

The community-based protection generally aims to provide a community against flood risk by introducing measures that effectively reduce the potential impact of flooding. For instance, by allocating a defence system for the community by modifying the river characteristics to increase the conveyance capacity. Floodwalls and embankments have been shown to be the preferred long-term protection for communities across the UK, with thousands of kilometres of flood embankments and hundreds of kilometres of floodwall alongside UK rivers and streams (Great Britain, n.d.). Although failure modes for flood defence vary from structural, geotechnical to functional failure (Long et al., April 2011), a good structural design and maintenance regime would enable the defence to withstand flood discharge that is within its designed capacity. Hence, it is recognized that the most common type of failure for flood defence is the functional failure (i.e. an overflowing of flood water when river flow exceeds its design threshold) (Great Britain, n.d.; e.g. Jonkman et al., 2009a).

Modifying river channel by increasing the channel capacity may be an effective solution (Mays, 2011). However, it has been suggested that during large events the storage provided by the dredged river channel is typically insignificant when compared to the natural storage of the floodplain (Chartered Institution of Water and Environmental Management, February 2014). A study on effectiveness of channel modification has found that an effective design protection of the measure is 1 to 4-year return period, hence ineffective for higher return period floods such as a 100-year return period (Arroyave and Crosato, 2010). The ineffectiveness of channel modification to reduce potential damage of a higher flood magnitude, and also the higher maintenance required to remove siltation over time are some of the main reasons for its unpopularity compared to other community-based protection measures.

However, there are claims that the inclusion of such option as part of the efforts to reduce flood consequences might be worthwhile and it may offer significant benefit to the vulnerable community. For example, the case of Somerset flood in winter 2013/14 has led the EA to establish

a 20-year flood action plan involving dredging rivers within the affected area (Great Britain, December 2014). This is despite initial suggestions that dredging of rivers in the area would only provide a limited impact on the extent and height of flooding (Chartered Institution of Water and Environmental Management, February 2014). Preference of the channel dredging, nonetheless has a basis in that the effective water level reduction of the flow discharge in reducing damaging consequences depends on the hydraulic characteristics of the channel and the flood plain and also the susceptibility and exposure of the elements at risks. This fact suggests that a relative damage reduction of such a measure might not be substantial for some flood prone areas but might be worthwhile for other areas. However, the cost-effectiveness of the measure is questionable in most cases (e.g. Great Britain, December 2014).

Another scope of intervention of 'hard measures' is the property-level protection that offers direct protection to targeted individual properties in a flood prone area. In recent years, reliable property-level protection measures have been developed, shifting from using the typical sand-bag protection approach to a more effective type of protection measures. The property-level protection measures can generally be applied by retro-fitted measures of dry- or wet- proofing types, or by raising buildings to higher elevation (Great Britain, Aug, 2010). Dry-proofing generally offers resistance to flood damage up to 0.6 meter high (Great Britain, Dept for Environment, Food and Rural Affairs, Aug 2012) whilst wet-proofing is equipped with home finishing that helps to minimize flood damage. The main difference between the dry- and wet- proofing is that the dry-proofing aims to completely prevent flood water from flowing into the protected property whilst wet-proofing allows the water to enter the property. Property-level protection is known to be more suitable to prevent damage from frequent flood events with lower flood extent and more likely to be considered for places where flood defence scheme is unjustifiable (Great Britain, Dept for Environment, Food and Rural Affairs, Aug 2012).

Today, the perspective on property-level protection has slowly moved from the last resort of flood management option to a possible cost-effective option. Property-level protection could be much adoptable in the future, especially with schemes that promote contributions from both homeowners

and local authorities such as the 'Partnership funding' introduced in the UK (Great Britain, Dept for Environment, Food and Rural Affairs, 2016). A chain of studies had been conducted by DEFRA from 2007 until recently to evaluate the cost-effectiveness related to property-level protection implementation (e.g. Thurston, Finlinson and Breakspear, June 2008;Great Britain, Dept for Environment, Food and Rural Affairs, Aug 2012;2016). The most recent findings from the studies indicate that property-level protection corresponds to 1 in 20 year return period is the most cost-effective solution with benefit-cost ratio of more than 5. The design protection was adopted in the flood risk management plan for the Lower Thames (Great Britain, Aug, 2010).

Although the chain of studies of the cost-effectiveness of property-level protection has made a great contribution in advancing the understanding of the adaptability of the intervention option, the suggested protection design is in the form of return period. This means that the concept of the risk-based decision making is not fully embraced in the guideline. This indicates that the possible variation of spatial distribution of the elements at risks and the contributing hydraulic properties to flood propagation in targeted areas are neglected if the guideline is adopted. As a result, some of the most vulnerable properties in those areas might be left out. Despite this limitation, the study by DEFRA has place property-level protection measures in context with other community-based protection measures. Such study provides the opportunity to obtain a meaningful hierarchical relationship of alternative options (Great Britain, Dept for Environment, Food and Rural Affairs, Aug 2012), what more from a rigorous risk-based studies involving property-level protection and other community-based protection measures.

A long-term plan of flood risk reduction involves a careful selection of a number of appropriate options that are suitable for the scope of decision. These options are typically arranged within a set of portfolios in ways that are matched to the options characteristics, such as life expectancy and maintenance regime (Environment Agency, April, 2010). Establishing portfolios of options enables a dynamic protection plan to be developed (Hallegatte et al., 2012) and allows a common currency to be used in comparing between alternatives (Hall, 2014). Strategic plans in implementing the portfolios of measures can concurrently be developed according to identified needs or limitations.

There is no one-size-fits-all best strategy (Ranger et al., September 2010) and given the uncertain future change, strategic plans are not only about answering where and how to approach the problem but also on when to respond (Matalas and Olsen, 2000;Kind, 2010). A decision will often need to be made on whether to design 'now' for climate change or to design at some point in the future. Planning led intervention of a 'no-regrets' action might adopt a precautionary approach (i.e. proactive approach), but could be prone to under- or over-estimate due to very partial information. On the other hand, to wait for several more years to decide (i.e. reactive approach) might gain better information that lead to a more reliable investment decision. However, the delay in investment of flood protection might incur damaging consequences of incurring extreme flood events during the waiting time (Twigger-Ross et al., 2015, p. 14). Similar to the reactive approach is to design in a way that allows further expansion or heightening at some point in the future (Great Britain, n.d.), for example the concept of real options (Woodward, 2012). The flexible options is also prone to unprecedented damaging impacts from possible future extreme flood events due to involvement of many stages of the design over the future period though with possibly less losses as compared to the reactive approach.

A vital and most recognized approach to assess the relative merit of alternative portfolios and strategies such as those mentioned above is the use of economic assessment of the costs and benefits involved. Although it is well acknowledged that appraisal of alternatives should not be solely economic (Environment Agency, 2010a), economic indices have been fundamental in guiding appropriate investment and highly desirable to policy makers. There is a variety of ways to evaluate economic performances of decision. Apart from the dominant cost-benefit analysis (CBA), there are also cost-effectiveness (CEA) and least-cost analysis (Michael, 2011).

The cost-effectiveness quantifies the courses of actions but is not restricted to monetary units only and may use different units. This type of analysis adopts the multi-criteria or multi-objective analysis where objectives such as ecological and health and social disruption are included (e.g. Rasekh, Afshar and Afshar, 2010). Optimizing the multiple objectives might require a more sophisticated decision tools such as Pareto optimal front, which applies evolutionary or genetic

algorithm approach (e.g. Woodward, 2012). The least-cost analysis, on the other hand, is a special case of CBA and CEA, where the benefits are identical for all courses of action such that only evaluation of the costs is required. This thesis will adopt the CBA for the exploration on the basis of compromising the need to adequately model the economic aspect and the need to reduce computational expenses in achieving the aim of the study. Section 2.3 looks into the discussion surrounding CBA and how CBA can be employed in flood risk management decision making.

2.3 Cost-benefit analysis in flood risk management decision making

The aim of reducing adverse impacts of flooding to deliver greatest benefits to the society entails difficult decisions about allocating scarce resources (Environment Agency, 2010a). As resources are limited and implementation of intervention can take decades, a wise public money spending on flood risk reduction requires careful analysis of the costs and benefits of the considered alternatives (Harvey, Hall and Peppé, 2009). Cost-benefit analysis has been used extensively in guiding decisions and offers vital information for investment prioritization. For example, a national scale study of 6000 FEMA grants distributed between 1993 and 2003 revealed that the benefit-cost for projects across earthquakes, floods, and extreme wind events was 4 to 1 (Mason, 2006). Similar policy guide has also been adopted in the UK (Great Britain, Dept for Environment, Food and Rural Affairs, 2016).

In theory, the CBA seeks to weigh up all the costs of the planned action and the benefits of the avoided damages (Michael, 2011). Though the concept is easy to digest, in practice the CBA has proven to be a challenging task predominantly due to the difficulty in transforming intangible costs and benefits in economic terms (Table 2.1). The suggested treatment for such cases is that either the intangible costs and benefits are given economic values (e.g. Broekx et al., 2011;Priest, Parker and Tapsell, 2011;Great Britain, Dept for Environment, Food and Rural Affairs, Aug 2012) by which they can be included in the CBA, or by formulating the costs and benefits in such a way that valuation of the intangible is not necessary. Many studies have avoided monetising intangible components in CBA (e.g. Rasekh, Afshar and Afshar, 2010;Jonkman et al., 2009b;Dawson et al., 2011;Mens et al., 2011) and in practical application the intangible components often qualitatively

assessed alongside CBA rather than within it (e.g. Environment Agency, April, 2010). The well-known reasons for the negligence of intangible components are that such valuation is prone to inadequacy due to subjective judgement and sensitivity issues with regard to monetizing loss of lives (Rosqvist et al., 2013). As a general rule, economic analysis should not aim to cover every single benefits and costs very accurately and precisely. The analysis should instead seek to include the most important benefits and costs which have the greatest effect upon the benefit-cost ratio so that a decision can be confidently taken as to which alternatives to adopt (Klijn et al., 2009, p. 14).

Table 2.1: Examples of some costs in different categories that might incurred in flood mitigation analysis, as compile in Messner et al. (2007) and Meyer et al. (2013).

	Classifications	*Tangible costs*	*Intangible costs*
Damage costs (for damage reduction benefits)	*Direct*	Physical damage to assets (buildings, contents, infrastructures)	Loss of life Health effects
	Indirect	Induced production lossess of supplies and customers of companies directly affected by the hazard	Inconvenience of post-flood recovery
Flood risk mitigation costs	*Direct*	Set-up infrastructure Operation and maintenance	Environmental damage due to mitigation infrastructure
	Indirect	Induced costs in other sectors	

CBA in flood risk management deals with long-term allocation of protection measures (Harvey, Hall and Peppe, 2012). With different options within each considered portfolio, the stream of costs and benefits over a specified appraisal period should be explicit for transparency. Each option may reflect a different useful lifetime that would require careful allocation of the costs and benefits over the appraisal period (Environment Agency, 2010a). For example, flood defence might have a lifetime of 100 years, whereas property-level protection measures is deemed to be replaced after 20 years (Great Britain, Dept for Environment, Food and Rural Affairs, Aug 2012). Therefore, the stream of costs of each considered option within each designed portfolios, which depends on the time of allocation/construction and the maintenance regime, should be appropriately identified.

For engineering-based intervention, capital costs at the start of a projects' life contributes the most to the total costs of intervention (Michael, 2011). The capital costs include direct costs of construction, such as materials and labours, and indirect costs, such as overhead costs. However, fixed costs, which are fixed regardless the level of output such as overhead costs and mobilisation are often eliminated in cost estimation of CBA (Samuelson, 2012, p. 257). The estimation of the construction costs of a project can be obtained by interpolating (or extrapolating) costs from other studies or previous project (e.g. Speijker et al., 2000;Stijnen et al., 2014). Other references such as national civil engineering works cost estimation guide books or information from contractors or responsible agency can also be used for the estimation (Environment Agency, 2010b).

Apart from the one-off costs during the year of project implementation, maintenance regime of the protection measure throughout the lifetime of the scheme is also contributing to the total costs (Hamill, 2011, p. 510). Recurrence of the maintenance costs usually considered annually and may be introduced to the overall costs as a percentage from the capital costs (e.g. Great Britain, Aug, 2010). Transaction costs, for example costs for land compensation, might also add to the overall costs. However, unless the considered protection measures would significantly result in substantial transaction costs, they are usually not included in CBA due to its subjective nature hence difficult to monetised (e.g. Meyer, Priest and Kuhlicke, 2012).

In relation to the community-based protection that has been discussed in the previous section, property-level protection requires much lower capital investment compared to the other community protection (Great Britain, Dept for Environment, Food and Rural Affairs, Aug 2012). It has been suggested that property-level protection is the lowest in cost, followed by channel improvement and embankments as the most expensive (Hamill, 2011). However, the approaches to estimate the costs of engineering-based intervention may vary depending on the purpose of study and the stage at which the costing is undertaken (e.g. feasibility study or detailed design). It can be either a detail list of cost components (e.g. Woodward, 2012), a moderately designed cost function based on a spatial boundary condition and past studies (e.g. Stijnen et al., 2014) or a rough estimation based

on heuristic cost function (e.g. Al-Futaisi and Stedinger, 1999). The second and third approaches should provide satisfactory results for feasibility or exploratory study.

The benefits of portfolios are much harder to quantify. Given that benefit is the expected risk avoided by the allocation of the measures, the probability of hazard and the degree of vulnerability of the elements at risks with and without the measures should first be quantified. In this case, a 'do-nothing' base case is introduced to allow for comparison (Great Britain, May 2011). The base case assumes that no intervention or further maintenance is undertaken. The discussion on flood risk assessment including the probability of and vulnerability to flood hazard is presented in Chapter 3.

To have a common time reference for comparison of the costs and benefits, the present value of the costs and benefits involved is typically used. The present value is calculated on the basis that a given cost or benefit at present is more valuable than the same cost and benefit in the future. The assumptions behind this is that (1) people are better off in the future in terms of the wealth, and (2) due to impatient attitude and preference of things now rather than in the future. The former is related to the annual growth rate (g) and the latter reflects the social time preference (ρ). Both constitutes the formulation of the discount rate; $r = \rho + \eta g$, where η is elasticity of marginal utility of consumption. For project appraisal, the HM Treasury recommends a discount rate of 3.5%. This percentage comes from assumptions that ρ = 1.5%, η = 1 and g = 2%. The selection of discount rate, nevertheless, is controversial because it is an estimation based on the assumption of society's preference and future conditions. Hence, different studies might use different discount rates. For example, it is suggested in the Stern Review of Climate Change that r = 1.4%, generated from the assumptions that ρ = 0.1%, η = 1 and g = 1.3% (HM Treasury, 2015). For the US, the discount rate may be taken as 3 or 7% depending on the assumption on the rate of pure preference for the present (1 or 4%), and the rate of economic growth of the US economy (2 or 3%) (Hallegatte, 2010). However, it is found that Jonkman et al. (2009b) in their study uses a discount rate of 4% for the analysis of flood defence economic performance for the New Orleans and further adjusted the value to accommodate potential increase in the economic growth over the appraisal period. Given that there is no single discount rate that is appropriate for all budgetary processes, selecting a common

discount rate of the specific localities is seemingly appropriate. As a general rule, the discount rate should be proportionate to the economic growth of the locality under study (Jonkman et al., 2009a).

The NPV and BCR are the most common economic indicators that describe the relative merit or desirability of a portfolio of actions. NPV reflects the difference between the benefits and costs involve (i.e. net benefit) and BCR provides the economic benefit over a unit cost of intervention. Net in this context means that the difference can be applied either to a particular year or to a pair of present values of benefits and costs derived by discount rate (Michael, 2011). Using an appropriate discount rate *r*, the costs and benefits over the appraisal period can be transformed to present value, $PV = \frac{cost\ or\ benefit}{(1+r)^n}$, where n is the number of years of the respective cost or benefit. The BCR can be computed by solving the ratio of discounted benefits and costs. They can be expressed as:

$$NPV = \sum_{t=0}^{n} \frac{1}{(1+r)^n} (\text{Benefit } (t) - \text{Cost } (t)), \text{ or}$$

$$NPV = \sum_{t=0}^{n} \left(\frac{Benefit\ (t)}{(1+r)^n} \right) - \sum_{t=0}^{n} \left(\frac{Cost\ (t)}{(1+r)^n} \right)$$

$$BCR = \frac{\sum_{t=0}^{n} \left(\frac{Benefit\ (t)}{(1+r)^n} \right)}{\sum_{t=0}^{n} \left(\frac{Cost\ (t)}{(1+r)^n} \right)}$$

For a fixed investment intervention, a positive NPV indicates a positive return of investment, whilst the value of BCR indicates the desirability of adopting an intervention measure (Klijn et al., 2009). Commonly, BCR more than 5 is regarded as cost-effective, whilst BCR more than 1 but below 5 is said to be cost-beneficial (Great Britain, Dept for Environment, Food and Rural Affairs, Aug 2012). Given that intervention related to engineering-based measures predominantly involves a range of technically mutually exclusive alternatives of the same option, such as the height of flood defence, or of different portfolios of measures, a maximum NPV that reflects the most value for money courses of actions is sought (Hall and Solomatine, 2008).

A similar indicator that would also direct decision to an optimal solution is the total present value cost (TPVC). This concept is well-established and has been widely used in flood risk management

options appraisal, though sometimes with different terminologies (Tung and Yen, 2005;Jonkman et al., 2009b;Kind, 2010). TPVC is the sum of the expected implementation costs and the residual risks of the course of actions in present value; TPVC = Risk + Cost (Tung and Yen, 2005). A minimum TPVC indicates the most cost-effective response to the flood management problem. Though a maximum NPV implies a minimum TPVC, using the TPVC to identify the optimal solution highlights the holistic approach of the risk-based optimization methodology in FRM decision making. Furthermore, solving the TPVC formulation does not require an assessment of the expected risks of the status-quo base case, hence reducing the expenses of recursive computation.

In the context of local-scale flood risk reduction, there has been a wide recognition on the importance of the approach of risk-based optimization particularly in flood defences scheme appraisal (e.g. Jonkman et al., 2009a;Kind, 2010;Rosner, Vogel and Kirshen, 2014). A wider adoption of the risk-based optimization approach to protection measures other than flood defences allows a more valuable comparison to be made. Risk-based appraisal of a range of flood risk management options is focuses on reducing harmful outcomes cost-effectively rather than merely relying on prescriptive treatment (Apel et al., 2009;Merz et al., 2010a). However, the question of how the risk-based optimization methodology can be adopted for other measures or for combined measures, for example combined flood defence and property-level protection, such that a larger set of alternatives can be evaluated to select the most cost-effective option, has not yet rigorously explored. Such efforts require quantification of the vulnerability of elements at risk conditional to the physical existence of the interventions.

Probably one of the most concerning issues on the use of the CBA in flood risk management decision making is the degree of uncertainty involves (e.g. Hallegatte, 2010). As mentioned in the earlier sections of this chapter, uncertainties cascading from the characterisation of the hazard to the decisions economic performances challenge decision making in flood risk management. Decision making under severe uncertainties requires rigorous process of decision making that may involves computer aided decision-making tools. The subsequent section discusses some of the

approaches of long-term plan of flood risk management focusing on uncertainty and sensitivity analysis.

2.4 Long-term planning of FRM

Conventional practice of flood risk management utilizes past observations to make an inference about the future. However, it is well known that the prediction based on observations of historical data alone is insufficient. Figure 2.1 illustrates the difference between present certainty based on previous (hydrological) data, and a range of possible future condition. The Cylinder of Certainty represents projecting the future from the past, whilst the Cone of Uncertainty represents uncertainties that grow over time (Walker, Haasnoot and Kwakkel, 2013). Furthermore, the prediction based on climate model is also uncertain given the control period in generating the future flows. As flood risk management decision making deals with long-term assumptions of unforeseen future state, robustness in decision making and decisions are vital.

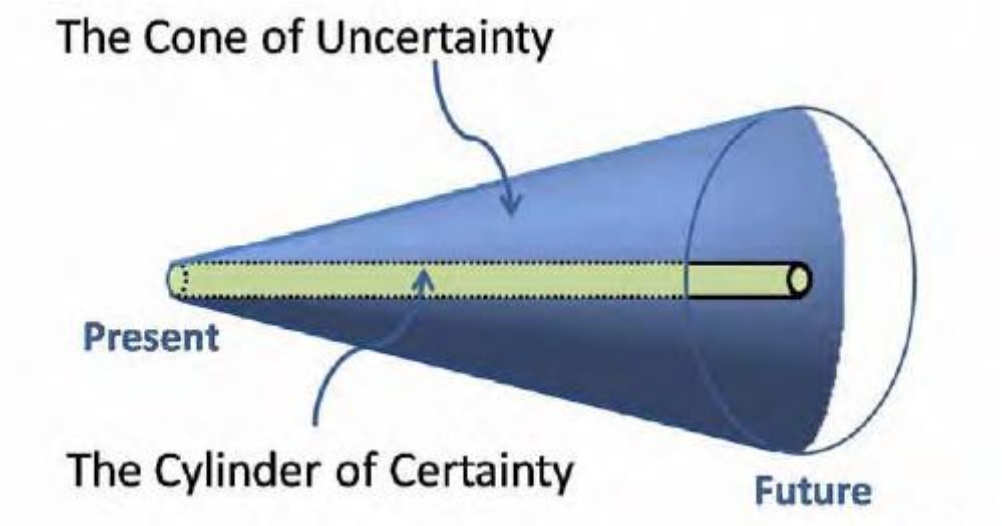

Figure 2.1: Schematic figure of the limited certainty of future based on current knowledge and the large uncertainty (Waage, 2010)

Many studies related to climate risk have explicitly associate robustness with uncertainty and have greatly emphasise the importance of robustness in long-term decision making to future uncertainties (e.g. Dessai and Hulme, 2007;Ranger et al., September 2010;Hallegatte et al., 2012). Similarly, reports and studies of flood risk management also emphasise the importance of robust decision making (Klijn et al., 2009). Hall and Solomatine (2008) and Sayers (2012, p. 79) have defined a

robust decision in flood risk management as a choice that continues to be desirable under a wide range of plausible future conditions. The efforts to attain a robust decision hence imply the acceptance of uncertainty in the decision making (Hallegatte et al., 2012).

It is also acknowledged that sensitivity analysis is important in ensuring robustness in decision making and decisions. Sensitivity analysis can generally be seen as the extension of uncertainty analysis (de Moel, Asselman and Aerts, 2012). Whilst uncertainty analysis focuses on the effects of uncertain inputs on outputs, sensitivity analysis attribute output uncertainties to the inputs (Mun, 2006). As far as the unknown future is concerned in flood risk management, the different input settings to the sensitivity analysis may be determined by the possible future scenarios related to changing in climate or flow regime as discussed in Chapter 1 and later in Chapter 3. In the case of appraising alternative flood risk reduction options, the scenarios can be related to the different alternative options/portfolios (e.g. Moel, Vliet and Aerts, 2014).

The different approaches of decision analysis incorporating uncertainty and sensitivity are depicted in Figure 2.2. Traditional planning involves identification of several possible outcomes from a number of possible scenarios and develops strategies based upon the sensitivity analysis. A robust decision-making process advances the method by exploring the possible outcomes from multiple hundreds of possibilities. Classic decision tree and real options involve estimating the probabilities of reaching various points on the cone and determine strategies to minimize expected future costs. There is no one-size-fit-for-all and the adoption of any planning approach depends on the needs and limitations. However, the advanced computational efficiency promotes adoption of the robust decision-making approach for a more rigorous analysis of decisions performance.

Although the general concept of robustness is easy to understand, there is no universal or normative criterion for robustness (Hine and Hall, 2010). For example, many studies have independently attempted to address uncertainties through decision analysis with distinct quantitative approaches (e.g. Hine and Hall, 2010;Harvey, Hall and Peppe, 2012). A few consistent characteristics of robust decision making nevertheless can be found from the studies and worth highlighted: (1) Robust decision making processes acknowledges that information is valuable and emphasis on rigorous

quantitative analysis. (2) The rigorous analysis accounts uncertainty and/or sensitivity of the decisions performance. (3) The results are reflected in quantitative and qualitative graphical representations.

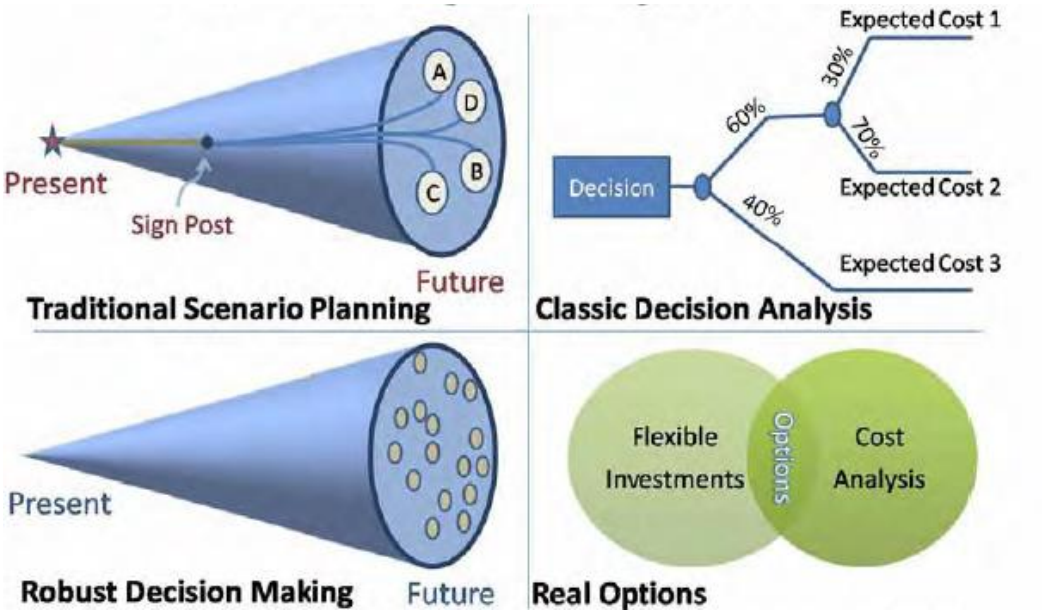

Figure 2.2: Four different approaches to flood risk management planning (Waage, 2010))

Sufficient and reliable information is the key for a robust decision-making process (Kundzewicz, 2012). Whilst the importance of information is widely recognized, analysis related to flood frequency is beset by limited number of observed extreme flows. The limited sample size poses two types of uncertainty: aleatory uncertainty due to the natural variability and epistemic uncertainty caused by imprecision of model formulation, parameterisation and input data (e.g. Apel et al., 2004). For long-term plan on flood risk reduction, predicting on uncertain future state based on observations remains one of the major challenges faced by flood managers owing to the aleatory and epistemic uncertainties. Whilst historical records are no doubt of importance, relying only on the observations for flood frequency analysis is inevitably questionable, especially in the context of changing climate (Kundzewicz et al., 2005;Kundzewicz, Hirabayashi and Kanae, 2010).

The uncertainty range of the outputs can be explored using simulation methodologies (Serinaldi and Kilsby, 2015). The Monte Carlo simulation methodology basically adopts a stochastic model to capture the probabilistic outcomes of variable of interests (Hall, 2014). In the case of flood risk

management decision analysis, the propagation of errors in the characterisation of hazard is implicitly transmitted through the modelling chain and reflected in the final results. Much effort has been demonstrated on exploring the implication of these uncertainties in flood risk estimation through Monte Carlo simulation methodology (e.g. Mkhandi, Kachroo and Guo, 1996;Apel et al., 2004;Merz and Thieken, 2009). Efforts to explore the uncertainty range of economic performances of decision alternatives, such as the economic damage and NPV, using the Monte Carlo simulation methodology have also emerged, though with different levels of complexity in the modelling effort (e.g. Goldman, 1997;Al-Futaisi and Stedinger, 1999;Harvey, Hall and Peppé, 2009;Su and Tung, 2013). The appropriate number of possible series to be generated via the Monte Carlo simulation methodology is subjective (e.g. hundreds or thousands), but in general should be sufficient to illustrate the general tendencies in the illustrative results presented (Moody and Brown, 2013). By default, a large number of simulations would give more precise estimates and should be considered to draw definitive conclusions.

For cases where uncertainty and sensitivity analysis is applied through a simulation methodology to tests the economic outcomes of different investment portfolios or strategies, the most straight-forward way of characterising uncertainties is via the mean-value criterion and the mean-variance criteria. The mean-value criterion is most widely used in engineering practice (Su and Tung, 2013) where the information of the variance is isolated. On the other hand, the mean-variance criterion provides the opportunity to look at the dispersion of the possible outcomes to identify the alternative with a higher expected outcome and/or a smaller variability (Su and Tung, 2013). The latter might be a better way to assists a robust decision making, but for cases where a project poses higher values of both the expectation and variability, there would be no definite ordering of preference between the participating alternatives. This further lead to subjective judgements to be made. Ayyub (2014) has developed a cost-benefit index that utilizes probabilistic information of the costs and benefits of alternatives. The index allows a definite ordering of alternatives to be built from the mean and standard deviation of the possible costs and benefits. Despite the advantage offered, the feasibility

of the index in the context of flood risk management decision making has not yet been fully explored.

Scenarios used in a sensitivity analysis basically represent new information based on realistic and plausible reasoning (Hallegatte et al., 2012). Scenarios can also be associated with the difficulty of predicting human behaviour (Hall and Solomatine, 2008), such as the different portfolios of flood risk management that may be taken during the long-term future. Many studies to understand the implications of future scenarios for the performance of flood risk management decisions have emerged. For example, O'Connell P. E. et al. (2010) explore the performance of two alternative strategies (i.e. proactive and reactive strategies) upon different degree of persistence in extreme flow series. Harvey, Hall and Peppe (2012) test the performances of alternative options (i.e. raise dike in 2030, raise dike twice and flood proofing 50% in 2030) against future increase in sea level whilst Zhou et al. (2012) test future performances of decision alternatives of pluvial flood risk management based on observations and climate change-induced projection. Broekx et al. (2011) on the other hand analyse the sensitivity of decisions to different economic growth and sea level rise scenarios whilst Tsvetanov and Shah (2013) investigate the sensitivity of timing of coastal protection (i.e. at the start of each future decade over 100 years) against varying plausible rates of future sea level rise. As a general rule, scenarios that are known to be unrealistic should be avoided for serious consideration in the decision analysis (Hsu et al., 2012). Nevertheless, the possible future scenarios to be included in the sensitivity analysis strongly depends on the future unknown to which decision makers would like the decisions to be robust (Mens et al., 2011).

Recent development has made available future flows projections that were derived based on IPCC future scenarios, such that developed and documented in Prudhomme et al. (2012). Although the projection has been made available, the call to adopt the information for a rigorous flood risk management decision analysis is relatively new. Given a hypothesis that flood risk could remain virtually constant despite the changes in its causal factors as a result of effective compensation, Kundzewicz (2012, pg. 16) brings an interesting question on what would be the relative

performance of decisions from projected future flows and observations. Such exploration is needed to explore the robustness of decisions under different assumptions of future state.

Analysis that focuses on capturing the uncertainty range and sensitivity of decision in flood risk management and its performance under a wide range of plausible scenarios could lead to information of greater value to decision makers (Harvey, Hall and Peppé, 2009). Combining scenario and uncertainty analysis within a simulation framework would help identify a robust decisions and decision-making approach. Integrating the risk-based optimization methodology into the decision analysis would further lead to optimality being part of the robustness analysis. Despite the strong emphasis for robust decisions in the face of uncertain future (e.g. Ranger et al., September 2010;Hallegatte et al., 2012), there are only a few studies that apply uncertainty and sensitivity analysis concerning performance of decisions in flood risk management against plausible future realization of different scenarios. Even less work has attempted to investigate robustness of decisions with the risk-based optimization methodology being part of the decision making. The reason behind this might be associated with the complexity to resolve in appropriate detail the components of flood risks management decision analysis (i.e. hazard, vulnerability and costs functions conditioned to intervention portfolios). Furthermore, the need to integrate the risk assessment components for them to be easily accessible and flexible for recursive computations might be even more challenging. Nevertheless, the selected approach for the decision analysis, for example by applying the traditional or robust decision analysis, depends on the needs and limitations of the given problem (Waage, 2010).

It is worth mentioning that uncertainty and sensitivity analysis might not necessarily increase our certainty. The analysis allows explicit quantitative assessment of the potential consequences from an uncertain key variable. Further, it provides the opportunity to understand and act rationally based on the given information, such as re-visiting the options considered earlier for flood risk reduction or developing a strategic approach to prepare for those possible conditions (Stijnen et al., 2014). In the case of conflicting assumptions and prediction of the future, exploratory data analysis in the

form of graphical and numerical outcomes are essential before proceeding to confirmatory data (Serinaldi and Kilsby, 2015).

2.5 Summary

This chapter presents the literature review of some of the critical elements of flood risk management decision making that should be understood in designing FRM decision analysis framework. In Section 2.1, the general overview of FRM is presented including the concept of risk-based flood management. Section 2.2 then proceeds on discussing appropriate intervention actions of 'hard' structures that often considered in FRM decision making. The discussion has focuses on local flood management measures by which alternative portfolios of actions can be developed. The cost-benefit analysis approach in FRM decision making is then discussed in Section 2.3. In view of the importance to attain robustness in FRM decisions, Section 2.4 continues with the discussion surrounding the notion of robustness of FRM decision making processes and decisions. It is clear from the literature that there has not been much investigation on the performance of alternative FRM actions accounting rigorous uncertainty and sensitivity analysis with regard to possible actual future states. Furthermore, studies have isolated the risk-based optimization methodology of cost-benefit analysis by which a cost-effective solution can be estimated. Given the need for a robust decision making process, a decision analysis framework that embeds the risk-based optimization methodology will be proposed in this study.

It is also crucial to further understand in more detail the modelling components of flood risk system, namely the probabilistic representation of flood hazard and the elements that would influence the flood vulnerability of a flood prone area. As mentioned earlier in this chapter, these two components are of importance in the assessment of flood risk. Chapter 3 therefore continues by reviewing literature around flood risk assessment, in particular some of the well-accepted method of flood frequency analysis and modelling approaches to address flood vulnerability of elements at risk. In aiming to explore the influence of nonstationarity to FRM decisions performance, Chapter 3 also reviews the way changes in flood frequency analysis can be characterized.

Chapter 3 Literature Review: Characterisation of fluvial flood hazard and vulnerability for flood risk assessment

Essential to flood risk management decision making is the estimation of flood risk. In order to understand how flood risk can be quantified, the literature on characterisation and approaches to model flood hazard and vulnerability and how the two components can be integrated to estimate flood risk are reviewed in this Chapter. Appropriate interacting modelling components are identified in seeking to develop an appropriate flood risk management decision analysis framework.

Section 3.1 presents flood frequency analysis, which is necessary for probabilistic estimates of flood events. Section 3.2 reveals characterisation of changes in extreme flow time series and distribution, focusing on persistent and nonstationary distributions. Section 3.3 discusses on the components and appropriate approaches for vulnerability assessment, which is another part of risk assessment. Finally, Section 3.4 provides a summary of the present chapter.

3.1 Flood frequency analysis

Flood frequency analysis is a widely recognized approach in flood risk assessment that takes advantage of stochastic properties of random hydrological variables. The analysis involves gathering relevant dataset of flow discharge and assigning an appropriate probability distribution through suitable estimation methodology. The probability distribution is then used together with a damage function to estimate a range of probability weighed damage that can be integrated to obtain an estimated value of flood risk.

Conventionally, a probability distribution is often selected based on empirical comparisons and suitability (Strupczewski et al., 2011), given the uncertainty inherent from small sample size and model specification (Rao, 2000). El Adlouni, Bobee and Ouarda (2008) has summarises some of the works undertaken in some region to identify adequate distribution. Based on a study that compared a number of distribution functions for 10 USA stream flow set of observations, the USA

has adopted the Log-Pearson type 3 (LP3) distribution in flood frequency estimation. Australia also is said to have adopted the LP3 distribution, whilst Generalized Logistic distribution is recommended to fit the flood frequency curves for the UK catchments (Reed and Robson, 1999) and China with the Lognormal distribution.

However, in exploration study related to sensitivity analysis of flood risk or its components, a probability distribution is typically chosen on the basis of deductive reasoning of limiting distribution of extremes in random samples (Strupczewski et al., 2011). The asymptotic limiting distribution according to the statistical extreme value theory suggested that Generalized Extreme Value (GEV) distribution is suitable for a block maxima dataset. While for peak over threshold dataset (POT), Generalized Pareto (GP) distribution is appropriate (Coles, 2001, p.78). Block maxima dataset of extreme flows is represented by annual maxima flows of water years. Different countries may have different water years hence the selected range should follow the climate pattern of area under study. For POT dataset, the threshold of extreme flows should at least represent the discharge that may triggers an overbank flow. This is related to the geometric representation of GP distribution that forms the distribution tail. For that reason, it is important to have sufficient local knowledge specifically on the relationship of the discharge and depth to determine an appropriate threshold.

POT generally provides higher instances of extremes, averaging 3 to 5 events per year in some countries (Hannaford and Marsh, 2008), hence provides the opportunity of obtaining higher sample size than AM. Nevertheless, an additional step is often required in POT frequency analysis to ensure that the observations are suitable for the intended flood frequency analysis (i.e. not correlated). Furthermore, simulation from GP distribution only generates estimates of the extremes whereas analysis maybe interested in simulating realistic series of events. Although this can be treated by coupling another empirical distribution for flow discharges less than the threshold value with the GP distribution (e.g. Cai, 2011), to simulate the required process requires additional computation time which might not be worthwhile for uncertainty and sensitivity analysis of flood risk adaptation study. For recursive simulation studies, a parsimonious model that is able to simulate the dominant

process is often sought. The disadvantages of using POT and GP might be some of the reasons why in many instances of such studies, GEV is often preferred owing to the convenient AM approach as compared to POT and GP distribution (e.g. Kay and Jones, 2012a).

There is a variety of well-adopted approaches to estimate distribution parameters. The most widely used method for 3-parameter GEV distribution is the maximum likelihood and L-moments (Ailliot, Thompson and Thomson, 2011). The maximum likelihood (ML) has since been extended to the Generalized Maximum Likelihood (GML) to eliminate potential invalid values of the shape parameter when using ML (Martins and Stedinger, 2000). L-moments is the extended version of probability weighed moments. Given a sample data, the probability weighed moments of the samples can be quantified and the linear combination of the results would provide the L-moments. Using the quantified L-moments, the summary statistics for the probability distribution of concern can be estimated (Hosking, 1990). The advantages and disadvantages of both approaches excerpt from Hosking (1997) and Coles (2001) are documented in Table 3.1.

Table 3.1: Advantages and disadvantages of estimation approaches of Maximum likelihood and L-moments (Hosking, 1990)

Methods	**Maximum likelihood or GML**	**L-moments**
Advantages	The model structure is adaptable/flexible to changes.	Work more effective for small sample size.
Disadvantages	When sample size is small, it will be less efficient in estimation.	It is not easily adapted because the distribution parameters need to be expressed in terms of L-moments.
	Provide direct estimates of uncertainties	Requires bootstrapping to estimate uncertainties

Regardless theoretical or empirical-based distribution choice, establishing an appropriate distribution for a given data should go through some kind of exploratory data analysis. This may be undertaken by performing goodness-of-fit of estimated distribution to data, which can be either in quantitative (e.g. Kolmogorov-Smirnov or chi-square tests) or qualitative forms (e.g. overlaying the theoretical probability density function (PDF) or its inverse to the empirical data). The

goodness-of-fit indicates how well the distribution fits to the data. It is common for the distribution to have a best fit for more frequent flood magnitudes (central range of the sample) and less prominent on the upper tail due to the scarcity of observations of the extreme flood magnitudes. Another approach that can be adopted to compare competing probability distribution is the AIC or BIC criterion (Di Baldassarre, Laio and Montanari, 2009).

Beside the goodness-of-fit tests, adequacy of the fitted distribution to AM flows can also be reflected through the shape parameter of the GEV distribution. The shape parameter is often used to indicate the behaviour of GEV distribution tail (e.g. Martins and Stedinger, 2000). UNESCO (2005, p. 25) suggests that a GEV distribution with a shape parameter within a range of -0.4 to +0.2 is consistent with a typical PDF of AM flood flows, whilst Martins and Stedinger (2000) suggests that based on hydrologic experience, shape parameter between -0.3 to 0 is the most likely range for AM flow series. Owing to the scarcity of low frequency flow magnitudes that leads to the difficulty to estimate the distribution tail (Katz, Parlange and Naveau, 2002;IPCC, 2007), the suggested range above should not be taken as rigid rules.

Flood frequency analysis has relies on the classical theory of Extreme Value. For AM flows, the theory assumes that observations in the time series are serially independent and identically distributed (IID) (Coles, 2001). The return period, *T*, which is the inverse of exceedance probability of any particular flood event is in fact formed upon the IID assumption, and can be denoted as (Serinaldi, 2015):

$$\mathrm{T} = \frac{\mu}{p} = \frac{\mu}{\mathbb{P}[X>x]} = \frac{\mu}{1-F(x)}$$

Where X is a random variable or realization describing the process, in this case the annual maxima flows, $\mu > 0$ represent the average inter-arrival time between two realizations of the process, which refers to one for the annual maxima, $p = \mathbb{P}[X > x]$ is the probability to observe realizations exceeding a specific value x, and $F(x) = 1 - p = \mathbb{P}[X \leq x]$ indicates the distribution function of X. Under the IID assumption, the exceedance probability is expected to be constant over the period of appraisal owing to the assumed constant of the distribution parameter vectors. This implies the

notion of stationarity of the PDF, which is fundamental in the classical extreme value theory. The implication of such assumption to flood risk assessment is that the computed risk is assumed to be annually constant, which leads to the description of risk as the average annual damage (Dawson et al., 2011).

The two major assumptions behind the conventional analysis of flood frequency (IID over the period of appraisal) may hold given that the distances between observations are sufficient enough to exhibit no apparent seasonal variation disturbance (Maidment, 1993, p. 19.3;Hosking, 1997) or provided that the average state of flow series is constant through time. Some even suggest that because it took thousands of years to notice climate change, the effects it has to geophysical time series may only be noticeable after a few hundred years. This may further suggests that designing a 100-year design life of a hydraulic structure may still be valid with the assumption of identical distribution through time. Nevertheless, it is still plausible that anthropogenic climate change may exacerbate the rate of change in the climate which may effectively change the hydrological pattern. In this case, the conventional assumption may no longer tenable. Moreover, the anthropogenic climate change might imply some sort of persistent pattern in the atmosphere and might also affects the catchment storage that persistent and nonstationary conditions are plausible (Arnell, 1996, p. 106) (as discussed in Chapter1).

With concerns over the traditional assumption in flood frequency analysis, the subsequent section presents some of the ways to accommodate different perspective of change in flood frequency analysis that can be adopted for the exploration research. It is worth highlighting that the literature review in the subsequent section is focused on understanding persistence in time series and nonstationarity of distribution as plausible characteristics of change in flood frequency analysis.

3.2 Characterisation of changes in time series and flood frequency distribution

3.2.1 Persistence in flow series

Stationarity of the underlying distribution is an important assumption made in order to simplify statistical inferences about a structure of a stochastic process (Cryer and Chan, 2008). An

independent sequence of random variables is the most general version of a stationary series, but a stationary series can also corresponds to a series whose variables are mutually dependent. In both conditions, the stochastic properties of a stationary series that can be represented by the PDF parameters are homogenous through time (Coles, 2001). Series with independent variables can be regard as strictly stationary process, whilst series with mutually dependent variables can be referred to as weakly stationary process (Chan and Chan, 2010).

The strength of persistence between two observations (i.e. separated by lag) in a time series can be quantified using the autocorrelation function (Malamud and Turcotte, 2013). The function will return an autocorrelation value given input data of observations separated by a defined lag. The autocorrelation value is the key variable in determining the significance of a given observations not being correlated. Various statistical techniques can be used to test the significance of persistence hypothesis. One such test is the ljung-box test that examines the overall randomness of a given sample based on autocorrelation values of associated lags (Watsham and Watsham, 1997, p. 241).

Persistence in a time series can be distinguished as either having a 'short-range' or 'long-range' persistency. These characteristics are based on the behaviour of 'memory' in the series (Khaliq et al., 2006). 'Long-range' persistence in a time series represents a non-negligible dependence between distant observations (Malamud and Turcotte, 2013). This may reflect the long-term variability of the underlying process. It has been referred in different terms, for example the 'Hurst Phenomenon' or 'long memory' (Koutsoyiannis and Montanari, 2007). Whilst the 'long-range' persistence indicates that the influence of the past never cease, the 'short-range' persistence reflects a future that is only influence by the present time instant (Koutsoyiannis and Montanari, 2007). In other words, short-range persistence is when the current state of the dynamic system already summarises everything in the past that is relevant for the future (Tijms, 2012, p. 460). A correlogram of autocorrelation function can be used to assists identification of short- or long-range persistence series. The autocorrelation function will rapidly die out for short-range memory and slowly decaying for long-range memory.

The concept of 'short-range' and 'long-range' persistence, however, is hard to verify when it comes to practical application involving hydroclimatic time series. Either models have been used to represent persistence in daily, monthly or annual flow series. Numerous studies on persistence in hydroclimatic time series are mentioned in Chen and Grasby (2009) and Koutsoyannis and Montanari (2007) and among those mentioned are studies indicating the long-range persistence in time series of river flows. In cases where the persistent time series is intended to be used for any independent-based assumption statistical tests, the series can be treated by declustering (Stahl et al., 2010). The declustering technique is the most widely adopted method to filter independent observations (Boniphace and Willems, 2011). However, Hosking (1997) comments that correlation between observations may not provide significant influence to estimated quantiles in flood frequency analysis. This suggests that the declustering technique might be of little use in flood frequency analysis. Although the suggested insignificant influence of persistence to the estimated quantile may indicate that persistence is not an issue in flood frequency analysis, our understanding of how significant the implication of under-protection of decisions made based on the assumption of IID whilst the underlying state is persistence is currently limited.

It is obvious that persistence is common in monthly or smaller time scale (Beaulieu, Chen and Sarmiento, 2012) but not in yearly time series. Nevertheless, there are concerns about future decadal persistence of flows due to the atmospheric oscillation pattern (as discussed in Chapter 1). Studies that try to quantify the effects of persistence are mostly limited to statistical effects (e.g. Koutsoyiannis and Montanari, 2007;Boniphace and Willems, 2011;Stedinger and Griffis, 2011) and few have tried to quantify the effects of persistence in effort to investigate the long-term performance of structural designs (e.g. O'Connell et al., 2010). In view of the importance of such information to assist flood risk management decision making, investigation of the effects of persistence to decisions performance is crucial.

A number of adaptation studies that explore plausible implication of flow series with persistence to decisions outcomes has typically adopted a simple model of autoregressive with lag 1 (AR(1)) to simulate plausible persistent extreme flows (e.g. Ward et al., 2013). The fact that AR(1) is a simple

time series model that can present persistence makes it a favourable choice for simulation studies (Koutsoyiannis and Montanari, 2007). Another model to simulate persistence that may be used for simulation of extreme flows is autoregressive and moving average (ARMA) model, which represent the 'long-range' persistence (e.g. O'Connell et al., 2010). Among the issues of using a time series model for simulation purpose is the fact that the stochastic process is based on Gaussian distribution assumption. Whilst this may be the case for most world problem, the normality assumption might not be reasonable for extreme value datasets. For annual maxima datasets, it may be necessary to model persistent series using a non-Gaussian distribution (e.g. O'Connell et al., 2010;Palma and Zevallos, 2011).

3.2.2 **Nonstationarity**

Emphasis on the nonstationary flood frequency analysis has emerged strongly in Milly et al. (2008). They have suggested that 'stationary is dead and should no longer serve as a central, default assumption in water resource risk assessment and planning'. Although some studies have already ventured into statistical analysis of nonstationary flood frequency just a couple of years before the paper is published (e.g. Olsen, 2006;El Adlouni et al., 2007;Leclerc and Ouarda, 2007), the remarks from Milly et al. (2008) triggered huge interests on exploring nonstationary extreme water-related problems.

Koutsoyiannis and Montanari (2015) have performed a critical review on the historical origin and the concept of stationarity. They highlight that in the case of a dynamic system, stationary characteristics are associated with a probability density function that remains unchanged in the course of time, citing a similar definition from Kolmogorov. This means that stationary is a stochastic process, which not to confused with characteristics of a time series that may not necessary be associated with a stochastic process (Koutsoyiannis and Montanari, 2015) (e.g. observations of random variables realizations of a stochastic process or merely 'noise'). Through the same concept, nonstationarity is also defined as a stochastic process that has one or more statistical characteristic that change systematically over time (Coles, 2001;Koutsoyiannis and Montanari, 2015).

In recent years, the concept of nonstationarity involving time-variant statistical parameters of probability density functions is well-adopted in studies related to investigating changes or the implication of flood frequency analysis. The mean (i.e. for two-parameter distribution) or location parameter (i.e. for three-parameter distribution) of the PDF represents the central tendency of the data whilst the variance of the scale parameter indicates the dispersion (Kay and Jones, 2012a). Di Baldassarre, Laio and Montanari (2009) explains that increase in the (mean) location parameter has the effect of shifting the whole PDF upward and an increase in the scale parameter causes a greater increase at higher return periods than in lower return periods in the case of stationary. Similar to the classification by Di Baldassarre, Laio and Montanari (2009), Castellarin and Pistocchi (2012) has considered three possible changes in the PDF (Figure 3.1): type 1 is a systematic increase of a constant value, type 2 deals with increase in extreme events of higher return period when more frequent events (low return period) remains unchanged. Type 3 described as increase in intensity of more frequent events (low return period) and vice versa for less frequent events (higher return period), but unchanged of intensities at a given design return period. The suggested representations of changes are plausible, but should be adapted with caution. It is necessary to fit the statistical model and to test the model strength to ensure that a given dataset is appropriately characterized.

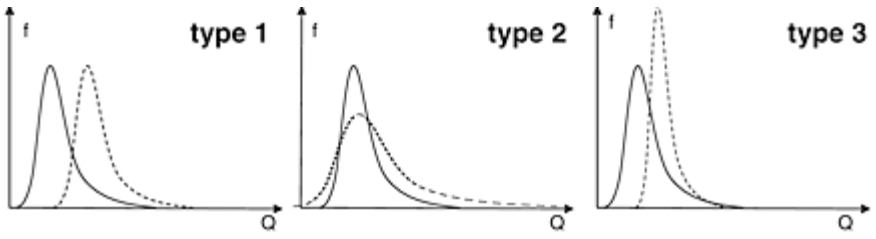

Figure 3.1: Conceptual variation in the probability distribution of extreme events. Left: change in the central value (type 1); middle: change in the dispersion (type 2); right: joint change in central value and dispersion (type3).

Most studies that apply nonstationary distributions to AM river flows have used nonstationary GEV distributions in characterising the changes (e.g. Seidou, Ramsay and Nistor, 2012a;Salas and Obeysekera, 2014;Rosner, Vogel and Kirshen, 2014;Condon, Gangopadhyay and Pruitt, 2015), whilst some uses the log-normal distribution (e.g. Prosdocimi, Kjeldsen and Svensson, 2014). Other possible distributions suitable to model nonstationary extreme flows are summarised in Serinaldi

and Kilsby (2015). Nonstationary parameters of the distributions for flood frequency analysis are typically attributed to time when the concerns on nonstationary are related to the implications of anthropogenic- and climate-induced changes. Covariates introduced within a nonstationary model can be of an actual scale of time (e.g. yearly time scale) or a time series of climate indices. Studies have used one or more covariates in characterising the nonstationary distribution. Time (or time series data of climate indices) as covariate allows future scenarios to be considered in a decision analysis (El Adlouni et al., 2007;Seidou, Ramsay and Nistor, 2012a).

For the log-normal distribution, the mean and standard deviation of the distribution may be assumed varying and for the GEV distribution, the covariates can be introduced in the location or scale parameter. The changes may be in the form of a linear trend or a more complex exponential function for the scale parameter (Coles, 2001). The exponential parameter for the scale parameter is to ensure that a positive value is used when estimating the parameter (El Adlouni, Bobee and Ouarda, 2008). Although it is known that the shape parameter (in this case of a GEV distribution) is the most crucial in characterising the probability of the extreme events, it is the hardest to estimate with precision. This is mainly the reason why it is unrealistic to consider the shape parameter with covariates (Coles, 2001).

Much efforts have been put into estimating potential nonstationarity in probability distribution of extreme flows, particularly in AM flows. The way the nonstationarity is characterised in the distribution parameters varies between studies. Prosdocimi, Kjeldsen and Svensson (2014) uses a nonstationary log-normal distribution with a linear trend in the mean to investigate changes in the peak flow data for catchments in the UK. They use time and 99^{th} quantile daily rainfall as the covariates. Condon, Gangopadhyay and Pruitt (2015) tested nonstationary GEV distributions with trend in location and scale parameters respectively with monthly total precipitation and mean temperature for the explanatory variable. The work has been demonstrated for two USGS gauges. Similar forms of nonstationary GEV distributions have also been adopted by Seidou, Ramsay and Nistor (2012a) for a case study in Canada. They tested several nonstationary GEV distributions with linear trend in location and scale parameters respectively and GEV distribution with linear

trends in both parameters, all with a range of different covariates of maximum average flows attributed to a period of days and time. Salas and Obeysekera (2014) tested GEV distributions with linear trend in location and scale parameters to annual peak flows of two river basins in the US with time as the covariates.

A number of approaches to estimate the nonstationary GEV distribution parameters have been proposed and explained in El Adlouni (2007); Maximum likelihood, generalized maximum likelihood and Monte Carlo Markov Chain (MCMC). In practical application, ML and GML have shown to be more favourable as compared to MCMC (e.g. Salas and Obeysekera, 2014;Condon, Gangopadhyay and Pruitt, 2015) as the former is less intricate as compared to the latter (e.g. Seidou, Ramsay and Nistor, 2012a). Given that a number of probability distributions are usually being contested, appropriate techniques can be adopted to indicate the statistical model that best represent the data. Similar to the selection of the best stationary model, the AIC can be adopted for this purpose (e.g. Salas and Obeysekera, 2014;Condon, Gangopadhyay and Pruitt, 2015). Other techniques that have been suggested and used to indicate a preferred model in nonstationary flood frequency related studies are the deviance statistics (Coles, 2001;Salas and Obeysekera, 2014) and bayes factors (e.g. Seidou, Ramsay and Nistor, 2012a). Through these methods, the likelihoods of each model are compared through a standard formulation respective to the selected approach. Indicative results would then suggest whether a more complex model considered is worth adopting for the given data as compared to a relatively simpler model.

Corresponding to plausible nonstationarity of probability distribution from observed peak flows, there have been much efforts in transforming the concept of return period of stationary assumption into one that corresponds with nonstationarity. For the case of increasing extreme events, the attempt was first demonstrated by Olsen et al. (1999) whereby the theoretical formulation of binomial distribution is manipulated to accommodate possible changes of the exceedance probability over the design life. Salas and Obeysekera (2014) later elaborated the same concept with improved derivation approach based on the geometric distribution. Consequently, new formulations of return period along with associated probabilistic equations are proposed. What has

been highlighted further in Salas and Obeysekera (2014) is the extended concept of 'risk of failure', which is the probability to observe a critical event at least once in a design life period under nonstationary conditions. Salas and Obeysekera (2014) have compared the 'risk of failure' curves under stationary and nonstationary conditions for a selected range of design life and a number of initial return periods. Although they suggested that the risk curve could be used for making decisions for projects experiencing nonstationary conditions, the way this can be done is not explicitly demonstrated in the paper.

Taking forward the concept of the 'risk of failure', Condon, Gangopadhyay and Pruitt (2015) demonstrated the usefulness of the method in investigating the so-called 'risk profile' (i.e. 'risk of failure' curves as used in Salas and Obeysekera (2014), but expanding the demonstration by incorporating projections of precipitation and temperature in the nonstationary flood frequency analysis. In addition, increase changes in the 'risk of failure' was investigated between observations and future projections. However, Condon, Gangopadhyay and Pruitt (2015) similarly isolate attempts to demonstrate the feasibility of the concept for making decisions under nonstationary conditions.

The advantage of the concept introduced by Olsen et al. (1999) and Salas and Obeysekera (2014) has also been highlighted by Serinaldi (2015). They further manipulated the mathematical formulation of the 'risk of failure' to allow computation of a design flood (or what they called return level) for a specified range of allowable 'risk of failure' and a targeted design life. It is interesting, however, to find that the formulation is not further adopted in a follow up paper by Serinaldi and Kilsby (2015) in effort to examine a practical application of the concept. Rather, Serinaldi and Kilsby (2015) perform uncertainty and sensitivity analysis of the 'risk of failure' and the 'return level' for stationary and nonstationary conditions. The findings from their work will be discussed later towards the end of this section.

What should be highlighted at this point is that the direct characterisation of the hazard using the probabilistic terms to represent nonstationarity in peak flow events promotes a shift from the widely used concept of return period to a more holistic concept of risk. The return period is commonly

used in c limate impact studies to characterise changes of flood frequency from projected extreme flows (e.g. Dankers and Feyen, 2009;Kay and Jones, 2012a). Communicating the changes in terms of the well-known return period might deemed as a more friendly approach. However, it is prone to misleading statements (Serinaldi, 2015). For example, a 100-year return period under stationary assumption widely understood as 'a rare event that is expected to occur on average once in every 100 years' whereas it is actually saying that 'there is 1% probability to observe the rare event each year' if one year time interval of duration is used.

It is important to point out that the 'risk of failure' should not be confused with the 'risk' term that has been defined in Section 2.1. The 'risk of failure' in the context of nonstationary conditions is defined as the failure of the defence system owing to the first arrival of floods exceeding a specified design load within a design life n or at year n and can be computed with time varying exceedance probability determined from a given nonstationary distribution and specified design load (Salas and Obeysekera, 2014). The 'risk' that is explained earlier in Chapter 2 represents the integration of the probability of the flood hazard and the consequences (i.e. $\int p(x)D(x)$). Considering the probability distribution of the flood hazard is changing every year, the 'risk' integration to estimate the probability-weighed damage is performed uniquely for each year. This means that the limiting distribution is conditional to the year it is represented.

Although the new concept introduced in Salas and Obeysekera (2014) has the potential to be adopted for an integrated risk-based flood analysis, for the time being it seems that it is more suitable for exploring changes in future flood hazard rather than incorporating into a comprehensive analysis of decision making in the context of nonstationarity. On the other hand, the applicability of the risk-based approach in FRM decision making has been demonstrated in Rosner, Vogel and Kirshen (2014) for nonstationary conditions, where the probability-weighed damage for each year is computed.

Up to this point, the way to ascertain nonstationarity for a given peak flow data and some of the recent approaches in characterising nonstationary flood hazard have been reviewed. Attempts to adopt nonstationary models in flood risk management applications entail a more complex procedure

as compared to the traditional stationary assumption (e.g. tests to be adopted to select the best nonstationary model and additional intermediate procedure for risk computation). Furthermore, it is well known that although the bias is reduced with a higher number of model parameters, the variance is increased. This can be illustrated as Figure 3.2 by Burnham and Anderson as presented in Di Baldassarre, Laio and Montanari (2009).

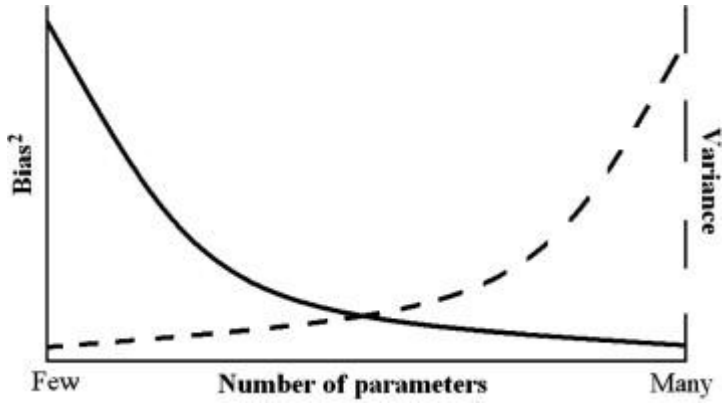

Figure 3.2: The principle of parsimony: the conceptual trade-off between squared bias (solid line) and variance (dashed line) versus the number of model parameters (from Burnham and Anderson) (Di Baldassarre, Laio and Montanari, 2009)

The possible discrepancies stemming from nonstationary model choice have been specifically highlighted by Serinaldi and Kilsby (2015) through uncertainty and sensitivity analyses of 'the risk of failure' and 'return level' curves. They suggest that outputs of a large uncertainty range from nonstationary model and a relatively small uncertainty range from stationary model 'provides no real justification' to switch from simple but clear framework of stationary assumption to the more complex nonstationary assumption approach that does not guarantee better future predictions. However, this statement should not be generalised to flood risk management decision-making problems as the relative effects of the competing models to flood risk management decisions has yet to be explored.

In view that communicating the ultimate performance of flood risk management decisions is influenced by the subjectivity of model choices would be more insightful in guiding flood risk management decision making as compared to the intermediate variable (e.g. design values), the uncertainty and sensitivity analysis may be extended to compute the statistical summary of resulting

economic outcomes (e.g. NPV). Merz et al. (2010a) have suggested that this can be done by (1) introducing time-dependence flood frequency analysis, albeit extrapolation of flood quantiles into the future may turn out to be different when the future unfolds, and (2) using simulation models incorporating assumed changes. Available software packages and simulation tools (e.g. Gilleland and Katz, 2011) have made possible such simulation study. With the issue of whether or not nonstationary assumption should be of concern being actively discussed and debated (Prosdocimi, Kjeldsen and Svensson, 2014;e.g. Milly et al., 2008;Stedinger and Griffis, 2011), exploration studies concerning the influence of the contested model choice and possible actual future conditions in the investment context of flood risk management is deemed valuable.

3.3 Vulnerability assessment

Vulnerability of elements at risk to flood impacts is another required information for flood risk assessment. Vulnerability assessment requires an understanding of the potential damaging consequences of a given flood scenario. Hence, it involves the prediction of damages of potential future flood events. As far as flood risk management decision making is concern, the predicted damages would be one of the essential inputs for quantitative flood risk assessment to support economic analysis for investment appraisal. The economic analysis will helps to identify appropriate risk reduction measures. Another potential use of outcomes from vulnerability assessment is flood risk mapping, which helps to raise awareness on the potential severity of flood impact.

Investigation on flood damage has been undertaken since mid-1970s (Merz et al., 2010b) but only a decade ago has been considered more seriously in the context of flood risk assessment (e.g. Tung, 2005;Kron, 2005) and decision-making processes (e.g. Messner et al., 2007). Flood damage assessment has been represented in different terminologies and components. Discussion on the different conceptual framework will be discussed later on in Section 3.3.4. It is worth to mention that this thesis will interchangeably uses flood damage assessment and vulnerability assessment to represent the same thing.

3.3.1 **Micro, Meso and Macro-scale assessment**

Flood damage assessment can be undertaken on different spatial scale; Micro, Meso or Macro-scale assessment (Messner et al., 2007;Merz et al., 2010b). Micro-scale assessment is an object-oriented study whereby damage is estimated to individual elements at risk. For example, Arrighi et al. (2013) has adopted the micro-scale assessment to estimate flood damage for a local area approximately 10 km along a river reach in Italy. Hence, it is suitable for local assessment and deemed appropriate for cost-benefit analysis of project appraisals (Apel et al., 2009). Meso-scale assessment is based on spatial aggregations of elements at risk to appropriate classes, typically based on land use classes. A meso-scale assessment has been adopted in Meyer, Priest and Kuhlicke (2012) for their two case studies located in Germany. Macro-scale assessment incorporates large-scale spatial units such as municipalities, region or countries. This means that the element at risk over a relatively large area may be assumed simply as an equal spatial distribution, hence disaggregation is not involved. An example of a macro-scale assessment for a pan-European scale flood risk assessment has been performed by Feyen et al. (2012), de Kok and Grossmann (2010) for Elbe River in Germany and Yu et al. (2012) for counties of Taihu Basin, China where high level aggregation data is used (100 – 500 m^2). Typically for Meso and Macro-scale assessment, resolution data at order of 100m from CORINE 2006 land cover database (EEA, 2009) is adopted (e.g. Apel et al., 2009;de Kok and Grossmann, 2010;Feyen et al., 2012;Jongman et al., 2012).

Although there is no clear spatial resolution distinction and no exact approach for the different assessment type, Messner et al. (2007) have depicted the relative differences between the spatial-scale damage assessment groups as Figure 3.3. The differences shown are in terms of size of area under investigation, costs per unit area and precision. Assessment classified according to the spatial scale focuses on the flood extent either directly or indirectly. It is obvious that risk quantifications for planning and cost-benefit analysis of flood mitigation measures requires very detailed spatial information to capture the flood extent. The way this can be satisfied is by improving the spatial specification, such as the spatial resolution of data on the area of interests (e.g. Apel et al., 2009).

Very few studies, nevertheless, have attempted to perform micro-scale assessments owing to the required detail.

Furthermore, a systematic approach on estimating flood damage for micro-scale assessment has yet to be developed, anticipating difficulty when flood damage is to be estimated for a range of flood scenarios and/or a number of competing flood-mitigation measures related to the risk-based assessment. As far as computational expenses of a rigorous risk-based assessment and decisions analysis are concerned, it is necessary to develop an effective algorithm-based approach to assist the quantification of flood damages for a range of flood scenarios.

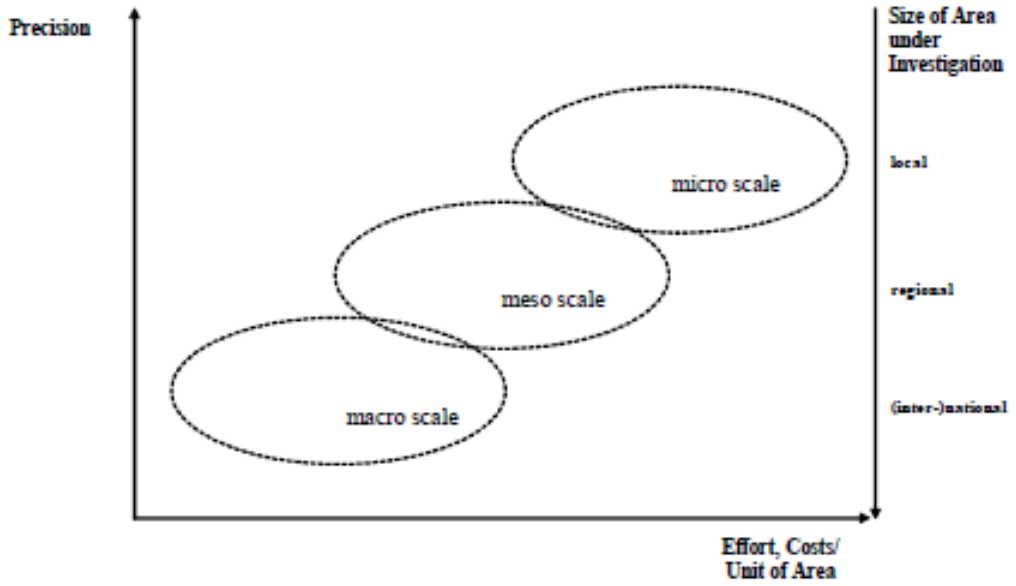

Figure 3.3: Different groups of damage assessment and their relative characteristics (Messner et al., 2007)

Micro, meso and macro-scale classifications have also been used to represent methodological distinction isolating the distinction based on the spatial scale (Merz et al., 2010b). For example, Boettle et al. (2011) has specified damage functions for individual buildings damage evaluation as macroscopic damage functions although the application is demonstrated for a local level.

3.3.2 Damage models

There is no single damage model that fits all purposes and places. Currently, there is a variety of established damage estimation approaches around the world, more prominently in the European

countries, that have been used for years in effort to assess total economic losses of actual flooding and predict flood-damaging consequences. The various damage models was independently developed, but most of them have the similarities of using water depth as the indicator for flood damage. The relationship between the depth and damage acts as the core function in the damage estimates.

The damage models can be differentiate according to a number of characteristics. Some of the characteristics, which are worth highlighting in this thesis are listed below (adapted from Jongman et al., 2012):

1. Scale of application (e.g. local, regional),
2. Units of analysis (e.g. individual objects or land-use classes),
3. Damage influencing factors (e.g. depth, duration, velocity),
4. Data method (i.e. either from empirical data from past flood events or synthetic data from 'what-if' analyses of a simulated potential flood),
5. Damaging cost base (i.e. replacement or depreciated/repair costs. Replacement costs refer to estimated new values of the elements at risk. Depreciated/repair costs are estimate of the present-day cost of replacement or reparation, which express real economic loss. The former is two-fold higher than the latter.),
6. Empirical validation (refers to validation of the damage model on the basis of reported flood damage data)
7. Damage functions (i.e. as a relative damage function with respect to a pre-defined maximum damage value or the absolute monetary loss with depth)

Table 3.2 lists a number of damage models developed for simulating direct and tangible flood damage and their associated characteristics (adapted from Jongman et al., 2012). The initial establishment of each model was mostly triggered by flood damaging experience in the country. For example, the FLEMO damage model of private sector was first developed based on survey data to 1967 private households that were effected by flood in 2002 (Apel et al., 2009), whilst HAZUS was developed by the USACE based on 20 year empirical damage data (Jongman et al., 2012).

Hence, the associated depth-damage functions were constructed on the basis of flood damage database experienced by the country (e.g. FLEMO, HAZUS, Rhine Atlas) (Jongman et al., 2012). Alternatively, synthetic data were used to derive the function (e.g. Damage scanner, MCM, Flemish model) (Jongman et al., 2012). For example, synthetic data for object-based damage function can be found from depth-damage function of MCM, where the standard buildings are defined by their typical size, construction and inventory components (Penning-Rowsell et al., 2010). The values of the components are assessed and the proportional damage to flood depth is estimated. The total damage of the specific building type corresponds to the water depth are then summed up to finally derived the depth-damage function. Regardless either ways, local expert judgements are somewhat involved in adjusting the model (Messner et al., 2007;Jongman et al., 2012). It is also important to note that regardless the approaches, the estimations are based on national prices.

The fact that the models are constructed based on national estimates implies that the models are not easily transferrable to other regions. The possible way for a model to be used elsewhere is when there are similarities between the two areas (Merz et al., 2010b), albeit some necessary modifications might need to be made (e.g. Jongman et al., 2012). For meso- or macro-scale assessment that involves aggregation of damage to land-use classes, the damage models might be transferrable for similar areas. However, adoption of damage models might not be appropriate in the case of micro-scale damage assessment due to the required local-knowledge of the elements at risk involved, such as the distribution of elements at risk and the hydraulic properties.

Table 3.2 highlights the use of water depth as the indicator for flood damage where other influencing parameters such as flow velocity and contamination are commonly neglected from damage assessment because of their heterogenous nature in space and time, difficulty to predict and limited information on their quantitative effects (Merz et al., 2010b). The many efforts to use other potential influencing parameters in estimating flood damage have been well documented in Merz et al. (2010b) and is not intended to be presented here. However, in almost all models that exists today, the estimation of direct flood damage has used depth as the determining factor for expected damage (Jongman et al., 2012).

Table 3.2: Some examples of damage models and their associated characteristics (adapted from Jongman et al., 2012)

Damage model	Rhine Atlas	MCM	HAZUS-MH	Flemish model	Damage scanner	FLEMO
Scale of application	Local and regional	Local and regional	Local and regional	Regional and national	Regional and national	Local, regional and national
Units of analysis	Surface area	Individual objects	Individual objects and surface area	Surface area	Surface area	Surface area
Damage influencing factors	Depth	Depth	Depth, Duration, Velocity, Debris, rate of rise and	Depth	Depth	Depth and contamination
Data method	Empirical and synthetic	Synthetic	Empirical and synthetic	Synthetic	Synthetic	Empirical
Number of unit classes	5 to 10	> 20	> 20	5 to 10	5 to 10	5 to 10
Costs base	Depreciated values	Depreciated values	Replacement values and depreciated values	Replacement values	Replacement values	Replacement values
Empirical validation	No	Limited	Yes	No	No	Yes
Function	Relative	Absolute	Relative	Relative	Relative	Relative

In relation to the risk-based decision analysis, it is crucial to ascertain that the determining parameters of flood damage model should be the same as the exogenous variable of the PDF. This is because a common variable is required to solve the integration of the probability and the damaging consequences to obtain the expected risk. Hence, if water depth is chosen as the determining parameter for the damage estimation, then the PDF should be described as the probability of extreme flow in height unit (e.g. Jonkman et al., 2009a;Kind, 2010). However, for fluvial risk assessment it might be more appropriate to use flow discharge as the determining parameter rather than water depth (e.g. Rosner, Vogel and Kirshen, 2014). Transforming the total damage as a function of depth to a function of discharge would require careful attention on the modelling chain involved and would isolate any transformation of the PDF of extreme flow discharges.

3.3.3 **Types of flood damage**

Flood consequences can be classified as either direct or indirect damages. Of both types, the damage can be in the form of tangible or intangible (Smith & Ward 1998; Parker et al. 1987; Penning-Rowsell et al. 2003; Messner & Meyer 2005). The classifications are similar with those discussed in Section 2.3 and provided in Table 2.1. Direct damages are harm related to the immediate physical contact of flood extent to humans, property and the environment. Indirect damages can be in the form of physical or economic-linkages disruption, such as traffic chaos and business interruption caused by the broken supply chains because of the failures of transportation systems. Tangible damage consists of damages that can be monetised, such as damage to properties and loss of industrial production, whilst intangible damages are not measurable by monetary unit, such as loss of lives and damage to environment (Tung, 2005). An element at risk to flooding can fall under direct tangible, direct intangible, indirect tangible or indirect intangible. However, most studies that demonstrate quantitative assessment of flood damage only consider direct and tangible damage for simplicity (e.g. Apel et al., 2009;Jonkman et al., 2009a;de Kok and Grossmann, 2010;Boettle et al., 2011) and little has incorporate indirect and intangible damages into the assessment (e.g. Broekx et al., 2011).

Evaluating indirect and intangible losses requires establishment of indices for damage assessment and an appropriate survey methodology (C. Yu et al., 2012). Nevertheless, obtaining accurate data on indirect losses is problematic and where these losses are relevant, they are often difficult to estimate (Messner et al., 2007). Furthermore, monetising intangible losses for cost-benefit analysis can be unethical. This explains why most damage models focuses only on direct tangible type of damage, for example in depth-damage model of MCM (Penning-Rowsell et al., 2010), or by taking indirect damage as percentage on top of direct damages (Jongman et al., 2012).

3.3.4 **Conceptualising vulnerability assessment**

Recognizing the importance of detailed micro-scale assessment required for flood mitigation studies, it is essential to identify the main modelling activities involved in estimating flood damage. In order to do this, the thesis intend to review the terminologies used within the risk-based concept in relation to the damage assessment. Although the analysis of flood damage is sometimes undertaken without any attempt to conceptualise the activities involved (de Kok and Grossmann, 2010;Broekx et al., 2011), many studies have put efforts to address the contributing elements of flood damage in a more systematic way.

Flood damage is usually defined as a product of hazard, vulnerability and exposure (e.g. Kron, 2005;De Wrachien, Mambretti and Schultz, 2011;Kebede and Nicholls, 2012;Jongman et al., 2012;Feyen et al., 2012;Arrighi et al., 2013;Merz et al., 2014). This definition denotes 'vulnerability' as the depth-damage function, whilst 'exposure' is defined by the type and value of elements at risk exposed to hazard (e.g. assets, private housing). Susceptibility of the elements at risk is considered implicit within the vulnerability function. Flood damage assessment has also been conceptualised as a product of vulnerability assessment, which means that vulnerability assessment also represent flood damage assessment, similarly describing the tendency of elements at risk to experience damage. Following this description, 'Vulnerability' assessment is the societal condition composed of exposure, susceptibility and response capacity (Merz et al., 2010a). Adopted from Merz et al. (2010a), the definition of the terms are as follows: 'Exposure' represents the attributes of the 'receptors', such as the type and value of assets at risks and the location of the assets relative

to the source of hazard. ‘Susceptibility’ is the degree to which the system is prone to be damaged by certain floods. For example, given the same ‘exposure’ of two assets to flooding, the one that is protected by some kind of measures is less susceptible to flood impact. ‘Response capacity’ describes the ability to respond to and recover from flood, for example, a building owners would have a greater financial capacity to repair damage and to recover (Merz et al., 2010a).

The characterisation of the factors that influence the ‘vulnerability’ as introduced by Merz et al. (2010a) is attractive, but may be difficult to incorporate in modelling activities owing to indefinite boundaries between the components. However, explicit segregation to some extent allows a systematic approach to modelling flood damage, which promotes a closer look on the physical processes and impacts associated with the flood propagation. As micro-scale damage assessment is a better approach for a local flood mitigation options appraisal, the classification is deemed reasonable to be considered for this research.

Harmonizing the concept of vulnerability introduced by Merz et al. (2010a) with the concept of SPRC (Section 2.1), some of the key components that required attention in flood damage modelling can be illustrated in Figure 3.4. The factors that influence the susceptibility and exposure of elements at risk and the ways they can be modelled are provided in Section 3.3.5 and 3.3.6 respectively. The response capacity, however, is not considered further in the thesis due to its indirect contribution to the vulnerability assessment.

The different ways of conceptualising the flood damage assessment/vulnerability assessment nevertheless comprise the same main activities: identification of flood hazard, predicting flood inundation, identifying flood receptors and linking information of flood inundation and flood receptors to estimate expected damage for a given scenario. For flood risk assessment, the modelling chain might not be strictly sequential as mentioned, but typically involves transforming flow discharge into flow depth by means of a reasonable hydraulic model and spatial inputs. Concurrently, the types and values of assets of interests on the floodplain are gathered. The inundation and the receptors can then be linked using geodatabase information that allows total damage to be computed for a given scenario. Subsequently, flood risk for a number of flood design

or corresponding return period in the case of stationary condition from a generated PDF can be quantified.

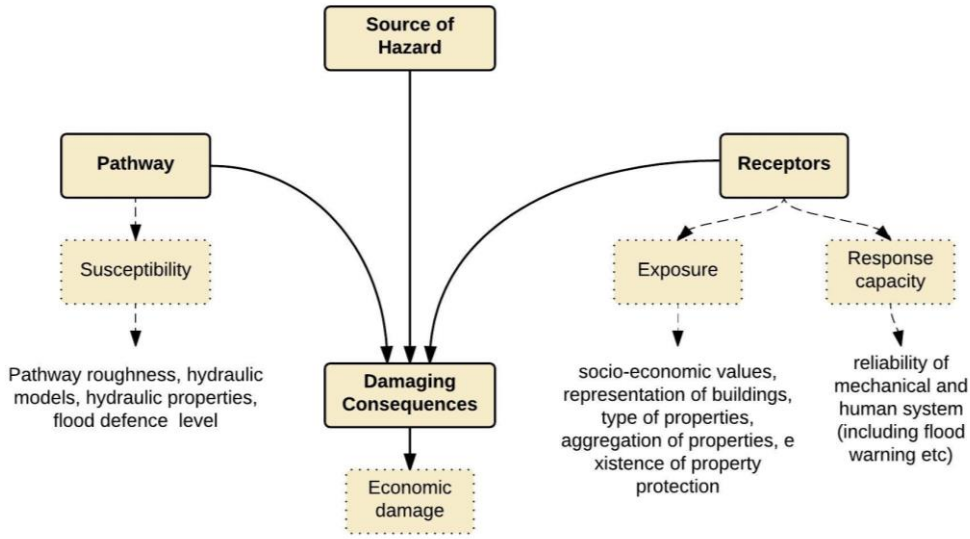

Figure 3.4: Conceptual illustration of the main components of vulnerability assessment

In traditional practice of flood risk management, assessment of damage is often treated as a separate component from risk-based investment decisions. Usually, the focus is at a specific defined protection target rather than an optimal risk-based solution (e.g. Heidari, 2009;e.g. Meyer, Priest and Kuhlicke, 2012). Adding to the drawback is the concept of return-period of stationary assumption that is widely used in damage modelling (e.g. Ward, H.de Moel and Aerts, 2011;Feyen et al., 2012;Meyer, Priest and Kuhlicke, 2012). This has constricting the usability of the model for stationary-based analysis only. Towards a more holistic application of risk-based decision making and identification of optimal decisions, it is advantageous to design a damage model that is adaptable for the risk-based optimization assessment. Such a model may be constructed with flood loading as the exogenous variable as opposed to the probabilistic return-period to further expand its adoptability in the context of nonstationarity.

A rigorous derivation of damage models using the spatial information is essential for alternative options appraisal, but may not be suitable for capturing the Monte Carlo based uncertainty of decisions under different assumptions and possible actual future conditions. Studies that attempt to explore the latter often use simplified damage functions to place emphasise on the relative

difference of the outcomes rather than absolute values, hence reducing the computational costs (e.g. Hine and Hall, 2010). For example, Boettle et al. (2011) uses logarithmic, square root, linear and quadratic representation of flood damage. Similar application of simplified functional form of damage function can also be found in Dutta, Herath and Musiake (2003), Al-Futaisi and Stedinger (1999) and O' Connell et al. (2010). The simplified functional forms have some desirable characteristics as an approximation and are at least plausible (Messner et al., 2007). Furthermore, it helps to eliminate the cumbersome of an end-to-end complex derivation of a flood damage function, especially for studies that aim to investigate the influence of an exogenous variable on the resulting damage or other particular indices and not aiming for absolute value in the damage estimates.

3.3.5 **Susceptibility related to flood propagation**

Susceptibility of the elements at risk can conceptually be related to the physical properties of the flood pathways by which the water propagates from the source (i.e. river) to the receptors (i.e. objects of interest) in the case of fluvial flooding. This definition expand the definition of susceptibility given by Merz et al. (2010b), which defines susceptibility as a function that relates the damage of the elements at risk and the characteristics of the inundation, i.e. the depth-damage function. The physical properties of the flood pathways, such as the roughness caused by vegetation, or existing flood protection such as embankment, may reduce the susceptibility of buildings to flooding. The susceptibility of elements at risk can be visualised by relating the source of flooding from the river (e.g. flow discharge) to an appropriate flood influencing parameter (e.g. inundation depth).

Whilst susceptibility analysis is often handled implicitly in flood damage modelling (e.g. Arrighi et al., 2013), taking into account the factors that may influence the susceptibility of elements at risk to flood impacts may improve flood damage estimation. In view that an explicit representation of the susceptibility of the elements at risk is important for a systematic approach of vulnerability assessment, this section attempts to review factors that may influence the susceptibility of the elements at risk and how they can be accounted for in the vulnerability assessment.

Traditionally, the relationship between flow discharge and water depth is estimated using a standard 'rating curve' (Di Baldassarre, 2012). The 'rating curve' is a power function that can be established using hydrometric data from a gauged river flow. For the past few decades, many studies on flood damage modelling have applied relatively more sophisticated hydraulic assessment to simulate flood inundation scenario as oppose to adopting the simple power law approach of the rating curve (Di Baldassarre, 2012, p. 86). Hydraulic models have shown to be useful in reducing inaccuracies due to the extrapolation for higher flow discharges when using the rating curves. Furthermore, available open source and commercial software of hydraulic models have made possible a wide application of the relatively more advance approaches. It is not the intention of this thesis to review the vast hydraulic models available for flood modelling, but rather to have an overview of the different approaches in order to select an appropriate approache for this research.

Hydraulic computation of flood propagation are widely classified as 1D, 2D, 3D or combined techniques. 1D modelling technique is constructed based on the simple assumption of steady flow typically using the manning equation (Knight et al., 2010), or unsteady flow using the St. Venant equation (Horritt and Bates, 2002), whilst 2D modelling approach is relatively more sophisticated in which depth average velocity is incorporated (Horritt and Bates, 2002). 3D modelling approach considers turbulence effects in the river system that can be solved using the Reynolds Averaged Navier Stokes equation (RANS).

1D technique is relatively simple to use and has been widely implemented in a number of commercial codes including ISIS, MIKEII, HEC-RAS (Wainwright and Mulligan, 2013, p. 98). A number of studies has adopt the simple 1D steady flow assumption for uncertainty and sensitivity analysis related to flood risk assessment and decision making (e.g. Hine and Hall, 2010) and for macro-scale assessment of flood damage study (e.g. Feyen et al., 2012). The basic requirement for a 1D hydraulic model is a cross-section line approximately perpendicular to the direction of flow (Di Baldassarre, 2012). For a given river stretch, a recommended distance between cross-sections along the river is 10 to 20 fold of the river width and a larger distance should be used for a larger river (Di Baldassarre, 2012, p. 33). The input data of the river and adjacent floodplain cross-section

for the 1D technique can be derived either by traditional ground surveys, or extracted from high-resolution DTMs. However, it is recognized that the DTM provide poor information on inundated terrain. Hence, the river geometry obtained from the DTM might need to be crosschecked with available ground surveys.

In cases when topographic variation is significant and detail assessment accounting the spatial variability is desired, a 1D model may not be adequate (Wainwright and Mulligan, 2013, p. 98). The limitation is usually overcome by applying a 2D modelling approach (Kourgialas and Karatzas, 2013). 2D models are able to simulate minute of hydraulic details (Kuiry, Sen and Bates, 2010). Some of the commercial 2D modelling codes are MIKE 21, TELEMAC2D and TUFLOW. Accurate estimation of the out-of-bank flow, flood inundation extent, water depth and surface flow velocity of 2D model, however, is a difficult task when considering a full 2D representation of floodplain (Feyen et al., 2012). Furthermore, the complex 2D models might prove difficult to apply because of the large amount of data to parameterized (Di Baldassarre, 2012, p. 47).

To ease the computational expenses, a quasi-2D model that uses a simplified equation to represent the floodplain flow was introduced a decade ago (Kuiry, Sen and Bates, 2010). The quasi-2D model eliminates the estimation of the complex fluid dynamic properties such as flow velocity, but still accounting floodwater movement. Similar to the full 2D model, terrain data are manipulated in the quasi-2D model to conceptualizing the flow domain as a cluster of arbitrary shaped storage cells, which are considered as interlinked compartments for the modelling of the water flux (Kuiry, Sen and Bates, 2010). The mass continuity equation is used to relate the net flow into a cell with its corresponding change in volume (e.g. Kuiry, Sen and Bates, 2010;Arrighi et al., 2013). The quasi-2D approach for fluvial flood risk assessment is most suitable to be used when the lowest part of the storage cell is the closest to the river, because realistically floodwater will start to propagate from the lowest part of the cells system. The representation of the storage cells for the modelling is subjective; conventionally, consistent grid size based on a raster grid resolution is used (typically 10 to 50 m), but studies have also used increased mesh density by the application of Triangular irregular network (TIN) (Kuiry, Sen and Bates, 2010).

In modelling flood inundation, it is common that 1D model is used to describe the river reach and 2D or quasi-2D storage cell models for the simulation of river-floodpain flows (Kuiry, Sen and Bates, 2010;e.g. Yu et al., 2012;Arrighi et al., 2013). The combined 1D/2D or 1D/Quasi-2D approach is attractive as it compromises between high computational time and accuracy of the 2D application (Kourgialas and Karatzas, 2013) and has since shown to successfully simulate real world flood inundation events (Kuiry, Sen and Bates, 2010). A standard broad-crested weir equation can be adopted to represent the movement of water in time between the river and the floodplain that is being protected and along the cells system in the floodplain area. Using the continuity equation and the weir law, the volume of the storage can be associated with the flow discharge from the river (e.g. Dawson, Hall and Bates, 2005;de Kok and Grossmann, 2010;Arrighi et al., 2013). In this case, information of the flood hydrograph is essential in estimating the associated overflow volume corresponds to a given flow discharge (or associated return period under stationary assumption).

Although the coupled 1D/2D or 1D/quasi-2D model is well-accepted, it is difficult to incorporate the model in a Monte Carlo simulation framework of flood damage assessment (de Moel, Asselman and Aerts, 2012). Instead of considering the flux between storage cells, alternative approach can be undertaken by pre-processing information of stage-storage relationship from the DTM using GIS processing tools. Similar to the storage boundary delineation of high resolution DTM undertaken for quasi-2D model, TIN can be applied on the topographic data and computation can directly be made to obtain the volume and area for a given maximum inundation elevation. By repeating the process for a range of appropriate inundation water level, the outcomes can be stored as a look-up table for subsequent assessment (e.g. de Moel, Asselman and Aerts, 2012). This include configuration of a parametric form of the stage-volume relationship (e.g. Arrighi et al., 2013) and. The cumulative flood volume reached up to the point of the specified maximum inundation can be obtained from the look-up table.

Wright and Hargreaves (2013) point out that the influence of interface between the main channel and floodplain that causes turbulence effects can be captured using a 3D model. However, 3D

modelling approach to simulate a river system requires extensive computing resources that it still a predominantly research activity rather than applied for practical risk assessment (Wright and Hargreaves, 2013). Nevertheless, effort to improve and assist flood extent estimation has been undertaken by Knight et al. (2010), where they establish a software called the Conveyance Estimation System and Afflux Estimation System (CES-AES) that 'is more than a 1D model', with 'certain 3D flow features embedded in it' (Knight et al., 2010, p. 275). The model was developed based on large experiments and validated against an extensive range of experimental data, including detailed turbulence data. Furthermore, it has been tested against a number of full scale rivers in the UK and overseas, for which there is measured data, as well as laboratory data (Knight et al., 2010, p. 275).

Regardless the approaches, there are mainly two distinct assumptions in modelling the susceptibility of elements at risk in relation to the maximum inundation level of a flood event: (1) The maximum water level in-river and on the floodplain is considered as a planar, where flood protection measures along the pathways are not taken into account (e.g. de Kok and Grossmann, 2010;Feyen et al., 2012). (2) The maximum water level is varies, in particular when overtopping flood embankment and/or the quasi 2D modelling is considered. The latter assumption is more appropriate when one attempt to analyse the susceptibility of the elements at risk conditional to the functionality of flood embankment.

It is worth highlighting that the common 'stage-discharge' terminology to relate water level and flow discharge is technically different for the two assumptions. Whilst under the first assumption the stage-discharge refers to the corresponding consistent water level between the river and the floodplain, under the second assumption it refers to the in-river water level. Establishing the relationship of inundation level and flow discharge requires additional steps to transform discharge to volume and from volume to inundation level, utilizing the information from the stage-storage relationship obtained from the storage cells model. It is important to note that the volume can also be regarded as the flood influencing parameter. In this case, volume-discharge relationship can be

established and used for the damage assessment alternative to the typical water level-discharge relationship (or equivalent stage-discharge relationship).

3.3.6 **Exposure related to flood receptors**

As mentioned before, the term 'exposure' in vulnerability assessment usually refers to the attributes of flood receptors. These include the receptors' socio-economic condition and spatial distribution, usually with static assumption. The classification of the receptors according to the economic sectors can be found in Merz et al. (2010b) and it is apparent from their study that available and accessible datasets are hardly found for most of the sectors possibly due to strict privacy requirements or trade regulations (Arrighi et al., 2013). Majority of datasets related to private households are easily accessible, which explains one of the reasons why private households have been the primary focus of direct tangible damage type in many flood damage studies (e.g. Penning-Rowsell et al., 2010;Arrighi et al., 2013).

The analysis of exposure can be performed using different spatial settings. The different spatial settings can be categorised according to the way vulnerability assessment is classified; a much coarser aggregation of receptors for the exposure analysis is aligned with the macro scale assessment whereas a more detail analysis follows that of the micro-scale assessment (Section 3.3.1). The land-use or area-based classifications of receptors can be associated with the meso and macro-scale assessment, whereas object-based receptors can be associated with the micro-scale assessment. There is no standard method for direct tangible exposure analysis. Whilst meso and macro scale analyses may identify flood receptors as 100 (e.g. Meyer, Priest and Kuhlicke, 2012) to 500 m^2 (e.g. Yu et al., 2012) grid cells, micro scale analysis may consider the object-based receptors according to sub-categories (e.g. commercial category such as hotels and restaurants, or household category such as terrace, bungalow and flat) or simply as the average value of the sectors (e.g. residential sector average) (e.g. Penning-Rowsell et al., 2010;Arrighi et al., 2013). In general, the micro-scale exposure analysis is expected to be more accurate as compared to meso or macro-scale assessment, illuminated by the importance of receptors' location in proximity to the hazard source (e.g. Molua, 2012;Kebede and Nicholls, 2012). Although the effort to identify the attributes

of the receptors can be longer for a micro-scale assessment, acceptable delineation time can be expected for a relatively small study area. Furthermore, accessible aerial map and GIS processing tools help to reduce the need for ground surveys (Mason, Schumann and Bates, 2011) and provide the opportunity for the micro-scale approach to be widely adopted (e.g. Arrighi et al., 2013).

An effective way to represent flood exposure of flood receptors to flood impact is through the depth-damage function. An appropriate depth-damage function for a flood damage study depends on how one characterised the related flood receptors. For example, depth-damage functions for residential buildings may vary according to the different types of the residential buildings, or may be represented by the average value of the sectors. In the case where individual property protection or flood defence is considered, the depth-damage function is usually truncated up to a threshold representing the protection level, usually up to a 0.6 m high from ground floor elevation level (e.g. Great Britain, Aug, 2010;Arrighi et al., 2013). Truncated depth-damage function is also found to be adopted for embankment protections (e.g. Heidari, 2009;Hine and Hall, 2010). This means that the protection measures are assumed to be fully functional and structural failure is not taken into account in the assessment. Using the truncated depth-damage function for vulnerability assessment involving the embankment protection also indicates that the embankment is considered to be fully submerged once the design threshold is exceeded by the in-river water level.

The location of the protection measures relative to the river and the receptors affect the flood vulnerability of the element at risks differently. For example, embankments are located near the river whilst property-level protection are for individual houses. This should be reflected in the appraisal process (Great Britain, Dept for Environment, Food and Rural Affairs, Aug 2012).

Applying the depth-damage function to affected receptors and aggregating the results would produce a corresponding total damage. Many studies have computed flood damages to individual affected receptors based on depths of water above the ground or street level of affected receptors before aggregating the total damage (e.g. Meyer, Priest and Kuhlicke, 2012;Arrighi et al., 2013). In conducting a full risk assessment that considers a wide range of extreme events and for a range of alternative mitigation options and optimization procedure, a manual computation for individual

affected receptors are considerably time consuming and deemed inefficient. To our knowledge, there is yet an automated method in computing total damage of a range of different flood scenarios. An automated approach using reasonable algorithms can be developed by taking into account a reference datum to relate the varying water level affecting the area of study and the receptors' locations.

It is worth recalling that the estimation of total damage with respect to flood hazard is essential to derive a damage function to undertake flood risk estimation of a given case study. There is a variety of ways the damage function can be derived. It may depends on a pre-set scenario, such as an inundation level or a return period for stationary case. For a risk-based options appraisal, the process of generating the damage function should aim for a consistent exogenous variable across participating functions. Given that extreme flow discharges are commonly used to drive probability distribution function, the flow discharge might be the most reasonable exogenous parameter for a risk-based options appraisal.

The following is steps towards configuring a damage-discharge function that were adopted in Arrighi et al. (2013) and de Moel, Asselman and Aerts (2012). For a given inundation level, the associated flow discharge should first be interpolated from an appropriate stage-discharge function. This will return the required damage as a function of discharge that can later be interpolated (or extrapolated) in the frequency domain to obtain the corresponding flood probability. Note that the method is applicable for the assumption of consistent water level in-river and on adjacent floodplain. As mentioned before in Section 3.3.5, volume-discharge relationship can be used for the case where the water level is considered different between in-river and on floodplain. This means that the volume is directly used to indicate the consequent damage, which can be obtained using volume-damage relationship. The volume-damage relationship and the volume-discharge relationship from preceding susceptibility analysis can then be used to derive the required damage as a function of discharge.

3.4 Summary

This chapter reviews the essential components to model flood propagation and impact. This includes the flood frequency analysis for flood hazard probabilistic analysis, the different representations of extreme flow series and the state-of-the art of flood damage modelling techniques. Appropriate statistical techniques for identification and characterisation of extreme flow series and distributions, and suitable models for simulation of flow series have been identified. The literature review has focused on independent and persistent flow series as well as stationary and nonstationary distributions. In aiming to model appropriate damage function for the risk-based decision analysis, susceptibility and exposure components of flood vulnerability have also been reviewed. The primary questions highlighted in Chapter 1 are sufficiently answered from the literature review from this Chapter and the previous Chapter 2.

Some of the findings from the literature review and the implication they might place for the modelling effort of this research are highlighted below. These findings are sorted according to the main components of the risk-based options appraisal:

1. Flood hazard model
    - It is recognized that persistent extreme flows does not contribute substantially to error in an estimated quantiles. Nevertheless, our current knowledge on the effects of flow series with persistence to the economic performance of decisions is limited. Furthermore, evaluating the effects of persistence would be a good starting point before including nonstationarity into the experiment.
    - The concept of return period may be expanded for nonstationary conditions. However, the concept may be negligible in practical application of risk-based optimization of flood protection, where an exogenous variable for the risk computation and the optimization procedure may adopt the initial parameter that governs the flood frequency analysis. In the case of fluvial flood management, the exogenous parameter of the flood hazard model is the extreme flow discharge. Hence, the allocation of

extreme flow discharge as the decision variable is more reasonable for computational efficiency.

2. Vulnerability assessment/Flood damage model
    - Flood damage model for risk-based options appraisal with regard to community flood protection requires detail attributes of flood receptors at risk. Furthermore, addressing the existence of flood protection measures in flood damage modelling might increase the accuracy of estimates; the distribution of receptors and the physical dimension of protection measures should, therefore, to be taken into account especially when preparing for a risk-based options appraisal. This gives rise to the preference of adopting a micro-scale assessment.
    - It is recognized from the literature review that micro-scale vulnerability assessment is currently limited. Furthermore, the few studies that have applied the micro-scale assessment have neglected a full range of flood scenarios of risk assessment. A systematic approach to capture the relationship between the source of hazard and the consequential damage for a risk-based assessment is yet to be developed. A systematic approach is vital to ease the assemblage of flood damage modelling components for the risk estimation.
3. Risk assessment and optimization procedure
    - Adopting the risk-based optimization methodology implies the cost model to be driven by the same exogenous variable as the risk model. The cost model should also be derived according to the micro-scale approach by which the dimensions of the measures in relation to the physical topographic of the area are taken into account.
    - In aiming to capture both the uncertainty and sensitivity of decision outcomes and its performance related to the assumption and possible future conditions, it is necessary to adopt less complex derivation techniques for damage and cost models. The less complex derivation of the models would ease the computational expenses for the thousands of simulations of decision makers' assumptions and possible actual future states.

- Sensitivity analysis allows the economic performance of alternative community-based options to be tested under stationary or nonstationary conditions, with the incorporation of the complexities of the multi-models of the risk-based optimization methodology. A systematic approach for vulnerability assessment can be developed more rigorously, and at the same time permits a more realistic results. To this end, little attention has been put into developing a systematic framework of vulnerability assessment that can easily be adopted and implemented for a practical risk-based analysis of options appraisal.

Overall, the reviewed literature from the present and preceding chapter has led to several research objectives that are highlighted in Section 1.7 in Chapter 1. These objectives are set to be accomplished in the subsequent Chapter 4 until 7. Progressively, objectives that are more specific are defined in the beginning of each chapter to have a more focus objectives in each study.

Chapter 4 Simulation study part 1: Decision analysis in the context of flow series with persistence

4.1 Introduction

The previous two chapters have reviewed some of the challenges in flood risk management decision making and the different possible characterizations of changes in extreme flow series and distributions. Concerns over the potential adverse consequences over the adoption of the IID assumption in the face of possible future changes have led to interesting questions on the possible effects to the performance of flood risk management decisions (Section 3.2). As pointed out in Section 2.4, it is also questionable whether a proactive decision based on limited information is more cost-effective than a later decision with a relatively more information.

Studies that incorporate a rigorous end-to-end technical evaluation in attempt to answer the questions are limited (as highlighted in Chapter 3). This Chapter aims to address the research questions, with emphasise on persistence in flow series and the implication to decisions' performance. A decision analysis framework is to be set up to satisfy four identified objectives. These objectives are:

1) To have insights on the resulting bias in PDF estimators due to IID assumptions in flood risk management decision making against actual persistence in extreme flow series, and owing to the alternative time-dependent decision making.
2) To have insights on possible flood damages over a design life period considering IID assumptions in flood risk management decision making and actual persistence in extreme flow series.
3) To have insights on the resulting economic performance of decisions from alternative time-dependent interventions accounting the effect of sampling error and persistence in extreme flow series.

4) To have insights on the relative performance of the alternative time-dependent decision making when the actual extreme flow series exhibit persistence.

The Monte Carlo simulation methodology is adopted to capture the effect of modelling and temporal uncertainties related to IID assumptions, natural variability and persistence in extreme flow series. The temporal uncertainties from sampling error is captured by simulating decision makers' behaviour in deciding upon flood protection designs whilst limited with finite historical records. Persistence in extreme flow series will be introduced using a GEV distribution and AR(1) model. Furthermore, the study attempts to capture uncertainty ranges of decisions performance influenced by to the strength of persistence in the extreme flows. Hence, a set of varying degree of persistence in the underlying properties is introduced.

Simulations of decision-making processes that involve rational acts of decision makers are undertaken in this study. It is assumed that the decision makers employed the risk-based optimization methodology to decide upon optimal protections. Performance of the decisions over a design period is subsequently assessed using perfect information of the underlying conditions. A comprehensive framework consists of the simulations of the decision-making process and evaluations of the economic performance of the decisions is presented in Section 4.2. Section 4.3 presents a methodology that is adopted to simulate extreme flows with persistence. Section 4.4 provides discrete formulations incorporating the time-dependent interventions within the simulation framework. The search for suitable underlying distributions for simulations of realistic extreme flows is presented in Section 4.5, follows by an example application of the proposed decision analysis to a case study. The results and discussions of the application are presented in Section 4.6. The conclusions from the main findings are highlighted in Section 4.7.

4.2 Development of a risk-based decision analysis framework

This section proposes a risk-based decision analysis framework that allows the propagation of uncertainty to be captured explicitly. Uncertainty from the natural variability and persistence of extreme flows are of the main focus. These sources of uncertainty in flood risk reduction decision

making inevitably influence the long-term economic performance of decisions. The characteristic of the underlying distribution of extreme flows is fundamental to this exploration work. It represents the state of the nature that is inherently unknown to decision makers, and can only be determined realistically based on a large sample size and expert knowledge on the appropriate statistical model. The decision analysis framework extends the work by O'Connell, Blenkinsop et al. (2010) by incorporating uncertainty analysis through the use of Monte Carlo simulation methodology. Damage and costs functions from the initial work are also re-parameterized to address the complexity of the area chosen for the implementation of the framework.

Figure 4.1 shows four layers of activities represented in rows that construct the decision analysis framework. The first row presents the process of generating multiple extreme flow series from an appropriate underlying distribution. Each time series consists of 'historical' and 'future' period. The 'historical' records is transformed into the second layer of the framework. Here, the decision-making process is undertaken through the risk-based optimization methodology and an estimated optimal protection is assumed to be materialized. Meanwhile, the generated 'future' series is brought into the third layer of the framework. The series is assumed as the actual future over the design life, hence the economic performance of the decisions can be evaluated.

The final layer compiles the outcomes of the multiple simulations of the same underlying process. Uncertainty range can then be tabulated to visualize the frequency curve of the economic indices. Applying the framework to a different underlying process allows the implication of persistence and natural variability to be captured and compared.

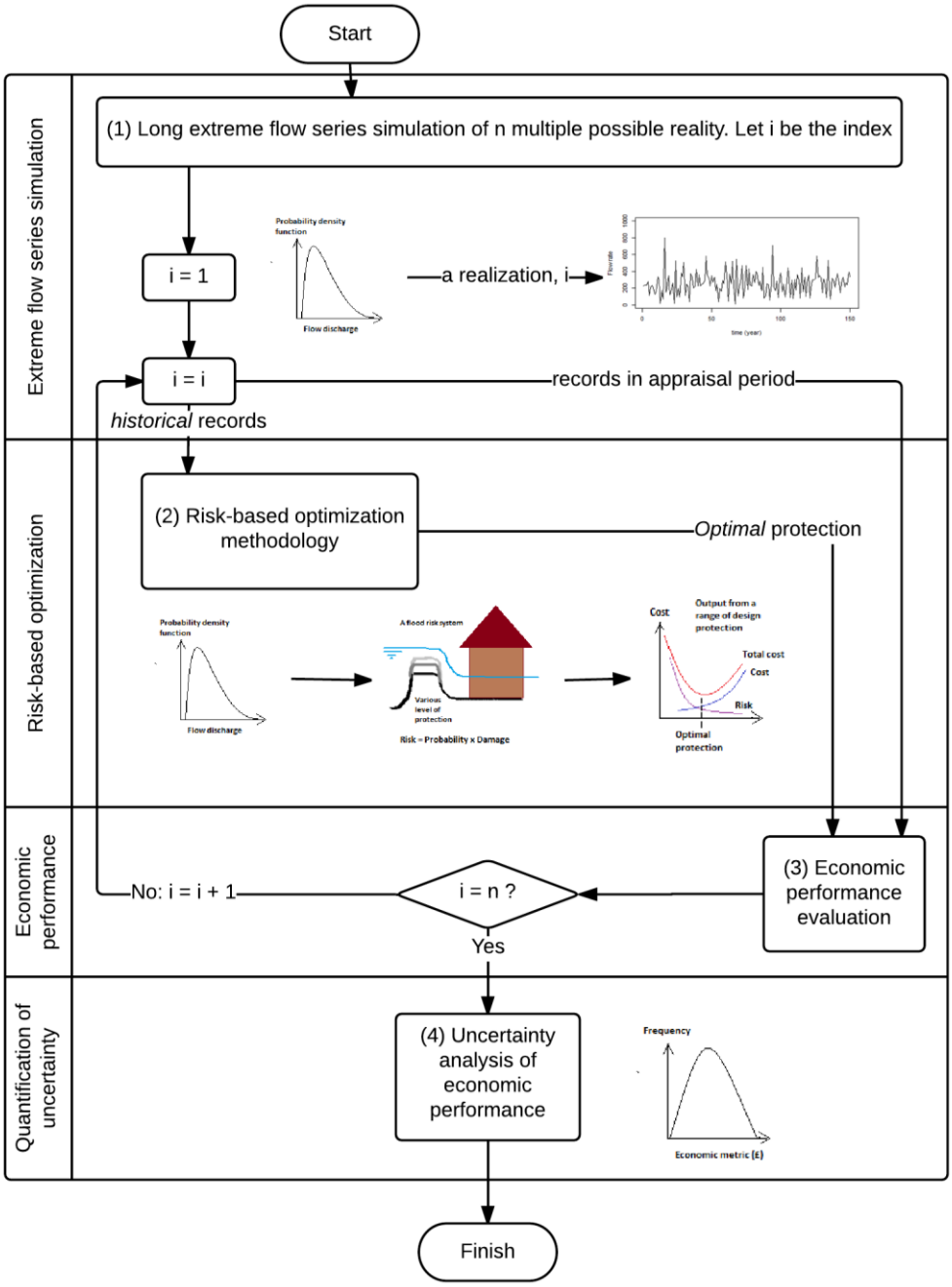

Figure 4.1: Main steps in the flood risk management decision analysis framework

The steps towards the uncertainty quantification, as explained and presented in the figure can be categorized into four distinct stages as follows:

(1) Box 1: Resampling of multiple possible long time series consisting of *historical* and *future* extremes from a *parent* distribution. The statistical extreme distribution model for this task is given in Section 4.2.1. Section 4.2.1 also explains how bias due to the

flow variability can be quantified. The approach to incorporate persistence scenarios in the simulated series is described in Section 4.3.

(2) Box 2: Simulation of decision makers' behaviour through the use of the risk-based optimization methodology. The models required to complete the risk-based optimization methodology are described throughout Section 4.2.2 to 4.2.5, and the ultimately assembling of models is explained in Section 4.2.6.

(3) Box 3: The quantification of economic performance using the simulated *future* series is undertaken. The criteria of economic performance are given in Section 4.2.7.

(4) Box 4: The empirical quantification of uncertainty from the ranges of possible economic outcomes. The work is presented in the results section (Section 4.6).

Distinct flood risk management strategies that are defined to initiate the propagation of different degree of uncertainty to the final economic performance are presented in Section 4.4. The time-dependent adaptation action would modify the proportional length of the simulated historical and future flow series. Eventually, the uncertainty associated with the sample used and the time preference of intervention would influence the decisions and the corresponding economic performance. The outcomes from the competing time-dependent interventions and different levels of persistence can be plotted graphically to capture their variability due to the inherent sampling error. Visual comparison of the outputs further indicates the degree of uncertainty one could expect from the inherent uncertainty.

4.2.1 Stationary GEV distribution, estimators and bias and error

An important step in generating a realistic series of extreme flows is the choice of the distribution function. As mentioned in Chapter 2, statisticians have pointed out that the GEV distribution is the limiting distribution for block maxima dataset. A long time series of annual maxima river flows can therefore be generated using the GEV distribution. Table 4.1 provides the GEV model equations (Hosking, 1997) for $\kappa \neq 0$ that can be traced back to Jenkinson's 1955 paper (El Adlouni et al., 2007). u is the location parameter, α is the scale parameter and κ is the shape parameter. The

estimates of extreme quantiles $x(F)$ of the AM distribution can be obtained by inverting the cumulative distribution function (CDF) $F(x)$. It is important to note that the CDF and PDF $f(x|u,\alpha,\kappa)$of the GEV distribution will exist if $1-\kappa(x-u)/\sigma \geq 0$. Given the condition, the reverse Weibull distribution (κ is positive) has an infinite lower bound and a fixed upper bound by $u+\frac{\alpha}{\kappa}$; the Frechet distribution (κ is negative) has an infinite upper bound and a finite lower bound given by $u+\frac{\alpha}{\kappa}$. Information of the upper bound of the GEV distribution is important to account for a full range of probability of extreme flows in the risk estimation. Section 4.2.5 will discuss more on how this can be achieved.

Table 4.1: GEV distribution functions for the stationary conditions.

Cumulative density function (CDF)	$F(x) = exp\left[-\left(1-\kappa\frac{(x-u)}{\alpha}\right)^{\frac{1}{\kappa}}\right]$
Quantile estimation	$x(F) = \begin{cases} u+\frac{\alpha}{\kappa}(1-(-\log(1-F))^{\kappa}), & \kappa \neq 0 \\ u-\alpha\log(-\log(1-F)), & \kappa = 0 \end{cases}$
Probability density function (PDF)	$y = \begin{cases} (1-\frac{\kappa(x-u)}{\alpha})^{\frac{1}{\kappa}}, & \kappa \neq 0 \\ e^{-\frac{x-u}{\alpha}}, & \kappa = 0 \end{cases}$ $f(x\|u,\alpha,\kappa) = \frac{1}{\alpha}y^{1-\kappa}e^{-y}$

GEV distribution used in this chapter were parameterized using the L-moments estimators. Although bias due to the sampling error to flood frequency estimates is well-acknowledged in the scientific literature, limited studies have quantitatively linked the error propagation to corresponding economic performance (e.g. Harvey, Hall and Peppé, 2009).Bias that stems from the variability of the finite sample size that effects the decisions' performance was captured using a simple yet robust statistical metrics. These are the Coefficient of L-variation (L-CV) and L-location (λ_1) as given in equation 4.1 and 4.2.

Hosking (1990;1997) introduced the measures as part of the L-moments measurement. L-CV is an analogue of coefficient of variation of a normal distribution where steepness of a given distribution is measured by dividing the L-moments scale parameter with its location parameter. λ_1 is the first L-moments that represents a conventional mean of the distribution. Both L-CV (Equation 4.1) and λ_1 ((Equation 4.2) measures are often used in hydrological study for different purposes with some within the scope of bias estimates (Viglione et al., 2012). Instead of estimating the L-CV and λ_1 by a single value as in the many hydrological studies, Monte Carlo simulations allows the measurement to be computed for a range of possible estimates, which leads to the quantification of bias from the estimates. $\Gamma(x)$ in Equation 4.2 is the gamma function whilst definitions of other notations have been mentioned earlier.

$$L - CV = \frac{\alpha}{u} \tag{4.1}$$

$$\lambda_1 = u + \alpha\{1 - \Gamma(1 + \kappa)\}/\kappa \tag{4.2}$$

The dispersion of the statistical metrics of estimates of each GEV parameter can further be quantified using the standard deviation (SD) and the relative mean square error (RMSE). Standard deviation indicates the dispersion from the mean, whereas RMSE measures the reliability of the statistical metric of the estimates as compared to the one from perfect information of the underlying parameters. The larger the magnitude of SD and RMSE, the more significant is the bias, and *vice versa*. Let the statistical metrics of the estimates be θ_i and the one from perfect information of the underlying parameters be $\hat{\theta}$. To obtain the RMSE for each statistical metric (Equation 4.3), the sum of differences between θ and $\hat{\theta}$ at each i estimated distribution is averaged by n total estimates before applying the square root function. The calculation can be repeated for different input conditions, in this case those which entail different sample sizes and persistence levels to allow comparisons.

$$RMSE = \sqrt{\frac{\sum_{i=1}^{n}(\theta_i - \hat{\theta})^2}{n}} \tag{4.3}$$

4.2.2 Stage-discharge function

Flood risk assessment involves identification of the relationship of water stage and flow discharge. The relevant literature on how the stage-discharge relationships can be formulated has been discussed in detail in Chapter 3. This section attempts to form a simple yet realistic stage-discharge function for preliminary decision analysis. The configured stage-discharge function is used to further configure damage and cost function for the economic analysis.

As widely known, Manning equation is one of the most commonly used open channel hydraulics equations to estimate the relationship of water discharge and inundation in flood damage modelling (Hine and Hall, 2010). In the present study, the Manning equation is used to configure the stage-discharge relationship. Note that the term 'stage' is used by assuming a planar inundation level over the main channel and the floodplain. However, the term is interchangeably used with the term 'level' throughout the Chapter whenever deemed necessary. The Manning equation for a rectangular channel can be constructed using the following properties. Bed width (w), flow stage (h), longitudinal bed slope (S_o) and Manning's roughness (n). w and h are typically in meters, whilst S_o is a ratio. h for a given discharge and other required properties can be obtained by pivoting the solution around its highest power with the use of a fixed-point iteration method (Equation 4.4). Fixed-point iteration helps to arrive at a new depth of flow normal depth, h_{j+1} from a previous depth of flow h_j. Eventually, the reiteration will arrive to an ideal solution of h (Knight et al., 2010). The 'normal' depth is associated with a long reach with a constant slope and roughness, and the slope of water surface and channel bottom is the same so the water depth remains constant (Knight et al., 2010, p. 16).

$$q = \frac{(wh)^{\frac{5}{3}} {S_o}^{1/2}}{n(w+2h)}$$

$$h_{j+1} = \left[\frac{qn}{{S_o}^{1/2}}\right]^{3/5} \frac{(w+2h_j)^{2/5}}{w} \tag{4.4}$$

The input parameters of n, S_o and w can be identified by simplifying the geometric features of the river and the flood pathway of the flood risk system. This can be obtained either by land survey, or based on available imagery and GIS application.

4.2.3 Damage function

This section proposes a damage function for the decision analysis. As highlighted in the literature review in Chapter 3, the damage function is one of the main components in flood risk assessment. The present study proposes a simplified damage function in the form of a square root function of a discharge-damage relationship (Equation 4.5). Given that the case is only a hypothetical and only the relative outcomes are considered, a constant (a) is used to amplify the damaging consequences. The damage is attributed to the relative magnitude of yearly AM flows and the no-damage threshold, where three sub-functions are assigned. Each is constrained by the limitation imposed by the relative magnitude.

$$D_t(q) = \begin{cases} 0, for h_d = 0, q \leq q_o or\ q \leq \hat{q} \\ a\left(h_d(q)\right)_t^{0.5}, for h_d \neq 0, q > \hat{q}\ (with\ defence) \\ a\left(h_d(q)\right)_t^{0.5}, for h_d \neq 0, q > q_o\ (without\ defence) \end{cases} \quad (4.5)$$

The damage (D) is determined by the water stage (h) above the river bed (d), corresponding to a flow magnitude (q). The selection of flow discharge as the determinant is deliberate to ensure a consistent exogenous variable for the risk-based optimization of protection design.

Assuming that a flood defence is proposed along a riverbank, the first case of no damage (i.e. $D_t(q) = 0$) indicates a lower h_d relative to the riverbank or flood defence threshold. This means that a higher q than the status quo discharge threshold (q_o) or the defence design discharge ($\hat{q}$) (when intervention is considered) will yield a damaging flood event and *vice-versa*. The second case refers to q exceeding $\hat{q}$, whilst the third case refers to q exceeding q_o. These conditions imply that damage will incur whenever the flood discharge (or corresponding flood level) is above the given thresholds.

The function is designed in such a way that the stage-discharge relationship from equation 6.4 can be incorporated for the damage estimation. Assignment of the constant values for the stage-discharge relationship should, therefore, aim for realistic values of consequential damages. Furthermore, a realistic magnitude of q_o should be selected based on available real information of a particular river system, and a reasonable a over a range of possible q can be identified based on several trials. The function with all the moderation is simple yet reasonable for a preliminary exploration study.

4.2.4 Cost function

Another key component in the risk-based optimization methodology and economic performance evaluation is the costs of intervention measures. As this study considers flood defence as the risk reduction measure, the rough estimation of investment costs in this study is associated directly with the height of the flood defences. Following a cost function derived by Al-Futaisi and Stedinger (1999), this study adopts a power function that allows the cost to increase faster than the height of the defence. Despite the same form of power function used, the $h_g(q_o)$ being part of the determinants of the costs estimation is derived differently. Furthermore, Futaisi and Stedingers' study is purely hypothetical whilst this study attempts to provide cost values that represent real economic values (i.e. in pounds), in attempt to illustrate a real-world problem. Given the above distinction, the magnitudes of A and B used in this study are not comparable with the ones used in Futaisi and Stedingers'.

The yearly cost (C_t) of the intervention adopted is denoted in Equation 4.6. Similar to the damage model, the determinant for the intervention costs is flow magnitudes (q). The stage- discharge relationship from Equation 4.4 is also embedded within the cost function. Two cases are considered; a case of no intervention (i.e. $C_t(q) = 0$) and a case where flood defence is considered. The variable that determines which function to be used is the height of the flood defence crest level (h_c) and the threshold level of the status quo (h_g) triggered by $\hat{q}$ and q_o respectively. The marginal difference of height ($h_c - h_g$) represents the flood defence height, which is converted to cost using constant parameters *A* and *B*.

$$C_t(q) = \begin{cases} 0, & for h_c - h_g = 0 \\ A(h_c(\hat{q}) - h_g(q_o))^B, & for h_c - h_g \neq 0 \end{cases} \quad (4.6)$$

4.2.5 Residual risk function

In this study, flood risk is denoted as an integration of the whole range of probability-weighed damage of flood events (Equation 4.7). $\rho_t(q|\, u, \alpha, \kappa)$ in equation 4.7 represents the PDF of extreme flows, specifically the GEV distribution (Section 4.2.1). $D_t(q)$ is the flood damage function, which for this particular study follows the one derived in Section 4.2.3. The risk function is associated with a particular year (t) acknowledging the possible variation of risk across the temporal scale. As this chapter limits the study to stationary conditions, the yearly risk will be constant. The integrations' lower limit is represented as a discharge threshold from the base case (q_o) or the defences' design discharge ($\hat{q}$), depending on the case considered. The upper limit of the function (q_L) is conditioned to the value of κ, which means that q_L may be either finite or infinite. The upper limit can be identify using the distribution parameters.

$$R_t = \int_{q_o or\ \hat{q}}^{q_L} \rho_t(q|\, u, \alpha, \kappa) D_t(q) dq \quad (4.7)$$

4.2.6 Risk-based optimization of the costs and benefits

This section explains in much detail the concept of risk-based optimization used in the study to reflect decision makers' action in reducing flood risk (Second row in Figure 4.1). The risk-based optimization is a powerful tool that trades off the cost of an intervention and the estimated risks associated with the intervention in obtaining the most cost-effective solution for the problem: the minimum total present value costs (TPVC) over the project lifetime period is sought. (Equation 4.8). It involves recursive computations that minimizes (i.e. optimizes) the TPVC including the expected damage and the cost across a wide range of possible protection design. Whenever applicable, a standard social time preference rate is used to transform yearly projects' cost and flood damages to present value.

The objective function of the optimization problem can be expressed as equation 4.8. C_t is the cost of intervention and R_t is the estimated risks. n_{str} is the design life and r is the discount rate. The optimization procedure requires an input of a unimodal function constructed based on the TPVC of

a range of appropriate protection design $\hat{q}$. The $t = 0$ in the equation represents the initial year the flood defence is constructed. For an exploration purpose, r can be of any reasonable value that may be recommended by experts. For the UK, 3.5% is the suggested rate (HM Treasury, 2015).

$$\min_{\hat{q}} TPVC = \sum_{t=0}^{n_{str}} \frac{1}{(1+r)^t} \left(R_t(\hat{q}) + C_t(\hat{q})\right) \qquad (4.8)$$

In solving this one-dimensional problem, the search operation for the optimum theoretically will start from a higher interval point of reference and repeated automatically until the global minimum is found. An inbuilt search optimization function in R, which is available form package *stats*, is adopted for this purpose to reduce the computational time of multiple operations. An assigned lower limit represents the starting reference point of the operation and an assigned upper limit represents the termination of computation indicating no optimal solution is an assigned upper limit. Hence by default, the upper limit should be of a higher value compared to the optimal. Appropriate assignments of both limits will ensure successful execution of the search operation and smooth implementation of the Monte Carlo simulation. This study uses q_o as the lower limit as it indicates the discharge threshold of the base case. The upper limit represented by the upper boundary of the PDF used for the risk estimation (see Section 4.2.1 for the formulation of the upper boundary). Given a correct set-up of the function, a minimum TPVC that indicates the most optimal solution for the given problem can be obtained. The optimal solution from the application of the risk-based optimization methodology is influenced by the variability of the 'historical' records affecting the estimated PDF, which will ultimately result in an inherent bias within the estimated optimal design.

4.2.7 Evaluation of economic performance

In this study, formulae used to evaluate economic performance of decisions are the net present value (NPV) and the benefit cost ratio (BCR). Both are denoted in Equations 4.9 and 4.10 respectively. Notations used in the equations have the same descriptions as the ones used in the previous Sections. As a prerequisite to solve the formulae, benefits and costs of a given flood risk intervention should first be calculated. The benefits here are computed based on the damage reduction of with project ($\mathrm{D}_t(q > \hat{q})$) from the base case of do-nothing ($\mathrm{D}_t(q > q_o)$). The damage function formulated in

Section 4.2.3 is applied in the benefits calculation. The main inputs for the function are annual extreme flow discharges over a pre-defined appraisal period that should be readily simulated prior the appraisal, as depicted in Figure 4.1. The cost function is adopted from Section 4.2.4 and depends on the $\hat{q}$. The NPV and BCR can then be quantified using the information of the streams of annual benefit and costs associated to the estimated optimal protection from the decision-making process. Equations 4.9 and 4.10 represent how the NPV and BCR are quantified in this study. Repeating the procedure for multiple possible decisions would return a range of NPV and BCR respectively.

$$NPV = \sum_{t=0}^{n_{str}} \frac{1}{(1+r)^t} (\mathrm{D}_t(q > \hat{q}) - \mathrm{D}_t(q > q_o)) - \sum_{t=0}^{n_{str}} \frac{1}{(1+r)^t} (\mathrm{C}_t(\hat{q})) \quad (4.9)$$

$$BCR = \frac{\sum_{t=0}^{n_{str}} \frac{1}{(1+r)^t} (\mathrm{D}_t(q>\hat{q}) - \mathrm{D}_t(q>q_o))}{\sum_{t=0}^{n_{str}} \frac{1}{(1+r)^t} (\mathrm{C}_t(\hat{q}))} \quad (4.10)$$

4.3 Initial set-up for AM flow series simulation

Section 4.2 describes a proposed framework incorporating associated key components for the exploration of decisions performance due to the inherent uncertainty of interests. This section further elaborates the approach adopted in this study to impose IID and persistence characteristics in AM flow series, respectively, where the GEV distribution model was adopted. Flow series with persistence were configured using the autoregressive model of lag 1 (i.e. AR(1)) representing the short-range correlation scenarios.

The construction of IID flow series is well-established and can easily be generated using 'random' functions in computer programs (Press, 2007). The procedure is known as the inverse probability integral transform. Given a real dataset of a long uncorrelated AM flow series having subsequent n values, parameters of GEV distribution ($\widehat{\boldsymbol{\theta}}$) for the IID series can be estimated. The inverse CDF having the GEV distribution parameters (see Section 4.2.1 for the equation) is then used to convert each $F(x_n)$ value to corresponding values of x_n. $F(x_n)$ is randomly assigned between [0,1] from a uniform distribution.

Whilst generation of extreme flow series with IID characteristic is widely applied in scientific studies, only a number of studies have attempted to generate extreme flow series having persistent

characteristics (e.g. O'Connell et al., 2010;Boniphace and Willems, 2011;Ward et al., 2013). In this study, the identified GEV distribution of the uncorrelated series is used to impose persistence in AM flow series. The remainder of this section describes the approach to modelling extreme flow series with persistence, having the same underlying characteristics of the GEV distribution as the stationary IID series.

The study adopts the first-order Markov chain model (i.e. the lag-1 autoregressive (AR(1)) model) to simulate extreme flow series with persistence. Assigning GEV as the underlying distribution, the model can be denoted as AR(1) – GEV. The lag-1 notation indicates a one-year time step correlation between the extreme flows in the series. The equation of AR(1) is denoted in Equation 4.11.

$$Y_t = \emptyset Y_{t-1} + \varepsilon_t \tag{4.11}$$

where Y is the process of interest (in this case AM flow series), $\emptyset$ is a lag-polynomial and ε is *innovation* (Cryer and Chan, 2008). Both Y and ε are magnitudes in a series of t years, respectively. For AR(1) process, the autocorrelation function at lag 1, denoted as ρ_1, is equal to the lag-polynomial to the power of 1, i.e. $\emptyset^1$. The value of lag-polynomial in the AR(1) process is, therefore, equal to the degree of autocorrelation assigned. Stationarity of this process is only if $|\emptyset| < 1$. When $\emptyset$ equals to zero, the characteristic of Y is equal to ε by which it is expected to have the IID characteristic. On the contrary, when $\emptyset$ is near to ± 1, strong autocorrelation can be expected in the process (Cryer and Chan, 2008). An assigned distribution type for ε would also result in the same distribution type for Y due to the linearity of the function. As the study focuses on using the GEV distribution as the underlying limiting distribution, the ε is assigned to have an underlying GEV distribution ($\varepsilon \sim GEV(u, \alpha, k)$).

The series is set to have similar distribution mean ($\widehat{\lambda_1}$) and variance ($\hat{\sigma}_{gev}$) of the IID series. Such arrangement is vital to have a valid final comparison of the economic performance outcomes. As the Y_t in the AR(1)-GEV equation is numerically innovated by ε_t, a linear transformation of desirable characteristics of GEV distribution of Y to the characteristics of ε's distribution should first be established. The characteristics of the distribution of ε can then be used alongside a

desirable autocorrelation to generate persistent flow series of Y_t following the AR(1)-GEV equation. Although this transformation is theoretically easy, in practice, it is not as straightforward. A detailed methodology on how this is to be undertaken is described as follows.

The properties of the underlying distribution of the IID series; $\lambda_1$and $\hat{\sigma}_{gev}$ should first be identified using available information of $\widehat{\boldsymbol{\theta}}$ using Equations 4.2 and 4.12 respectively (UNESCO, 2005). Let the underlying distribution of the persistent series have the same mean and variance as the IID. Defining μ_Y as the mean of the persistent distribution and σ_Y as the variance, the notation can be denoted as $\mu_Y = \widehat{\lambda_1}$ and $\sigma_Y = \hat{\sigma}_{gev}$. Subsequently, the distribution mean of ε denoted by μ_ε can be obtained using Equation 4.13, and by applying a desirable $\emptyset$ and the previously calculated μ_Y. Simultaneously, the variance of ε denoted by σ_ε can be calculated using the assigned $\emptyset$ and the covariance σ_Y using Equation 4.14. Recall that the assigned autocorrelation indicates the level of persistence that can be expected from the simulated series.

Having quantified the mean and variance of ε distributions, the GEV parameters of ε can then be determined. This is essential to initiate the generation of ε_t and subsequently Y_t. First, let the GEV shape parameter (κ) of ε be consistent with the shape parameter from $\widehat{\boldsymbol{\theta}}$. The associated scale parameter (α) of ε is then obtained by solving Equation 4.12 with $\sigma_{gev} = \sigma_Y$. Next, all the computed input variables required for Equation 4.2 is used to solve for the location parameter (u) of ε. The three parameters of GEV distribution of ε obtained from the calculations enables the generation of persistent series having the same $\lambda_1$and limiting $\hat{\sigma}_{gev}$ as the IID series.

Acknowledging that realistic extreme flows should only represented by positive magnitudes and follows a certain criteria, Equation 4.12 of $\kappa \neq 0$ and $\kappa > -1/3$ is considered in this study (UNESCO, 2005).

$$\sigma_{gev} = \frac{\alpha^2\left(\Gamma(1+2\kappa) - \Gamma(1+\kappa)\right)}{\kappa^2} \tag{4.12}$$

$$\mu_Y = \frac{\mu_\varepsilon}{1-\emptyset} \tag{4.13}$$

$$\sigma_Y = \frac{{\sigma_\varepsilon}^2}{1-\emptyset^2} \quad (4.14)$$

In selecting an appropriate magnitude of autocorrelation for the generation of the extreme flow series with persistence, several trials may be required before ultimately selecting a realistic autocorrelation value. If no evidence on correlation between annual maxima is found from available reference historical records, an initial autocorrelation for the simulation trials can be assigned using knowledge on the range of the extremes from the records. The trials should be undertaken ideally until the generated series presents no negative extreme discharges. As a general rule, a smaller autocorrelation is more suitable to be imposed on actual IID annual maxima flow series with relatively low flow magnitudes.

It is also important to note that the geometric mean and variance of the underlying distribution are the same for the different autocorrelation setting, but the arithmetic mean and variance of the generated series might be different due to the weak stationary properties of the persistent series.

4.4 Formulation of time-dependent risk reduction strategies

This section specifies two alternative time-dependent strategies of flood risk management that are designed to capture uncertainties from finite sample size and natural variability in the samples. The first considered strategy is a Proactive Strategy (PRO), defined as an adaptation action at a present time to decide upon a flood defence protection design in reducing potential flood risk. The second strategy is a Reactive Strategy (RCT), which refers to an adaptation action that is postponed to a future time. The RCT decision-making process will be triggered when the status-quo threshold is being exceeded. These strategies are of practical examples that are often surfaced in discussions among flood risk managers, stakeholders or decision makers alike. The competing strategies often arise due to conflict of interests on whether to secure societal safety from unforeseen flood consequences proactively or to prioritize limited resources and act when more information is at hand.

In general, both alternatives have their advantages and downsides. In terms of societal benefit, PRO strategy allows the protected community to be resistant from early on by securing them with flood

protection. One of the downsides of PRO intervention is the possibility of significant under or over estimation of the $\hat{q}$ due to relatively limited information, i.e. given by the sample size, which is used in PDF estimation. PRO strategy also requires investment to be allocated at a present time, which might result in serious repercussion of overspending due to possible severe sampling error. With the downsides of the PRO strategy, the RCT strategy might be more attractive as it potentially increases the reliability of risk estimation hence promote a good investment decision. Furthermore, it relatively reduces present value spending of public funds with the delay in investment. However, RCT strategy also brings a negative effect of possible significant consequences due to unforeseen flood events within the waiting time. Perhaps these are among the reasons why in practice, PRO intervention usually applied 'for cities that are of greatest importance to the national economy, with a RCT approach is taken elsewhere' (O'Connell and O'Donnell, 2014).

To fit the strategies into the decision analysis framework, they are formulated with respect to a discrete timeframe that represents a complete view of key periods in flood risk management plan. The timeframe includes historical period of observations, present time and future period of appraisal. For ease of execution, the intervention action will be simulated by a one-off investment of flood defence over the considered future timeframe. Let t be a consecutive yearly time steps of $[1,150]$ with $t_P = 51$ as the present time. Let also m be a period into the future from t_P representing a waiting time before a random simulated first flood occurs. As defined previously, PRO strategy implies deciding upon flood intervention at t_P while RCT strategy is triggered after the first flood occurs. As to allow valid comparison between PRO and RCT strategy, decisions of RCT will only be undertaken when the extreme flow exceeds the status-quo threshold at a point of time within a waiting period of 75 years. This corresponds to the fact that a later investment would not provide sufficient discounted benefit (O'Connell et al., 2010). Therefore, the time limit for RCT strategy to be valid is represented by $t_P + m = 75$. For both strategies, the construction of flood defence is assumed to occur in the year of intervention.

In the case of decisions based on estimated parameters, PRO strategy will use $[1, t_P)$ historical records to estimate the parameters of the PDF for the risk estimation. The historical records are set

to comprise of 50 years annual maxima flows. For the UK, the period is reasonable based on a typical length of available flow record from gauging stations across the UK (O'Connell and O'Donnell, 2014). 50 years of records is also said to be a reasonable number of flood samples for analysis of extreme flow series (Kundzewicz and Robson, 2004). RCT strategy, given the waiting time, poses advantage of having extra information to fit the PDF distribution that leads to better estimation. The historical data used in RCT strategy PDF estimation corresponds to $[1, t_P + m)$.

In executing the risk-based optimization in the decision-making process of PRO or RCT strategies, it is assumed that the discount rate r is 3.5% throughout the design life period. The 'historical' records ultimately will yield an estimated optimal protection from the search operation. The estimated design protection in flow discharge is then brought forward to calculate the annual damage over the appraisal period of $[t_P, 150]$ (i.e. 100 years) using the 'future' series. For PRO strategy, any 'future' annual extreme flows that exceed the protection design discharge ($q > \hat{q}$) are assumed to cause flood damage. As for RCT strategy, the first flood occurs waiting time is assumed to cause flood damage. Furthermore, the remaining 'future' annual maxima is assumed to cause damage when the estimated optimal protection of RCT intervention is exceeded. Hence, in computing the damaging effect, flood damage is computed in two phases of the appraisal period; one is during the waiting time when simulated extreme flows exceed the status-quo discharge threshold ($q > q_o$) and another is after the intervention ($q > \hat{q}$). The flood damage is calculated empirically using Equation 4.5. Having the information on intervention costs and damage of do-nothing and with-project over the appraisal period, the economic metrics as given in Section 4.2.7 can then be calculated for each strategy. The calculation process is repeated for each simulation.

A detailed workflow that distinguishes the process of obtaining the economic performance of decisions associated with the respective strategies is illustrated in Figure 4.2. This workflow encapsulates the imprecise knowledge that a decision makers have when performing the risk-based optimization. Some boxes in this figure are numbered to attribute them to the numbered boxes in Figure 4.1.

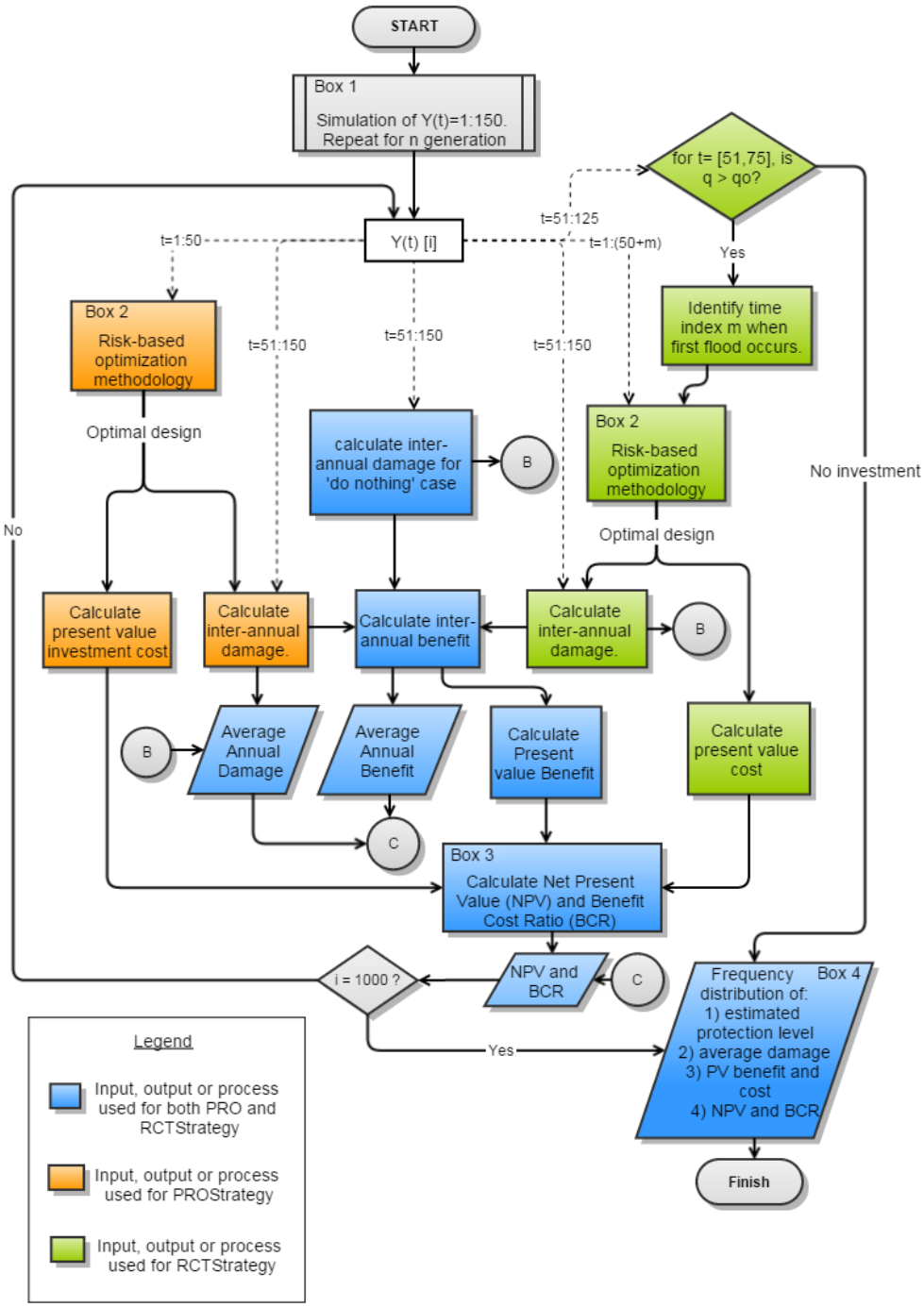

Figure 4.2: Detail steps for uncertainty computations of PRO and RCT economic performance for 1000 simulations.

4.5 Application

This section presents the application of the designed methodology using partial information of a real case study to parameterise the modelling components of the decision analysis. The information includes available historical time series of river flow discharges and spatial properties of an area downstream of the gauging site. The historical records and the spatial properties of the area were

used to establish a realistic limiting PDF and to configure the damage and cost functions for the case study, respectively. A brief background of the time series used in this study is presented in Section 4.5.1. Section 4.5.2 will test the independency of the time series and fit a probability distribution to the data. The simulation of the IID and persistent series are presented in Section 4.5.3, followed by configurations of the damage and cost functions in Section 4.5.4.

4.5.1 Background of referred historical records

This study uses daily mean of October 1883 to September 2011 from the Thames at Kingston gauging station flow records (Centre for Ecology and Hydrology, 2014). The annual water years (Oct to Sept) were extracted and used to obtain a limiting distribution for the simulation study (see Section 4.6.1 for the model fitting). The Thames at Kingston historical flow records is widely used in literature for various research purposes and examinations. Its long historical record is a vital source of information for hydrologists to understand the many aspects of the river system and incurred changes (e.g. Marsh and Harvey, 2012).

In this study, the available long time series is crucial to represent the limiting distribution for the simulation. The unnaturalised flow records were used considering that frequency and magnitude of extreme flows are of important characteristics when designing engineering structural measures. There are studies that used naturalised discharges to understand the behaviour of 'unaffected, natural' flow series. In the latter case, the annual maxima time series of the Thames at Kingston has shown to exhibit no significant trend (Marsh and Harvey, 2012).

4.5.2 Independence and goodness-of-fit tests

The application of the decision analysis to the stationary case requires identification of suitable GEV distribution parameters for the initial underlying probability distribution. The parameters are used to simulate multiple flow series to reflect the natural variability. As mentioned in detail in Section 4.3, series of IID characteristic are generated using these parameters. As for series with persistence, mean and variance of the initial distribution are used to ultimately determine the GEV distribution parameters of ε before the series are generated.

Having the long time series of extreme flows from the Thames at Kingston as the basis for the initial GEV distribution, an important first step is to test whether the series is inherently independent and better represented by a stationary distribution model. An independent statistical test was therefore applied to the series using Ljung-box statistical method (Cryer and Chan, 2008) whilst a typical goodness-of-fit test was used for the model fit.

The Ljung-box statistical method tests the magnitude of correlations as a group, not at individual lags of the given series. The null hypothesis for the test is defined as the data being independently distributed up to order m, where m refers to lag of the series. The null hypothesis cannot be rejected if the value of the test statistics is higher than the 'significance level'. The returned p-values for selected lags and a significance level of 5% are given in Table 4.2. As can be seen, even for lag 1 the p-value is significantly higher than 0.05, and increases for larger lags. The results strongly suggest that the data is independently distributed.

Table 4.2: Summary of Ljung-Box test result for Thames at Kingston annual maxima flows.

Lag, K	p-value
1	0.1438
2	0.1642
3	0.2738
4	0.4209

Using L-moments as given in Section 4.2.1, the GEV distribution with the estimated parameters was fitted to the extreme flow series data. The parameter estimation was undertaken using an in-built L-moments function in R (Asquith, 2012). The estimated PDF is depicted in Figure 4.3 alongside the goodness-of-fit of its CDF. The parameter values are also provided in the PDF figure. The goodness-of-fit of the CDF represents a comparison between the estimated quantiles (pink dashes) with those from observations (black dots). A good fit can be observed from the figure suggesting that the GEV distribution parameters are suitable as the initial underlying GEV distribution parameters.

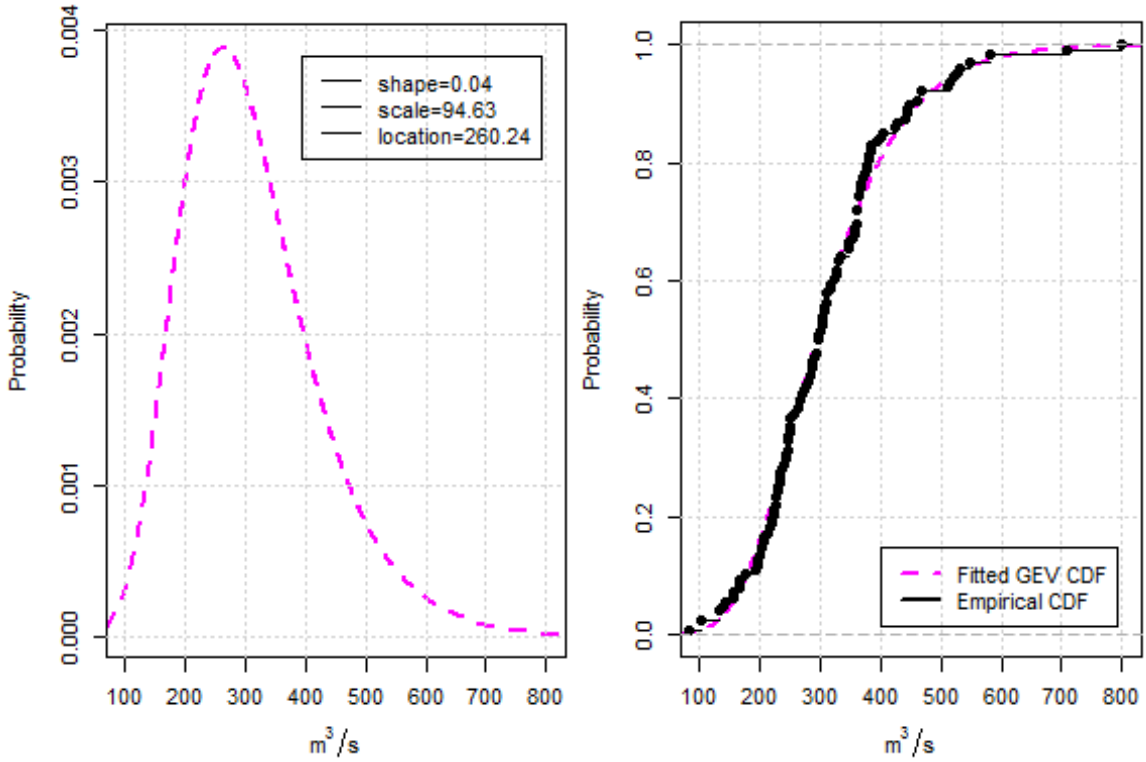

Figure 4.3: PDF and CDF of fitted GEV distribution for Thames at Kingston annual maxima flows.

4.5.3 Simulation of flow series

In search of the GEV parameters of ε for the persistent series simulation, the method described in Section 4.3 was executed. Two scenarios of persistence were chosen; autocorrelation of 0.2 and 0.4. Initial investigation indicated that a relatively higher magnitude for $\emptyset$ (i.e. higher than 0.4) result in some generated flows to be of negative values. In the remainder of this Chapter, the resulting outcomes associated with the simulated IID series and the two persistent scenarios will be referred as P1, P2 and P3 respectively.

Histograms of 10,000 mean flow discharge from 150 years simulated annual maxima series of the three scenarios are illustrated in Figure 4.4 to visualise the effects of autocorrelation on the variability of the flow series. As expected, P3 scenario shows the highest variance, followed by P2 and P1. For flow series with higher persistence, the resulting variability of the generated flow series tends to be greater. 1000 sets of the simulated series of each scenario were subsequently brought forward for the exploration of the decisions performance. The results are presented in Section 4.6.

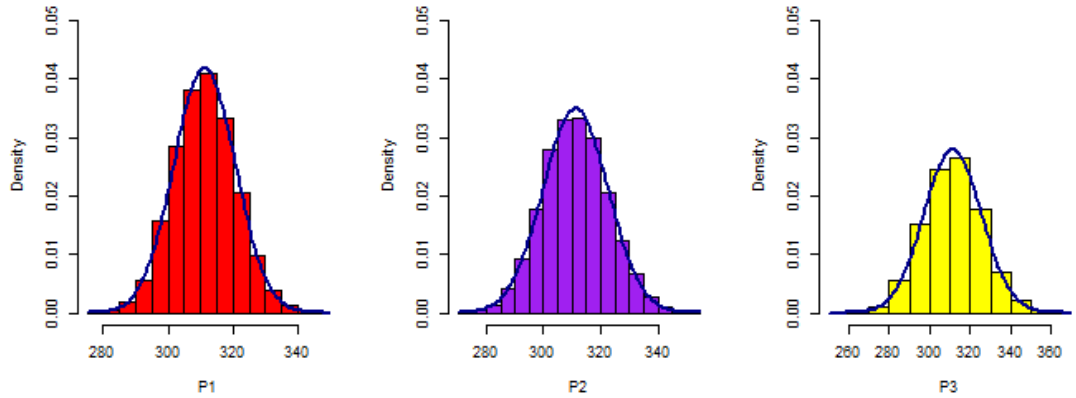

Figure 4.4: Histograms each with 10,000 values of average flows over 150 years simulated AM flow series. IID *(red),* $\emptyset = 0.2$ *(purple) and* $\emptyset = 0.4$ *(yellow) scenarios.*

4.5.4 Configuration of damage and cost functions

A flood risk system of the downstream area of the Thames at Kingston gauging station was used to represent the source-pathway-receptors components for this specific study. The spatial features were simplified and used to configure damage and cost functions. The required input variables to establish the functions are related to the variables that govern the stage-discharge function denoted in Equation 4.4. Other required inputs are the constants of the damage and cost function. .

Table 4.3 provides the assigned values for the configuration of the damage and cost functions. The river slope was assumed based on a typical slope of most rivers in the UK (i.e. Ward, 2000). The roughness coefficients of the river and the neighbourhood area assigned based on survey evidence given in the CEH website (2014) and satellite imagery, with reference to the typical roughness coefficients suggested in Knight et al. (2010). Approximate widths of the river and the floodplain were extracted by overlaying available aerial map and geospatial information in ArcGIS (ESRI, 2012). q_o was chosen based on a given peak over threshold discharge of the gauging station from the CEH website (2014).

Substituting the values into the functions, Figure 4.5 shows the range of flood damages and investment costs against extreme flows and protection designs, accounting a number of possible constant values of A, B and a. Compared to a documentation related to real evaluation of costs of options from the Environment Agency (April 2010), which estimated approximately £3.5 million per annum of capital and maintenance costs of community-based flood protections, the estimated costs here are realistic. The sensitivity of the functions, however, indicates the extent to which the

values of the constants may influence the results of the analysis. For this study, only one value of each constant were brought forward into the decision analysis to focus on the sensitivity of the economic performance caused by the different time-independent strategies and persistent flow series. It is important to note that the constants A, B and a are highly uncertain and a more accurate representations of damage and cost functions require further refinement.

Table 4.3: Summary of inputs for the cost and damage functions.

Constants	***River***	***Property area***	***Source***
Roughness Coefficient, n	0.05	0.03	(Arcement and Schneider, 1984)
Slope, S_o	0.0001		(Knight et al., 2010)
Width, w	100 m	900 m	Approximation from aerial map
Status-quo of flow threshold, q_o	300 m^3/s		-
Cost constant, A	1,100,000		-
Cost constant, B	4		-
Damage constant, a	700,000		-

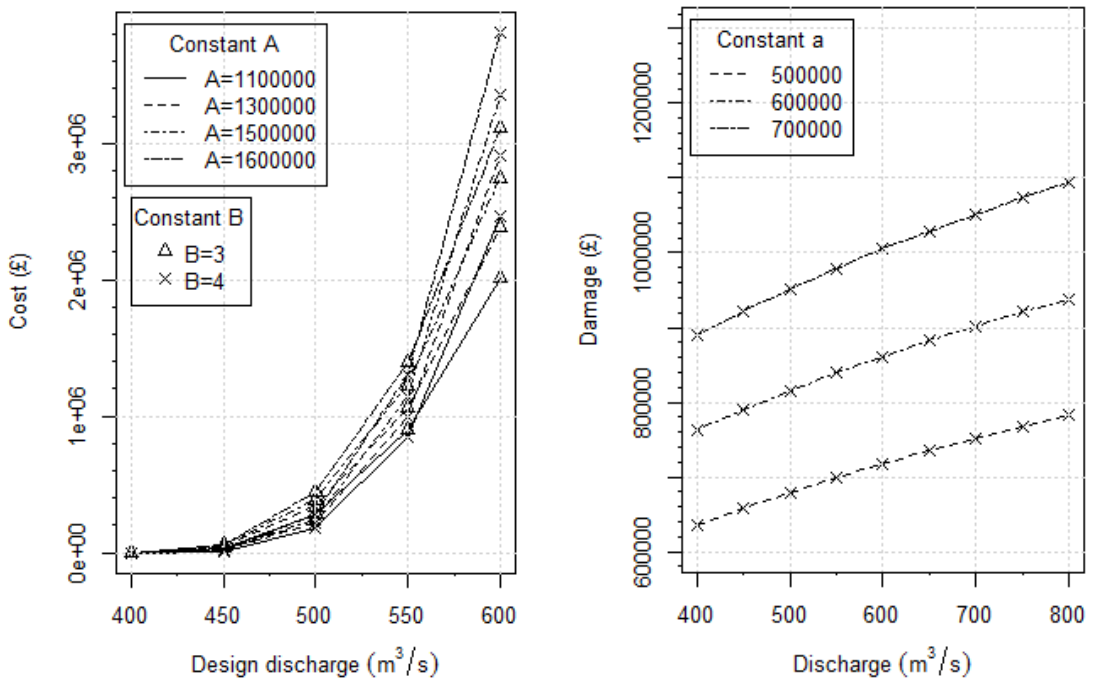

Figure 4.5: Estimated investment costs and flood damages against a range of flow discharges. Different curves represent the different constants used in estimation.

4.6 Results and discussion

This section provides results from the application of the decision analysis framework. The bias in PDF estimates caused by sampling error and persistent flow series are presented in Section 4.6.1, followed by the effects of persistence on do-nothing damage calculation in Section 4.6.2. The economic performance that are influenced by the deliberate variety of the flow series are presented in Section 4.6.3. The preferred strategy between PRO and RCT based on a benefit-cost index is presented in Section 4.6.4.

4.6.1 Bias and error calculation

The 10,000 generated flow series of 150 years annual maxima of P1, P2 and P3 scenarios in Section 4.5.3 were first divided into three classes of different sizes of 'historical' records; 50, 75 and 100 years of sample size, respectively. GEV distribution model with parameter estimations by L-moments was fitted to each of the simulated series of each case. The returning estimated GEV parameters of each case were then used to calculate the statistical characteristics of the samples; L-CV and λ_1 through Equation 4.1 and 4.2, and the results are then grouped according to the 'historical records' and scenarios. The dispersion of the L-CV values was measured using the SD function whilst the estimated λ_1 is compared with the known $\widehat{\lambda_1}$ (i.e. from the perfect information) using the RMSE.

The results in Figure 4.6 show that bias is higher for the smaller sample sizes in both L-CV and λ_1 estimates. Furthermore, it is steadily increases from higher persistent scenarios. The results are consistent with findings from previous studies that lead to the importance of sample size in statistical model fitting (e.g. Kumar and Chatterjee, 2005;Strupczewski et al., 2011).

4.6.2 Effects of persistence to flood damage

To have insights on the relative range of potential flood damages, the multiple sets of the simulated AM simulations of P1, P2 and P3 were individually fed into the damage function of do-nothing case derived in Section 4.5.4. The annual flow of damages from each 10,000 input series were averaged over the 150 years respectively. The resulting frequency of averaged damage for the entire

simulations with respect to each scenario was then distributed in a histogram against a range of damage magnitude (Figure 4.7).

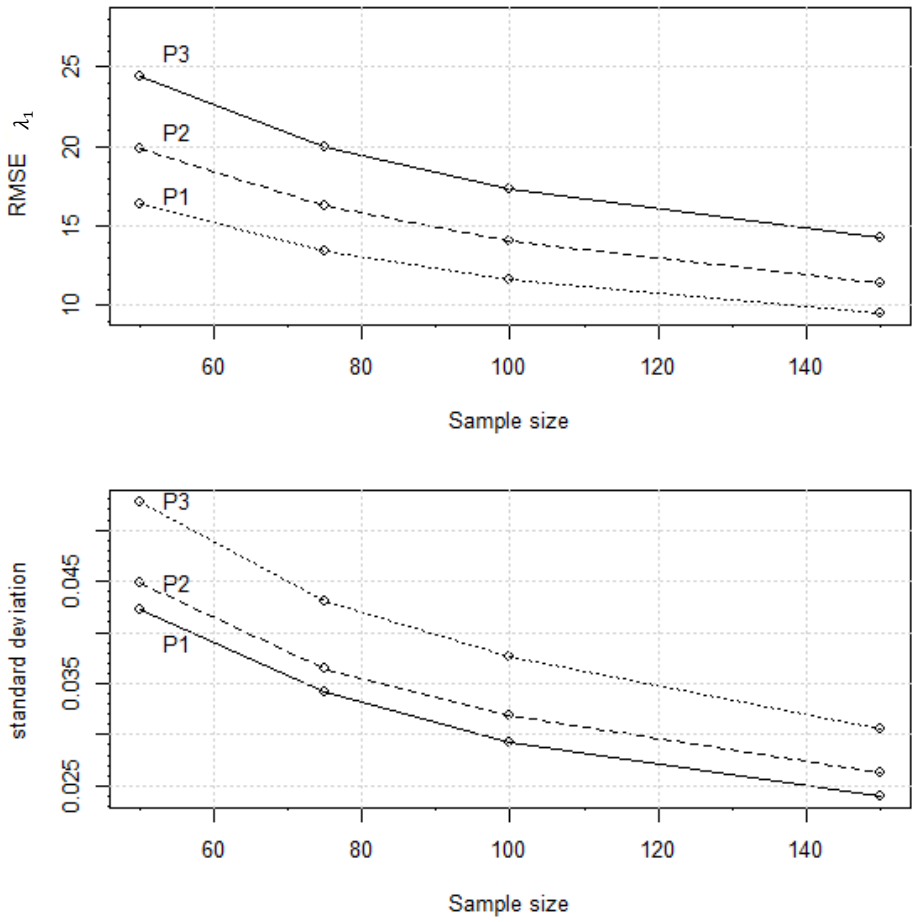

Figure 4.6: Standard deviation of estimated L-CV and RMSE of the estimated L-location across different sample sizes and scenarios.

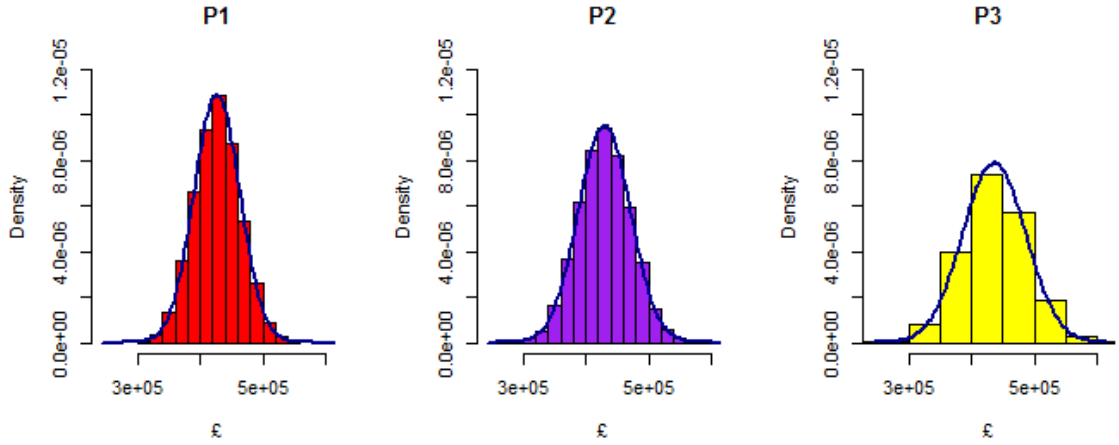

Figure 4.7: Histograms each with 10,000 values of average damage over 150 year of do-nothing case. IID *(red),* $\emptyset = 0.2$ *(purple) and* $\emptyset = 0.4$ *(yellow) scenarios.*

A higher number of instances from lower and higher average damages can be seen from P3 followed by P2 and P1. The behaviour suggests a more frequent generation of 'flood rich' and 'flood poor' periods from the higher persistent flow series. These illustrations are consistent with the tabulated results in Figure 4.4 and Figure 4.6.

4.6.3 Effects of sampling variability and persistence to decisions performance

This section presents the outcomes of the simulated decision makers' risk-based optimization operation for PRO and RCT strategies under each considered scenario. The focus is to visualize the influence of flow variability due to the combined effects of sample size and persistence. The workflow depicted in Figure 4.2 was therefore applied using 1000 generated flow series from Section 4.5.3. Through the process, the intermediate economic metrics (i.e. residual damage, cost and benefit) and the ultimate economic performance in terms of BCR and NPV of decisions were calculated. They are presented and discussed in the following paragraphs.

The distributions of the estimated optimal protections associated with the different degree of persistence, respectively, are presented in Figure 4.8. From the box-whisker plots of PRO and RCT strategies, it can be seen that the median of each distribution associated with scenarios of different persistence differs slightly. Comparisons of medians of design protections of PRO and RCT strategies under the same persistence scenario show that the design protection under IID scenario is indistinguishable, whereas higher median values of RCT strategy as compared to the median values from PRO strategy can be seen under persistence scenarios of P2 and P3, respectively. Compared to a perfect information of the underlying distribution, i.e. represented by the median optimal protection of IID scenario, this indicates an inclination to over-estimate the optimal protection when the degree of persistence in flow series is greater. Furthermore, the uncertainty range can be seen smaller for decisions under IID scenario due to the agreement with the decision makers' assumption in the decision making process. Whilst under the P2 and P3 scenarios, the uncertainty range can be seen increases, owing to the greater variability imposed by the persistent flow series.

The risk-based optimization methodology trade-off the costs and benefits of the range of design protections considered. This means the magnitude of cost and damage functions (i.e. the latter determine the benefit) strongly affect the estimated optimal protection. If the relative magnitude of costs is lower than the one that is used here, the estimated optimal protection might be higher. The same goes to the relative magnitude of the damage. This is discuss in more detail in Section 7.5.

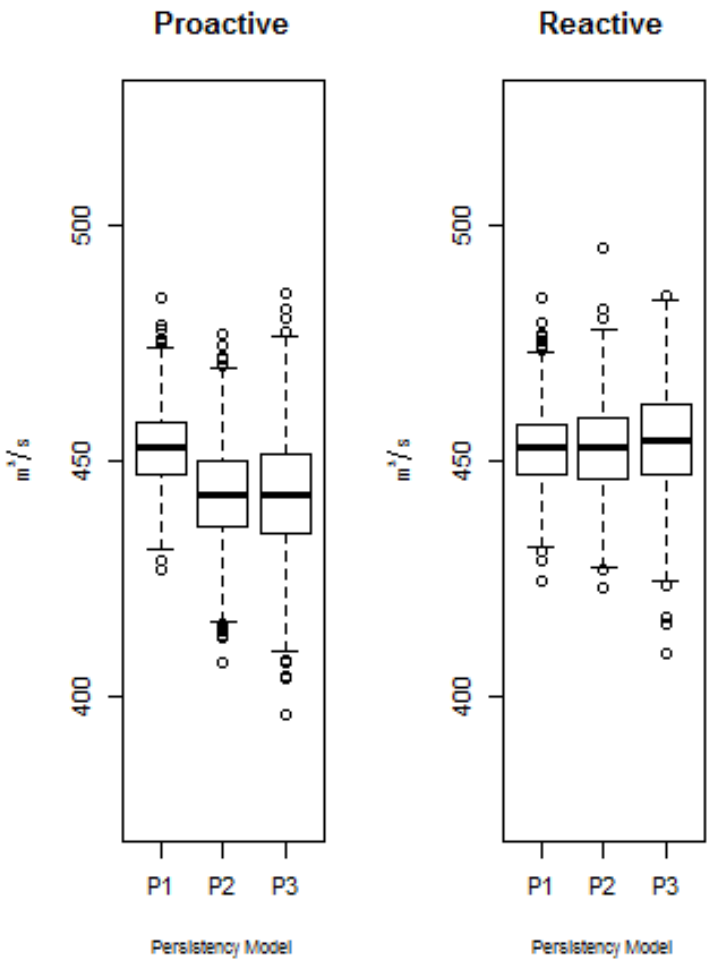

Figure 4.8: Box and whisker plots of estimated optimal protection level for PRO and RCT strategies across 1000 simulations of different scenarios.

The corresponding average damage over the 100 years appraisal period of each series are displayed in Figure 4.9. The figure clearly shows that the damage of the do-nothing case is the greatest and the RCT action poses a slightly greater expected damage as compared to the PRO action. The greater expected damage from RCT intervention is a result of the damage incurred due to the waiting time.

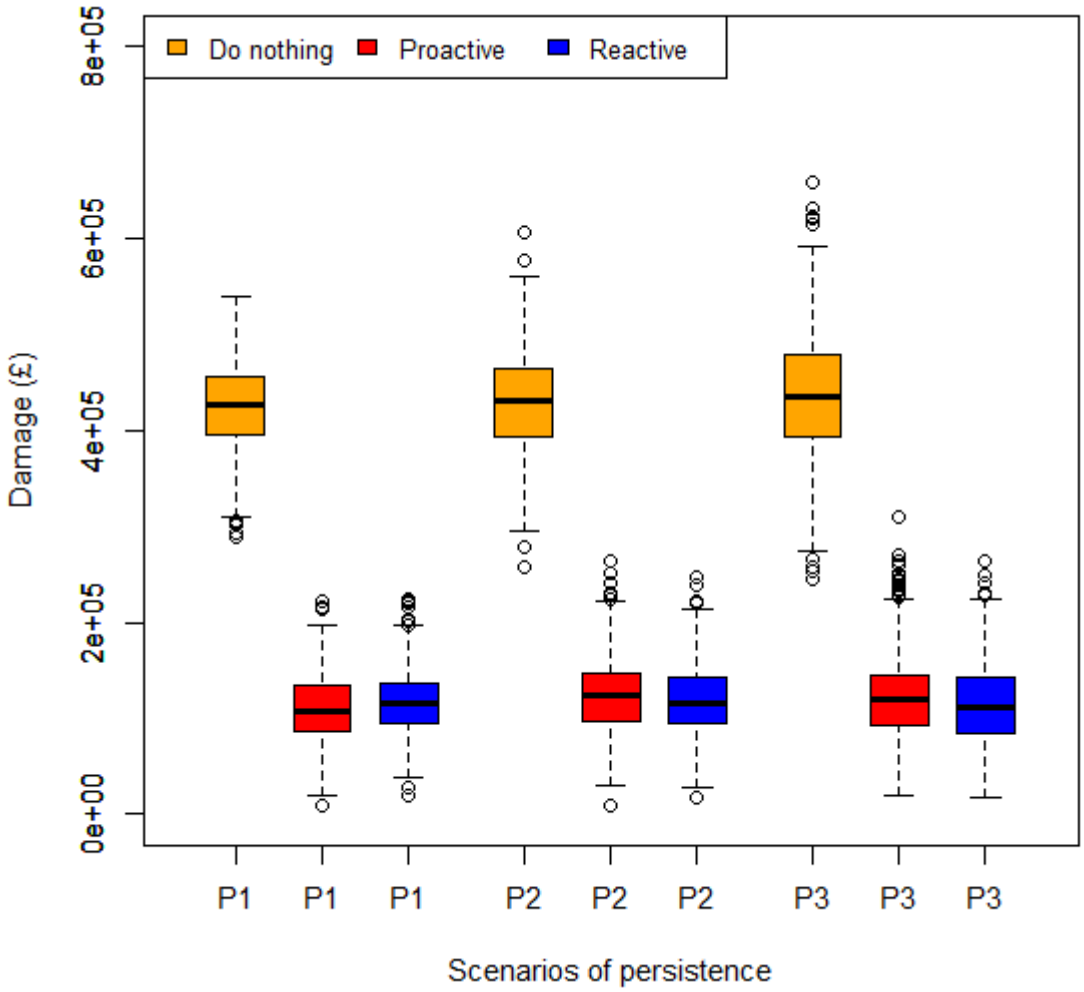

Figure 4.9: Box and whisker plots of mean annual damage of do-nothing, PRO and RCT strategies for 1000 simulations, respectively.

The distributions of benefits and costs in present value (PV) for PRO and RCT strategies for each scenario were subsequently calculated using the annual damage of do-nothing and with-project, respectively. The results are displayed in Figure 4.10. The PRO strategy, although is expected to yield higher benefits as a result of an early intervention as compared to the RCT strategy, shows only a minor difference of the expected PV benefits compared to that of RCT strategy across all scenarios. To some extent, this may be due to the smaller sample size used in PRO decision making that contributes to a higher estimation error and leads to the PV benefits being compromised. The PV costs also show a minor difference between the competing strategies, similar to the difference in PV benefits. A slightly greater variance for PRO strategy and higher persistence can be found from the results due to the greater instability of estimates from smaller sample size and from greater persistence as shown in Table 4.4.

The distribution of PV benefits and PV costs are also dependent on the relative year of intervention between PRO and RCT along the timeframe. Plots that show the time occurrences of interventions over the appraisal period are useful to explain the previous findings. Tabulated investment costs associated with PRO strategy (blue dots) and RCT strategy (red dots) over a 30-year appraisal period is depicted in Figure 4.11. The time window of 30 years of appraisal period is selected to magnify the difference since all RCT interventions happened to occur within this period regardless scenarios.

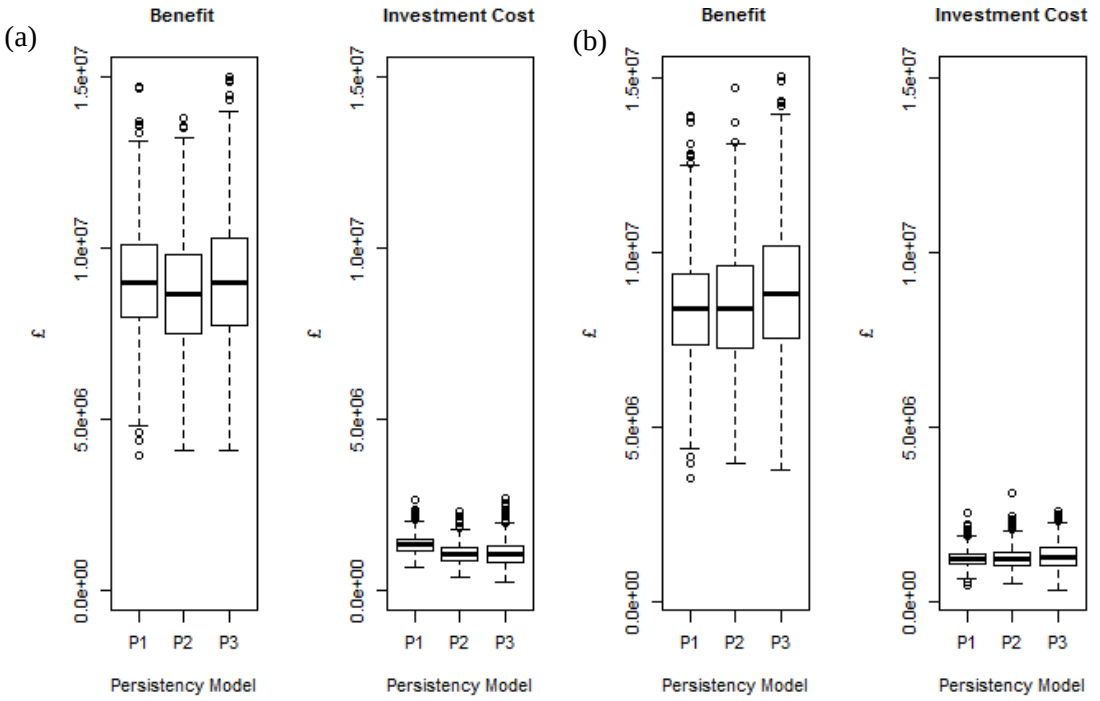

Figure 4.10: Box and whisker plots of PV benefits and PV costs of different scenarios of (a) PRO strategy and (b) RCT strategy for 1000 simulations, respectively

The investment costs of PRO interventions are scattered only in the first years of all three scenarios due to the fixed year of intervention. RCT interventions, on the other hand, are scattered from year 2 onwards and can be seen faded out after the first 10 years. The early interventions of RCT strategy indicate a high vulnerability condition due to a lower magnitude of q_o as compared to the annual maxima flows, and due to the hydraulic properties of the flood risk system. The clusters of RCT interventions within the first 10 years of the appraisal period implies that the size of the 'historical' records used in the PDF estimation of RCT interventions is not significantly different to PRO strategy. The small difference explains the minor difference of the resulting PV costs and PV

benefits between RCT and PRO strategies across all scenarios. It is also notable from the figure that RCT intervention occurrences fade out earlier in P1 as compared to P2 and P3. The finding suggests that an underlying higher persistence will lead to a higher variability of investment costs, such that presented in Figure 4.10.

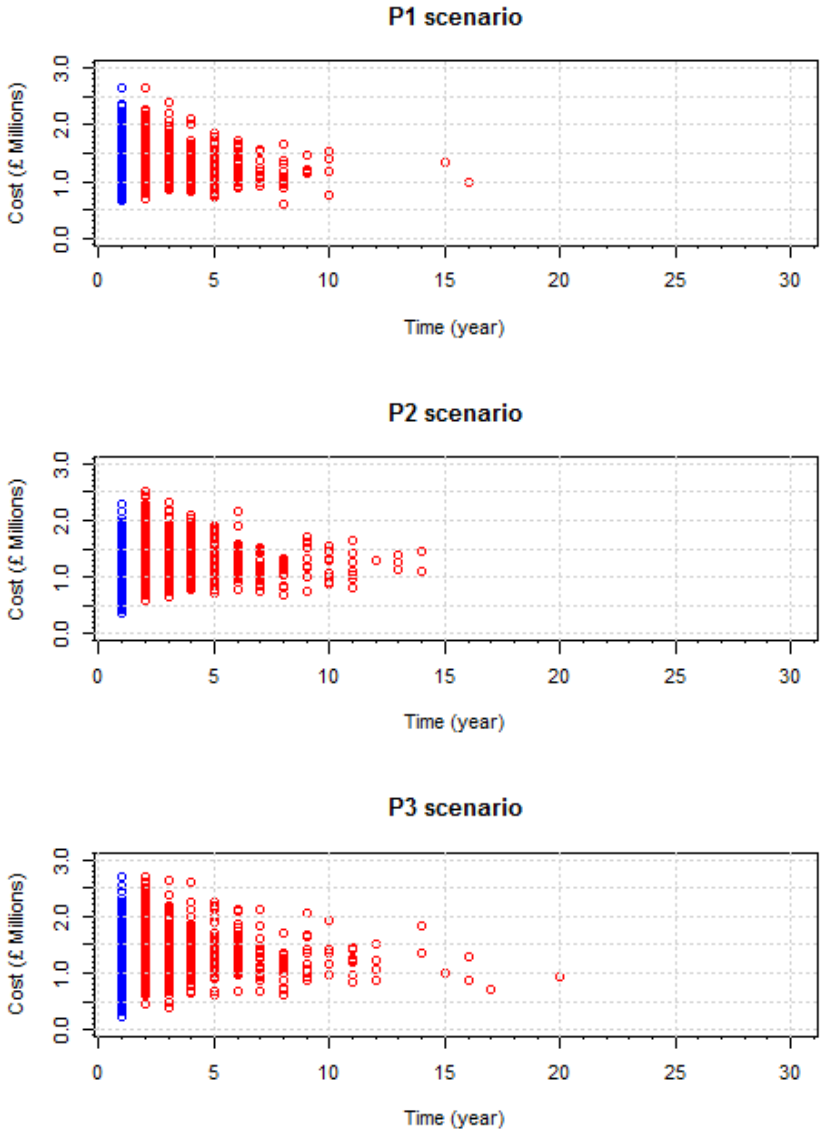

Figure 4.11: Scatter plot of PRO (blue dots) and RCT (red dots) across 1000 simulations of different scenarios. (a) P1 scenario (∅=0), (b) P2 scenario (∅=0.2), and (c) P3 scenario (∅=0.4).

Figure 4.12 displays box-whisker plots of NPVs and BCRs calculated from the PV benefits and PV costs of each simulation set. In both strategies, the variance of the economic indices can be seen greater for scenarios with higher persistence magnitudes, which in agreement with the previous findings. In terms of the expected values, the PRO strategy yields higher medians as compared to

the RCT strategy under all considered persistence scenarios, but more apparent from P3. The higher NPV and BCR of the PRO strategy is due to a higher reduction in damages from the PRO strategy that outperforms a lower costs from RCT strategy. Between NPV and BCR outcomes, NPV shows a more stable distribution as compared to that of BCR, consistent with what is highlighted in Michael (2011).

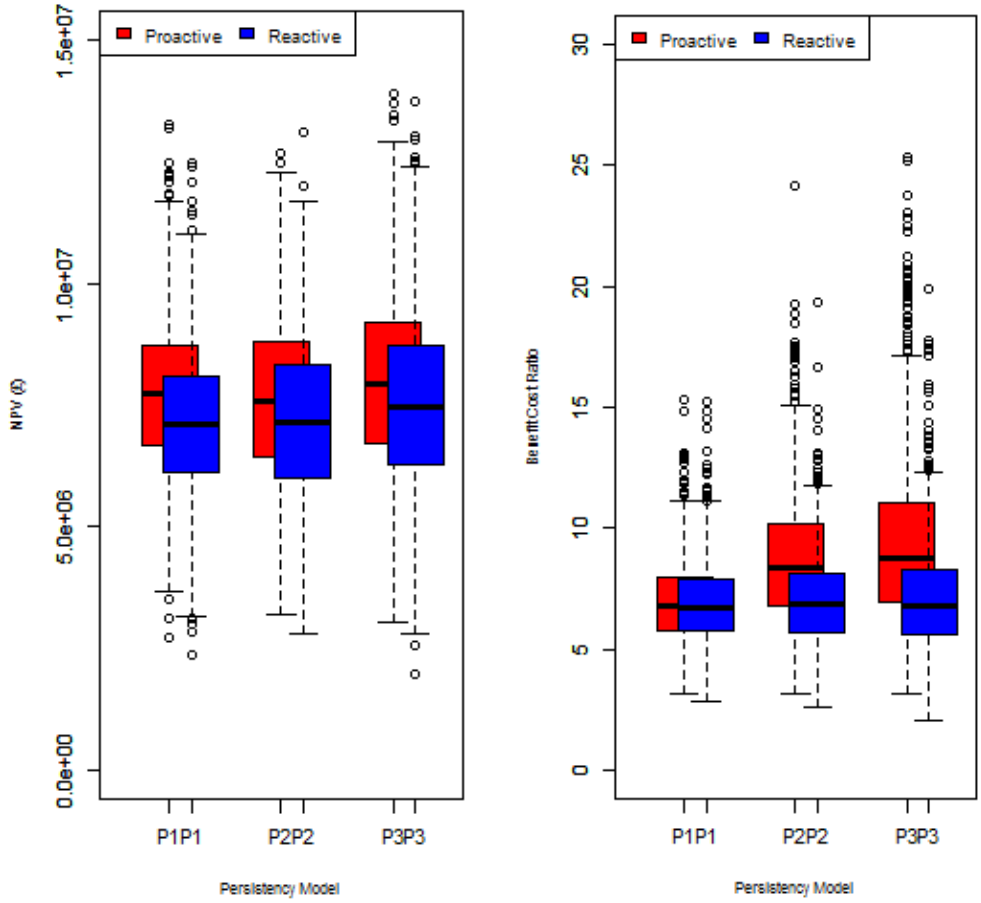

Figure 4.12: Box and whisker plots of NPV and BCR of PRO and RCT strategies across 1000 simulations of different scenarios.

4.6.4 Analysis of ultimate preferred strategy

This section proceeds to investigate the performance of decisions of the PRO and RCT strategies by accounting the range of possible costs and benefits associated with the decisions that have been previously quantified. Using the statistical information of the dispersions, a benefit-cost index $\beta_{B/C}$ introduced by Ayyub (2014) was employed to seek for a preferred strategy. The benefit-cost index is a powerful tool that accounts the randomness of the possible benefits and costs of the considered strategies to return a comparable index of the economic performance associated with each strategy.

To compute the index, the distributions of benefits (B) and costs (C) of the strategies are assumed to follow a lognormal distribution that can be denoted as Equation 4.15 (Ayyub, 2014, pg 453). The mean and coefficient of variance associated with the strategy were computed arithmetically from the simulation outcomes.

$$\beta_{B/C} = \frac{\ln\left(\frac{\mu_B}{\mu_C}\sqrt{\frac{\delta_C^2+1}{\delta_B^2+1}}\right)}{\sqrt{\ln\left[(\delta_B^2+1)(\delta_C^2+1)\right]}} \tag{4.15}$$

where,

μ_B = the mean of benefit of the intervention.

μ_C = the mean cost of the intervention.

δ_B = the coefficient of variation of the intervention benefit.

δ_C = the coefficient of variation of the investment cost.

Table 4.4 provides the mean and standard deviation of the PRO and RCT strategies of all scenarios that were used in the calculation, respectively. The table also shows the resulting metrics from the application. A preferred strategy for each scenario can be identified based on the highest index value between the competing strategies.

As clearly shown in the table, the PRO strategy returns a higher metric as compared to the RCT strategy, which is consistent across all persistence. The results also indicate that the confidence to select the PRO strategy as compared to the RCT strategy is more evident in a strong stationary condition (i.e. P1) and less in a relatively weaker stationary condition (i.e. P3).

The benefit-cost index considering the alternative strategies of proactive and reactive in reducing flood risk proves to be useful. The end results provide quantitative justifications on the preferred strategy, accounting the probabilistic outcomes of the economic performance. The findings suggest that a proactive response to reduce flood risk should be the main agenda for a greater economic net benefit even with relatively limited information in the risk estimation. The results indicates that this holds true regardless the level of persistence in the extreme flow series. .

Table 4.4: Summary of benefit-cost index appraisal for PRO and RCT strategies for the different scenarios.

Proactive				
Economic indices (£)	Statistics	P1	P2	P3
Benefit	Mean	9,023,255	8,677,750	9,046,176
	SD	1,657,815	1,711,332	1,855,431
Cost	Mean	1,336,297	1,055,683	1,064,134
	SD	266,490	277,222	347,989
Performance index ($\boldsymbol{\beta_{B/C}}$)		7.12	6.55	5.74
Reactive				
Economic indices (£)	Statistics	P1	P2	P3
Benefit	Mean	8,389,742	8,430,297	8,823,664
	SD	1,605,508	1,733,934	1,933,721
Cost	Mean	1,249,567	1,247,257	1,307,152
	SD	259,552	310,248	374,572
Performance index ($\boldsymbol{\beta_{B/C}}$)		6.82	6.02	5.43

It is important to note that although this study proves that the proactive response is a better choice compared to the reactive response to flood risk for all considered persistent scenarios, O' Connell (2010) in their study has found that the reactive strategy outperformed the proactive strategy in terms of the average net benefit at a very high level of persistence. The contrast findings may have been influenced by the distinct persistent model representation and the parameterization of the underlying distribution for the simulation of persistent series.

It is also found that the relative difference of outcomes across the different persistent scenarios are small, suggesting that the conventional assumption of IID in flood frequency analysis is still valid under persistent conditions. The quantitative findings support what have been mentioned in Hosking (1997) and Coles (2001) and further highlights the advantage of simulation study. Furthermore, the study shows that the preference of the proactive strategy over the reactive strategy is justified only with a small margin, indicating the insignificant effect of the sampling error and also the robustness of the risk-based optimization approach in flood risk management decision-making process.

4.7 Conclusion

The risk-based decision analysis framework has successfully been demonstrated in this Chapter. The study has advances the work of O'Connell et al. (2010) by exploring not only the expected value of outcomes from the simulation, but also provide quantitative evidence on the effects of the cascading uncertainty in decision making related to partial information and persistent series. Moreover, the application of the cost-benefit index as demonstrated in this study reveals that the index can be a powerful tool in providing insight into the preference ordering of strategies.

The decision analysis has proven to be useful in providing invaluable insight on the influence of uncertainty due to sample size and persistence. Valuable information especially in the form of quantitative and qualitative comparisons such as presented are essential in improving understanding in flood risk management decision making. Furthermore, the framework can be applied to similar case studies to suggest relevant and defensible action to be proceeded. Listed below are the findings related to the objectives defined earlier in this chapter.

1) Simulation methodology allows analysis to be undertaken probabilistically, accounting the influence of natural variability into the assessment. In this study, the variability in flow series is propagated into the economic performance, enabling a wide range of possible outcomes to be captured. The probabilistic outcomes were ultimately used in the benefit-cost index computation, which is a powerful tool that provides comprehensive insights on the relative outcomes of the alternative strategies.
2) The influence of bias and estimation error in the L-CVs' SD and L-locations' RMSE due to the sample size and persistent series were apparent from the intermediate economic performance and the NPV and BCR. The resulting uncertainty ranges of the economic performance provide additional information that might be more meaningful to decision makers and stakeholders as compared to the estimation bias and errors.
3) The results from the benefit-cost index computations indicate that the proactive adaptation is preferred as compared to the reactive regardless the degree of persistence.

The higher benefit of the proactive intervention, in this case, is justified although proactive approach comes with an expected higher cost and a greater sampling error.

The findings nevertheless are influence by the modelling and simulation set-up, and also the input data. The use of different constants and variables values for the participating functions might lead to a different findings. Similarly, a different records of annual maxima series for the GEV parent distribution might offer different results.

The decision analysis framework designed in this chapter focuses on stationarity of extreme flow distribution with emphasise on persistent flow series. As the thesis is also interested in exploring the effects of nonstationarity of extreme flow distribution to decisions performance, the framework presented in this chapter has provide an appropriate groundwork for further exploration. Adoption and further necessary refinement of the framework are undertaken in Chapter 5 to explore the effects of nonstationary underlying conditions additional to stationary conditions in the context of economic performance of flood risk management decisions.

Chapter 5 Simulation study part 2: Decision analysis in the context of nonstationary extreme flow distribution

5.1 Introduction

Chapter 5 advances the work from Chapter 4 to understand the possible consequences that arises from contrasting prediction of future flood probability in risk-based decision making. In particular, the chapter seeks to expand the flood risk decision analysis developed in Chapter 4 to incorporate nonstationary models. The main aim is to understand the relative decisions performance when adopting stationary and nonstationary models and the relative decisions performance considering a range of plausible future state. A simulation framework which includes a number of different pathways combining possible decision makers' model preferences in adapting to future flood risk and plausible future changes were developed.

Following the literature review in Chapter 2 and Chapter 3, and simulation study in Chapter 4, further refinement of the research objectives for this particular study are as follows:

1) To demonstrate the usability of the developed decision analysis framework for flood defence protection design in the context of nonstationarity.

2) To quantify the implication of differing projected risk against plausible future states.

3) To visualize the performance of flood protection decisions through uncertainty and sensitivity analysis of the stationary and nonstationary model choices and possible future states.

The chapter is organised as the following. Section 5.2 provides the extension of the decision-analysis framework of Chapter 4, which include some of the relevant approach when considering nonstationary models. Plausible pathways of decision making on flood protection and possible future scenarios with stationary or nonstationary underlying distributions are specified in the section. Section 5.3 describes two simulation set-ups developed for the study; (1) with uncertainty

consideration, and (2) without uncertainty consideration. The application of the simulation methodology along with the qualitative and quantitative results are provided in Section 5.4 accounting the relative implication of the stationary and nonstationary model choices and the range of possible future. Section 5.5 discusses and conclude the findings.

5.2 Development of a risk-based decision analysis framework considering nonstationary distribution

In exploring the performance of risk-based flood protection decisions, the decision analysis in Chapter 4 has emphasised on flow series with persistence. This chapter further looks into the implication of adapting to future change considering nonstationary prediction and possible underlying nonstationary distribution of future extreme flows. The concept of risk-based optimization in the decision analysis framework from Chapter 4 was again applied.

Three modules were designed incorporating predictive models that reflect decision makers' assumption on the future underlying distribution (i.e. stationary or nonstationary). Stationary or nonstationary possible actual conditions of the future were also incorporated. These modules, therefore, were designed to incorporate possible pathways decision makers might take in effort to reduce future flood risk (Figure 5.1). Within each Module, decisions performance against possible actual future states can be assessed, corresponds to each alternative pathway. All three modules assume decisions are made through the application of the risk-based optimization of flood protection.

The first and the second modules were designed to capture the implication of the alternative model choices (i.e. subjective uncertainty) in predicting the future state. Stationary and nonstationary models (second column in Figure 5.1) were individually employed to predict the probability of extreme flows for each module. With the assumption that the decision makers are proactively intervening to reduce future flood risk, the study simulates the decision-making process by applying the risk-based optimization, taking into consideration the investment cost and the estimated residual risk. Through the designed pathways, a stationary model is assumed adopted in the decision-making process in search for an optimal flood protection when an initially preferred nonstationary model

predicts a decreasing change (row 1 and 2, column 3 of Figure 5.1). On the contrary, when the fitted nonstationary model predicts an increasing change, the nonstationary model is assumed to be used. This is to reflect decision makers' rational approach in the sense that preventive action is still being undertaken despite the negative signal of change from the fitted nonstationary model. The first two modules also seek to examine the effects of natural variability (i.e. aleatory uncertainty) to the decisions performance. In accounting these uncertainties, the decision analysis framework of Chapter 4 illustrated in Figure 4.1 were employed. In each module, multiple possible AM extreme flows over the historical and design life period were simulated from a specific underlying distribution, and individually used within the decision-making process to return distributions of performance outcomes.

Note that the primary difference between the first and the second modules is the actual underlying distribution considered for the historical and the design life (refer column 1 Figure 5.1); Module 1 assumes a stationary underlying distribution, whilst Module 2 assumes a nonstationary underlying distribution. Whilst stationarity implies non-changing statistical characteristics of the extreme flow distribution, nonstationarity here is associated with the rate of change (u_1) of AM flows. A range of different rates of changes were included to examine and evaluated through sensitivity analysis within Module 2. This enables a deeper insight on the impact of a range of possible future changes to decisions performance.

The third module focuses on nonstationary underlying conditions, but isolating the uncertainty range in the simulation set-up. This means that the effect of the natural variability is neglected in the decision analysis and the primary focus is on the sensitivity of the economic performance of decisions when false prediction is made.

Apart from the designed modules, the decision analysis concerning nonstationarity was also applied using real historical records and climate model (CM) projections to examine the relative effects of using the two alternative sources of information. . For the historical records, the study employed the long time series of Thames at Kingston from the Centre for Ecology and Hydrology (2014), whilst the CM projections were taken from the projected future flows published in Prudhomme et

al. (2012). Similar to Module 3, the application of the decision analysis framework on the real datasets isolate the effects of natural variability and focuses on the sensitivity of the decisions performance of the alternative predictions. Therefore, direct comparison of the results with the ones from Module 3 can be undertaken.

Section 5.2.1 introduces the nonstationary GEV model, associated estimators and adopted model selection method employed in this study. Section 5.2.2 provides a brief explanation on the proposed risk-based optimization methodology concerning the alternative prediction and possible future of stationary and nonstationary conditions. The risk-based optimization employed in this study, although similar to the one used in chapter 4, has distinct formulations to accommodate the nonstationary model and computation of expected value. Section 5.2.3 further describes how the economic performance of flood protection decisions will be evaluated.

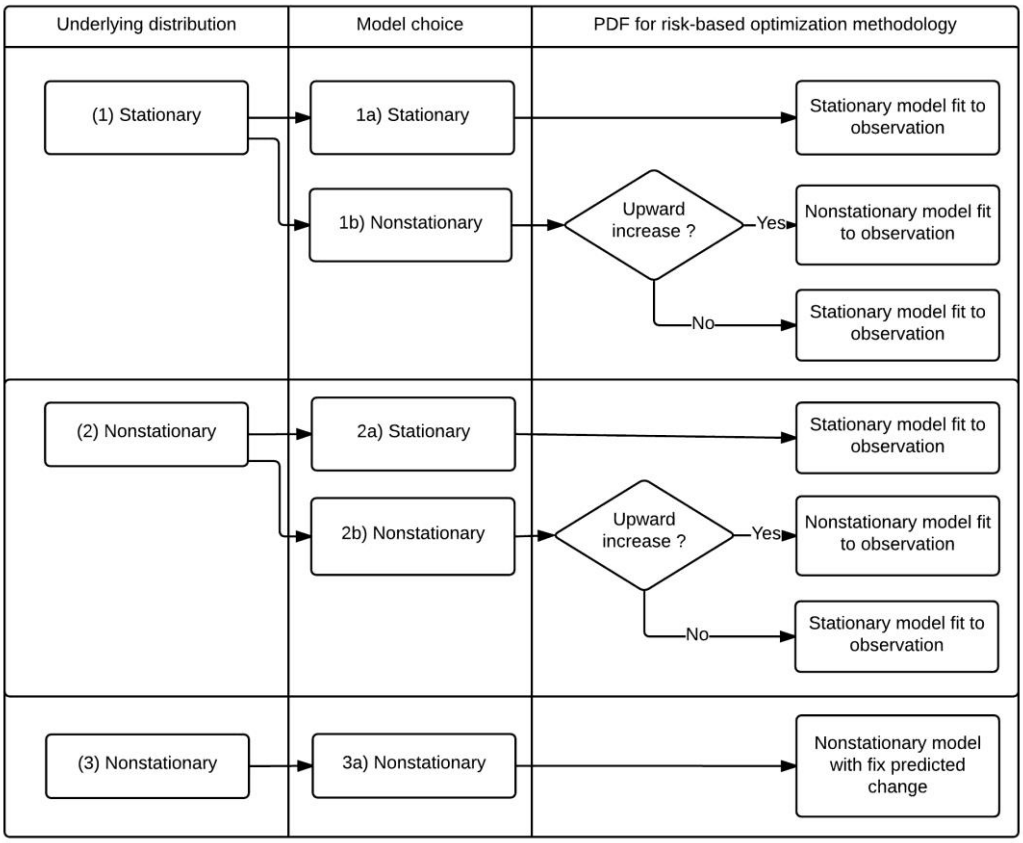

Figure 5.1: Three unique Modules that link the state of the underlying distribution, the model choice by decision makers and the final model used in the risk-based optimization.

5.2.1 Nonstationary GEV distribution, estimators and model selection method

The GEV model adopted in Chapter 4 has stationary characteristics where the parameters do not change over time. In this particular study, a time covariate was introduced in the location parameter to account for nonstationary in the underlying distribution. Using the same notation as used in Chapter 4, the nonstationary GEV model PDF and quantile computation are given in Table 5.1, where t represents the time covariate and u_1 as the rate of change in m^3/s/year. The upper and lower bound of the distribution are time-dependent, which depends on the characteristic of the location parameter.

Table 5.1: GEV distribution functions for nonstationary conditions.

Probability density function (PDF)	$y = \begin{cases} (1 - \frac{\kappa(x-u_t)}{\alpha})^{\frac{1}{\kappa}}, & \kappa \neq 0 \\ e^{-(x-u_t)/\alpha}, & \kappa = 0 \end{cases}$ $f(x\|u_t, \alpha, \kappa) = \frac{1}{\alpha} y^{1-\kappa} e^{-y}$
Quantile estimate	$x(F) = \begin{cases} u_t + \frac{\alpha}{\kappa_t}(1 - (-\log(1-F))^{\kappa}), & \kappa \neq 0 \\ u_t - \alpha \log(-\log(1-F)), & \kappa = 0 \end{cases}$
Location parameter	$u_t = u_0 + u_1 t$

The quantile estimate was used to simulate AM flow series for Module 1 and 2 through the Monte Carlo simulation methodology (Section 5.4.1), whilst the PDF was applied in each Module and real dataset case study to simulate decision makers' behaviour in estimating flood risk. Specifically for Module 1 and 2, the parameters of the PDF were estimated using the maximum likelihood (ML) method, which is compatible with nonstationary GEV models. The likelihood function with parameters $\boldsymbol{\theta}$ can be denoted as Equation 5.1.

$$\ell(X; \boldsymbol{\theta}) = \prod_{i=1}^{m} f_X(x_i|\boldsymbol{\theta}) \tag{5.1}$$

where m is the sample of AM series of river flow compiling observations $x_1, x_2, \ldots, x_m$ and $f_X(x_i|\boldsymbol{\theta})$ is the pdf of the variable X. $f_X(x_i|\boldsymbol{\theta})$ represents the GEV nonstationary distribution. To estimate the parameters, log-likelihood of the function is maximized with respect to parameter

vector by numerical solutions (Coles, 2001). An inbuilt 'extRemes' toolkit made available by Gilleland and Katz (2011) in R software was applied for the nonstationary model fitting.

In simulating the decision makers' behaviour of choosing between alternative models, this study isolates the typical rigorous step that is usually applied in flood frequency analysis. For example, Deviance statistics or Akaike Information Criterion (AIC) may be used to ascertain a preferred model. The pathways designed here directly incorporate the assigned model choice into the decision-making process (Refer column 2 Figure 5.1). While it is acknowledged that the use of the supporting tools such as the AIC might influence the final preferred model, the pathways were designed such that unnecessary complexity in the simulation study can be reduced.

The underlying distribution to represent the possible actual future conditions should be realistic. This requires a reasonable assignment of the distribution parameters for both stationary and nonstationary cases. In this case, the study applied the AIC on the available real dataset to yield a better representation of the statistical properties of the possible actual underlying distribution for the simulation study (demonstrated in Section 5.4.1). The AIC as derived by Akaike can be written as Equation 5.2 as presented in Salas and Obeysekera (2014).

$$\mathrm{AIC} = -2(llh) + 2K \tag{5.2}$$

where llh refers to the negative log likelihood estimated for a model fitted with K parameters. The best model will be selected based on a pairwise comparison of AIC scores of the competing models, whereby the model that returns a smaller AIC will be the preferred model (Katz, 2013).

5.2.2 Risk-based optimization methodology for nonstationary conditions

For each Module, it is assumed that the decision makers apply the risk-based optimization methodology in the decision-making process. The associated functions and search operation procedures of the risk-based optimization are exactly the same as the one used in Chapter 4 (see Section 4.2.6). The annual risk, damage and cost functions are also consistent with the ones from Chapter 4 (see Section 4.2.5, 4.2.3, 4.2.4). The only difference is that the configuration of the risk function in the present study considers for both stationary and nonstationary PDFs.

To distinguish between the estimation of risk according to the two conditions, let T be the possible underlying distribution. The annual risk R_t with respect to the distribution can therefore be denoted as R_{t_T}. For the stationary conditions, the distribution parameters are constant throughout the year. The nonstationary conditions is characterised by constant scale and shape parameters and a time variant location parameter, which is denoted as u_t. It is important to note that due to the time variant location parameter from the nonstationary PDF, the upper limit for the optimization operation is defined accounting the time covariates in the location parameter. A careful allocation of the conditional function of the operation, in this case the upper limit of the GEV distribution, would allow smooth runs of the simulations and help to reduce the computational time.

5.2.3 Evaluation of economic performance of decisions

Evaluation of the economic performance in this study focuses on the intermediate results, such as the total damages and total benefits of the decisions, and also on the final indicators; i.e. the NPV and BCR. Where the effect of natural variability is of concerns, the annual damages of with-project case will be calculated by comparing yearly-simulated AM flow series over the design life with an associated protection design discharge ($\hat{q}$). The total damages and total benefits can then be computed based on the series of annual damages associated with having the protection, and also based on a series of calculated annual damages of do-nothing case. Repeating this procedure for all simulated series from a specific scenario of future change will provide a unique distribution of the economic performance for the specific case (see Figure 4.2 for the workflow). Applying the routine for a range of future change scenarios will lead to multiple ranges of distributions of the economic performance.

Similarly where uncertainty range is of concern, the NPV and BCR computations can be applied for a range of decisions associated with a specific scenario of future change. The same routine as the one presented in Chapter 4 (Section 4.2.7), where the benefit is represented by the annual marginal damage (Equations 4.9 and 4.10), is similarly applied for this case. For the sensitivity analysis where effects of natural variability is neglected, instead of using the annual marginal damage, the annual benefits associated with the given scenario (B_{t_T}) are computed as the difference

between the associated annual risks of do-nothing ($R_{t_{T,q_o}}$) and the associated annual risks of with-project ($R_{t_{T,\hat{q}}}$). The risks should be quantified using the perfect information of future condition and the associated protection design discharge, i.e. based on the decision makers' prediction on future condition. Note that the annual risks will vary from year to year due to the time varying parameter values of the nonstationary distributions. With this specification, the NPV and BCR can be quantified as Equations 5.3 and 5.4. Notations used are the same as the ones used in Section 4.2.3, 4.2.4, 4.2.5, and 5.2.2.

$$NPV = \sum_{t=0}^{n_{str}} \frac{1}{(1+r)^t}\left(R_{t_{T,q_o}}(\mathrm{q}) - R_{t_{T,\hat{q}}}(\mathrm{q})\right) - \sum_{t=0}^{n_{str}} \frac{1}{(1+r)^t}(\mathrm{C}_t(\hat{\mathrm{q}})) \quad (5.3)$$

$$BCR = \frac{\sum_{t=0}^{n_{str}} \frac{1}{(1+r)^t}(R_{t_{T,q_o}}(\mathrm{q}) - R_{t_{T,\hat{q}}}(\mathrm{q}))}{\sum_{t=0}^{n_{str}} \frac{1}{(1+r)^t}(\mathrm{C}_t(\hat{\mathrm{q}}))} \quad (5.4)$$

5.3 Computation framework for capturing uncertainty range and sensitivity of outcomes

As defined within the list of objectives in Section 5.1, it is of interests of this study to have insights on the uncertainty range of the economic performance resulting from the combined influence of aleatory uncertainty and decision choice. At the same time, it is of interests to understand the sensitivity of the decisions outcomes by focusing on the full characteristics of the limiting distribution.

This section presents step-by-step workflows accounting these objectives. Figure *5.2*(a) replicates what has been demonstrated in Chapter 4 to capture the effects of natural variability, whilst Figure *5.2*(b) proposes a workflow to compute the economic performance of decisions without the uncertainty range. The work flow can be applied independently, but to examine the difference between the performance of flood protection decisions based on predicted risks and that of perfect information (the word 'perfect' hereafter will interchangeably referred to as 'actual'), results from the computation of the workflow in Figure *5.2*(b) can be overlapped with results from the workflow in Figure *5.2*(a).

In relation to the designed Modules (Figure 5.1), Module 1 and Module 2 attempt to capture both uncertainty and sensitivity of the results, hence the application of both workflows. Module 3 and the application to real data focuses only on the sensitivity of the results, hence the adoption of workflow without consideration of uncertainty.

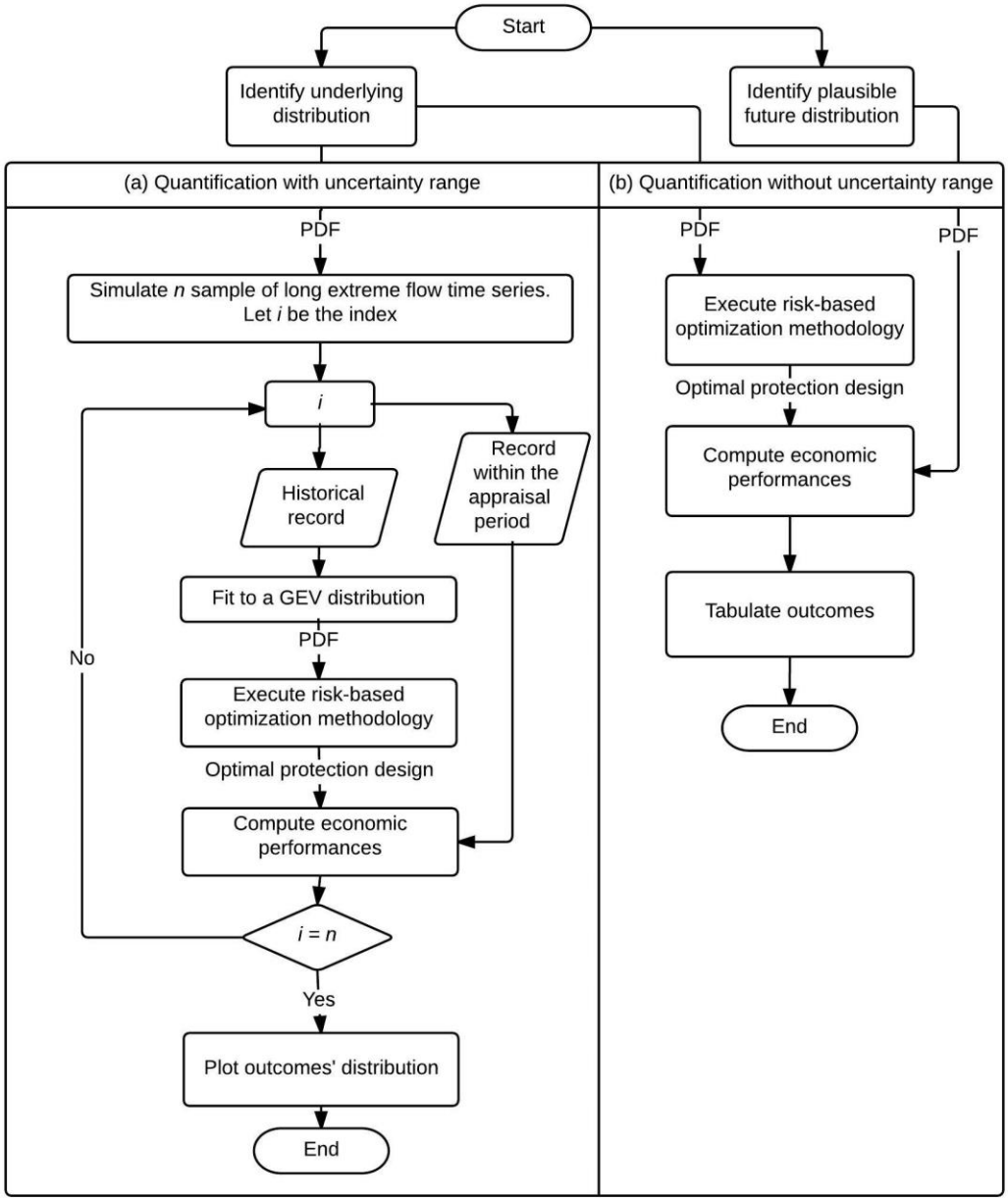

Figure 5.2*: Workflows for computation of economic performance of decisions (a) with consideration of uncertainty, and (b) without consideration of uncertainty.*

5.4 Application and results

This section presents example applications of the proposed methodologies of the decision analysis involving nonstationarity. Section 5.4.1 presents the identification ofsuitable underlying distribution and the approach to simulate annual maxima flows for computations concerning uncertainty from natural variability. Section 5.4.2 to 5.4.4 provides the qualitative and quantitative results of the three modules, respectively. Section 5.4.5 provides the results from the application of the methodology to real historical records and CM projections, respectively.

5.4.1 AM flow series simulation

Similar to the AM flow series simulation in Chapter 4 for PRO strategy, historical periods here were designed to be 50 years and the design life is the subsequent period of 100 years. The historical records represent the samples that decision makers used to infer the future underlying distribution and further decide upon the optimal level of protection. Whilst the design life period is the appraisal period of the decisions performance. Because of the replication of the set-up to the decision analysis framework of the previous chapter, the workflow in which the economic performance is analysed with respect to aleatory uncertainty in this study follows the workflow in Figure 4.2 of Chapter 4.

A realistic underlying distribution for simulation of AM flow series used in this study is taken from the long available data from the Thames at Kingston (water years 1883-2012; 128 annual maxima data). The dataset was also used in Chapter 4 for the same purpose. However, an approach to ascertain whether a stationary or nonstationary model is better representing the data was further undertaken in this study. Stationary GEV distribution, along with the nonstationary GEV distribution with the following characteristics and time as the covariate were considered: (1) a linear trend in the location parameter, (2) a linear trend in the scale parameter, and (3) a log-scale parameter. Rather than taking the previously estimated stationary GEV distribution by L-moments from Chapter 4, the maximum likelihood method was applied to all considered models for a consistent estimation method across the models. The AIC was subsequently computed for each fitted results to identify the preferred model for the dataset. The corresponding AIC for the stationary model is the smallest, i.e. 1570.24, whilst the nonstationary model with a linear location

parameter gave AIC = 1571.68, which is the second preferred model. Nonstationary distributions with a linear scale comes third with AIC = 1572.02, followed by the distribution with the log-scale parameter with AIC = 1571.99. The results indicate that the stationary GEV distribution is the best model to represent the AM flow series. The finding confirms with the goodness-of-fit figure presented in Figure 4.3.

The stationary GEV model having estimated parameters of $u = 260$, $\alpha = 95.88$, $\kappa = 0.045$ were taken forward as the underlying distribution of historical and future flow series for Module 1 simulation study. The underlying distribution for Module 2, which requires an assignment of a nonstationary distribution for the simulation, used the second best model i.e. the linear location parameter of GEV distribution for the flow series simulation. As provided in Table 5.1, the model encompasses an expected rate of change with time as the covariates. With reference to the fitted nonstationary parameters and several trials of simulations, a realistic set of nonstationary GEV parameters of u_o= 250.65, u_1= 0.2, α = 95.7 and κ = - 0.046 was selected for the simulation.

The inverse CDF of the given distribution with the estimated parameters was then used to generate multiple series of 150 years of AM flows. Although the method for random-number generations is well-established for the stationary distributions, simulations from a nonstationary distribution requires an innovative simulation set-up to account for the covariate. A workflow presented in Figure 5.3 is adopted to simulate AM flow series for a given nonstationary distribution. The simulated flow magnitudes are strictly conditional to the year they occur relative to the starting year the change is imposed.

To have an illustration on how the rate of change of u_1= 0.2 influences the pattern of AM flow series over the 150 year period, 300 generated AM flow series associated to the imposed change were averaged respective to their years of occurrence (Figure 5.4). It is evident from the plots that the average flows increases over the period due to the nonstationarity of the underlying distribution.

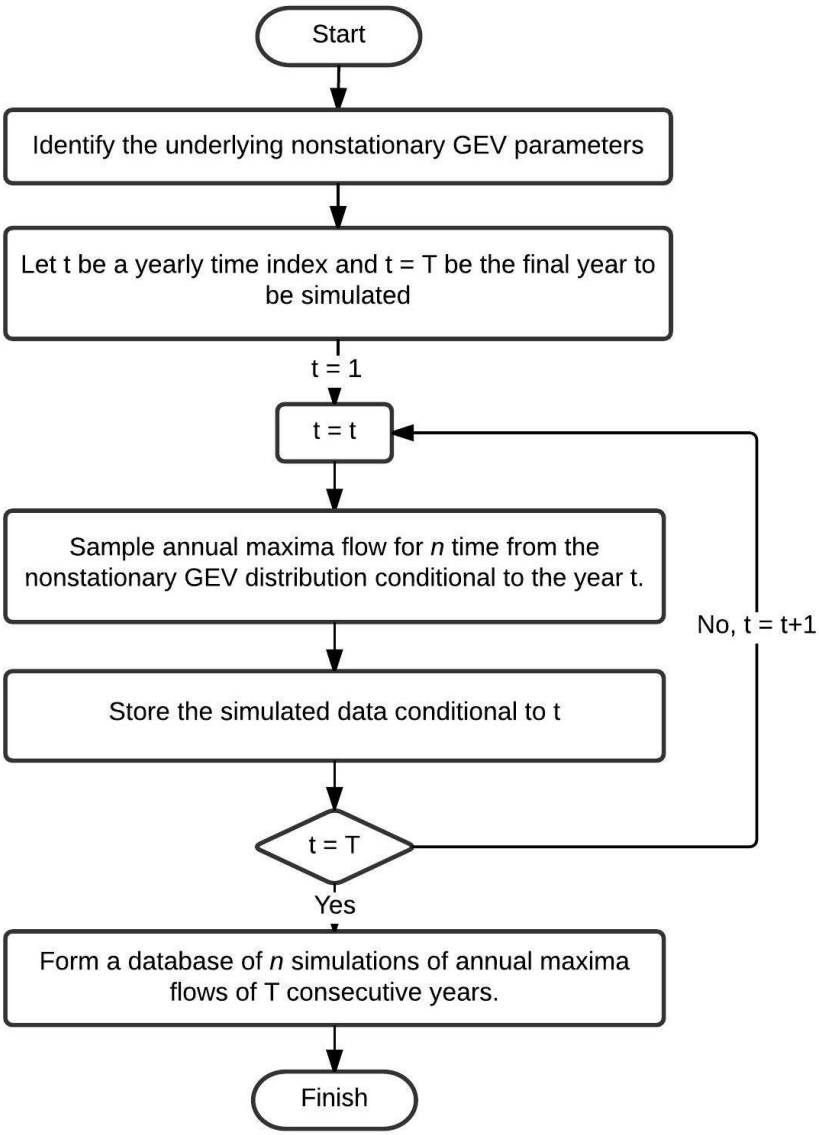

Figure 5.3: Steps to simulate multiple sets of nonstationary flow series (adapted from Seidou, Ramsay and Nistor (2012b)).

In preparing for the sensitivity analysis, the set of plausible rates of change to be imposed on the underlying distribution should be reasonably selected. A range of plausible rate of change of flow series over the future (u_1) ranging from 0 to 1.0 m^3/s/year is chosen for the study. 0 m^3/s/year means that the underlying distribution is having a stationary distribution characteristics, whilst 1.0 m^3/s increase per year will cause a consistent increase of discharge over the years and expected 100 m^3/s increase of flow rate at the end of the 100-year appraisal period.

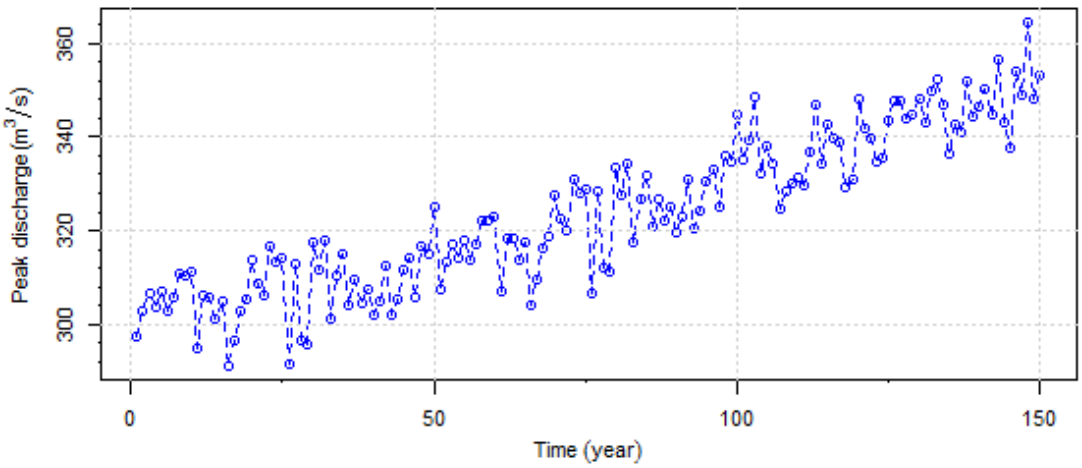

Figure 5.4: Simulated mean flows over the historical and future 150 years period when $u_1 = 0.2$.

The u_1 and u_o and the constant shape and scale parameters are the essential input variables required to generate flow series with nonstationary underlying distribution for a given time horizon (refer to the quantile estimate in Table 5.1). Simulating a realistic change between the historical and design life period with a smooth transition can be undertaken using arithmetic rules by linearly transforming the nonstationary location parameter equation (refer to the nonstationary location parameter function in Table 5.1). The smooth transition can be obtained by setting the expected flow series at $t = 51$ of the design life to be equal to that of the historical period, whilst the u_1 of the two periods have different magnitudes.

First, the location parameter at $t = 51$ (i.e. $u_{t=51}$) of the historical period is quantified using the perfect information of the rate of change. Using a targeted rate of change u_1 of the next 100 years of the design life, the computed $u_{t=51}$ of the historical period were then used to compute the corresponding u_o of the linear location parameter function. A complete set of parameters of the design life from the calculation with the specific u_1 of the historical period are then used to simulate the future flow series. A set of computed u_o associated with a set of assigned u_1 of the design life are provided in Table 5.2. Note that the values in the table were based on the historical $u_1 = 0.2$.

Considering the case for Module 2, Figure 5.5 shows the trends of the average AM flow across the 150 years when the historical $u_1 = 0.2$ and the design life $u_1 = 0.4$ and $u_1 = 0.7$, respectively. Only realizations from the two future scenarios are considered here to show the distinct effect of

the different rates of change. Upward trends from all three distributions are evident from the figure with the steepest trend caused by $u_1 = 0.7$. It is clear that the higher the rate of change is, the greater the average magnitude of flows can be expected in a specific year. Furthermore, the marginal average magnitude of flows between the different scenarios increases over years.

Table 5.2: Summary of the nonstationary GEV location parameter components for the underlying future design life associated to the rate of change at t = 51.

Rate of change ($u_{t=51}$) (m^3/s/year)	**0**	**0.1**	**0.2**	**0.3**	**0.4**	**0.5**
u_o (m^3/s)	260.85	255.75	250.65	245.55	240.45	235.35
Rate of change ($u_{t=51}$) (m^3/s/year)	**0.6**	**0.7**	**0.8**	**0.9**	**1.0**	
u_o (m^3/s)	230.25	225.15	220.05	214.95	209.85	

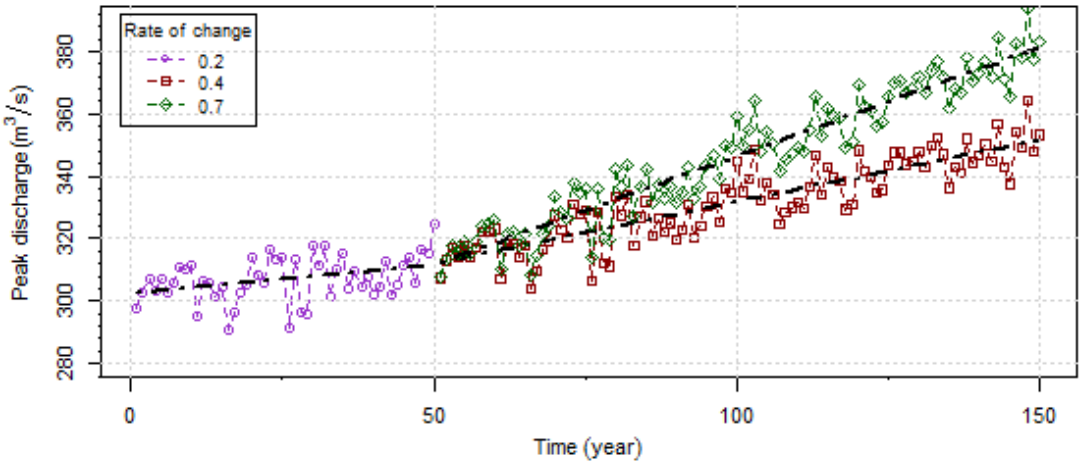

Figure 5.5: Mean AM flow associated with time over historical and future period for 300 simulated flow series.

5.4.2 Module 1

Module 1 simulation study focuses on stationary underlying distribution and the possible selection of stationary and nonstationary models by decision makers (Figure 5.1 (1a) and (1b)). 300 sets of 150 years AM flow series were generated using the GEV distribution parameters identified in Section 5.4.1, followed by the application of the decision-analysis framework depicted in Figure *5.2*. The resulting histograms of optimal design as estimated by decision makers' stationary and nonstationary model choices are illustrated in Figure 5.6. The red dotted vertical line overlaying the histograms represents the optimal design when perfect information of the underlying distribution was used (i.e. 453m^3/s). The box-plots at the bottom of the figure shows the associated investment

costs of the alternative models, and perfect information indicated by red crosses. Using the design discharge $\hat{q}$ estimated by the decision makers, the economic performance of each realization associated with stationary model choice (SE), nonstationary model choice (NSE), and perfect information (POP) were independently calculated following the procedure explained in Section 5.2.2. Figure 5.7 displays the box plots of total damage, total benefit, NPV and BCR attributed to the respective conditions.

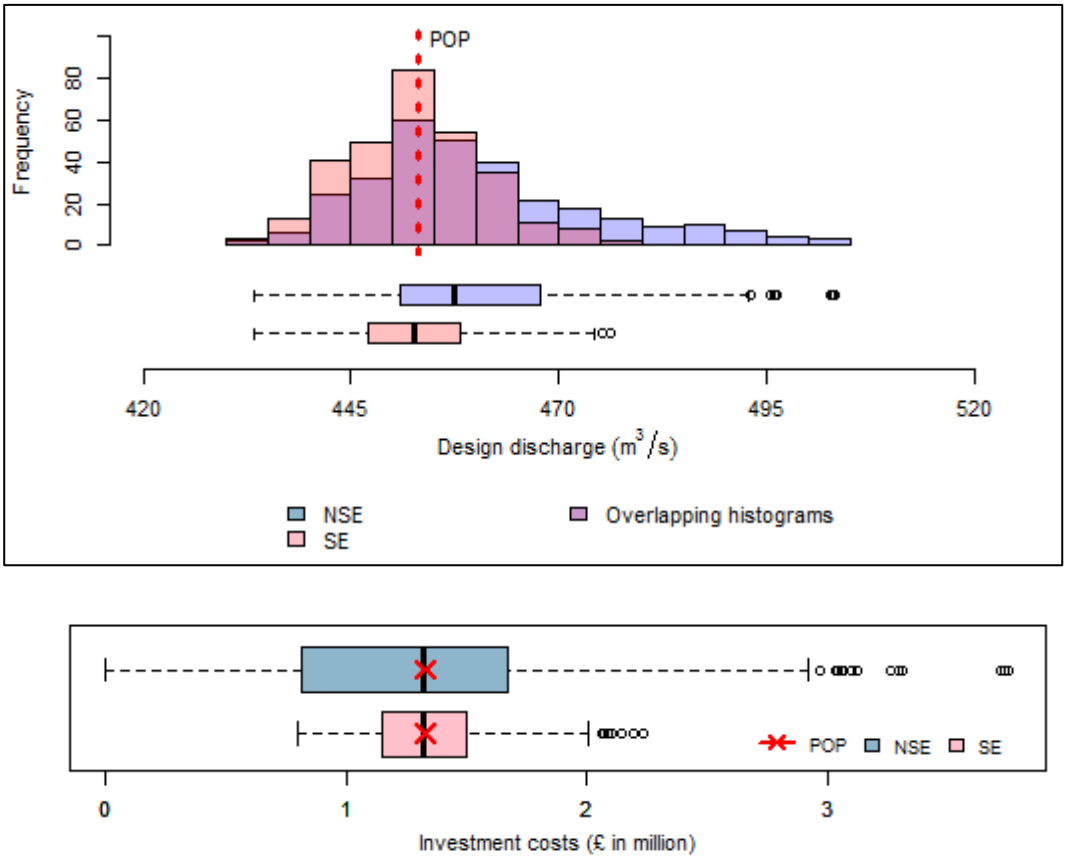

Figure 5.6: Histograms and box-plots of the protection designs and associated investment cost when underlying distribution exhibits stationary characteristics.

From Figure 5.6, it is clear that the uncertainty range of the estimated flood protection and the associated investment cost are larger for NSE than that for SE, which indicates a greater possibility of over-designed or under-protection. This is because the decision makers used the nonstationary model in the decision-making process whilst the underlying distribution exhibits stationary characteristics, leading to the larger discrepancies. Looking closely at the median and the distribution of outcomes, it can be seen that the effects of the higher median of NSE-based designs

(Figure 5.6) leads to a lower median of the total damage compared to that from SE and POP (Figure 5.7).

A higher median of the total benefit of NSE-based designs can also be seen from the top figures in Figure 5.7. The investment cost and PV benefit distributions seem to contribute little to the variability of the NPVs, but is clearly influence the variability of the BCRs (bottom figures in Figure 5.7). The larger amount of investment as compared to the slightly more benefit of the NSE-based designs as compared to the POP- and SE-based designs result in approximately 10% lower median BCR and slightly wider range of uncertainty from the NSE-based designs.

The results from Module 1 indicates the long-term implication of using stationary or nonstationary models to predict the future based on the variability of the limited historical records when the perfect information of the future underlying distribution exhibit stationary characteristics. The use of the false model (i.e. NSE) when the underlying distribution is stationary arguably return only minor differences of the NPVs and BCRs.

5.4.3 Module 2

Concerning stationary model choice when the underlying distribution is nonstationary, Module 2 involves the generation of extreme flow series from the nonstationary underlying distribution and the application of stationary or nonstationary model choice by decision makers (Figure 5.1 (2a) and (2b)). The workflow in Figure *5.2*(a) was executed using the nonstationary distribution parameters as defined in Section 5.4.1 to simulate 300 sets of 150 years annual maxima flows.

The resulting decision makers' estimated optimal design from SE- and NSE-based decision making are illustrated in the histograms and box-plots in Figure 5.8. The red dotted vertical line overlaying the histograms represents the optimal design (i.e. 456 m^3/s) based on perfect information of the 'historical' underlying distribution (POP). It can be seen from the figure that the estimated flood protection and the resulting investment cost does not converge with the values of POP. The non-convergence may be due to the strong variability of the simulated nonstationary AM flows. Another possible cause of the non-convergence may be due to the non-linearity of the damage function used.

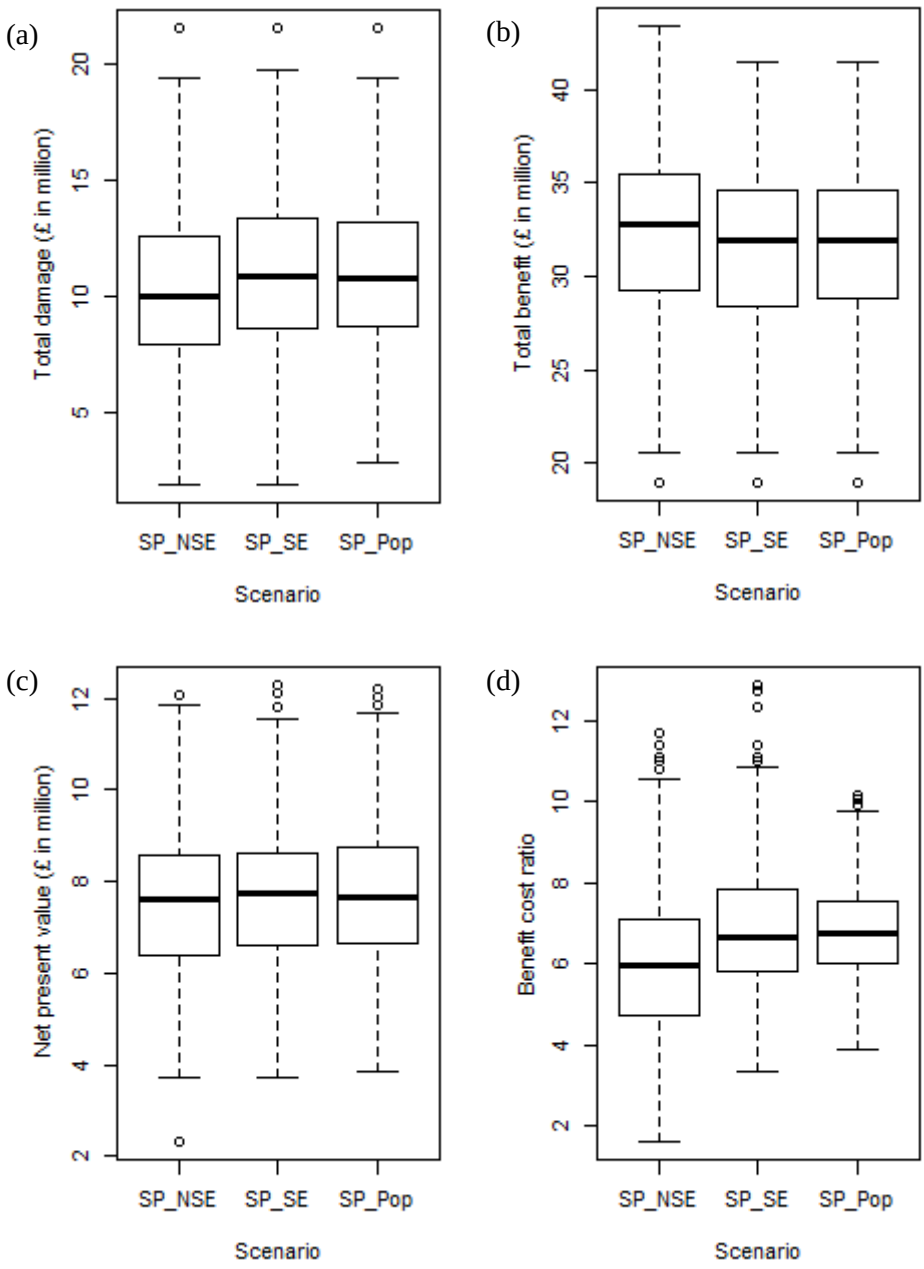

Figure 5.7: Box-whiskers plot of economic performance of nonstationary-based estimates (SP_NSE), stationary-based estimates (SP_SE) and perfect information (SP_POP) when the underlying distribution is stationary, i.e. Module 1. (a) Total damage, (b) Total benefit, (c) Net present value, and (d) Benefit cost ratio.

Although increasing the number of simulations might improve the results, increased simulated samples to 500 simulations returned no significant difference to the convergence. The difference between the median of the simulated and the ones from the perfect information only reduced the discrepancies from 0.48% (i.e. NSE-based $\hat{q}$ = 458.2m^3/s) to 0.39% (i.e. NSE-based $\hat{q}$ = 457.7 m^3/s). Because of the considerably small discrepancies, the effect of having a higher number of

simulations (i.e. from 300 to 500) is deemed to be insignificantly different. Moreover, the initial 0.48% non-convergence is small and can be considered negligible. Henceforth, the 300 realizations were maintained for the study.

In comparing between the NSE and SE-based flood protection and corresponding costs, NSE-based designs return smaller bias as compared to the SE-based designs. The results demonstrate the advantage of using a nonstationary model when the underlying distribution is nonstationary.

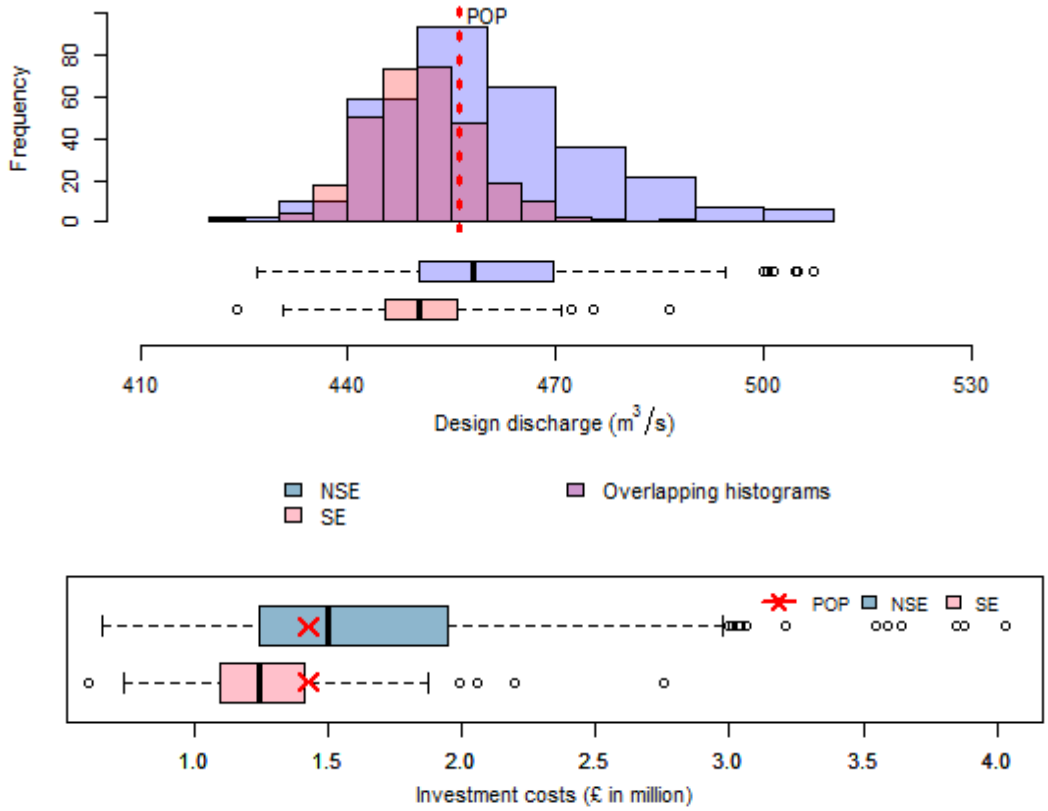

Figure 5.8: Histograms and box-plots of the protection designs and associated investment cost when the underlying distribution exhibit nonstationary characteristics.

To explore the sensitivity of the economic performance of the SE- and NSE-based decisions against a range of plausible future u_1, the simulation setup explained in Section 5.4.1 was executed. The computed u_1 and associated GEV parameters for the design life were then used to generate 300 sets of AM flow series, and randomly paired with the 300 sets of the historical AM flow series simulated earlier in Module 2. Note that 11 different future u_1 were considered for the exploration (Table 5.2), hence the workflow depicted in Figure *5.2*(a) was repeated 3300 times for the economic evaluation of stationary and nonstationary model choice, respectively. The associated $\hat{q}$ and the

corresponding cost of intervention estimated earlier from the historical series were brought forward together with the PDFs of the design life to calculate the range of economic performance (using Equations 4.9 and 4.10).

Progressively, the $\hat{q}$ and corresponding investment cost of POP for the 11 different possible future u_1 were also calculated following the workflow depicted in Figure *5.2*(b). The associated curves of PV costs, PV risks and TPVCs based on the perfect information of future u_1 are presented in Figure 5.9. The metrics and the associated results of NPVs and BCRs (using Equations 5.3 and 5.4) are given in Table 5.3. It can be seen roughly from the figure and shown quantitatively in the table that the minimum TPVC (i.e. optimum protection) and the resulting NPV increases very slowly as the underlying future change increases.

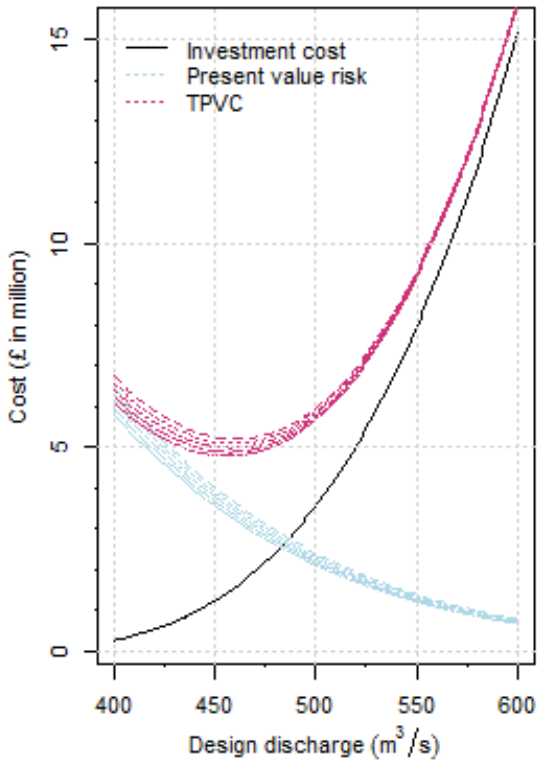

Figure 5.9: Curves of PV risks, investment costs and TPVCs correspond to the range of possible protection design and the range of possible actual future in the case of nonstationary underlying distribution.

Figure 5.10 to Figure 5.14 present the distributions of the computed economic performance associated with the u_1. The total damages of without intervention is given in Figure 5.10, followed by the distribution of total damages within the design life period considering the SE and NSE

intervention in Figure 5.11. The consequent total risk-reduction benefits from the simulations are given in Figure 5.12. The NPV and BCR that are computed using the investment cost and PV benefit of each simulated series are presented in Figure 5.13 and Figure 5.14, respectively. The red 'X's mark on top of each box-whisker plot represents the economic performance of decisions based on perfect information of the underlying distribution of the future, for the range of plausible futures considered.

Table 5.3: Economic metrics of the protection designs based on the perfect information and the resulting NPVs and BCRs attributed to the different rates of change.

Rate of change , u_1 (m^3/s.year)	Protection design, $\hat{q}$ (m^3/s)	Investment cost, C_t (£ in PV)	Risk of do-nothing, $R_{t_{T,q_o}}$ (£ in PV)	Risk of do something, $R_{t_{T,\hat{q}}}$ (£ in PV)	Benefit, $R_{t_{T,q_o}} - R_{t_{T,\hat{q}}}$ (£ in PV)	NPV (£ in PV)	BCR
0	454	1,361,111	12,307,849	3,151,774	9,156,075	7,794,964	6.73
0.1	455	1,394,082	12,547,888	3,207,081	9,340,807	7,946,725	6.70
0.2	456	1,427,620	12,791,315	3,264,979	9,526,336	8,098,716	6.67
0.3	457	1,461,728	13,037,675	3,325,572	9,712,103	8,250,375	6.64
0.4	458	1,496,415	13,286,463	3,388,962	9,897,501	8,401,086	6.61
0.5	459	1,531,683	13,537,122	3,455,253	10,081,869	8,550,185	6.58
0.6	460	1,367,540	13,789,048	3,524,547	10,264,501	8,696,961	6.55
0.7	461	1,603,992	14,041,601	3,596,943	10,444,659	8,840,667	6.51
0.8	462	1,641,042	14,294,111	3,672,536	10,621,575	8,980,533	6.47

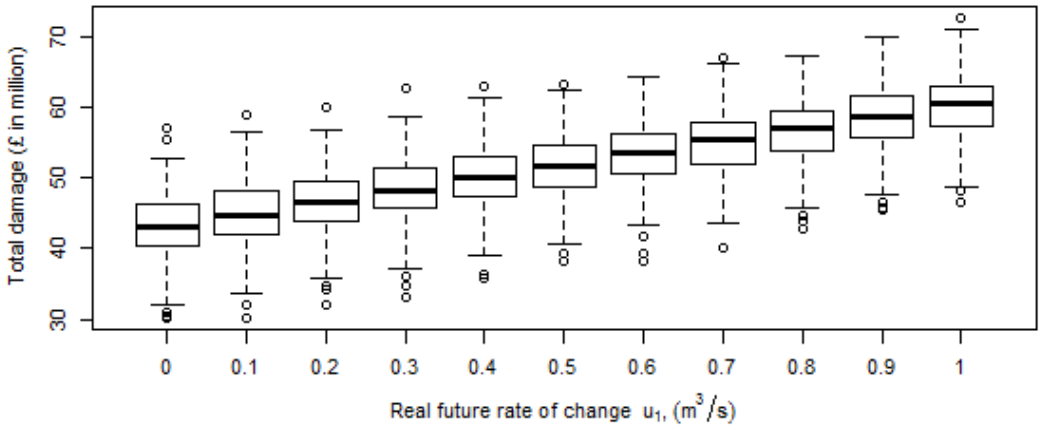

Figure 5.10: Distributions of total damage of do-nothing over the design life, based on the multiple simulations of historical and future extreme flows, stationary and nonstationary model choices across different possible future u_1.

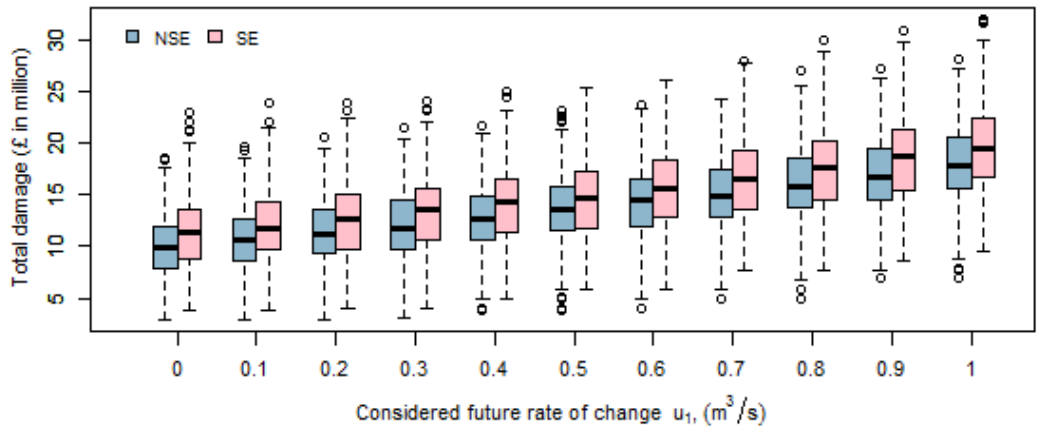

Figure 5.11: Distributions of total damage of with-project over the design life, based on the multiple simulations of historical and future extreme flows, stationary and nonstationary model choices across different possible future u_1.

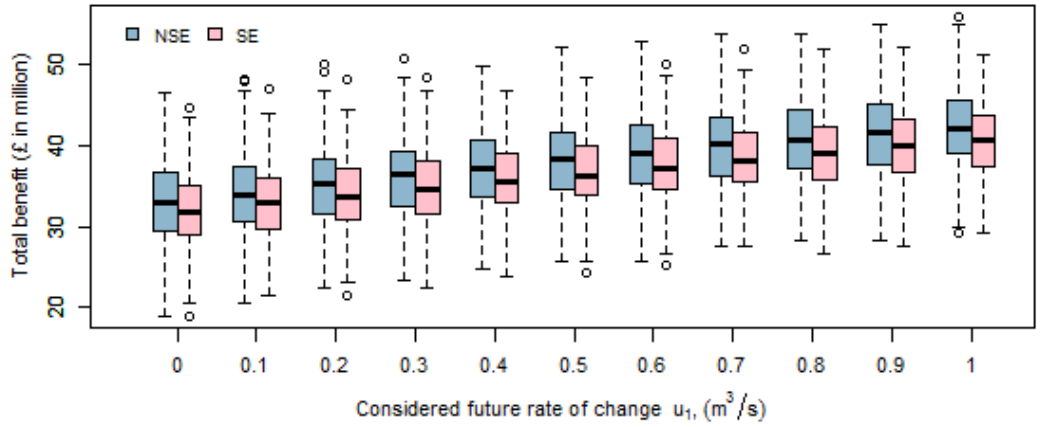

Figure 5.12: Distributions of total benefit of with-project over the design life of protection, based on the multiple simulations of historical and future extreme flows, stationary and nonstationary model choices across different possible future u_1.

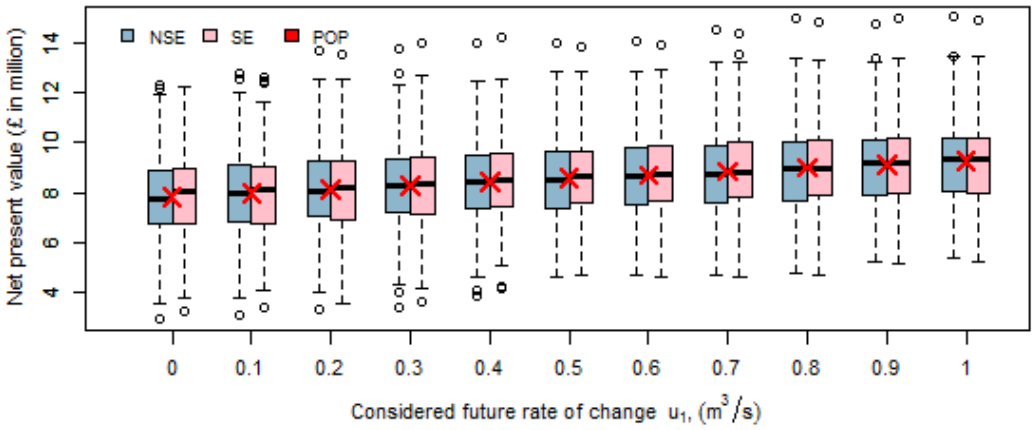

Figure 5.13: Distributions of NPV of with-project over the design life of protection, based on the multiple simulations of historical and future extreme flows, stationary and nonstationary model choices across different possible future u_1.

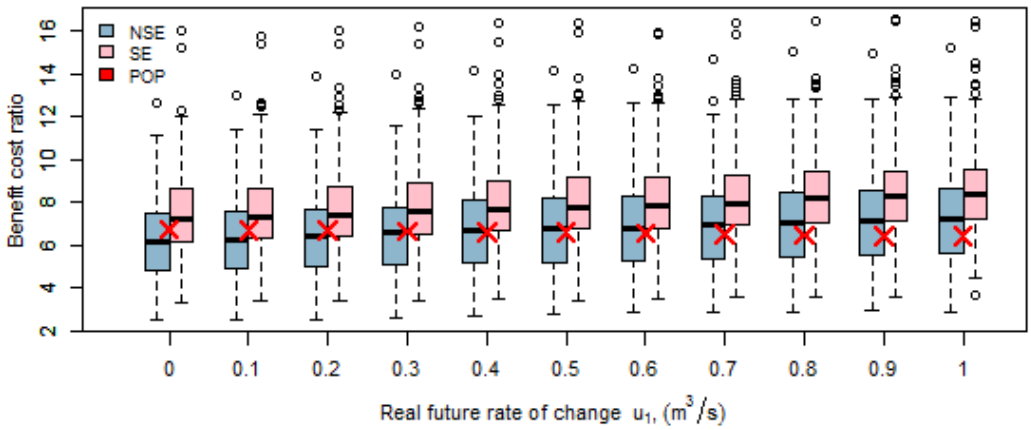

Figure 5.14: Distributions of BCR of with-project over the design life of protection, based on the multiple simulations of historical and future extreme flows, stationary and nonstationary model choices across different possible future u_1.

Figure 5.10 and Figure 5.11 indicates that the total damages potentially increases when the rate of change in the AM flows of the future is higher. Looking at any one particular scenario from the figure, it can be seen that the total damages are generally higher for SE-based designs due to the average condition of under-protection, causing a higher total benefit for NSE-based design. Upward patterns of median NPVs and BCRs against higher future u_1 shown in the figures are consistent with the higher total benefits and static investment costs respective to the SE and NSE model choice in the decision-making process across all future u_1 considered. The positive NPVs and the resulting BCRs above 2 and within a range of 6 to 8 from all possible decisions under any particular scenarios indicate the robustness of the intervention approach used in the simulated decision-making process.

The median of the NPVs can be seen converging with the NPV of POP for all considered u_1, but not apparent from that of the BCRs. This is likely due to the formulation of the NPV and BCR, where the NPV is the difference between the costs and benefits associated with the design protection, while the BCR is the ratio between the costs and benefits. Nevertheless, it is intriguing that the median of the BCRs based on the NSE designs at future $u_1 = 0.2$ m^3/s/year does not intersect with the BCR of POP, although the historical nonstationary underlying distribution is set to have $u_1 = 0.2$ m3/s/year. The reason behind this is probably the same as what caused the median of protection designs and investment costs of NSE designs to not align with the ones from

POP (Figure 5.8). Moreover, the instability of BCR from the Monte Carlo simulations as found in Figure 4.12 may also add to the cumulative effects of the non-convergence.

Figure 5.10 to Figure 5.14 generally suggest that the relative effects of the stationary and nonstationary model choices to the economic performance of decisions is generally not apparent. This raise an interesting question; On the basis of the economic performance as the output of interest, is it worth adopting the more complex nonstationary model against the simpler stationary model for the sake of adapting to possible future change. The investigation is continued in Module 3 to further explore the relative implication of the competing models with a range of possible actual futures.

5.4.4 Module 3

Module 2 has successfully captured the long-term economic outcomes considering the different possible futures and the conflicting model choices. The outputs in the form of uncertainty range, predominantly due to the natural variability, successfully provide insights on the relative range of outcomes of the considered scenarios. The performance of decisions based on the predictions of future change versus the ones from the possible actual future is further explored in Module 3. The module focuses on comparing the expected values rather than capturing the effects of sampling variability, as explained in Section 5.2.3.

The exploration was undertaken by first defining the possible predicted change in the form of rate of change in the location parameter that may be used by the decision makers in the decision-making process. The range of possible actual future change was also defined accordingly. This study takes five possible predicted future change and 11 possible future conditions, as shown in Figure 5.15. Hence, the total pairs of predicted and actual future u_1 is 55. The predicted and actual u_1 were used along with their associated GEV parameters from the set-up in Section 5.4.1 for the calculation of the economic performance.

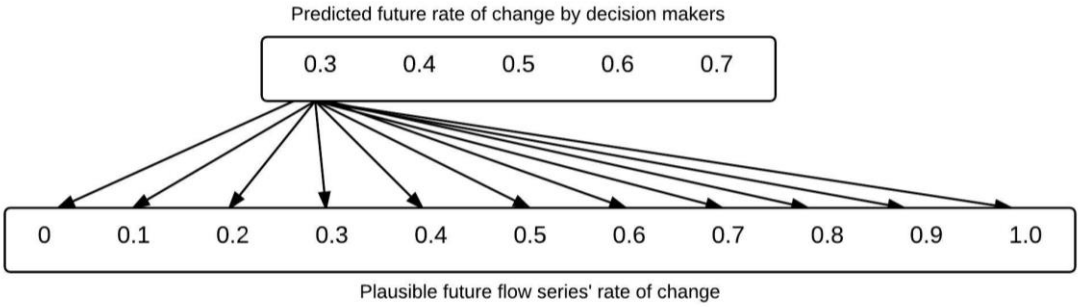

Figure 5.15: Predicted u_1 and possible future changes for the sensitivity analysis. Example combinations of predicted u_1 and possible range of future u_1 is shown.

Applying the workflow depicted in Figure *5.2*(b), the flood protection $\hat{q}$ based on the predicted u_1 and actual u_1 were first calculated. The investment costs and risks associated with the $\hat{q}$ of the individual pair of the predicted u_1 and the actual u_1 were then used to calculate the PV benefits, NPVs and BCRs. Equations 5.3 and 5.4 were employed for the NPV and BCR computations. Note that Module 3 adopts the same sets of GEV parameters that were used in Module 2. Hence the protection design, investment costs and the associated metrics of consequential risks, NPVs and BCRs of the actual future in Module 2 were taken forward into Module 3 exploration.

The percentage difference (% difference) between the expected values of prediction- and perfect information-based decisions were analysed through solving Equation 5.5. Let y_e be the economic metrics of the decisions. The subscript (P|T) refers to the condition when the actual future unfolds whilst flood protection decisions are based on the predicted change. The subscript (T) refers to the condition when the actual future unfolds whilst flood protection decisions are based on the full knowledge about the future.

$$\%\ difference = \frac{y_e^{(P|T)} - y_e^{(T)}}{y_e^{(T)}} \times 100 \qquad (5.5)$$

Figure 5.16 shows the interpolation of the % difference plots of the economic performance associated with the pairs of the predicted-actual future u_1 set-up earlier. The y-axis in each figure shows the % differences of the economic performance of the predicted-actual future and the x-axis refers to the possible actual futures. Plots on $y = 0$ represent conditions when predicted $u_1 =$

perfect information of future u_1, where there are no discrepancies in the resulting economic performance.

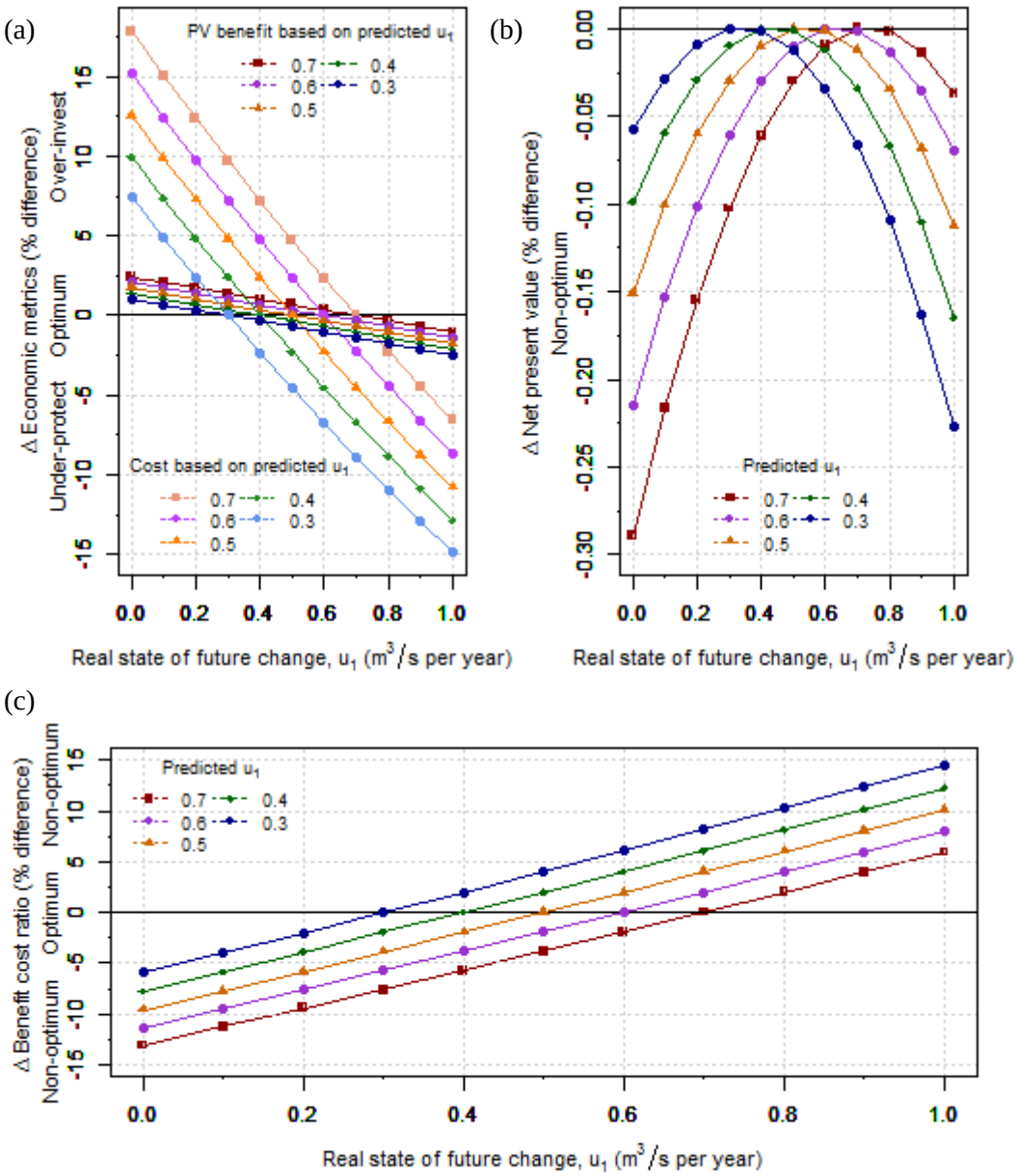

Figure 5.16: Plots of marginal difference of (a) investment costs and PV benefit, (b) NPV and (c) BCR of predicted and future u_1.

Over-predicting the future change lead to over-designing the flood protection and causes a higher PV benefits, as indicates in Figure 5.16 (a) from the positive % differences. On the contrary, under-prediction of future changes that result in under-design and consequential under-protection are apparent from the negative % differences in Figure 5.16 (a). As for the corresponding NPVs and BCRs in Figure 5.16 (b) and (c), positive or negative marginal differences reflect the non-optimal

protection caused by the over-design (i.e. over-prediction) or under-design (i.e. under-prediction). The maximum discrepancies of BCR is around 15%, which is when predicted $u_1 = 0.3$ m^3/s/year and future $u_1 = 1$ m^3/s/year.

It is also evident from Figure 5.16 (a) that the investment cost is more sensitive as compared to the PV benefit, reflecting the influence of the parameterization of the cost and benefit functions. The relative % differences between the points of the investment cost and PV benefit at any specific pair of predicted and actual future u_1 is more pronounce when the discrepancy between the predicted and actual future change is greater. This can be qualitatively seen, for example, when the predicted u_1 is 0.3 m^3/s and the future u_1 is 0.1 m^3/s, as compared to when predicted u_1 is 0.3 m^3/s and future u_1 is 0.6 m^3/s. As a result, the NPV and BCR tend to deviate farther from the optimal horizontal lines, respectively (Figure 5.16 (b) and (c)). These qualitative findings ascertain that a worst prediction would eventually lead to a severe regretful decision.

Such information brings insight in FRM decision making in the face of uncertain future. The findings from the sensitivity analysis from Module 3 enable decision makers and stakeholders to understand the consequences in terms of the expected relative difference of the decisions economic performance, due to subjective judgements of the potential future change. In an attempt to explore a more realistic and meaningful insights, the subsequent section explores the use of climate model-based projections against the conventional historical-based prediction through sensitivity analysis.

5.4.5 Historical data versus climate model-based predictions

To have a more realistic comparison on the influence of the alternative stationary and nonstationary models in the risk-based decision making, this section considers two alternative sources of information in predicting the future change; information from the historical observations- and information from the climate model-based future flows projections. Historical records of AM flows (water years) were taken from Thames at Kingston gauging records (Centre for Ecology and Hydrology, 2014) similar to the ones used in the simulation of flow series from a stationary underlying distribution (i.e. in Module 1 and 2) (Section 5.4.1). The climate model-based future

flows projections (CM projections) were also based on the Thames at Kingston gauging station, where there are 11 sets of CM projections made available by the CEH (Prudhomme et al., 2012). The CM projections for the year 2013 to 2060 of the water years were extracted from each of the ensemble. The year 2013 as the starting year of the AM flows of the CM projections was chosen to allow consistency of period between the projections and the targeted appraisal period.

The AIC test on the Thames at Kingston historical AM flow series indicates a stationary model as the preferred model (Section 5.4.1). For the CM projections, two out of 11 sets gave an AIC values smaller for the nonstationary model as compared to the stationary model, while for the nine others, the AIC values were smaller for the stationary model (Table 5.4). In aiming to use a nonstationary model to represent the CM projections alongside the stationary model from the observation-based prediction, the two CM projected series that better suit nonstationary models than stationary models were therefore brought forward. It was discovered that one projected series shows an upward trend (i.e. positive u_1) whilst the other one with a negative trend (i.e. negative u_1). As assumed in Module 1 and Module 2 simulation studies, an initial downward predicted change would lead to a stationary model being used by the decision makers in the risk-based optimization (Figure 5.1). As it would be more interesting to have a comparison analysis between contrasting models (i.e. stationary and nonstationary model), the CM projections with predicted upward trend was further used in the decision analysis.

Table 5.4: Summary of AIC readings of SE and NSE estimates for 11 dataset of predicted future flows. The bolded values indicate the preferred model.

Hydro-climatic model reference		**Q0_afgcx**	**Q3_afixa**	**Q4_afixc**	**Q6_afixh**	**Q9_afixi**	**Q8_afixj**
AIC	**SE**	773.64	772.60	769.66	801.03	794.52	766.59
	NSE	775.49	774.58	769.86	802.07	791.03	768.55
Hydro-climatic model reference		**Q10_afixk**	**Q14_afixl**	**Q11_afixm**	**Q13_afixo**	**Q16_afixq**	
AIC	**SE**	777.26	772.68	783.24	766.06	771.61	
	NSE	779.18	774.68	782.25	768.06	773.59	

The estimated nonstationary GEV parameters of the CM projections gave $u_o = 286.98, u_1 = 1.795$, $\alpha = 126.02$ and $\kappa = 0.353$, whilst the estimated stationary GEV parameters of the

historical records is given in Section 5.4.1. From the estimated nonstationary parameters, it is recognized that the κ parameter is slightly above the reasonable range of flood events ($-0.3 > \kappa > 0.3$) suggested by Martins and Stedinger (2000). However, the fact that the value is estimated using the CM projections through the well-accepted procedure of ML indicates that the estimated parameters are appropriate for the exploration.

Figure 5.17(a) illustrates the stationary PDF of the historical records and the nonstationary PDF of the CM projections at $t = 1$ and $t = 100$ representing the start and end of the appraisal period. While the stationary PDF is constant over the appraisal period, the nonstationary PDF vary in accordance with time. The distinct shapes of the stationary and nonstationary PDFs is a result of the different estimated parameters due to the different input data set. The location parameter of the nonstationary distribution regardless of time is greater than that of the stationary distribution (nonstationary $u_o = 286.98$, stationary $u = 260$), which causes the peak of the nonstationary distribution to be inclined towards the higher quantiles as compared to the peak of the stationary distribution.

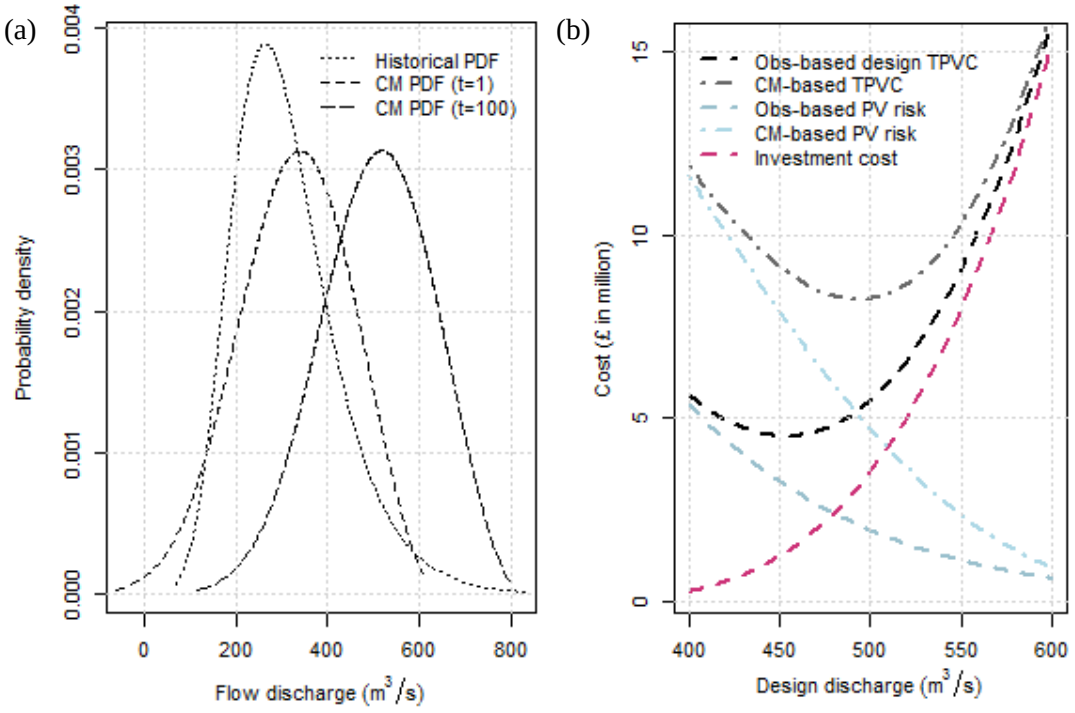

Figure 5.17: (a) PDF of observations and CM future flows at t=1 and t=100. (b) Curves of PV risks, investment costs, TPVCs of observations- (Obs-based) and CM-based prediction respectively.

Furthermore, the distinct κ parameters of the PDFs influences the relative behaviour of the distributions' tails. As can be seen from the figure, the stationary PDF from the historical records reveals a heavier (fat) tail owing to the smaller magnitude of κ (Martins and Stedinger, 2000). Heavier tail is said to return a greater risk associated with the hazard (e.g. Malamud and Turcotte, 2013), but this general rule does not necessarily apply. Flood risk as a product of hazard and vulnerability is based on the interaction between the distribution parameters (including the resulting upper limit), as well as the design discharge threshold, as denoted in Section 5.2.2. The computation of risks as a consequences of these factors are explained in the subsequent paragraphs.

In estimating optimal flood protections based on the two different sources of information, the PDFs from the historical records and the CM projections were individually incorporated into the risk-based optimization methodology in accordance with the workflow presented in Figure *5.2*. The PV costs and PV risks associated with a range of potential design discharges were interpolated in Figure 5.17(b). From the automated computation of the risk-based optimization procedure, the estimated flood protections $\hat{q}$ of the historical records and CM projections are 453 m^3/s and 493 m^3/s, respectively. The difference between the estimated $\hat{q}$ from the historical records and CM projections is 8.1%.

The curves in Figure 5.17(b) can further be visualized to study the differences between the risk-based design estimates of stationary and nonstationary PDFs. The investment costs curves of both cases are the same due to the non-dependence of the investment costs calculation to the PDF. PV risk curves, on the other hand, vary as a result of the distinct PDF properties in the risk calculations. It can be seen from the figure that the nonstationary PDF yields higher magnitudes of PV risk than stationary PDF over the whole range of the design discharge considered, albeit the less heavier tail (stationary $\kappa <$ nonstationary κ). The difference between the PV risks of both conditions, nevertheless, declines as $\hat{q}$ increases. This behaviour is likely the result of a declined lower limit of the risk calculation and also the isolation of relatively less severe flood events within the computation.

The influence of the distinct PDF characteristics and the considered flood protection design $\hat{q}$ can also be inspected by observing the associated streams of annual risks from both PDFs (i.e. the stationary and nonstationary conditions predicted based on the historical and CM projections, respectively). Figure 5.18 provide interpolation lines of computed annual risks associated with the two distinct PDFs and two possible flood protection designs (400 and 500 m^3/s). The annual risks decline when a higher design protection is used (i.e. 500 m^3/s as compared to 400 m^3/s) for stationary and nonstationary conditions, respectively. This is expected given a higher protection for the same future condition.

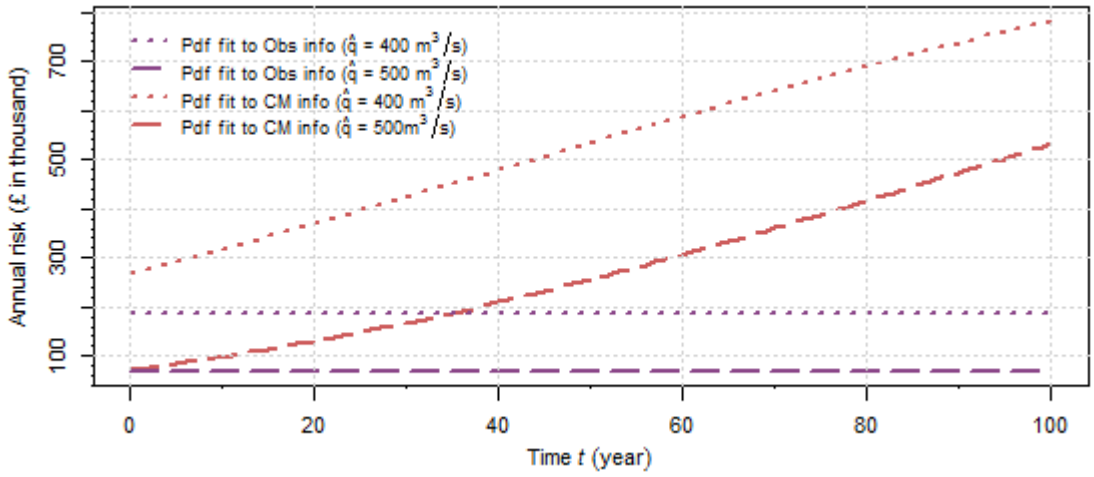

Figure 5.18: Annual risk streams for nonstationary PDF (estimated from CM information) and stationary PDF (estimated from observations). Two distinct $\hat{q}$ are considered.

The evolutions of annual risks between the stationary and nonstationary conditions are further compared from the illustrations. It is interesting to find that whilst the flood protection of 500 m^3/s under the nonstationary condition able to reduce the annual risks more than a lower flood protection (i.e. 400 m^3/s) under the stationary condition during the early period of appraisal, the lower protection in the stationary condition outperforms the higher protection in the nonstationary condition soon after approximately 50 years into the future. Higher margin can be seen as farther it gets into the future. This behaviour reflects how the transient nonstationary PDF over the appraisal period and the distance of the time of the annual risk from the initial time of the nonstationary evolution would influence the estimated PV risk and further the optimal design protection. The findings also reflect the combined effects of low probability-high consequences and high

probability-low consequences flood events, which both important in quantifying flood risk (Hall and Penning-Rowsell, 2011).

The estimated optimal protection $\hat{q}$ from the historical records and CM projections were then individually brought forward into the assessment of decisions performance against a range of possible future conditions. This is undertaken with the assumption that the optimal decision was estimated by decision makers and the flood protection functionality is now being assessed over the design life period. The range of possible future conditions over the design life period was first defined as having an underlying distribution following the statistics of either the (1) historical records (Set 1), or the (2) CM projections (Set 2). The consideration of the two scenarios provide the opportunity to have a wider range of possible future conditions to be assessed. The study further classified this as two sets of possible future conditions, each with a unique set of underlying parameters u_o, α and κ. However, the rates of change u_1 considered for the two sets were consistent to allow a valid comparison of the final outcomes. $u_1 = \{0, 0.4, 0.8, 1.2, 1.6, 2.0, 2.4, 2.8, 3.2\}$ were selected for the range of plausible future change, taking into consideration that the previously predicted nonstationary distribution of the CM projections gave $u_1 = 1.785$ m^3/s.

PV risks corresponding to the previously estimated $\hat{q}$ and the actual future PDFs of the considered rates of change of Set 1 and Set 2 were computed, respectively. Each was individually used to quantify the consequent economic performance of decisions associated with the predicted and actual future state (henceforward will be regard as predicted-actual future state). The optimal protection and the resulting economic performance assuming full knowledge of the actual future condition were also calculated for each considered rates of change of Set 1 and Set 2 using Equations 5.3 and 5.4, and following the computation settings explained in Section 5.2.2 and 5.2.3. The percentage difference between the economic performance of decisions based on the predicted future conditions and the perfect information was computed for all scenarios using Equation 5.5 (i.e. similar to what have been demonstrated in Module 3). Figure 5.19 (a) to Figure 5.19 (d)

illustrate the results of the economic performance of flood protection decisions under Set 1 and Set 2 possible future. Four broad scenarios according to the simulation setup can be defined as follows:

1) *Obs-based dec. Set 1*: Scenarios when the estimated optimal decision is based on the historical records, hence the stationary prediction. The range of possible actual future conditions follows the statistics of the PDF of the historical records.
2) *CM-based dec. Set 1*: Scenarios when the estimated optimal decision is based on the information of CM future flows projections, hence the nonstationary prediction. The range of possible actual future conditions follows the statistics of the PDF of the historical records.
3) *Obs-based dec. Set 2*: Scenarios when the estimated optimal decision is based on the historical records, hence the stationary prediction. The range of possible actual future conditions follows the statistics of the PDF of the CM projections.
4) *CM-based dec. Set 2*: Scenarios when the estimated optimal decision is based on the information of CM future flows projections, hence the nonstationary prediction. The range of possible actual future conditions follows the statistics of the PDF of the CM projections.

As can be seen from the figure, the curve of the CM-based dec. (Set 2) intersects with the x-axis exactly where the predicted u_1 is the same as the actual future u_1 (i.e. u_1 = 1.785 m^3/s). A similar behaviour can be seen from the curve of Obs-based dec. (Set 1), when predicted u_1 is the same as the actual future u_1 (i.e. u_1 = 0). These occurrences will return a 100% performance of the FRM decisions. In reality, however, a 100% performance would not be possible owing to the huge sources of discrepancies. Such errors are not only caused by the false model selection (e.g. stationary over nonstationary) or the discrepancy in the predicted rate of change, but also from the estimated values of the rest of the distribution parameters of the same model. For example, the CM-based dec. (Set 1) of having a predicted u_1 equal to the actual u_1 does not causing the curves to intersect with the x-axis at the u_1 value (i.e. u_1 = 1.785 m^3/s), and vice versa for the Obs-based dec. (Set 2).

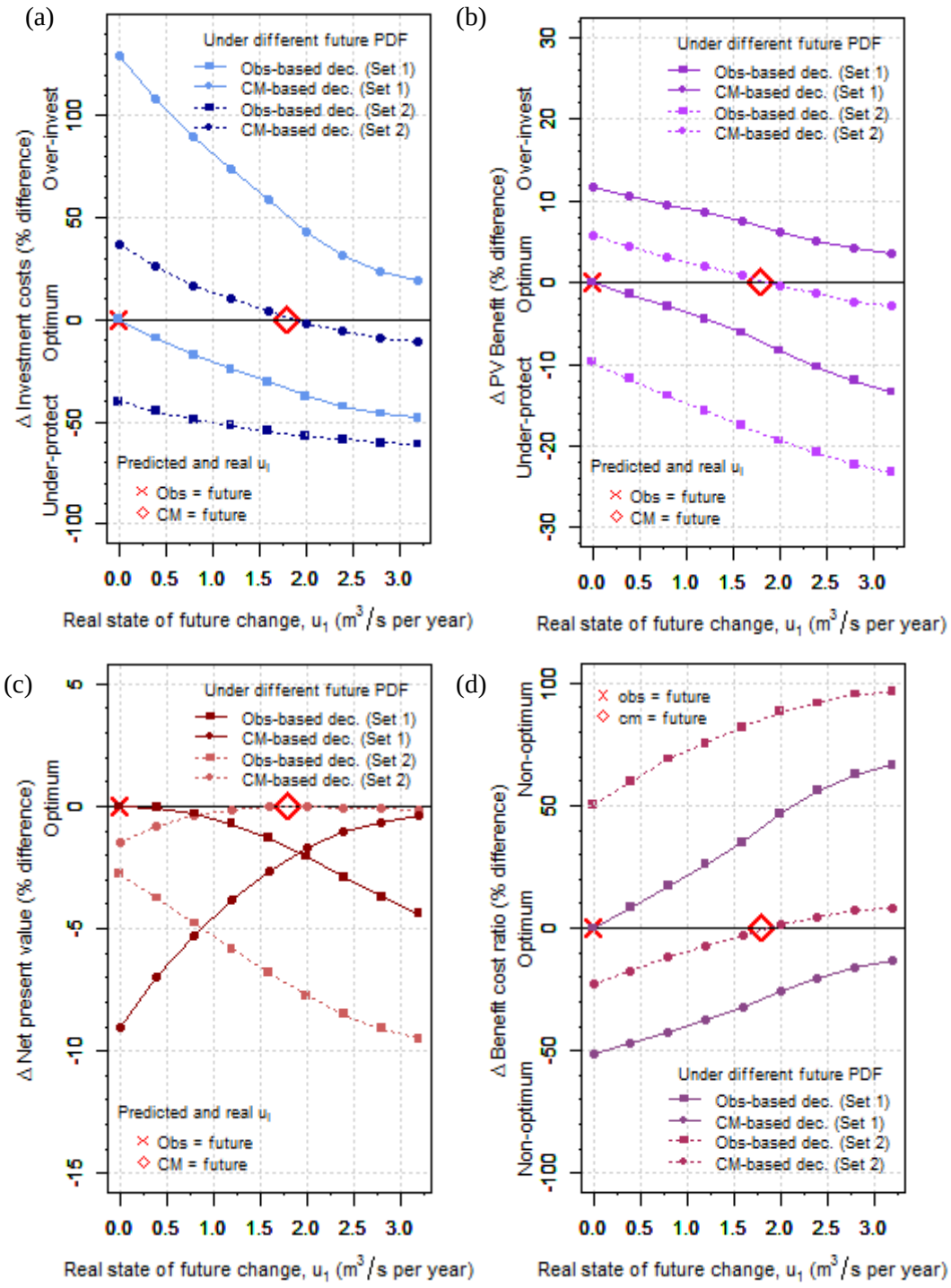

Figure 5.19: Plots and curves of % difference of predicted-actual future (a) investment costs, (b) PV benefit, (c) NPV and (d) BCR. Each figure contains tabulated results related to the discrepancies of the predicted change and the perfect information. (1) Obs-based dec (Set 1) refers to decisions based on the historical records, whilst the actual future is of Set 1. (2) CM-based dec (Set 1) refers to decisions based on climate projections, whilst the future is of Set 1. (3) Obs-based dec (Set 2) refers to decisions based on historical records, whilst the future is of Set 2. (4) CM-based dec (Set 2) refers to decisions based on climate projections whilst the future is of Set 2. The two red marks along the x-axis in each figure refers to the decisions performance when the PDF used in the decision-making process is the same as the actual future.

Analysis of the results from Figure 5.19 (a) and (b), however, confirms that the more over-designed a project is, the greater PV benefit can be expected. The opposite behaviour can be seen from under-designed scenarios where the project would bring less benefit due to the under-protection. Figure 5.19 (c) and (d) further shows how the % difference of the costs and benefits influence the % difference of the NPV and BCR. The results reveal that both over-designed and under-protected scenarios return a negative % difference of NPV. Whilst the implications are rather obvious for the NPV, this is not the case for BCR. A false prediction that result in an over-designed protection gave a negative % difference of the resulting BCR as compared to the BCR from the perfect information. This means that although the over-protected scenario increases the benefit, the marginal increase in cost is much higher (Figure 5.19 (a) and (b)), leading to a negative % difference of BCR. The opposite is true for under-designed protection. This can be observed from plots of similar scenarios of % difference in PV cost and PV benefit. Note that the % difference curves between NPV and BCR behave differently as a result of the underlying formulation of the indices; BCR is the ratio of the benefit to cost, whilst NPV is the net return in monetary value. The distinct behaviour and the curves of NPV and BCR % difference are consistent with results from the Module 3 exploration.

In attempt to understand the possible downfall of using the conventional stationary assumption (in this case from the historical records) against the nonstationary assumption (in this case from the CM projections), the results from the sensitivity analysis of the economic performance to the competing approaches under Set 1 and Set 2 were further analysed. For ease in interpretation, the analysis only focuses on the % difference of NPVs in Figure 5.19 (c). The results show that regardless the rates of change, if the actual future conditions follow those of Set 1, the use of CM projections in the decision making is generally preferred provided that the CM projections under-predicts the future by more than 6.4%. Else, the historical records would be preferred for a more cost-effective response to flood risk. Meanwhile, if the actual future conditions follow those of Set 2, using the CM projections gave a relatively lower percentage differences of NPVs as compared to using the historical observations. In this case, using the CM projections allows a more cost-effective solution. The findings are consistent with the fact that the shape and scale parameters of

the distribution of Set 1 follows the stationary statistics estimated for the historical records, and Set 2 follows the nonstationary statistics estimated for the CM projections.

Although the finding generally suggests that the nonstationary model (i.e. predicted from the CM projections) is preferred given certain conditions, it is interesting that the % difference of NPVs of stationary and nonstationary model choices are relatively small across the range of considered future. Furthermore, either the stationary or nonstationary model can cause a major increase in the % difference when the predicted distribution deviate farther from the actual distribution.

5.5 Discussion and conclusion

The study has successfully demonstrated the analysis of FRM decisions performance in the context of stationary and nonstationary conditions. Numerical simulation based on real data of historical flow records and CM projections were undertaken through uncertainty and sensitivity analysis aiming to observe and analyse the relative economic consequences of a number of possible adaptation pathways and a range of possible scenarios of historical and future conditions. The end-to-end framework of the decision analysis involves the simulation of flow series (from stationary and nonstationary underlying distributions), the simulation of decision makers' proactive action (model fitting to existing dataset and applying the risk-based optimization methodology) and the analysis of economic performance of decisions (given a possible future condition). In simulating the decision makers' preference in using a nonstationary model for the risk estimates, a risk-based decision analysis framework incorporating nonstationary model has been proposed and where applicable directly used in the decision-making process. This setting eliminates the need to incorporate a trend analysis before a nonstationary model is fitted (e.g. Rosner, Vogel and Kirshen, 2014).

The Monte Carlo simulation methodology adopted to capture the uncertainty range allows the influence of natural variability additional to the model error to be explicitly addressed. The GEV distribution is used throughout the study for the stationary and nonstationary cases. The nonstationary conditions are characterised by the linear trend in the location parameter of the GEV

model with time as the covariate. The characterization of the PDF accounted the information of the real dataset from Thames at Kingston historical flow records and also the information from the climate model projections of future flows. This provides the advantage of having realistic underlying distributions to simulate possible actual future conditions.

Although it is well recognized that a preferred probability distribution model for flood risk intervention decision is the one that closely represents the future underlying distribution, it was found that nonstationary predictions gave a larger variance of outcomes compared to the stationary prediction regardless the underlying distribution (refer Section 5.4.3). The behaviour is consistent with the expected higher variance of model with higher number of parameters as highlighted in Di Baldassarre, Laio and Montanari (2009). The findings arguably may give weight to stationary models despite an expected future nonstationarity. The preference on stationary model over nonstationary model further highlighted from the findings in Module 2 and 3, whereby stationary and nonstationary model choices in the decision making for all considered future state return positive NPVs, respectively.

The study continued by analysing the % difference of the expected values of economic performance of prediction-actual future distribution. In general, the resulting economic consequences are shown to be worse when the predicted change deviates farther from the future change. Some specific quantitative findings in terms of the relative preference of nonstationary and stationary model have also been identified with an indication that in most of the future scenarios considered, adopting the nonstationary model (i.e. predicted from the CM projections) can lead to a more cost-effective decisions. Nevertheless, it is interesting that the difference between the % difference of NPVs of stationary and nonstationary model choices are relatively small across the range of actual future conditions considered. Furthermore, either the stationary or nonstationary model can cause a major increase in the % difference when the predicted distribution deviate farther from the actual distribution.

On that basis, the conventional stationary approach may be preferred than the more complex nonstationary approach. This echoes the strong suggestion by Serinaldi and Kilsby (2015), that

stationarity should remain the default assumption even when the evidence of nonstationarity is apparent. Nevertheless, this does not mean that nonstationary model should be discarded (Milly et al., 2015). In fact if there is a clear evidence/prediction of future change and there exist modelling capabilities, comparison of simulation outcomes between stationary and nonstationary models will provide valuable insights to inform FRM decision making.

The use of nonstationary model predicted from the CM projections as demonstrated in this section has enabled quantitative comparisons to be made with the conventional approach of using the stationary model predicted from the historical records. In particular, the exploration considering the wide range of plausible future underlying distributions increases the robustness of the study. The proposed risk-based decision analysis in the context of stationary and nonstationary, and the incorporation of information from climate projection in the flood frequency prediction additional to the retrospective approach is also novel. The application successfully provides significant insights into the economic performance of decisions under stationary and nonstationary model choices and possible future conditions. The comparative response of stationary and nonstationary predictions discovered from this study advances the findings related to concerns on nonstationarity. This contributes to the discussion on nonstationarity that currently being actively debated in the literature (Milly et al., 2008;Stedinger and Griffis, 2011;Serinaldi and Kilsby, 2015).

The results from the application of the decision analysis framework, however, are greatly influenced by the input components of the modelling chain and the modelling techniques. As this study applies the framework using the Thames at Kingston historical and future predicted flows, the available long time series ensures a reliable parameterization of the PDF. Smaller sample size would inevitably cause discrepancies, but based on the present study, it can be argued that reliable outcomes can be obtained when using 50 years of sample size (Module 1 and 2). Similar exploration, therefore, can still be employed for other cases of available small sample size.

Adopting the exploratory framework for other case studies should account local factors in configuring the damage and cost models for more realistic absolute values of the economic performance. Different constant values of cost and damage function may be adopted for a more

robust outcomes. However, simulation studies should be equipped with fairly simple physical-based damage and cost models to ensure that the recursive computation run smoothly.

Another possible improvement to this study is to incorporate additional pathways of decision makers' attitude in managing flood risk. For example, it may be assumed that the decision makers might not intervene if the fitted distribution reveals a downward change, until a time in the future when damage occurs. In order to identify the realistic pathways, it is important to obtain local decision makers' opinions for the results to be relevant for policy recommendation.

To explore the effects of adopting a nonstationary model in addition to a stationary model in a real case study through a more realistic risk-based optimization of flood protection design, the damage and cost functions should be modelled with appropriate physical representation. Chapter 6 seeks to develop a conceptual framework to estimate flood damage corresponds to micro-scale assessment, and further demonstrates its applicability. The cost model derivation and the feasibility of both the damage and cost functions within the context of a risk-based options appraisal of stationary and nonstationary conditions are further addressed in Chapter 7.

Chapter 6 Damage modelling and flood vulnerability assessment: Incorporating spatial complexities

6.1 Introduction

The previous chapter explores FRM decision making in the context of nonstationarity additional to the conventional stationarity. Physically-based cost and damage functions in simplified forms were used. Recognizing the importance of micro-scale damage models in flood risk management, this chapter attempts to develop approaches to modelling flood damage associated with a number of potential intervention options, and further undertake assessments on associated flood vulnerability.

The development of the damage modelling takes into consideration a number of alternative engineering measures of community-based flood protections (Section 6.2), which has been reviewed in Chapter 2. The selected alternative measures were influenced by the study area selected, in this case an urban area in Teddington, west of Greater London, downstream of the Lower Thames River. A proposed flood protection scheme for the area by the EA has brought to light the suitability of community-based measures for the area (more explanation on the proposed intervention from the EA in Section 6.4.1). However, it should be stressed that the attempt to construct modelling approaches of flood damages correspond to the selected measures is mainly proposed by virtue of the gaps identified in the literature that was found later on when the risk-based optimization is aimed to be applied to the area. Furthermore as highlighted in Chapter 2, it was found that quantitative approaches in estimating flood vulnerability associated with alternative community-based measures, such as the property-level protection and/or embankments for cost-benefit analysis are still developing and knowledge on the relative performance of the measures is still limited. The objective of this study, therefore, focuses on micro-scale damage modelling. This includes developing approaches to modelling flood damage associated with a number of potential intervention options, and further undertake assessments on associated flood vulnerability.

The modelling approach designed in this study consists of consecutive pre-processing activities (Section 6.3) that incorporates the concept of vulnerability assessment discussed in Chapter 3. The damage functions targeted from the study use flood discharge as the determinant. This is to enable a consistent formulation with the PDF components in the risk-based optimization procedure, which will be undertaken in options appraisal later in this thesis.

The feasibility of the proposed methodology is examined by applying the vulnerability assessment to the selected options (Section 6.4). Information from DEM, historical flood events and spatial distribution of residential properties are used for the configuration of the damage model. The final outputs are in the form of damage-discharge curves associated with the options considered (Section 6.5). The chapters ended with discussions on the advantages and limitations of the proposed modelling approach and conclusion.

6.2 Intervention options

Four types of community-based flood protection options appropriate for local intervention were selected for this study (Table 6.1); flood embankments, property-level protection (PLP), channel modification and combined PLP and embankment protections. The embankment is the earth type embankment proposed to be constructed adjacent to the river, PLP considered is the resistant-type package suggested by DEFRA (Aug 2012). The PLP is assumed to enable the properties to be resistance from floodwater up to a 0.6 m elevation level from ground floor level, whilst the channel modification refers to the channel dredging activity.

The modelling approaches of Option 1, Option 3 and Option 4 as listed in Table 6.1 have been designed to allow flexibility for a convenient execution of vulnerability assessment considering a range of possible flood protection designs, whilst Option 2 is considered as a fix intervention with a 1 meter depth of channel dredging. A base case of do-nothing that represents the status quo of the local area is considered alongside the alternative options for the vulnerability assessment. This will allow comparison of outcomes and further preparing for the risk assessment to be undertaken for Chapter 7.

Table 6.1: FRM intervention Options considered for the flood damage assessment

Option	Approaches
Option 1	Earth embankment along the river side and adjacent floodplain.
Option 2	Channel deepening of 1m deep excavation of the river.
Option 3	Resistant type property protection protects up to a 0.6 m height of each individual protected houses.
Option 4	Earth embankment along the river side and adjacent floodplain, and resistant type property protection protects up to a 0.6 m height of each individual protected houses.

6.3 Development of flood damage modelling approach

The SPRC and the vulnerability concepts as reviewed in Chapter 3 are the cornerstone of the development of the modelling approaches in this study. The modelling approaches for the analysis of the susceptibility related to flood propagation and the exposure related to flood receptors were carefully configured by taking into account the influence that each intervention option has on the expected flood depth and extent. The modelling approaches were also tailored with respect to the physical properties of the case study area.

Taking into account the considered intervention options, two approaches were designed for the susceptibility analysis in simulating flood propagation and inundation. The first approach assumes a consistent maximum flood level between the river and the adjacent floodplain in the event of flooding. This assumption is applied for the base case and options with channel dredging and PLP, respectively. Although it is recognized that property protections may imply difference in water levels, the influence of PLP is assumed negligible since in general most buildings stand separately from one another (Boettle et al., 2011). This lead to a similar condition as to the base case, hence the same stage-discharge relationship. The effects of increasing capacity of the river by dredging, on the other hand, create a modified cross-section that will generate a different resulting stage-discharge function.

The second approach adopts a more elaborated approach, where varying water levels between the river and the floodplain due to embankments are considered. As reviewed in Section 3.3.5, flood propagation with embankment protection adjacent to the river may be modelled by considering the

overflow flood volume and floodplain storage capacity. This modelling approach, therefore, is adopted for Option 1 and 4.

The estimation of the stage-discharge relationship can be undertaken using one of the various techniques available (examples are given in the literature review in Section 3.3.5). This study adopts the CES-AES software from HR Wallingford (HR Wallingford Ltd., 2001) to generate stage-discharge relationships associated with the considered scenarios of flood protection. CES-AES model outputs are subjected to an assumption of a consistent flood level across the river and the floodplain during high flow events. Hence the adoption of the model for the second approach is only applicable for the in-river water level but not for the protected floodplain, unless the embankment is fully overtopped (The use of the software for the stage-discharge relationship is further explained in Section 6.3.1).

For the exposure analysis, a micro-scale assessment involving discretization of buildings that are exposed to flood risk and identification of their relative elevations are to be undertaken. Potential damages to each affected buildings associated with a range of flood levels will be interpolated from an appropriate depth-damage function. This study takes into account discrete data of depth-damage curve from MCM of Penning-Rowsell et al. (2010) and focuses on direct tangible damages to residential properties.

Given all the assumptions, the overall flood damage modelling approaches can be distinguished into two main modelling chains. A less extensive modelling chain is designed for options that do not consider embankments, i.e. Option 2 and Option 3 (Figure 6.1). A more elaborated modelling chain is designed concerning options with embankments, i.e. Option 1 and Option 4, (Figure 6.2). The latter considers overflow volume estimation. The methodological framework illustrated in Figure 6.1 is also applicable for option with embankments in conditions where inundation levels in the floodplain area exceeds the embankment crest-level.

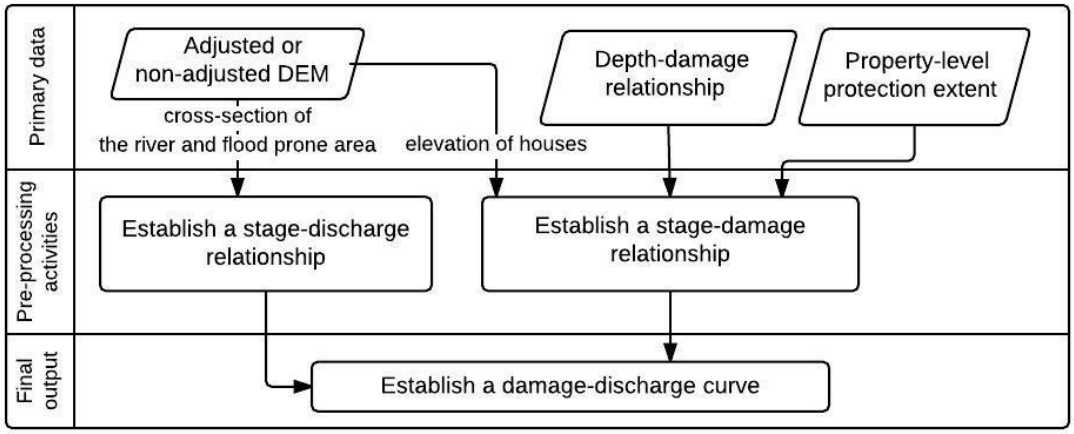

Figure 6.1: Main steps used in the study to estimate flood damage of local area without embankment protection (Option 2 and Option 3).

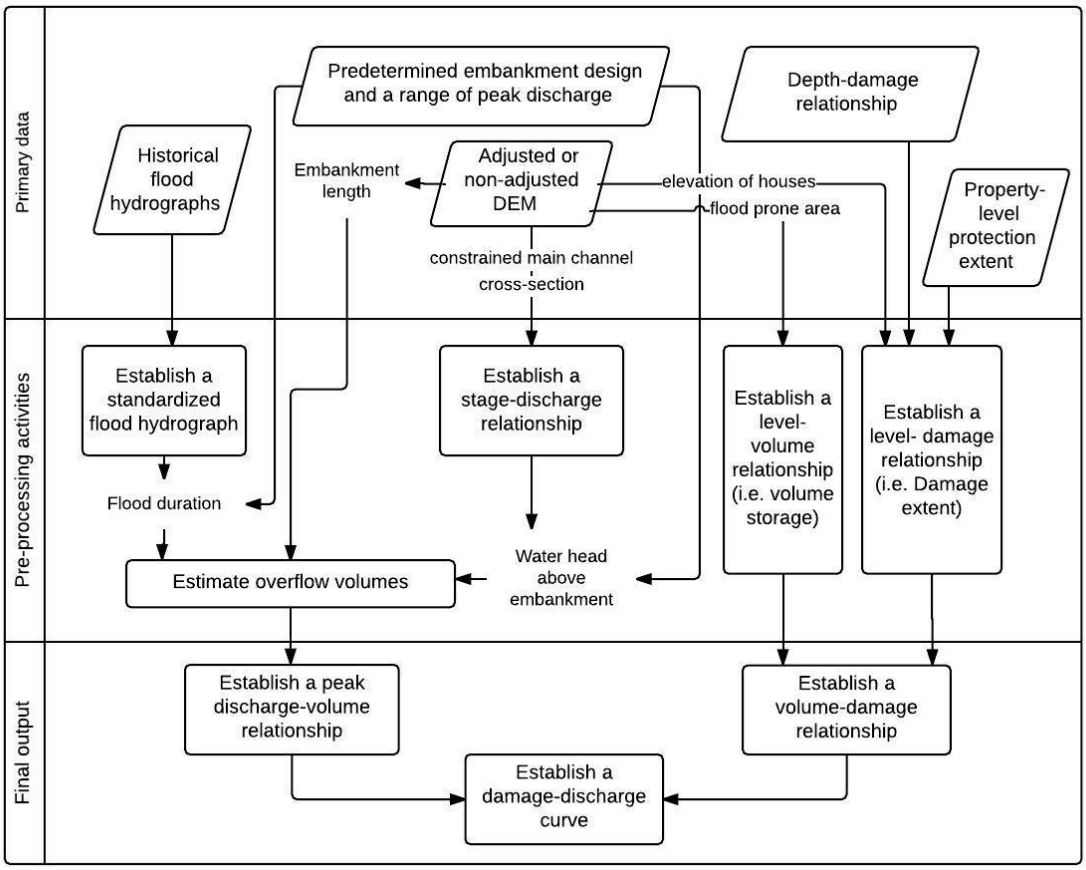

Figure 6.2: Main steps used in the study to estimate flood damage of local area with embankment protection (Option 1 and Option 4).

The modelling chain is built upon dominant steps (refer to the far left column of the figures): (1) Identifying primary information required for the modelling work. (2) Pre-processing activities of the primary input data to generate appropriate formulation for the final assemblage. (3) Assembling

data for the final outputs. Note that the susceptibility and exposure analysis are implicitly incorporated within the modelling chains. The final target from the modelling is to assess the vulnerability associated with each option in the form of a damage-discharge curve, respectively. Hence, the comparison of the final outcomes will be more of a qualitative rather than quantitative.

Section 6.3.1 to Section 6.3.4 describe the model construct related to the susceptibility analysis, whilst Section 6.3.5 propose a mathematical modelling to estimate the extent of flood damage. Section 6.3.6 provides the assemblage of associated modelling components to obtain a damage-discharge relationship of each considered option. The assumptions and limitations of the modelling approaches are discussed in more detail in Section 6.3.6.

6.3.1 Stage-discharge relationship

It is assumed that a particular maximum flood water level that exceeds the riverbank would form a plane of water in the floodplain area that is as high as the water level in the main channel, unless an embankment is considered between the river and the floodplain.A stage-discharge relationship estimated using the CES-AES estimation with the same assumption is adopted in this study. The CES-AES hydraulic estimation is considered adequate to model the stage-discharge relationship given a fairly regular floodplain geometry (Knight et al., 2010). The software comes with an intuitive user interface and requires specification of a cross-section, river slope and zones of the cross-section to run the inbuilt hydraulic model. The cross-section elevation data can be inserted into the CES-AES software and processed to return a stage-discharge relationship.

A cross-section of the area of interest can be extracted from available DEM using a GIS software by introducing a straight line approximately perpendicular to the river. The elevations along the line should be able to represent the whole area of interest. DEM is an effective source of information for spatial analysis, but it is known to return poor ground elevations for cells that are covered with water bodies (de Moel, Asselman and Aerts, 2012). A more accurate data, for example of a river geometry (e.g. to identify the bankful stage for hydraulic analysis), can be obtain using additional

information from surveys that is often made available by authorities or similar agencies (Arrighi et al., 2013).

Damage-discharge derivations of Option 2 and 3 directly uses the stage-discharge relationship (i.e. without a complex pre-processing activities as depicted in Figure 6.1). For Option 1 and Option 4, the damage-discharge relationships are derived through a chain of intermediate steps. For options considering embankment protection (Option 1 and 4), an in-river stage-discharge relationship generated from the CES-AES software is used to estimate the overflow volume (Figure 6.2). Another input to estimate the overflow volume is information of flood events duration. Section 6.3.2 describes how flood events durations can be extracted from standardized hydrographs. The proposed approach to estimate overflow volume in the case of having an embankment protection is proposed in Section 6.3.3.

6.3.2 Standardized hydrograph

The proposed methodology of vulnerability assessment considering options with embankments requires an estimation of overflow flood volume. A standardized hydrograph represents a simplification of information gathered from multiple historical flood hydrographs of flood events. It is dimensionless, hence is adaptable for different sort of analysis Different forms or names of standardized flood hydrograph can be observed from the literature (e.g. Sherwood, 1993;Dunsmore, 1997), but a typical standardized flood hydrograph builds upon discharge to peak ratio (q/q_p) against time. An overflow volume corresponds to a particular peak discharge and design discharge can be estimated using an appropriate standardized hydrograph of the area of interest. This can be undertaken by integrating the upper area of the standardized hydrograph to obtain the overflow volume, which is simply the average magnitude corresponding to the peak and threshold discharge assigned and not intended to reproduce an actual condition (Sherwood, 1993).

In calibrating the standardized hydrograph, a reasonable number of samples among the largest peak flow events should be identified from available historical records. Hydrographs of the selected events are then constructed from associated time series and standardized against their peaks to yield

a dimensionless hydrograph that return $q/q_p = 1$ as their peak. The peaks should be aligned together to form a unity peak. Taking the mean or median of the ordinates at each time step, the average standardized hydrograph can then be derived.

For each hydrograph from the historical records, it is important to carefully choose a start and end flow magnitudes that are larger than the expected smallest magnitude of flood that may cause damage to the most vulnerable receptors. It is also necessary to eliminate outlier events prior to quantify the average standardized hydrograph. The outliers can be of those caused by different flood-generating mechanisms, for example, events that are caused by localised precipitation instead of catchment response flood events (Dunsmore, 1997). These can be identified from available historical information or simply by visual inspection of the shape of the standardized hydrographs. . The elimination of the outliers is crucial to reduce bias in the median standardized hydrograph. Nonetheless, peculiar hydrographs should be removed with caution as to not discard unnecessarily. The process to obtain a standardized hydrograph is simplified in Figure 6.3.

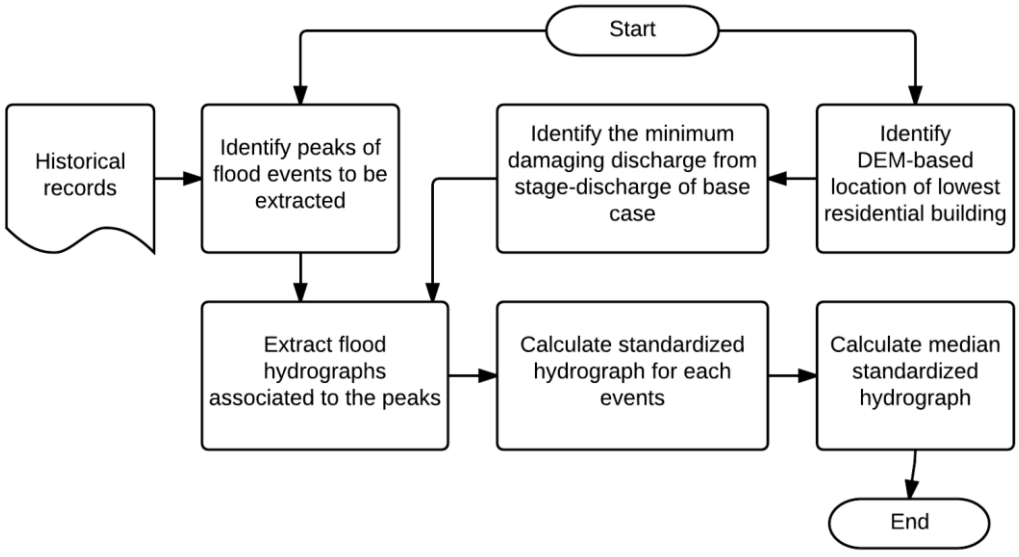

Figure 6.3: Flowchart to construct a median standardized hydrograph from a range of flood events.

6.3.3 Overflow flood volume

The assessment of vulnerability associated with options with embankments (i.e. Option 1 and Option 4) assumes that floods exceed the embankment crest level will cause an overflow that

consequently result in inundation on the protected floodplain area. The proposed estimation of the overflow flood volume (V_{ds}) follows the well-established weir equation (de Kok and Grossmann, 2010). The equation (equation 5.1) is driven by the inflow rate (q_{in}) and the duration of the flood event, which requires information on the length of the proposed embankment (L), the water head above the embankment (h_{ds}) and the start (t_L) and end time (t_R) of the flood event in days.

$$V_{ds} = \int_{t_L}^{t_R} q_{in}\, dt$$

$$q_{in} = 1.705L(h_{ds})^{3/2} \quad (5.1)$$

$$V_{ds} = 1.705L \int_{t_L}^{t_R} (h_{ds})^{3/2}\, dt \quad (5.2)$$

As previously highlight, the duration of the considered extreme flood event is obtained from a standardized hydrograph. The water head based on the difference between the design and peak water levels (m AD) is estimated by interpolating the stage-discharge relationship of the constrained main channel. The appropriate location of the embankment, which indicate an approximate length of the embankment, can be identified using the topographical elevations of the area. An appropriate length of the embankment is to be identified by specifying a maximum height of the embankment (e.g. 3 m maximum crest level) and establishing a straight line that intersects the maximum elevation of the DEM at both ends. This can easily be undertaken using GIS tools.

The standard weir equation presented in Equation 5.2 can account for backwater effects (e.g. Dutta et al., 2013;Arrighi et al., 2013). The backwater effects are more likely to happen when the head of water above a crest level downstream of the weir exceeds the critical depth, which is when the downstream water head is more than $0.66h_{ds}$ (Hamill, 2011, pg. 343). As the length of the crest level can be expected to be far greater than the inflow water head, the phenomenon might be unlikely to occur especially for high frequency flood events. Floodplain storage capacity is also intuitively large enough to accommodate overflow floodwater for such events before the critical depth is exceeded and causing the backwater effects. For the present methodology, we isolate the influence of the backwater effects in the analysis.

The overflow flood volume can be estimated for a range of peak discharges and a range of possible protection designs. A practical way to compute this is through an automated computation that can be repeated with a relatively large input datasets.A systematic automated approach can further eliminate manual multiple calculations (i.e. for the water head and flood duration corresponds to each given peak discharge and protection design), hence increasing the adaptability. Considering a range of peak flows (q_p), where each is associated with a constant design protection ($\hat{q}$), Figure 6.4 proposes a systematic way to model the overflow volume. The activities that supply inputs into the calculation process, i.e. the stage-discharge relationship and the standardized hydrograph derivations, are highlighted in the grey boxes. The final product is a peak discharge-volume relationship conditional to the $\hat{q}$.

The computation is designed to enable ease of handling multiple inputs of peak discharges conditional to a specified protection design. Furthermore, it can be repeated by varying the magnitude of the protection design. The proposed computational tool is particularly useful for a risk-based optimization, where multiple scenarios of flood events and possible range of protection designs are to be evaluated. The tool can still be adopted for a particular flood loading and/or protection design by specifying only one input to each of the respective variables.

The workflow in Figure 6.4 begins with the identification of a reasonable $\hat{q}$ and a set of q_p. Each q_p should have a higher magnitude than $\hat{q}$. The set of q_p is indexed (j) and used individually in the subsequent computation. For each q_{p_j}, a flood discharge generating sequence that represents the sequence of inflow floodwater (q_{in}) is formed conditional to the q_{p_j} and $\hat{q}$. The q_{in} is incrementally indexed (k) and transformed to a set of standardized discharges using the input information of q_p (i.e. in the form of ratio). Note that each of these standardized discharges is attributed to a start and end time of a flood event (denoted as t_L and t_R, respectively) using the previously derived standardized hydrograph. Hence, a pair of t_L and t_R corresponds to the flood generating sequence of k was subsequently interpolated for all k. To obtain the associated flood duration, an incremental flood event time step conditioned to the q_{p_j} and $\hat{q}$ is then established.

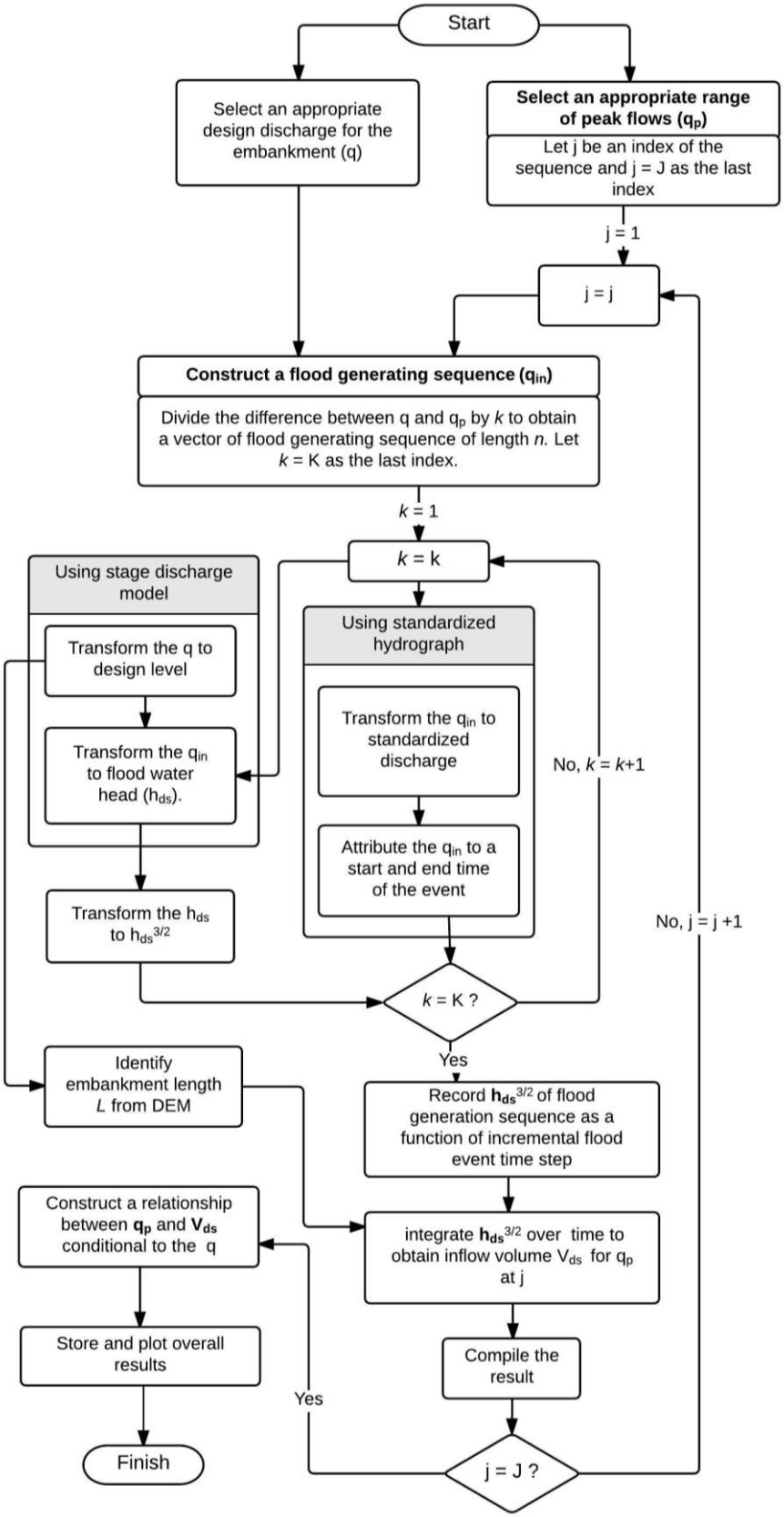

Figure 6.4: Flowchart to establish a peak discharge-volume relationship conditioned to embankment protection design. Pre-processed stage-discharge relationship and standardized hydrograph are embedded within the process.

The next step is to estimate the sequence of h_{ds} corresponds to the incremental q_{in}. First, the stage-discharge curve of the confined main channel that previously constructed is interpolated to obtain the embankment design level and water level correspond to $\hat{q}$ and q_{in}, respectively. The h_{ds} is subsequently obtained by subtracting the embankment design level from the water level. Note that the h_{ds} obtained resembles an incremental level of floodwater from the assigned $\hat{q}$ to q_{p_j}.

The sequence of h_{ds} of a condition of floodwater receding is then estimated following the same procedure. The dataset of water head of floodwater increasing and receding over the time period is established for the specified flood event and protection design. The resulting consecutive h_{ds} of the full event is then transformed into ${h_{ds}}^{3/2}$, and appropriately paired with the previously obtained incremental flood event time step. The V_{ds} is then solved numerically using the information of ${h_{ds}}^{3/2}$ and associated time of occurrence (Equation 5.2). The lower and upper limits for the integration are represented by the t_L and t_R associated with the particular $\hat{q}$ and q_{p_j}.

Repeating the above steps for the other q_{p_j} will return a range of overflow volumes associated with the considered range of peak discharge, hence returning a peak discharge-volume relationship. The repetitions for a number of protection designs will generate a multiple peak discharge-volume relationships conditional to the design discharges. For such simultaneous computations, the inputs comprising minimum and maximum magnitudes of design and peak discharges should be reasonably chosen in accordance to the specific area of interest. Through the development and testing of this tool, it became clear that a conditional function should be introduced prior to the execution of the automated computation to only limit the assessments for q_p that are higher than the assigned $\hat{q}$, and specify the output to be zero for $q_p < \hat{q}$. Attention should also be given to the assignment of input data in order to reduce unnecessary repetitions of trials and errors. Some recommendations are given below:

1) The considered minimum and maximum protection designs for the analysis should be reasonable. For example, a minimum 0.3 m and maximum 2.5 or 3 m crest height.

2) A minimum peak discharge set for the analysis should be higher than the predefined minimum design discharge, as to simulate events of flooding.
3) A ratio between q_{in} and q_p should be higher than the lower boundary of the configured standardized hydrograph. This means the maximum peak discharge should be realistically selected (presumably not too high) in order to successfully model the overflow volume. If for some reasons the assessment is to involve a higher peak discharge that result in a smaller ratio between q_{in} and q_p than the lower boundary, then the standardized hydrograph may need to be extrapolated. However, it should be aware that extrapolation might yield an unrealistic estimate due to the scarcity of the most extreme flood events used to derive the standardized hydrograph.

The estimated V_{ds} from the automated computation as described above can be verified using an alternative estimation approach. A discrete computation to solve Equation 5.3 can be used to verify the results of the previous approach. This equation is built upon a similar weir equation as the root function. The input variable of $\hat{q}$, q_p and L should be consistent with the data used in the automated computation for the verification to be valid. $q_{in_{i+1}}$and q_{in_i} in Equation 5.3 refer to q_{in} at time i. They can be obtained by solving the Equation 5.1 with h_{ds} extracted from the interpolation of the stage-discharge relationship of the constrained main channel. The associated t_{i+1} and t_i should be extracted from the standardized hydrograph. The summation of the discrete results for all n parts of the event ultimately return the total overflow volume.

$$V_{ds} = \sum_{i=1}^{n} \left(\frac{q_{p_{i+1}} + q_{p_i}}{2}\right)(t_{i+1} - t_i) \tag{5.3}$$

6.3.4 Floodplain storage

As given in Figure 6.2, another important activity to supply input for the damage model for options with embankments is the quantification of floodplain storages correspond to flood inundation. This information is required to generate a relationship between possible flood inundation levels and the corresponding volume within the floodplain area. Further, it is required to establish a connection between the flood hazard, i.e. the peak discharges, and the flood consequences, i.e. the expected

damages. Figure 6.5 presents a proposed methodology for the flood storage delineation and for the establishment of the water level-volume relationship.

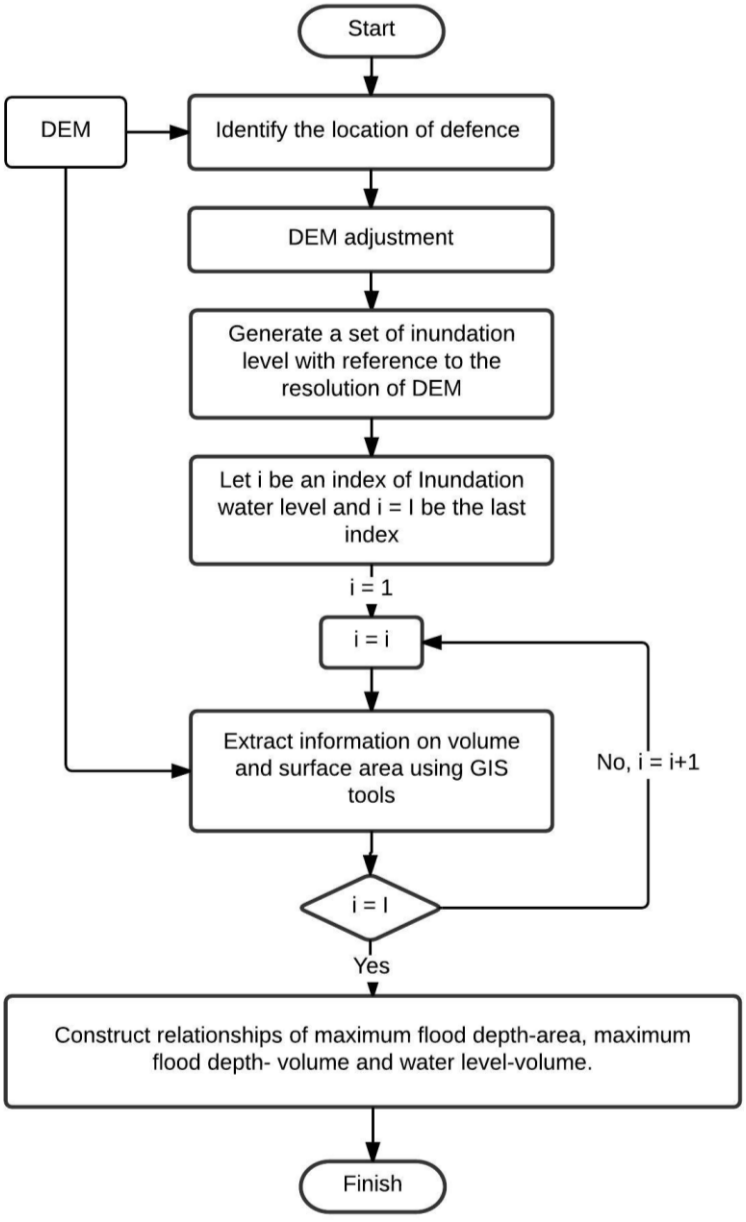

Figure 6.5: Flowchart of the storage volume estimation corresponds to a range of flood inundation levels for the water level-volume relationship. Relationships pertaining other relevant variables are also extracted from the method.

A range of hypothetical embankment crest levels should first be established in the DEM using the GIS tools. In the modelling chain designed for this study, the establishment of the embankment crest levels is to be undertaken during the modelling of overflow volume (Section 6.3.3). It is assumed that the embankment provide protection up to a stage where water level from the river exceeds the embankment crest level, hence the study only considers cases of functional failure. A

range of inundation levels on the protected area is subsequently established up to an associated embankment crest level. A range of corresponding horizontal planes of the established flood levels will then be introduced using associated contour lines as their boundary. Figure 6.6 provides an illustration of a horizontal plane and how it intersects with the topographical surfaces. For each established flood level i, associated information of volume and surface area, as well as the associated water depth are obtained using available functions from the 3D analysts toolbox (ESRI, 2012). The relationship of water level-volume and surface area-volume are subsequently constructed from the outcomes.

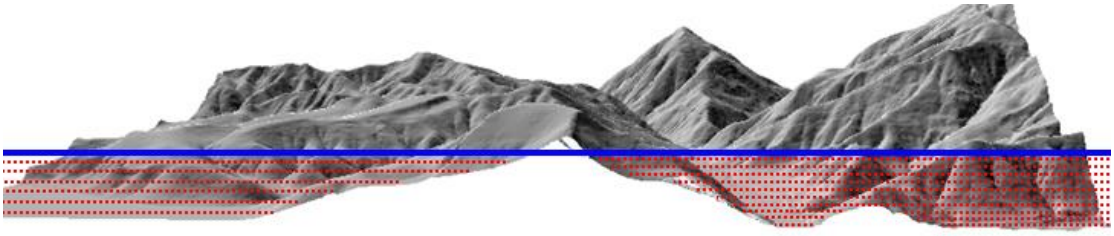

Figure 6.6: Schematic illustration of a storage volume estimation using a defined inundation level across a topographical location feature (ESRI, 2012)

The water level-volume relationship established from this task is brought forward in the modelling chain to establish the ultimate damage-discharge relationship. As presented in Figure 6.2, this requires the identification of damage extent in terms of the potential economic damage due to the flood level or flood volume. A rigorous approach that can be used to identify the damage extent is presented in more detail in Section 6.3.5.

6.3.5 Damage extent

A micro-scale assessment is adopted in this study. The approach considers exposure of individual objects/buildings to flooding, where direct and tangible flood damages of residential properties are of concerns. The key information related to the object-oriented assessment is locations of the buildings (i.e. ground floor elevation), density of buildings in the area of interest, and their values in the form of a depth-damage relationship.

The density of buildings of residential properties can be segregated according to types of houses, for example Semi-detached, Terrace, etc. This information can be obtained from land survey or

readily available database (Great Britain, Dept for Environment, Food and Rural Affairs, Aug 2012). A unique depth-damage relationship can be attributed to each housing type for the damage assessment, but this implies more time for data collection and modelling effort owing to the aimed micro-scale assessment and further risk assessment. This study, therefore, focuses on average monetary losses of the residential sector instead of the different types of residential buildings.

The density of the residential properties on the flood prone area is to be associated with their ground floor elevation level from DEM grid cells. A list of total number of properties at each incremental elevation step representing their ground floor elevation levels will be generated accordingly. If deemed necessary, the ground floor elevation levels associated with the buildings that are obtained from the DEM can be adjusted to account a higher residential ground floor elevation, for example 10 or 20cm extra (e.g. Boettle et al., 2011). In the case of flooding under base case and other non-PLP conditions, damages will only be considered when floodwater exceeds the ground floor elevation.

Damage extents can be conceptualised by establishing a connection between a range of flood inundation levels and possible flood damages, i.e. level-damage relationship. Note that the term 'level' is used instead of the common 'stage' term to consider the possible differences of water elevations in the main channel and flood prone area in the case of flooding. In order to derive a level-damage relationship suitable for the considered options, two cases are considered for the derivation; one that concerns over having PLP measures installed to buildings and another without PLP installed.

For buildings without PLP installed, a flood inundation depth affecting a building is obtained through substracting the buildings' ground floor elevation from the maximum flood inundation level, provided that the affected buildings' ground floor elevation is lower than the maximum inundation level. All buildings located on the same ground floor elevation are assumed to be experiencing the same consequences due to an assumed consistent flood depth. For example, a 10 m maximum flood inundation level will cause a 3 m flood depth for buildings located at a 7 m elevation level (i.e. 10 – 7 m AD). A consequent total damage for a given flood inundation level

and a given ground floor elevation, therefore, is determined by aggregating flood damages affecting the buildings at the same ground floor elevation level. The aggregated total damages for the flood event is then determined by taking all the total damages associated with each ground floor elevation level of the affected buildings. This procedure is similarly applied for buildings protected with PLP. However, the PLP introduces a resistance effect that reduces the expected total damage.

In reducing flood impacts to a community with the adoption of PLP, buildings located relatively near to the river and at the lower ground are usually the ones that are targeted to be equipped with PLP. Whilst the ones located at the higher ground may not be protected. In effort to construct a discrete mathematical equation for the total damage quantification, it is useful to introduce some referencing notations: Buildings equipped with the PLP measures and located at the highest elevation level as compared to the other protected buildings is referred as the 'highest protected buildings', whilst buildings equipped with the PLP measures and located at the lowest elevation level is referred as the 'lowest protected buildings'. Furthermore, algorithms for the discrete computations of total damages associated with a given maximum inundation level and a targeted PLP extent (i.e. protecting the nearest buildings to the river up to buildings located at a certain elevation level) can be constructed on the basis of several assumptions:

1) Buildings that are protected by the PLP are assumed to be individually resistant to flooding up to a standard height above their ground floor elevations.
2) When a maximum inundation level is lower than the threshold of the lowest protected buildings, all buildings are considered safe from damaging consequences. Otherwise, buildings are considered affected.
3) Once a maximum inundation level exceeds the threshold of the highest protected buildings, all protected buildings are considered affected.
4) When a maximum inundation level is higher than the ground floor elevation of the highest protected buildings, but lower than the PLP threshold level, flood will affects the unprotected buildings located higher than those of the highest protected buildings.

Considering the above assumptions, an algorithm to estimate total damages of flood events considering an area without PLP ($k1$) is denoted in Equation 5.3, whilst for an area with PLP ($k2$) is denoted in Equation 5.4. D_{k1} is to be used for the base case, Option 1 and Option 2, and D_{k2} is to be used for the Option 3 and Option 4. Note that D_{k1} is a special case of D_{k1}. This represents a condition where a maximum inundation level overtop the PLP extent of the highest protected buildings, i.e. the PLPs are no longer effective. The description of the notations used in the equations are explained in the following paragraphs.

$$D_{k1} = \sum_{i=0}^{n} \left(P_{g_{y=n-i}} D_{h_{z=i+1}} \right) \tag{5.3}$$

$$D_{k2} = \begin{cases} 0, \ for\ n < i_f \\ D_{i_f<n<i_p}, \ for\ i_f < n < i_p \\ D_{i_f<n<i_p} + D_{i_p \leq n<i_m}, \ for\ i_p \leq n < i_m \\ D_{k1}, \ for\ i_m < n \end{cases} \tag{5.4}$$

Where;

$$D_{i_f<n<i_p} = \sum_{i=i_f}^{n} \left(P_{g_{y=n-i}} D_{h_{z=i+1}} \right)$$

$$D_{i_p \leq n<i_m} = \sum_{i=i_P}^{n} \left(P_{g_{y=i+1}} D_{h_{z=n-i}} \right)$$

The total damages is influenced by the density of residential buildings (P) on each ground elevation (g), and damage (D) affecting individual buildings, which is determined by flood depth (h). The values of the mentioned variables are attributed to elevation steps of the area of concern. One way to extract the information is through discretization of DEM with reference to the overlaying topographic map. Discretization of the ground floor elevation levels of buildings should begin from the ones located at nearest to the river. Discretization of the flood depth should begin from a point of no damage. It is important to choose a consistent and appropriate length of the sequential steps for the density of buildings and flood inundation depths to allow a successful implementation of the equations. The equally spaced sequence of a consistent length of the variables is indexed with

i as a general reference. Three constraints attributed to i and in relation to the assumptions previously highlighted are introduced in the equations:

1) i_f refers to the elevation level of the PLP's threshold on the lowest protected buildings.
2) i_p refers to to the ground floor elevation level of the highest protected buildings.
3) i_m refers to the elevation level of the PLP's threshold on the highest protected buildings.

The algorithms are designed to solve for total damages by referring to the relative differences between the ground elevation levels of buildings and the maximum flood inundation level (n), and between flood depths and the point of no damage. Indices y and z are therefore introduced to refer to the relative differences, respectively, where both are influenced by the index i. The information of P_{g_y} and D_{h_z} attributed to the discrete elevation steps have to be stored in a look-up table accordingly to allow for referencing when executing the model. Whilst i_p can be obtained directly from the look-up table, i_f and i_m can be determined by accommodating the elevation levels of the PLPs' threshold with the information in the look-up table.

.

The damage functions as described above is easy to adopt for repeatable computations involving multiple possible maximum flood inundation. An assigned extent of the PLP on the flood prone area can be specified by setting a targeted design discharge for the PLP, for example by using the return period for stationary assumption, followed by an interpolation of an associated stage-discharge relationship to identify the corresponding stage. The corresponding stage reflects the ground floor elevation level of the highest protected buildings. Considering a range of PLP extents will ultimately provide a range of unique level-damage relationship, hence better insights on the relative effects. The resulting level-damage relationships are then brought forward into the final

6.3.6 Damage-discharge relationship

The aim of the modelling effort is to construct damage-discharge relationships influenced by the considered protection options. These relationships reflect the flood vulnerability of the given

conditions. The damage-discharge relationships for the conditions without embankment protections (Option 2 and Option 3) are directly obtained using the stage-discharge and level-damage curves from methodologies presented in Section 6.4.2 and Section 6.4.5, respectively (refer Figure 6.1 for the complete workflow). For the conditions with embankment protection (Option 1 and Option 4), additional consecutive steps are involve in the construction of the damage-discharge relationships (refer Figure 6.2 for the complete workflow). Hence this section is dedicated to explain how the outputs from previous modelling efforts can be assembled to construct damage-discharge relationships of Option 1 and Option 4.

As identified in Figure 6.2, two essential inputs in deriving the damage-discharge relationships of the options are the peak discharge-volume relationship and volume-damage relationship. The peak discharge-volume relationship with respect to a specified design discharge is obtained from the overflow volume estimation in Section 6.3.3. On the other hand, the volume-damage relationship is constructed by first compiling the databases of volume storage (Section 6.3.4) and damage extent (Section 6.3.5) according to a specified range of inundation levels. A volume-damage relationship is then formed from the set of pairs of volume storages (e.g. in m^3) and damage extents (e.g. in £), which is tabulated according to associated inundation levels.

The methodological setup in this study adopts the assumption that the water level on the floodplain is consistent with the water level in the main channel when a flood protection level is exceeded. This assumption leads to the use of the base case stage-discharge relationship for flood events that exceeds the limit (e.g. Heidari, 2009;e.g. Hine and Hall, 2010;Jonkman et al., 2009b;Mays, 2011). An indicator (Q_{lim}) that allows a running model to switch from using the default peak discharge-volume and volume-damage curves to using the damage-discharge curve of base case for the damage-discharge relationship configuration is therefore introduced. For the Option 4 where PLP is considered alongside the embankment, the configuration of the damage-discharge relationship is assumed to follow that of the base case when a given peak discharge is higher than the considered PLP extent. Therefore, an additional indicator for this condition ($Q_{p.lim}$) is introduced to the modelling arrangement of Option 4.

Taking into account the introduced constraints, the design workflows to obtain the damage-discharge relationships for Option 1 and Option 4 are depicted in Figure 6.7 and Figure 6.8, respectively. Both workflows are designed to allow multiple computations given a range of possible extreme events. They were also arranged to accommodate for a range of possible protection designs. These settings provide the advantage of ease in handling multiple datasets, especially when risk-based optimization methodology is to be adopted.

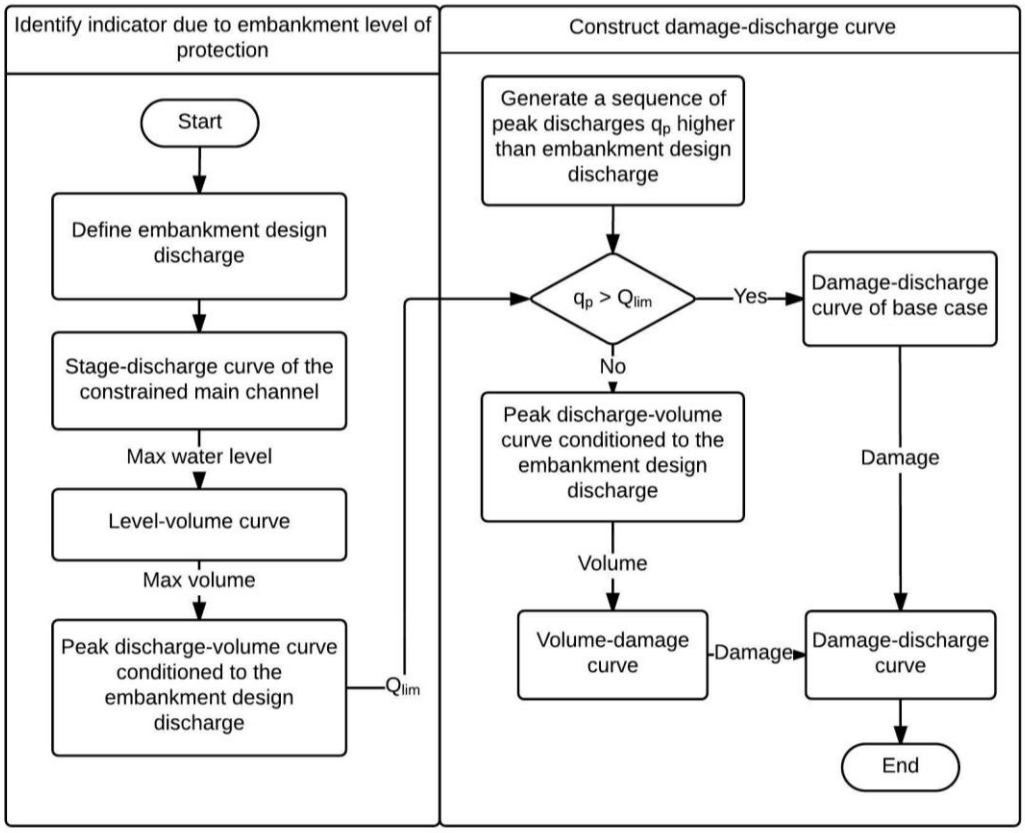

Figure 6.7: Flowchart of the damage-discharge curve derivation steps with indicators' function for Option 1.

As can be seen in Figure 6.7 the workflow is divided into two stages for Option 1. The first stage refers to the identification of Q_{lim} through the use of the pre-processing modelling outputs. The second stage involves comparing q_p of interest individually with the identified Q_{lim} to direct the computation to the appropriate next approach. If $q_p \leq Q_{lim}$, the corresponding overflow volume of the q_p is used to estimates the flood damage. Otherwise, the flood damage is estimated using the

damage-discharge relationship of the base case. The damage-discharge relationship of the base case, therefore, should be determined prior the damage assessment of Option 1.

In Figure 6.8, three stages were allocated to derive the damage-discharge relationship of Option 4. The first stage deals with the identification of $Q_{p.lim}$ through the use of input and output from the pre-processing modelling activities. $Q_{p.lim}$ is compared to the q_p of interest before directed to the next stage. If $q_p \leq Q_{p.lim}$, no damage is assumed due to the lower peak discharge as compared to the PLP design discharge. Else, the q_p is directed into the second stage where it is compared with the Q_{lim}. The identification of Q_{lim} is similar to the stage 1 of the Option 1, but slightly different in the consecutive stages. In the third stage, if $q_p \leq Q_{lim}$, the water level corresponding to the resulting overflow volume of the extreme discharge is used to estimate the flood damage. Otherwise, the damage is estimated using the level-damage relationship of PLP, triggered by the identified water level corresponding to the q_p from the interpolation of the stage-discharge relationship of the base case.

In preparing for further risk assessment, it is important to ensure that the data collected for the vulnerability assessment is sufficient to capture the damaging consequences of the low probability extreme floods. However, such information relies on past extreme events, which is scarce in nature. Hence, users might not have a solid basis in determining an appropriate extent of data to be collected. In the absence of historical information, an initial configuration and testing assemblage of the models is necessary. Iterative numerical computations and repetition of data collections are likely unavoidable. For example, one may have to collect more data as the specified initial range of water levels does not cover the full range of damaging flood events for the risk-based assessment. Consequently, this would lead to collecting more data on the density of flood receptors located on higher elevations, as their exposure will influence the overall flood damage. Unnecessary repetitions can be avoided by identifying an appropriate maximum extreme event through probabilistic exploration. The corresponding flood inundation level of the maximum discharge, and

the extent of flood receptors affected can then be identified. This will provide a good basis to determine the extent of data to be collected.

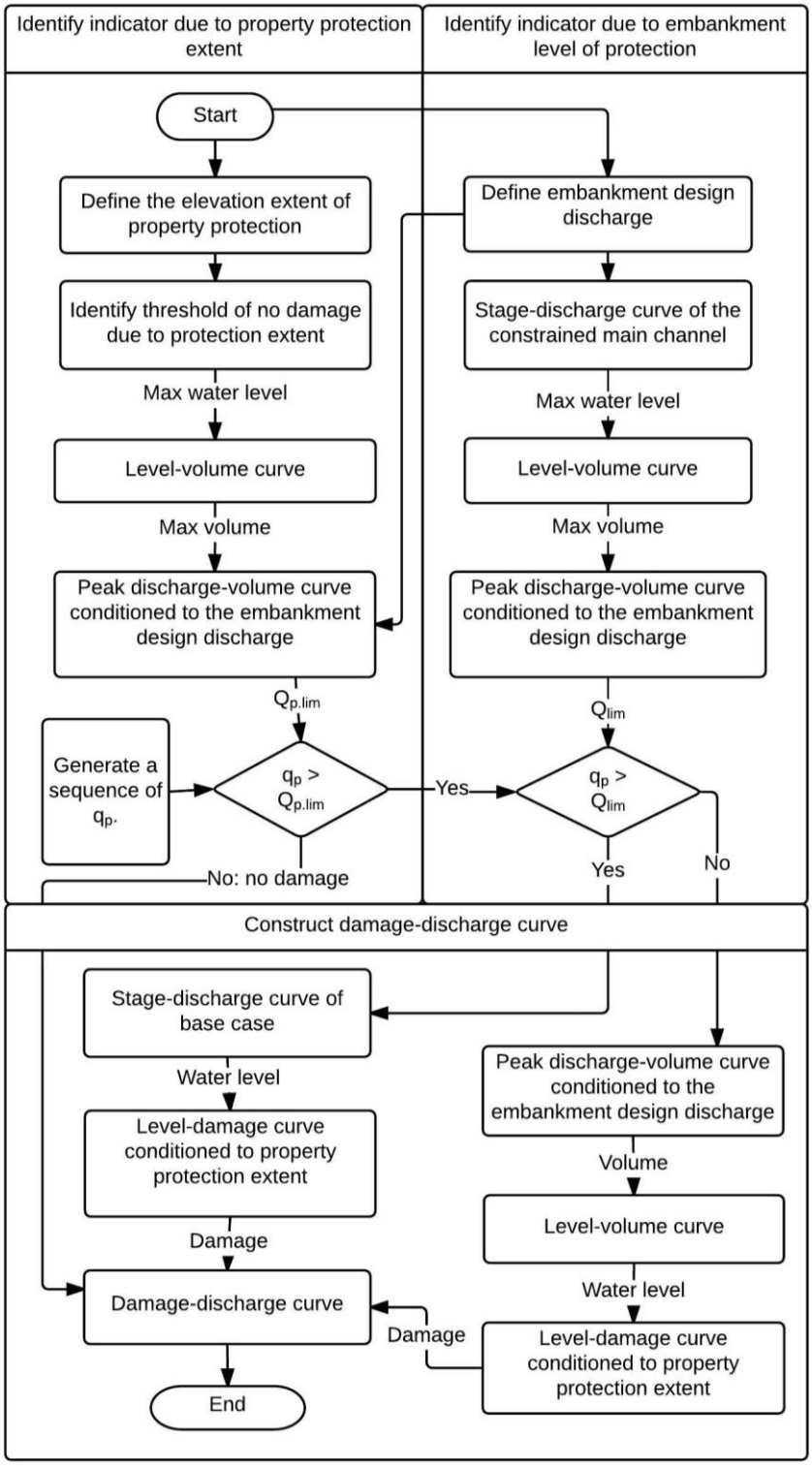

Figure 6.8: Flowchart of the damage-discharge curve derivation steps with indicators' functions for Option 4.

6.4 Application

6.4.1 Introduction to the case study

As mentioned before, the alternative options of the community-based protection chosen in the thesis were influenced by the location of the Teddington area in the Lower Thames. The location was further selected for the application of the proposed methodology. According to the Environment Agency (Aug, 2010), the Lower Thames is one of the largest and most at risk developed but undefended flood plains in England, with 21,000 properties and 50,000 people currently at a 0.5% annual exceedance probability flood risk or higher. Environment Agency anticipate that the consequences of flooding in some parts of the area are to be severe and suggest that climate change could exacerbate the impact (Aug, 2010). In 2009, the Environment Agency initiated a long-term strategic plan for reducing flood risk for the Lower Thames. The project, which was expected to costs approximately 500 million pounds at that time, developed a protection plan for the floodplain from Datchet to Teddington.

In their preliminary study, approximately 40km^2 area of Lower Thames that will be benefited from the plan is divided into two reaches, Reach 3 and Reach 4, due to distinct topographical characteristics. Reach 3 represents Datchet to Walton Bridge, and Reach 4 represents Walton Bridge to Teddington (Figure 6.11). Reach 3 is mainly a flat and wide floodplain with many branching and converging flood routes and compartments while Reach 4 is more of a confined and less extensive area exposed to flood risk (Great Britain, Aug, 2010).

The Environment Agency preliminary study concluded that a flood diversion channel would be an appropriate structural intervention for Reach 3 and the target date to commence construction is by mid-2019. Community-based flood protection measures including flood defence scheme and PLP was concluded as the appropriate intervention for Reach 4 due to its relatively lower risk. The protection intervention in Reach 4 is estimated to protect approximately up to 1000 properties that are most vulnerable to flooding. The preliminary stage appraisal also ruled out dredging because of possible ecological impacts. However, maintenance dredging has been considered for limited parts

of Reach 4 to compensate the effects of diversion channel in Reach 3, provided permitting findings from environmental surveys.

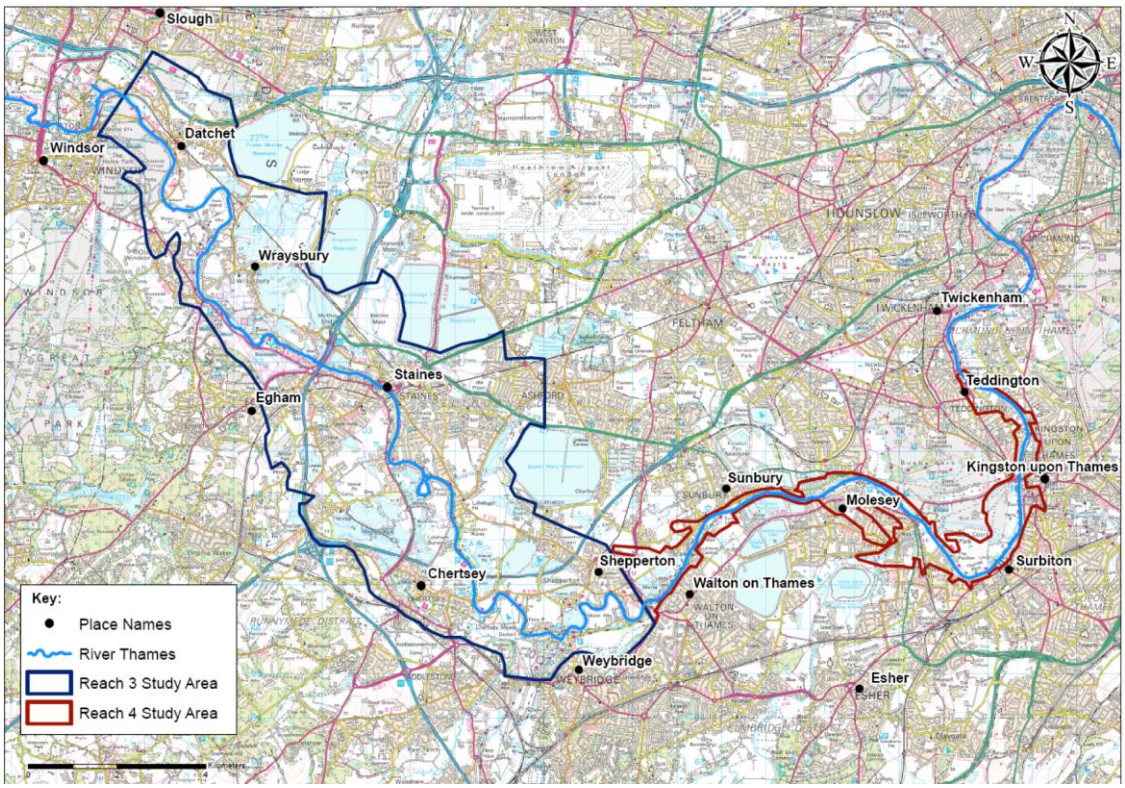

Figure 6.9: Map showing encircled Reach 3 (left hand side) and Reach 4 (Right hand side) of the Environmental Agency's Lower Thames Flood Risk Management Strategy. (Environment Agency, April, 2010)

The EA reported that it is difficult to be ascertained of an optimum level of protection for the community-based protection for Reach 4 (Environment Agency, April, 2010). Ultimately, they suggested a fixed standard protection with a minimum 1.33% annual exceedance protection (1 in 75 years return period) for the flood defence design level. This protection design is consistent with the ABI requirements for house insurance, and was said be refined in the future according to the topography and physical arrangement of the area (Environment Agency, April, 2010). For individual house protection, the EA suggested a minimum design standard of 5% annual exceedance probability (1 in 20 years return period), consistent with the recommendation from a PLP study by DEFRA (Aug 2012). These target protection is to be applied to a group or individual properties deemed practicable and subject to further revision (Environment Agency, April, 2010).

It is clear from this review that the risk-based optimization of the flood protection measures were not being undertaken.

To test the feasibility of the proposed methodology on a real location, we chose an approximately 1km stretch of a river reach across the suburban town of Teddington of Reach 4. The place is suitable as it is located exactly downstream of the gauging station of Thames at Kingston, where the source of flood hazard would be characterised. The selected area is protected from tidal surges by weirs located just downstream and by the high standard protection from the Thames Barrier located farther east (Penning-Rowsell et al., 2013). Teddington predominantly is a residential area that is heavily developed and urbanised.

The Teddington reach has undergone several human/engineering interventions in the past. One of such examples is a modification of the channel conveyance capacity in 1935 and another intervention following the 1947 flood (Marsh and Harvey, 2012). It is also gathered from the historical evidence that the 2003 flood with a magnitude of ~460 m^3/s did not cause any local overspill along the Teddington reach and no flood damage was reported. From the flood frequency distribution of the data in Chapter 4, a 460 m^3/s magnitude of flow discharge corresponds to approximately 10-year return period of stationary condition. This implies that no damage would be expected for flood discharge equal or lower than the flood of this scale.

The previously parameterized flood frequency distribution (refer Chapter 4) and the stage-discharge of status quo (refer Section 6.4.2) were used to identify the maximum flow discharge, i.e. an upper extreme discharge boundary, that is suitable for the application of the proposed damage modelling approach. This action is part of the effort to ascertain that the evaluation includes a reasonable maximum high magnitude of flow discharges for the modelling chain to work effectively. In addition, this is to ensure that a complete range of low probability flood discharge that may significantly contribute to the total flood damage is included for an accurate assessment of risk (the assessment of risk is undertaken in Chapter 7). A flow discharge of 1100 m^3/s corresponds to a 0.002 exceedance probability was selected as the upper extreme discharge boundary for the assessment. Prior investigation from an associated stage-discharge relationship of base case for the

area shows that the magnitude yield an appropriate stage (i.e. in meter AD height) of possible high damage. The flow magnitude corresponds to a 50,000-year return period. Figure 6.10 illustrates the behaviour of the probability curve against observed flow series and how the extrapolation might behave for higher magnitudes. Very extreme flow magnitudes (i.e. higher than 1100 m^3/s) that return very small probability of exceedances were eliminated from the assessment. Given the flexibility of the proposed damage assessment methodology as developed in Section 6.3, the upper limit of extreme discharge suitable for other case studies can conveniently be specified.

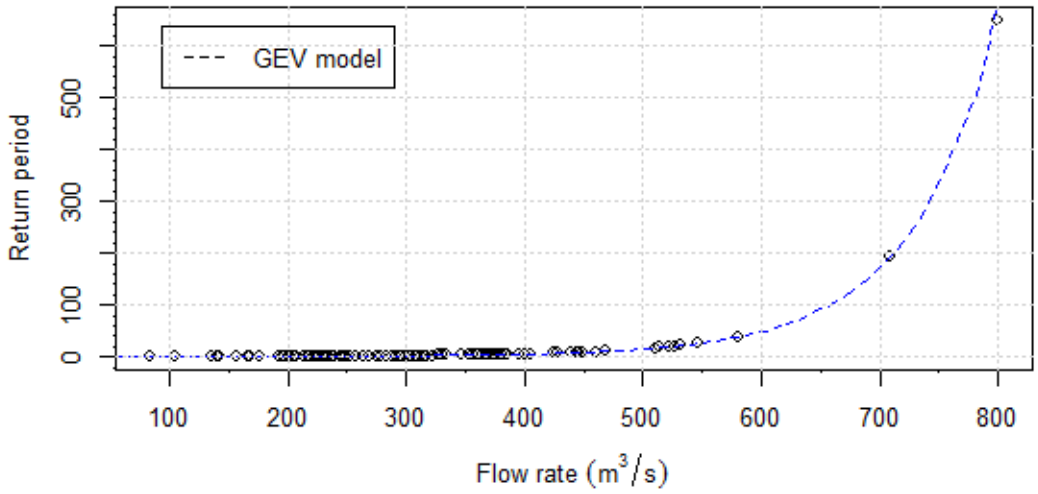

Figure 6.10: Probability curve of Thames at Kingston AM flow records. The plots represent the observations whilst the blue line represents the fitted stationary GEV model from Chapter 4.

The terrain information of the area was obtained using an available LiDAR-based DEM with a vertical accuracy of 10 cm and a grid cell of 1 m by 1 m (Great Britain, Environment Agency Geomatics, 2014). Figure 6.11 shows a raster map of the location with colour-coded terrain elevations. The pink-coloured bend shape on the northeast of the area represents the river stretch, and the flood prone area of concern is located west from the river. The legend of the different coloured contours of 1 m is included on the map. With the help of imagery data and the information from the DEM, the boundary of the flood risk system is defined as the contour of 5.4 m AD of the riverbank until an upper limit contour of 9 m AD of the potential flood risk area.

The assigned boundary served as the reference for data collections for the model configuration. Section 6.4.2 explains the configuration of the stage-discharge relationship. Section 6.4.3 presents the derivation of the standardized hydrograph for the area, followed by the estimation of the

overflow volume and floodplain storage in Section 6.4.4 and 6.4.5 respectively. The damage extent considering the receptors is presented in Section 6.4.6.

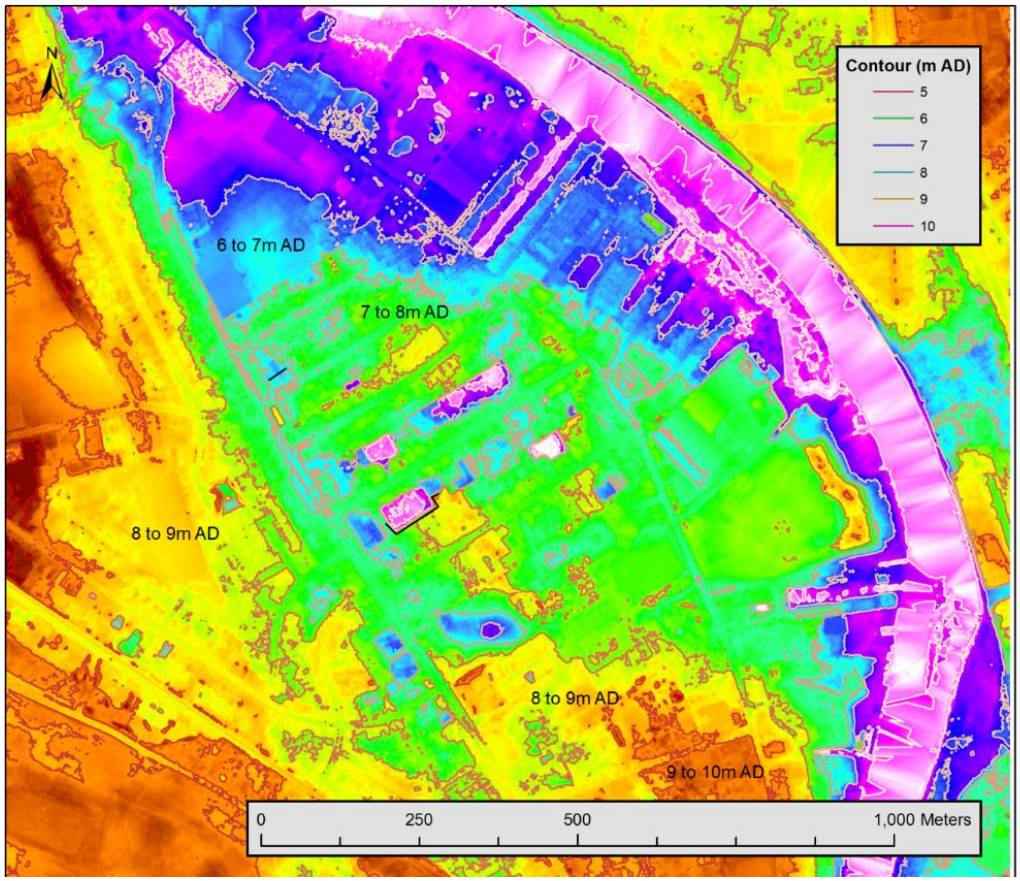

Figure 6.11: Raster map of the location selected for the case study with the range of elevations embedded. Upper right legend shows the different contour elevations. The pink-coloured bend shape on the northeast of the area represents the river stretch, and the flood prone area of the case study is located west from the river. Flood depths were determined by subtracting elevation levels from a specified maximum inundation levels.

6.4.2 Stage-discharge relationship estimation

One cross-section is used to represent the stage-discharge relationship of the study area. The cross-section is established by introducing a perpendicular line to the river and across the floodplain. A suitable location was cautiously selected to represent the terrain of the area. It is assumed that the maximum possible depth of the river follows the bankful stage given in the CEH website (2014), which is 4.77m. The channel depth was later reduced to approximately 1 meter depth to increase the possibility of more damaging flood events for the case study. This is mainly due to the evidence that the historical flood events caused no damaging consequences to the area, even when the flood

magnitude was as high as 460 m^3/s (Marsh and Harvey, 2012). The modification is deemed necessary to ensure that the outcomes of the proposed model can clearly be illustrated. In addition, the modification will further enhance outcomes from the planned risk-based optimization of options appraisal that will be undertaken later on.

Elevations from the established cross-section that were identified from the DEM, zone types of different land use along the cross-section and assumed unit roughness (Table 6.2) were embedded into the CES software to estimate the stage-discharge relationship. An imaginary zone called 'wall' was introduced to include a unit roughness for embankment wall to estimate a stage-discharge relationship of a constrained main channel. The unit roughness are estimated based on Roughness Advisor in the CES-AES software with reference to available imagery of the river reach. To facilitate the modelling for conditions with embankment, the base case cross section is imposed with an imaginary embankment of 9 m AD. The estimated unit roughness for the river bed can be seen to be exceptionally high. This may be due to the shallow depths of the river, where Manning values increase substantially at lower depths and can be up to 0.16 at certain rivers (Knight et al., 2010, p. 57).

Table 6.2: List of zone types and unit roughness assigned in the CES

Zone type (printed name in figure as in parentheses)	**Unit roughness**
River Bank (RBank)	0.0546
River Bed (RBed)	0.102
Wall	0.02
Housing plain (housing)	0.0381
Grass plain (FPlainGrass)	0.021

The estimation of the stage-discharge relationship was first undertaken for the do-nothing base case, and the results are exported and stored. Next, a stage-discharge relationship was estimated considering the channel dredging by adjusting the river bed to an additional 1 m depth representing the Option 2. Another stage-discharge relationship for in-river water levels constrained by embankment was also estimated with the imaginary wall between the river and the floodplain zones. The latter stage-discharge relationship is to be used to estimate the overflow volume of the

considered options with embankment, i.e. the Option 1 and 4. The stage-discharge relationship for the condition with PLP alone, i.e. the Option 3 was assumed to follow that of base case since most buildings are assumed to be separately located and mostly not adjacent (e.g. Boettle et al., 2011). Figure 6.12 presents schematic illustrations of the cross-sections for the conditions mentioned above. Zones are labels along the cross-sections and separated by red vertical lines. The bank markers on the cross-sections refer to the bankful stage. The resulting stage-discharge relationship of each considered condition is displayed in Figure 6.13.

Initial alteration on the channel cross-section to impose a higher damaging consequence of flood events have result in a stage-discharge relationship that is inconsistent with what can be expected in a real condition: From the Centre for Ecology and Hydrology (2014) website, a bankful water level of 4.77 m is said to yield a flow discharge of 459.5 m^3/s, whereas the estimated stage-discharge relationship for the base case yields 120 m^3/s of flow discharge of the same water level. Hence the resulting curves and the interpretation of quantitative outcomes is strictly based on the imposed adjustment and not the real condition. However, outcomes in qualitative analysis will not be affected.

From Figure 6.13, it can be seen that the curves of all conditions are less steep after they reach approximately 200 m^3/s of flow discharge, i.e. approximately 5 m AD. Investigation on the terrain characteristic from Figure 6.12 and Table 6.2 suggests that the elevation represents a transition point between the riverbank and the floodplain grass area. Therefore, the less steep rising curves reflects the higher conveyance capacity during higher flow events due to the overbank flow of water.

The channel deepening decreases the water level for low flow events as compared to the base case, but not for high flow events. This suggests that the channel dredging option may not be effective during high flow events, as have been reviewed from the literature in Chapter 2. For the constrained main channel, the in-river water level is indifference with that of base case for low flow events, but causes reduction on the natural conveyance with higher in-river water level as the river discharge increases. The stage-discharge curve of the constrained main channel, therefore, exhibits a steady

rise aused by the imposed embankment and continues to accelerate at a higher rate as compared to the base case due to the reduced conveyance capacity.

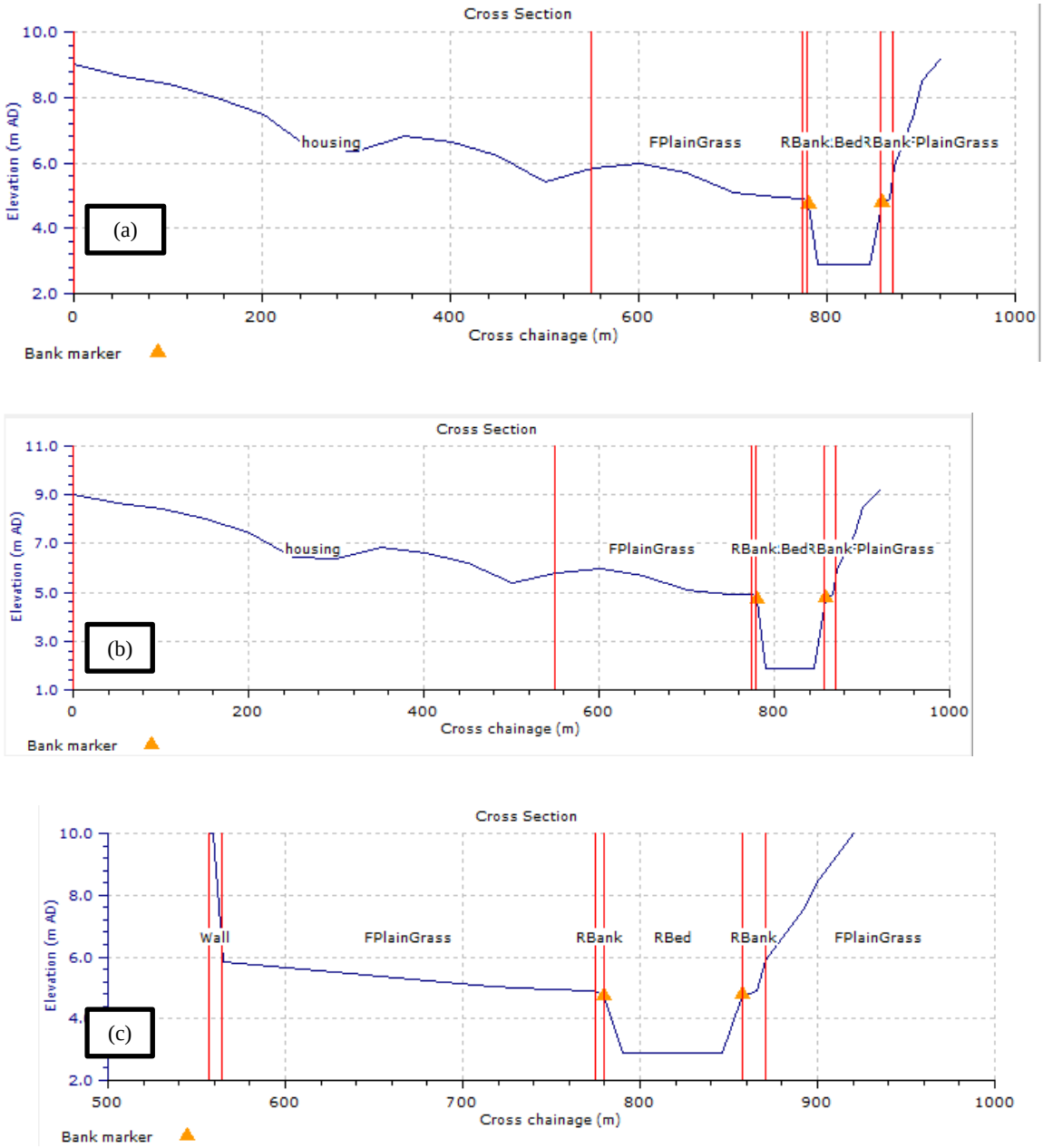

Figure 6.12: Cross-sections as delineated in the CES for stage-discharge relationship estimation; (a) the base case, (b) the dredged channel, and (c) the constrained main channel.

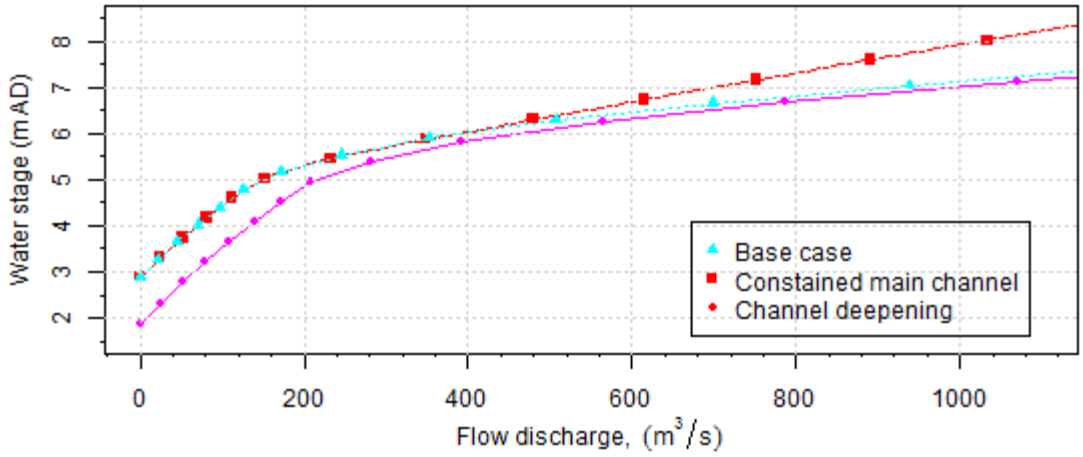

Figure 6.13: Estimated stage-discharge curves of the different conditions.

The stage-discharge curves were further used in the subsequent modelling stages. The stage-discharge curves of the base case, Option 2 and Option 3 were directly used for the damage-discharge relationship derivations (demonstrated in section 6.5), whilst the stage-discharge curve of the Option 1 and Option 4 were brought into a number of pre-processing activities before the derivation of the damage-discharge relationship can be undertaken.

6.4.3 Standardized hydrograph

A standardized discharge for conditions with embankment was configured following the procedure presented in Section 6.3.2. A number of hydrographs associated with out-of-bank peak flows was identified based on historical have peak flows. Only peaks that are high enough to represent damaging flood events were selected. In particular, the relevant peaks were set to be higher than the smallest magnitude of flow discharge that may cause a damaging flood event for the case study area. The smallest magnitude of flow discharge for the area was estimated by evaluating the extracted cross-section information, the satellite imagery of the area and the stage-discharge relationship of the base case (i.e. from Section 6.4.2. The minimum damaging flow records was estimated as 268 m^3/s. A total 21 samples of hydrographs were extracted from the Thames at Kingston daily flow records (Table 6.3).

Table 6.3: Historical flood events of Thames at Kingston flow records with associated peak discharges.

No.	Date	Peak discharge, Q_p	No.	Date	Peak Discharge, Q_p
1	18/11/1894	800	12	20/03/1947	709
2	21/02/1900	527	13	01/12/1954	446
3	15/02/1904	510	14	04/11/1960	444
4	05/02/1915	581	15	17/09/1968	581
5	04/01/1925	514	16	23/11/1974	531
6	04/01/1925	514	17	27/12/1985	395
7	07/01/1928	522	18	04/02/1990	405
8	13/12/1929	547	19	07/11/2000	440
9	18/03/1937	402	20	13/12/2000	431
10	09/02/1940	400	21	02/01/2003	461
11	02/02/1943	449			

Upon examining the hydrographs, a flood event duration of maximum 21 days was selected with a start and end flow magnitudes at least equal to the minimum flow discharge. Furthermore, historical evidence and visual examination of the hydrographs were undertaken to identify outliers. The flood event of September 1968 had a peculiar shape hydrograph, which caused by high precipitation over the lower areas of the catchment (Dunsmore, 1997), was eliminated. Hydrographs of year 1904, 2000 and 2003 flood events were further eliminated due to obvious peculiarities of the shape as compared to the other considered hydrographs. In addition, flood events prior to the year 1950s were included in the median calculation due to catchment wide-response flood events resulting from widespread precipitations (Dunsmore, 1997). For example, the 1894 flood was due to substantial rainfall over a 4-day period, and the 1947 flood was due to a passage of a warm weather that caused a prior heavy accumulated snow to melt rapidly over a still-frozen ground. Both trigger the most extensive and widespread floodplain inundation throughout the Thames basin (Marsh and Harvey, 2012).

The standardized discharges of all extracted hydrographs were averaged (Table 6.4). Figure 6.14 illustrates all the standardized discharges of the considered hydrographs in different solid coloured lines and the median hydrograph in a black dashed line. Note that the median standardized discharge towards the peak exhibit less variance than the smaller standardized discharges, indicating a more accurate estimation for a larger ratio between the peak flow and the embankment threshold.

Table 6.4: Resulting median standardized discharge for Thames at Kingston.

t_1	Med standardized discharge, Q_t/Q_p	t_2	Med standardized discharge, Q_t/Q_p
-10	0.452116	1	0.946984
-9	0.481069	2	0.848259
-8	0.515867	3	0.774194
-7	0.566479	4	0.733463
-6	0.583519	5	0.659533
-5	0.626898	6	0.559944
-4	0.711111	7	0.528736
-3	0.768018	8	0.547884
-2	0.853604	9	0.533145
-1	0.910499	10	0.489546
0	1	11	0.444973

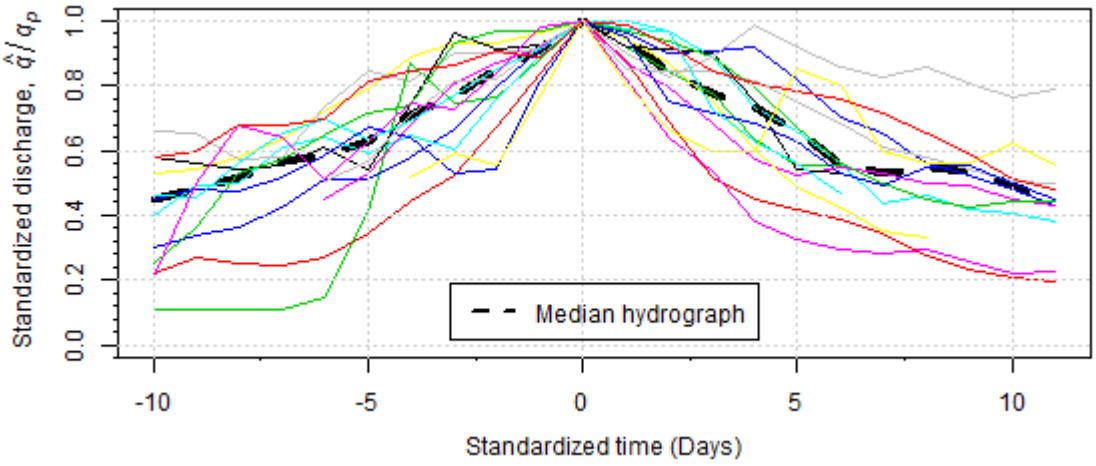

Figure 6.14: Standardized hydrographs for 19 flood events and corresponding median standardized hydrograph

6.4.4 Overflow flood volume

Another pre-processing modelling activity specifically for condition with embankment is the estimation of overflow volumes due to an exceeded embankment design discharge following the methodology proposed in Section 6.3.3. A suitable location for the embankment adjacent to the river was first established in the DEM using GIS tools. The maximum height of the embankment was set 3 meters and the length of approximately 1.8 km A sequence of design disharges q_p was then selected (i.e. 400, 450, 500, 550 and 600 m^3/s) based on their relative magnitude to the historical peak events. Using the previously configured stage-discharge relationship of condition with embankment, the sequence of design discharges were transformed to elevation levels and corresponding heights (i.e. 0.4, 0.8, 1.1, 1.4 and 1.7 m). These represent the elevation or height of the embankment crest.

A range of peak flows $\hat{q}$ ranging from 400 m^3/s to 1100 m^3/s were chosen, and alongside the specified design discharges, the workflow proposed in Section 6.3.3 was executed. The estimated overflow volumes against peak flows from 400 to 800 m^3/s are depicted in Figure 6.15. The overflow flood volume into the floodplain shows an increase magnitude at higher peak flows and at smaller protection design.

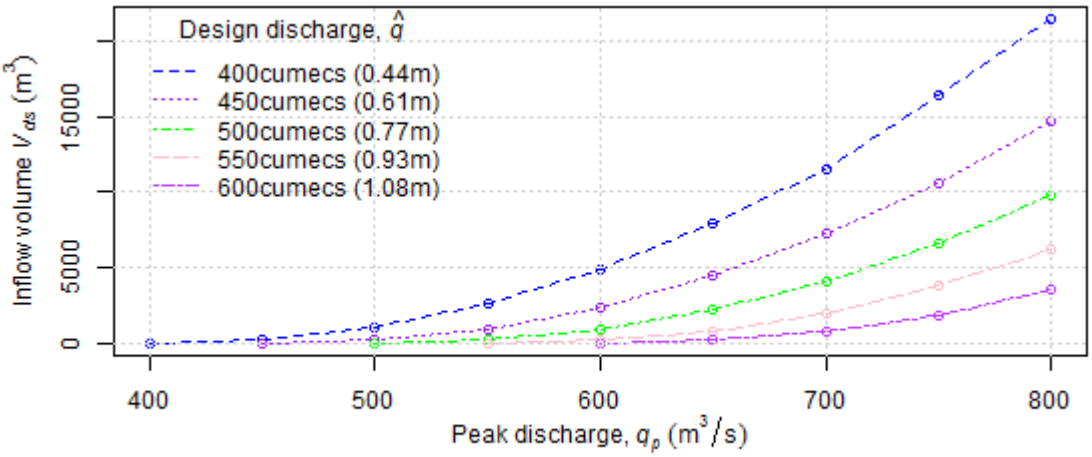

Figure 6.15: Overflow volume against peak discharge for different embankment design discharges (peak discharge-volume curves).

Table 6.5 tabulates the outputs from the computation when the protection design $\hat{q}$ is 500 m^3/s (corresponds to 0.77 meter height) and peak flow q_p between 550 and 1100 m^3/s. It can be seen that the automated computation had generated a variety of information associated with the assigned input of protection design and peak flows. Such information can be examined for reliability check of the designed model prior execution of large input datasets. From the table, the overflow volume can be seen increases moderately in response to higher peak flows q_p.

Figure 6.16 illustrates an example computed ${h_{ds}}^{3/2}$ over time for q_p 750m^3/s using the automated computation. The area under the curve was used to estimate the total overflow volume associate with the assigned input variables. Results from the alternative method of calculating the overflow volume for verification is given in Table 6.6 with time in days modified as a set of natural numbers. The total volume obtained from the alternative method is consistent with the automated computation, hence confirming the reliability of the model.

Table 6.5: Example results of overflow volume computation for 500m^3/s design discharge and various peak discharges.

$\hat{q} = 500m^3/s$								
Defence Max. Height (m)	Peak discharge, q_p (m^3/s)	Max. water level in the main channel (m AD)	Max. water head, h_{ds} (m)	Maximum standardized discharge, $\hat{q}/q_p$	Standardized time LHS ,t_L	Standardized time RHS, t_R	Flood Duration (day)	Volume , V_{ds}
6.367	550	6.525	0.158	0.9091	-1	1.4	2.4	172
6.367	600	6.684	0.317	0.8333	-2.2	2.2	4.4	849
6.367	650	6.841	0.474	0.7692	-3	3.1	6.1	2139
6.367	700	6.997	0.63	0.7143	-3.9	4.3	8.2	4058
6.367	750	7.153	0.786	0.6667	-4.5	4.9	9.4	6624
6.367	800	7.305	0.938	0.625	-5	5.3	10.4	9804
6.367	850	7.457	1.09	0.5882	-5.9	5.7	11.6	13513
6.367	900	7.609	1.242	0.5556	-7.2	6.7	13.9	18015
6.367	950	7.759	1.392	0.5263	-7.8	7.2	15	22936
6.367	1000	7.909	1.542	0.5	-8.5	9.2	17.7	29032
6.367	1050	8.058	1.691	0.4762	-9.2	10.3	19.5	35667
6.367	1100	8.207	1.84	0.4545	-9.9	10.8	20.7	42593

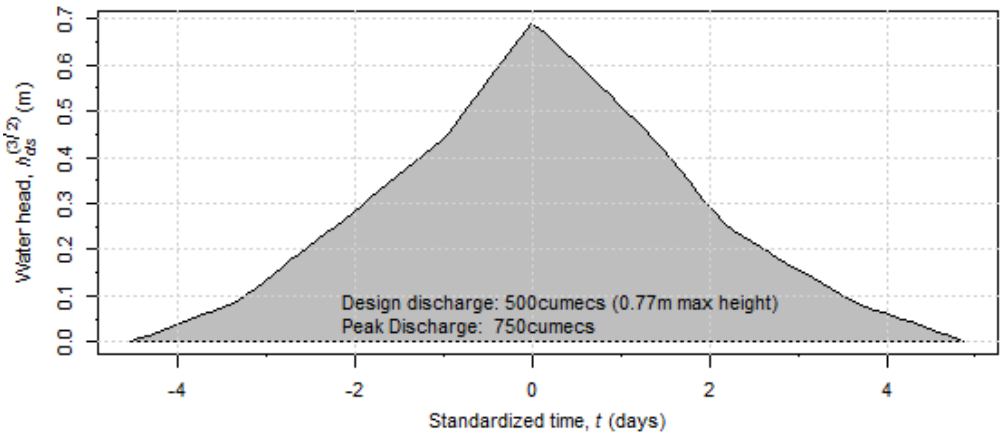

Figure 6.16: Hydrographs in the form of $h_{ds}^{3/2}$ over time for $\hat{q}$ = 500m^3/s and q_p = 750m^3/s.

Table 6.6: An example of manual calculation of overflow volume for $\hat{q}$ = 500m^3/s and q_p = 750m^3/s.

Discrete fragment, i	1	2	3	4	5	6	7	8	9	
Time (day)	0	1.2	2.3	3.6	4.5	5.8	6.7	8.1	9.4	
Water head (m), h_{ds}	0	0.198	0.396	0.591	0.786	0.591	0.396	0.198	0	
Overtopping flow rate (m^3/s), q_{in}	0	225.3	637.3	1162.0	1782.2	1162.0	637.3	225.3	0	
Overflow Volume, V_{ds}	136	466	1175	1370	1924	805	600	147	Sum = 6624	

6.4.5 Floodplain storage

This section presents the application of the proposed methodology to estimate the floodplain storage in Section 6.3.4. First, a range of contour elevations of 0.2 meter intervals was established to represent a range of possible maximum inundation level. The lowest contour level was selected to represent a stage of no damage, using the land-use information from the topographic map and the elevation data from DEM. A straight line was introduced in the DEM to represent the virtual embankment crest elevation level. The estimation of floodplain storage was undertaken for each contour level. Hence, the virtual embankment crest level was set to have a consistent elevation with the individual contour defined earlier. A horizontal plane between the contour and the embankment crest elevation level was then introduced in the DEM to represent the maximum inundation level. This enables the estimation of the area and volume storage using the triangular irregular network (TIN), facilitated using GIS tools. The maximum inundation levels associated with the considered range of contour levels were later transformed into flood depths by subtracting the associated ground floor elevation levels, respectively.

Table 6.7 presents the estimated areas and volumes of the considered range of maximum inundation depths, whilst Figure 6.17 tabulates the information to visualise and examine the relationship between floodwater level, storage and surface area. The overflow volume representing the floodplain storage can be seen increasing dramatically when the maximum inundation depth is higher than 1.5 m. In order to continue the vulnerability assessment, water level-overflow volume relationship was established and brought forward for the derivation of damage extent modelling (Section 6.4.6).

Table 6.7: Information related to modelling floodplain storage of the floodplain area of Teddington; overflow volume, surface area and maximum depth of condition considering embankment protection.

Maximum water depth (m)	Water level (m AD)	Volume with defence existence, V_{ds} (m^3/s)	Surface area (m^2)
0	5.6	0	0
0.2	5.8	1522	6527
0.4	6	3249	13454
0.6	6.2	5897	18861
0.8	6.4	11477	27626
1	6.6	19805	42067
1.2	6.8	29970	55037
1.4	7	41069	55674
1.6	7.2	103211	169002
1.8	7.4	143248	241680
2	7.6	202589	318795
2.2	7.8	257277	368802
2.4	8	350245	421761
2.6	8.2	457819	540795
2.8	8.4	576644	605776
3	8.6	694338	640705

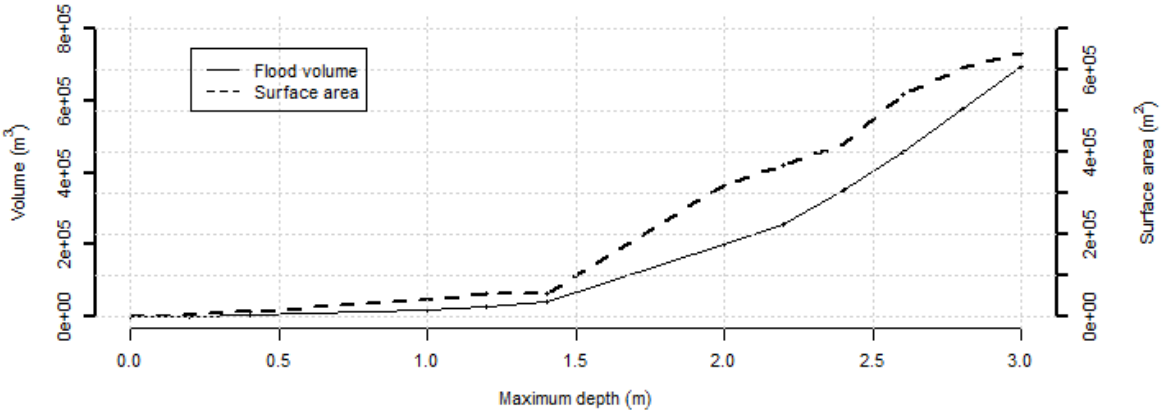

Figure 6.17: Relationship between maximum water depth and volume, and maximum water depth and surface area. Both are constructed with linear interpolations.

6.4.6 Damage extent assessment

Another important task for the construction of damage-discharge relationships following the proposed methodology is the estimation of potential economic damages in the events of flooding Section 6.3.5. The study employs the MCM database of estimated economic losses of a range of inundation depths, i.e. the depth-damage relationship, of flood duration of not more than 12 hours for residential sector average. The values of buildings consist of building fabrics (e.g. floors,

plumbing and electrical) and household inventories. Figure 6.18 illustrate the depth-damage relationship with the characteristics as mentioned.

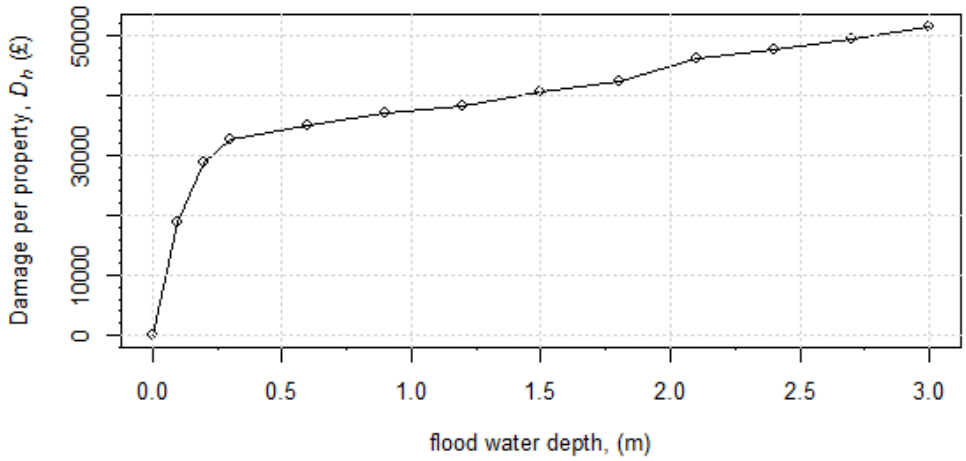

Figure 6.18: Damage-depth curve for 12 hours flood duration from Multi-coloured manual damage-depth relationship.

Another important input in the damage extent estimation is the density of houses within the boundary of flood risk defined earlier. Information from the DEM and satellite imagery indicates that the lowest ground flood elevation of the residential buildings on the area is approximately at 5.6 m AD. Before proceeding to the data extraction for the density of residential buildings, a maximum elevation limit for the density of the buildings was identified based on a suitable maximum inundation level. The maximum inundation level was identified according to the maximum inundation depth that can be interpolated from available depth-damage relationship, in connection with the ground floor elevation level of the lowest residential buildings. For the case study, the possible maximum inundation depth to be interpolated is 3 m according to the MCM depth-damage relationship. The highest elevation for the data extraction of the density of buildings was, therefore, decided to be 3 m higher than the ground floor elevation level of the lowest identified buildings on the area. In this case, the considered range is from 5.6 m AD to 8.6 m AD.

Following the proposed methodology in Section 6.3.5, the density of buildings P_g on 0.1 m elevation step was extracted up to a maximum 3 m from the ground floor elevation level of the lowest identified buildings. The DEM of the area is overlaid with an updated basemap of aerial imagery from ArcGIS (ESRI, 2012). Each property is discretized based on the aerial view, such as

chimneys and rooftops. The elevation information attributed to each discretized property was then compiled and the number of properties associated with the incremental elevation steps was computed respectively and stored in a look-up table. The 'depth' axis of the depth-damage relationship was similarly discretized with the same 0.1 m intervals up to a 3 m depth. The corresponding damages D_h were interpolated and also stored in the look-up table. The P_g and D_h were indexed as to enable further computations (first four columns in Table 6.8).

Table 6.8: Look-up table (Column 1 to 4) and resulting level-damage relationship for conditions without property protection and with protection design of 20-year return period, respectively (Column 5 and 6). The damage per meter depth for a property follows the 2005 prices.

Input				Total damage (£)	
Ground elevation (m AD)	Calculation index	Damage per water depth for a property, (£)	Number of residential buildings per elevation	Options without property protection	Options with property protection extent of 20 year return period
	i, n, z and y	D_h	P_g	D_{k1}	D_{k2}
5.6	1	980	4	-	-
5.7	2	18,925	3	75,700	-
5.8	3	28,859	3	172,210	-
5.9	4	32,754	1	274,367	-
6	5	33,476	3	337,668	-
6.1	6	34,199	5	421,119	-
6.2	7	34,921	7	556,664	-
6.3	8	35,606	6	758,291	142,426
6.4	9	36,292	20	970,708	251,987
6.5	10	36,977	21	1,449,432	742,104
6.6	11	37,418	13	2,086,298	1,379,685
6.7	12	37,859	24	2,639,719	2,024,866
6.8	13	38,299	17	3,339,270	2,889,631
6.9	14	39,061	18	4,000,408	3,790,881
7	15	39,823	53	4,663,180	4,663,180
7.1	16	40,586	53	5,987,334	5,987,334
7.2	17	41,220	76	7,672,664	7,672,664
7.3	18	41,854	64	9,941,232	9,941,232
7.4	19	42,488	96	12,244,904	12,244,904
7.5	20	43,690	71	15,161,471	15,161,471
7.6	21	44,892	66	17,930,351	17,930,351
7.7	22	46,094	92	20,526,799	20,526,799
7.8	23	46,650	68	23,535,321	23,535,321
7.9	24	47,206	46	26,375,694	26,375,694
8	25	47,763	103	28,700,979	28,700,979
8.1	26	48,332	63	31,849,059	31,849,059
8.2	27	48,901	94	34,754,194	34,754,194
8.3	28	49,470	28	38,107,933	38,107,933
8.4	29	50,133	49	40,434,921	40,434,921
8.5	30	50,796	82	42,676,033	42,676,033
8.6	31	51,459	43	45,558,105	45,558,105

This study assumes a PLP effective depth 0.6 m from the ground floor elevation level of a protected property (Figure 6.19) (e.g. Great Britain, Dept for Environment, Food and Rural Affairs, Aug 2012;Arrighi et al., 2013;Moel, Vliet and Aerts, 2014). Therefore, damaging floods were only considered when flood levels are above this threshold for cases with adoption of PLP.. As a first instance, the total damages influenced by 20-year return period protection of PLP and a range of flood inundation levels were considered (DEFRA, Aug 2012). A corresponding design discharge was first determined using the previously fitted GEV distribution. Subsequently, the design discharge was used to estimate the elevation through interpolation of the associated stage-discharge curve (Section 6.4.2). A stage of 6.3 m AD was then obtained which reflects the targeted maximum protection corresponds to the 20-year return period.

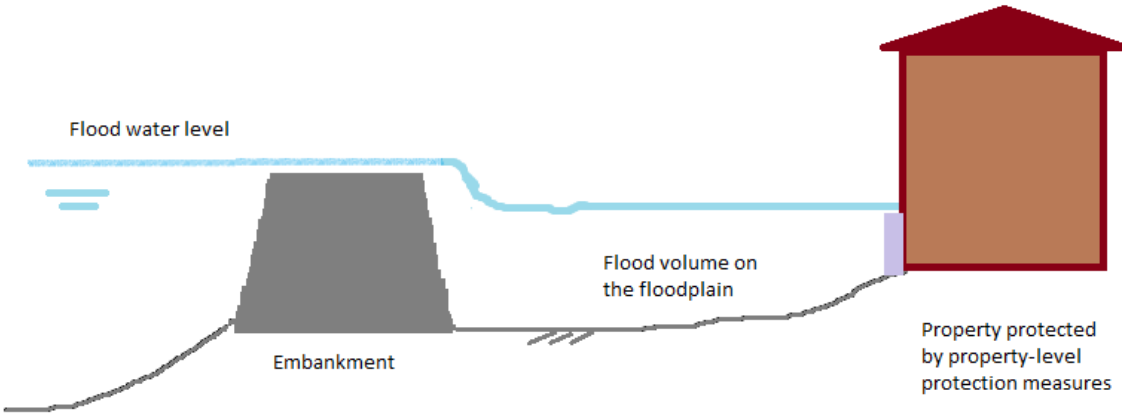

Figure 6.19: Schematic diagram of a cross-section of a condition where floodwater exceeds the property-level protection.

Based on the lookup table, the index of the ground floor elevation level the highest protected buildings associated with 6.3m AD was identified as $i_p = 8$. Given the PLP threshold height as 0.6 m from the ground floor of each protected houses, the index of the ground floor elevation level of the lowest protected buildings is i_f = 7 (i.e. 5.6+0.6m AD). The index of the PLP threshold of the highest protected buildings is i_m = 14 (i.e. 6.3+0.6m AD). The total damages were then computed for the range of inundation levels (n) in reference to the identified i_f, i_p and i_m using the proposed algorithm in Section 6.3.5. The final two columns in Table 6.8 provide the results from the

automated computations concerning options without PLP adoption and with the 20-year return period protection.

From the Table 6.8, it can be seen that the estimated total damage of the condition with PLP (D_{k2}) is the same as the estimated total damage of the condition without PLP (D_{k1}) starting at *i/n/z/y* = 15. This indicates a situation where the highest protected buildings are damaged by the flooding due to overtopped PLPs. The curves of the total damages against inundation levels for the conditions without PLP and with 20-year design PLP are illustrated in Figure 6.20. It is clear that the adoption of PLP can reduce flood damages until the PLPs are fully overtopped by a very extreme flood events.

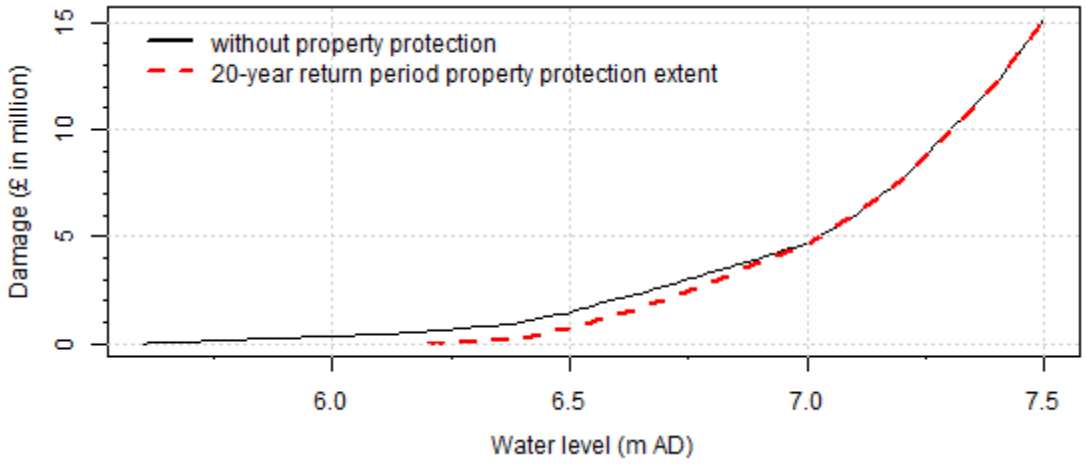

Figure 6.20: Level-damage curves of without-PLP and with a 20-year return period PLP conditions, respectively.

The verification of the results from the automated functions was undertaken by comparing with the results from manual calculations. Manual calculations were made for two scenarios: (1) considering inundation level at $n = 2$ of a condition without PLP and, (2) considering inundation level at $n = 9$ with 20-year return period design PLP extent. The results from the manual calculations are consistent with the results from the automated function shown in Table 6.8. This indicates the reliability of the automated computation.

$$D_{k1} = \sum_{i=0}^{n=2} \left(P_{g_{y=n-i}} D_{h_{z=i+1}} \right)$$

$$= (P_{g_{2-0}} \times D_{h_{0+1}}) + (P_{g_{2-1}} \times D_{h_{1+1}}) + (P_{g_{2-2}} \times D_{h_{2+1}})$$

$$D_{k1} = 3(980.20) + 4(18925.02) + 0(28858.73) = 78640.68$$

$$D_{k2} = \sum_{i_f=7}^{n=9} \left(P_{h_{g_{n-i}}} D_{h_{d_{i+1}}} \right) + \sum_{i_P=8}^{n=9} \left(P_{h_{g_{i+1}}} D_{h_{d_{n-i}}} \right)$$

$$= \left(P_{h_{g_{9-7}}} D_{h_{d_{7+1}}} + P_{h_{g_{9-8}}} D_{h_{d_{8+1}}} + P_{h_{g_{9-9}}} D_{h_{d_{9+1}}} \right) +$$

$$\left(P_{h_{g_{8+1}}} D_{h_{d_{9-8}}} + P_{h_{g_{9+1}}} D_{h_{d_{9-9}}} \right)$$

$$= \left(P_{h_{g_2}} D_{h_{d_8}} + P_{h_{g_1}} D_{h_{d_9}} + P_{h_{g_0}} D_{h_{d_{10}}} \right) +$$

$$\left(P_{h_{g_9}} D_{h_{d_1}} + P_{h_{g_{10}}} D_{h_{d_0}} \right)$$

$$D_{k2} = \left(3(35606.44) + 4(36291.82) + 0(36977.21) \right) + \left(20(0) + 21(0) \right)$$

$$= £\,251{,}987$$

A range of possible PLP extents ranging from 6.2 to 6.7 m AD with 0.1 m intervals is further considered in this case study. The selection was based on the previously gathered information of the density of buildings. The total damages correspond to water levels (i.e. level-damage relationships) were then estimated following the designed algorithms in Section 6.3.5. The level-damage relationship from the considered range of potential PLP extent alongside the estimated level-damage relationship without PLP adoption were brought forward to model the damage-discharge relationships (Section 6.5).

6.5 Results

This section presents the construction of damage-discharge relationships by taking the modelling outputs from Section 6.4 into the methodology described in Section 6.3.6. The resulting damage-discharge curve of each option is provided in Figure 6.21 to Figure 6.24. For the Option 1, 3 and 4, multiple damage-discharge curves were generated in the same figure, respectively. Each curve is associated with the considered range of protection designs.

The methodology of damage-discharge relationship derivation of Option 1 were applied for q_p ranging from 300 to 1100 m^3/s and $\hat{q}$ ranging from 400 to 600 m^3/s, with 50 m^3/s intervals (refer Section 6.4.4). The resulting damage-discharge curves of adopting the embankment protection

against that of base case reveals that the damage reduction is more pronounce for higher protection designs, which is anticipated. The figure also shows that the damage-discharge curves of the intervention reconcile with that of base case at certain peak discharges owing to the uniquely specified discharge indicators (Q_{lim}) for each $\hat{q}$. A higher $\hat{q}$ leads to a much larger storage volume before the embankment is fully submerged, leading to a larger Q_{lim} in the damage estimation. This reflects the influence of the protection design $\hat{q}$ to the overflow flood volumes.

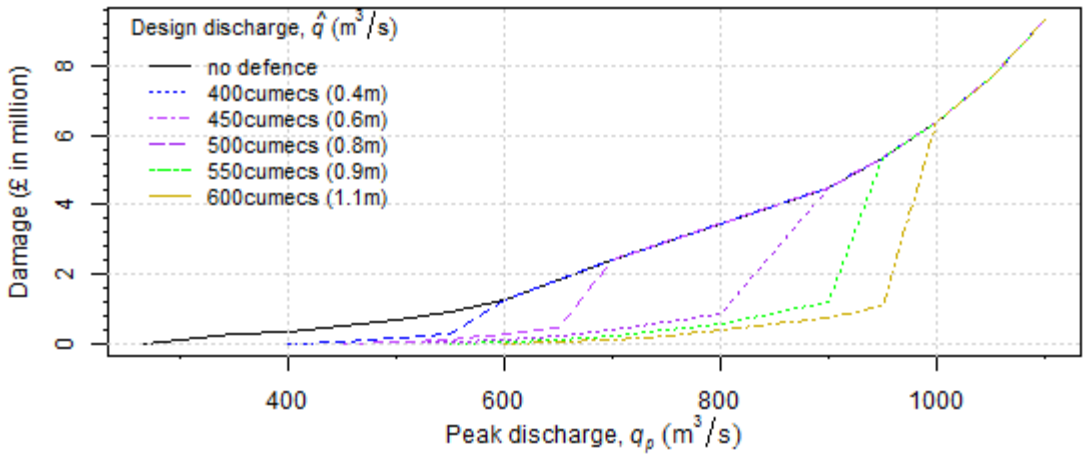

Figure 6.21: Damage-discharge curves of base case and Option 1 for various design discharges. The embedded legend shows the considered $\hat{q}$ and the associated maximum embankment height (in the parentheses).

Figure 6.22 illustrates the difference between the damage-discharge curves of the Option 2 and the base case. It can be seen that the potential flood damages are reduced as a result of floodwater level reduction from dredging (Figure 6.13). The potential damage reduction can be seen from the gap between the two curves. Although the difference between the stage-discharge relationships of the base case and of the adoption of channel dredging is relatively small at low probability flood events (Figure 6.13), the resulting difference in damages is relatively large (Figure 6.22). Upon examining the cascading effects more closely, it was found that this has been a result of a significant difference of resulting damages despite a small difference of inundation levels. For example, given a 1000 m^3/s flood peak, adoption of channel dredging reduces the inundation level to 0.1 m lower than the base case (i.e. from 7 m AD to 7.1 m AD extracted from Figure 6.13). The resulting total damage reduced is approximately £1.5 million (obtained from Table 6.8), which is consistent with the

quantitative findings depicted in Figure 6.22. This signifies the influence of the magnitude of variables, such as the density of houses and their values, to estimates of total damage.

It can also be seen from the figure that higher probability of flood events shows less reduction as compared to Option 1. For the low probability flood events, the damage reduction from the adoption of channel dredging is generally higher than that from embankment protection. This behaviour is most likely due to the model settings of overflow volume from Option 1. Nevertheless, the probability-weighed damage might not be substantial for the very extreme flow discharges and negligible for the risk estimation. This will further examined in Chapter 7.

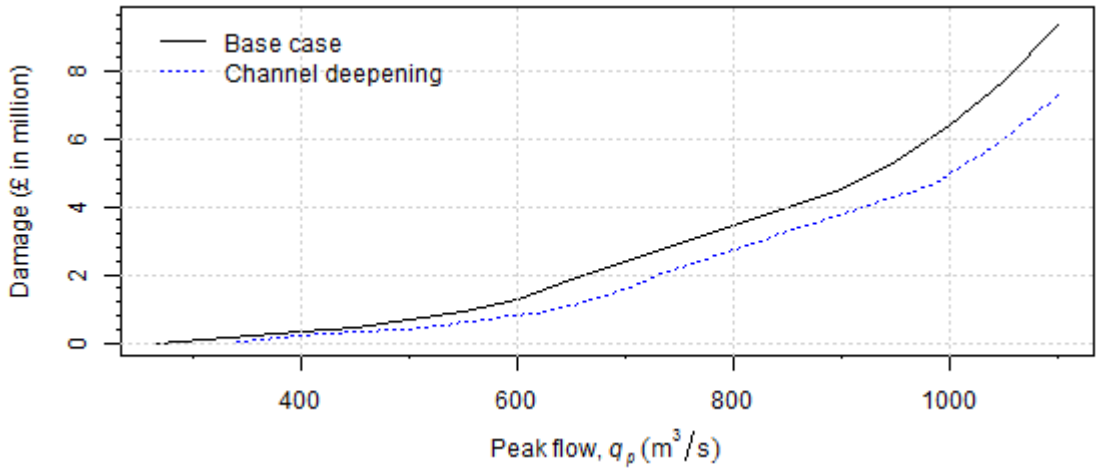

Figure 6.22: Damage-discharge curves of base case and Option 2.

The damage-discharge curves of the Option 3 for a number of targeted PLP extent (specified in Section 6.4.6) against the base case are presented in Figure 6.23. The distinct behaviour of the curves shows that the potential damage reduction increases when a higher PLP protection is adopted. The curves are steadily increase in a similar trend due to the constant PLP threshold adopted for all considered PLP extent. The curves are and independently reconcile with the damage-discharge curve of the base case at points where the PLP threshold of the highest protected buildings is overtopped. For example, the curve of the 20-year return period PLP design reconcile with that of the base case at ~900 m^3/s.

Figure 6.24 presents the damage-discharge curves of the Option 4 of the combined embankment and property-level protections. For clarity, only results from a designed embankment of 400 m^3/s

with a range of PLP extent were tabulated. It can be seen that a higher PLP design yield a greater damage reduction. The impact of flooding associated with the considered alternatives is expected to begin from the same peak discharge due to the similar buildings density and PLP height considered.

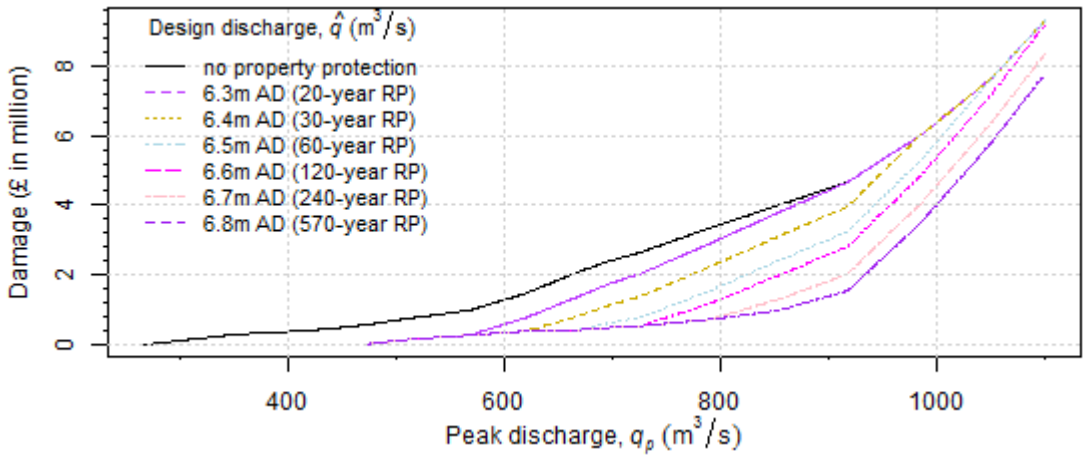

Figure 6.23: Damage-discharge curves of base case and Option 3 for various property protection extents. The embedded legend shows the ground floor elevations of the highest buildings protected and the associated return period in the parentheses.

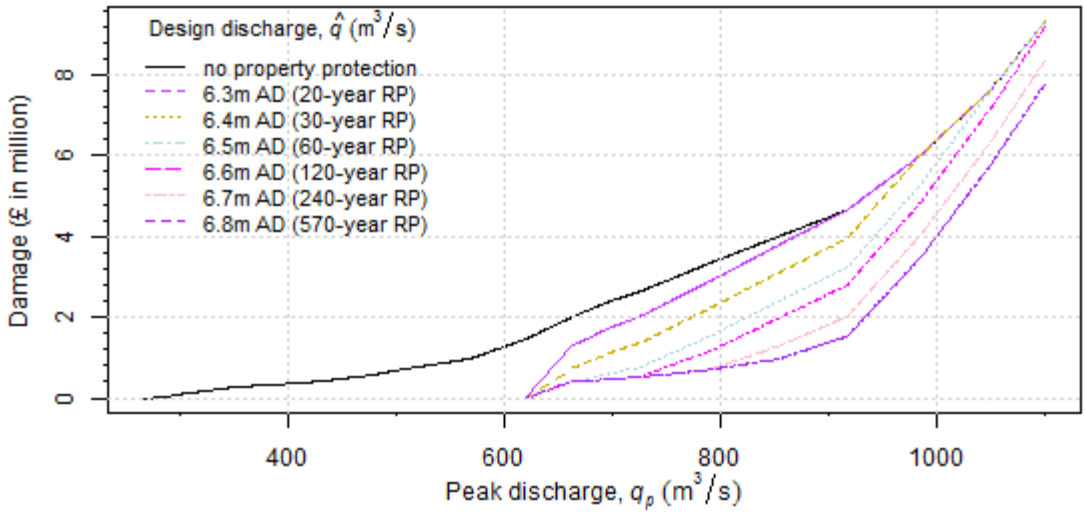

Figure 6.24: Damage-discharge curves of Option 4 for various property protection extents and 400m^3/s embankment protection. The embedded legend shows the highest elevation of houses protected and the associated return period (in the parentheses).

An apparent difference between the curves from the Option 3 and the Option 4 can be seen from the smaller design protection. The embankment existence in the Option 4 signifies the flood damage reduction as compared to the condition of without embankment in the Option 3. The behaviour

indicates the embankment functionality and also the potential benefit of having combined protection

6.6 Discussion and conclusion

This Chapter presents an integrated vulnerability assessment that was designed to incorporate a full range of possible flood events and a range of engineering flood protections with the aim for robustness in FRM decision making. A systematic arrangement of activities within the modelling chain takes into consideration the influence of the physical components of the flood risk system of local area including the effects of engineering flood protection measures. The arrangement of the modelling activities reflects on two distinct conditions; conditions where property-level protection is adopted and conditions without property-level protection. Relevant modelling tasks in accordance to the SPRC concept are carefully arranged in the modelling chain. Two-stage flood propagation was adopted for cases with embankment in effort to improve estimation. This includes extending the use of historical flood hydrographs for flood duration and volume estimation. The study also adopts the storage-based concept facilitated by the GIS high-resolution DEM to estimate the inundation depth relative to the flood discharge.

One advancement from the study is that the focus on micro-scale assessment has led to the development of novel algorithms to estimate flood damage to individual buildings. This involves discretizing the buildings most vulnerable to flooding to identify the relative position of the buildings from the hazard source. One can apply the automated damage model to any micro-scale assessment provided that a depth-damage relationship and a complete dataset of property counting are available. These information alongside the spatial influences of considered engineering measures were introduced into the flood risk system using high-resolution of DEM and GIS application.

The algorithms also allow flood vulnerability in the form of damage-discharge curves associated with the intervention measures to be assessed for a range of possible scenarios of inundation depth and protection designs. This leads to a shift from a specific fixed protection design or estimation of

damage corresponds to a particular extreme flood event to a more holistic risk-based approach, hence facilitates a practical application of the risk-based optimization of flood protection. Moreover, the isolation of return period estimation from the approach allows the subsequent flood risk assessment and economic appraisal to be undertaken directly using a variety of possible flood frequency distributions

The automated computation also advances quantitative vulnerability assessment related to property-level protection and combined protection of property-level protection and embankment. The tractability of the methodology provides the advantage to track down the quantitative results from the modelling chain and ease of cross-referencing, hence increase the confidence to the quantitative findings. Moreover, the explicit documentation of outputs from pre-process activities throughout the modelling chain allows the final results to be justified. The implementation of the modelling work to the local area of Teddington signifies the feasibility of the micro-scale vulnerability assessment. The final outcomes in the form of damage-discharge relationships of the different flood protection alternatives are provided by means of visual comparison with emphasise in both qualitative and quantitative outcomes As highlighted from the case study, the consideration of property-level protection and channel dredging alongside the ever-preferred flood defence allows a wider options to be evaluated.

The application of the proposed modelling to the case study of Teddington area involves adjustment to some input data to magnify inundation scenarios for clearer illustrations on the applicability of the methodological framework. Therefore, the absolute values from the vulnerability assessment demonstrated in this study are not representing the real case of the area under study. In cases where absolute values are of concerns, verification of the modelling outputs may be undertaken using information from historical flood events.

Further improvements to the application can be made on the characterization of the flood receptors such as their spatial distribution and economic values (i.e. depth-damage relationship). Datasets from Ordnance Survey for the area of interest can be adopted or extensive surveys may be undertaken for a more reliable input data. Despite the obvious advantage, readily available data

from Ordnance Survey may not be accessible and data acquisition from ground truthing (e.g. Suriya, Mudgal and Nelliyat, 2012) entails considerable costs and efforts. Nevertheless, it may be worth exploring the effects of a range of possible depth-damage relationship rather than the mean value. This is especially true given that a small difference of the depth-damage relationship can yield a very substantial difference of damage-discharge relationship (For example, refer the discussion in Section 6.5 on the difference between the damage-discharge relationships of the channel dredging and the base case). Further studies, therefore, may incorporate a range of depth-damage relationship, for example maximum, average and minimum estimates (e.g. Moel et al., 2012). It will be interesting to see the effects this brings to the vulnerability and further to the economic performance of alternative flood protection options. This can be undertaken as a sensitivity analysis. However, in practical sense it is rational to use the expected values rather than a range of values given that only one optimal protection will be adopted.

Other limitations of the proposed modelling are as follows. The inundation depth from the simulation is subjected to floodplain storage definition and delineation (Arrighi et al., 2013). Furthermore, it neglects the effects of water balance or dynamic routing through the relevant grid cells (Dutta et al., 2013). Further refinement for a more sophisticated treatment of hydraulic estimation may be worth exploring, but arguably might not result in significant difference to the final results.

Chapter 7 continues the work by integrating the vulnerability assessment into the risk-based options appraisal to explore the economic performance of alternative portfolios under stationary and nonstationary conditions. The intervention costs of the measures for the cost-benefit analysis is also estimated in Chapter 7 and further used in subsequent cost-benefit analysis.

Chapter 7 Performance of flood protection decisions in the context of stationary and nonstationary extreme flow distributions: Incorporating spatial complexities

7.1 Introduction

Chapter 6 presents the development of micro-scale damage calculators specifically for four community-based flood protection options; earth embankment, channel deepening, property-level protection and combined protection of earth embankment and property-level protection. The damage calculators were successfully applied to a case study area in Teddington and result in comparable outcomes of different degrees of flood vulnerability correspond to the different options and flood inundation scenarios. This Chapter seeks to explore the usability of the developed damage calculators for risk computations and further explore long-term economic performance of flood protections. Evaluation of the economic performance entails the need to demonstrate how the costs and benefits can be estimated for each alternative options. The risk-based economic evaluation with the focus of reducing risks to the most vulnerable in the most cost-effective manner will be of value in providing assistance in public spending prioritisation. In particular, this work is aimed among others to offer an example application of the risk-based options appraisal of property-level protection alongside other well-accepted protection measures. Furthermore, the study aims to examine the influence of flood protection decisions in the context of stationary and nonstationary conditions.

The risk-based economic evaluation that is demonstrated in this study adopts future prediction of stationary and nonstationary distributions following the ones fitted earlier in Chapter 5. The risk estimation accounts a wide range of possible flood probability and consequences. The latter was taken from the modelled damage-discharge relationships from Chapter 6. The economic performance of long-term protection portfolios involving the four alternative options as adopted in Chapter 6 is undertaken through applications of the cost-benefit analysis. Applications of the risk-

based optimization approach to a real representation of FRM problem in this particular study takes into account the complex physical influences. This further promotes the adaptability of the proposed approach to real world FRM problems.

The remainder of this Chapter is documented as follows. Section 7.2 elaborates on FRM alternatives of long-term protection portfolios. Section 7.3 presents developed approaches for the evaluation, or approaches developed in previous Chapters but required modification and further refinement for the purpose of this study. The applications of the methodology are demonstrated in Section 7.4 followed by discussions and conclusion in Section 7.5.

7.2 Portfolios of long-term flood protection

There are many potential components to a portfolio of structural and non-structural measures, and they can be implemented in many different ways through time (Hall and Penning-Rowsell, 2011). Continuing from the study in Chapter 6, the four alternative measures with the characteristics as described in Section 6.2 are adopted into five alternative portfolios. This study had specified 100 years of design life to each portfolio to establish consistent appraisal period. The appraisal period is deemed reasonable as to consider flood embankment with a typical planned lifespan of 100 years..

Table 7.1 describes the portfolios considered for the case study. Decisions of three portfolios (Portfolios 1, 3b and 4) are based on the risk-based optimization of flood protection design, respectively, whilst decisions of another two portfolios (Portfolios 2 and 3a) are based on fix protection designs. Although the main focus of the study was to have insights on the decision performance made by the application of the risk-based optimization methodology, the inclusion of fix protection designs represents the still widely practiced conventional approach and by comparing the outcomes of both approaches. Furthermore, insights on the advantage of applying the risk-based optimization methodology as compared to a fix design in terms of the resulting economic performance were sought. There are three portfolios that consider PLP, either as a single protection or as a combination protection with embankment. The consideration of PLP alongside the other community-based protection offers advantage in informing FRM decision making.

As described in Table 7.1, Portfolio 1 adopts embankment protection that is to be determined through the risk-based optimization methodology. Portfolio 2 adopts a channel improvement by 1 m river excavation. Portfolio 3 implies PLP with a protection threshold of 0.6 m from the ground floor elevation level of protected buildings. There are two considerations for Portfolio 3; (1) Portfolio 3a considers a fixed protection corresponds to a 20-year return period of a stationary condition. This means that all buildings located on and below the ground elevation level correspond to the 20-year return period will be benefited from the scheme. Under a nonstationary condition, Portfolio 3a will also considers a fixed protection of the same level as that of the stationary condition to allow for a valid comparison. (2) Portfolio 3b identifies a targeted protection design of PLP by implementing the risk-based optimization methodology. Portfolio 4 adopts both embankment and PLP, through the rsk-based optimization of combined protections over the future period.

Table 7.1: Descriptions of the considered portfolios.

Portfolio	Type of protection	Protection design
Portfolio 1	Earth embankment. Maintenance runs every year over the appraisal period.	Embankment level is optimized through the risk-based optimization of flood protection
Portfolio 2	Channel deepening. Maintenance runs every year over the appraisal period.	1m excavation of the river.
Portfolio 3a	Resistant type property-level protection. Protection is to be re-installed every 20 years.	Protection for each house is up to 0.6m high from ground level and implemented corresponds to 1:20 year return period of the stationary condition.
Portfolio 3b	Resistant type property-level protection. Protection is to be re-installed every 20 years.	Protection for each house is up to 0.6m from its ground level. Protection extent is optimized through the risk-based optimization.
Portfolio 4	Embankment and property-level protection. Embankment maintenance will runs every year over the appraisal period.	Protection for each house is up to 0.6m from ground level. Protection from embankment and property-level protection is determined through the risk-based optimization. (property-level protection is to be re-installed every 20 years).

It is important to note that upon evaluating the economic performance of the portfolios, only functional failure of the measures were considered throughout the appraisal period. It was assumed that the embankment and PLP are not exposed to structural failure. The structural failure often

considered unlikely for new structural developments due to good engineering practices and well-implemented maintenance regime over the lifetime of the assets.

7.3 Methodology

Figure 7.1 illustrates the designed consecutive steps of the main tasks involved for the portfolios appraisal. Arrows are used in the figure to distinguished pathways of the tasks associated to the different portfolios. Also included in the figure is the sections or/and chapters where each task is presented. Some of the tasks already undertaken in Chapter 5 for the determination of PDF and Chapter 6 for the configurations of damage-discharge relationships. The estimation of costs of each portfolio and the execution of the risk-based optimization methodology, where applicable, will be undertaken in this chapter. In particular, proposed approaches to estimate costs of each considered measures relevant to the portfolios in Section 7.3.1. Proposed approaches to evaluate the flood risk associated with the considered portfolios are presented in Section 7.3.2. Section 7.3.3 further presents the adopted approach to examine the economic performance of decisions.

7.3.1 Whole-life costs of protection measures

The whole-life costs of each portfolio were estimated accounting the implementation and maintenance costs. The study ignores costs related to land acquisition, resettlement or other transaction costs. Furthermore, constraints related to the data acquisitions of other factors contributed to cost may cause additional challenge for a representative quantitative analysis (e.g. Meyer, Priest and Kuhlicke, 2012). However, depending on the needs of a study, consideration of other type of costs may be necessary.

To have a reasonable estimates of the capital and material costs, spatial elements related to the allocation of the measures were considered (e.g. Stijnen et al., 2014). The following sub-sections present the proposed approach to establish cost functions conditional to the considered protection measures considered.

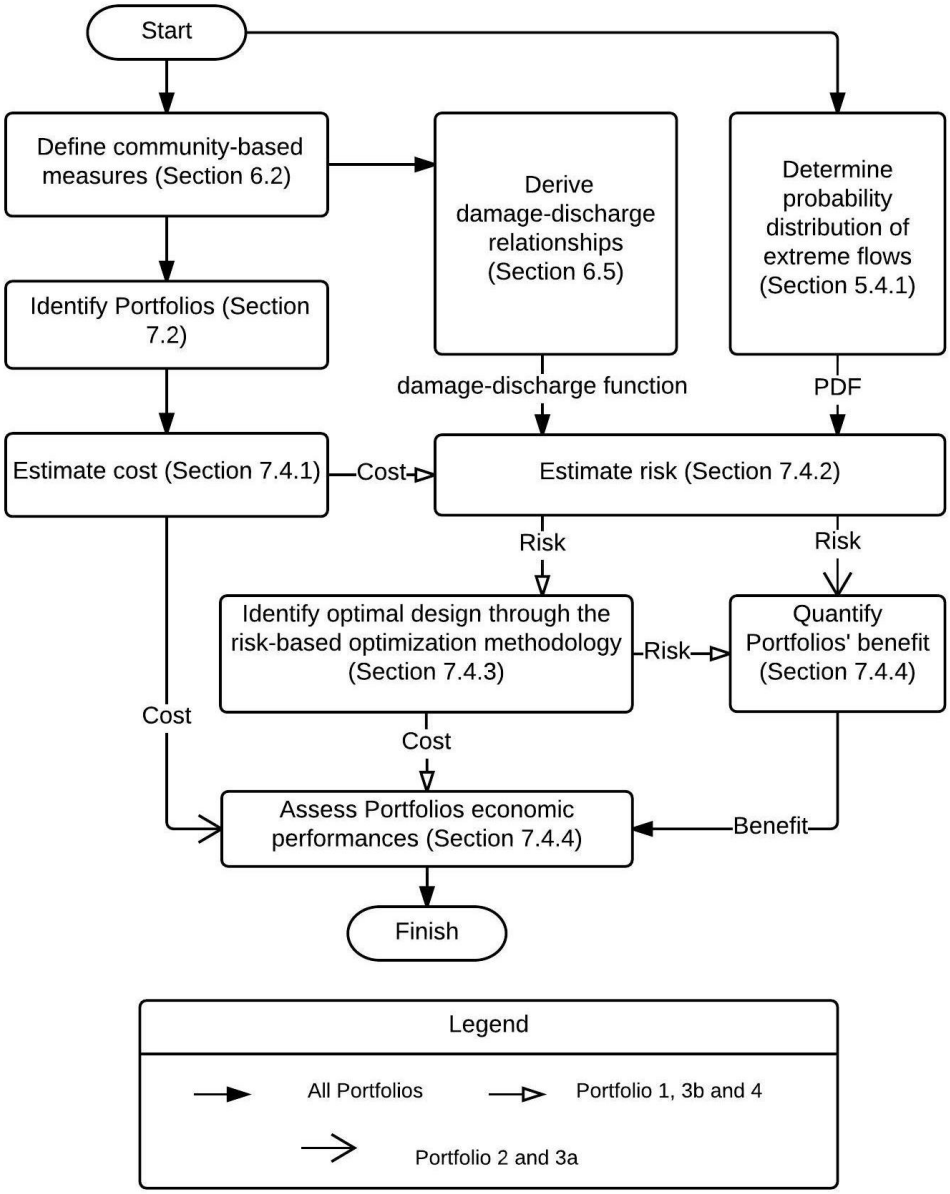

Figure 7.1: Steps of the main tasks of the portfolios appraisal.

Embankment

The type of material considered for the embankment flood defence is earth embankment/ The construction costs can be estimated based on the physical size of the embankment, i.e. the length of the embankment and its height, associated with an assigned crest height. The construction costs include material and labour costs, where both are more convenient to be estimated in a unit volume. A range of length of the embankment correspond to a range of crest heights was first established. The elevation levels of the base of the embankment regardless crest heights were assumed to be uniformed. Each length is divided into smaller divisions of similar length and the volume of each

division was quantified accordingly. The total volume associated with an embankment length was quantified by aggregating the volumes of all divisions. The ground elevation of each divisions was identified using the DEM. To ease the volume computation, the divisions with the same elevation level are grouped together. Upon comparing the elevation level of each group with the one having the lowest elevation level, the total volume conditional to the groups' elevation were quantified. Further aggregation of the total volume associated with each group returned a total volume of the given length.

An algorithm was established to ease the costs computations. Let k be the index of ascending ground elevations, where each k comprises more than one division and has a unique cross-sectional area (A). The estimation of an embankment cross-sectional area A_k typically follows the way a trapezoidal cross-sectional area is calculated. As depicted in Figure 7.2, input data required for the calculation is the slope of embankment, H:V where V is the vertical height of the defence and H is the horizontal width of the crest. The elevation level of an embankment crest level is considered consistent along the embankment length regardless the variability of ground elevation of the divisions. Therefore, the height of the defence at each division (y_k) can be determined by subtracting the ground elevation from the crest level elevation. By assuming that the horizontal width of the crest (x_k) is proportionately equal to y_k and the H:V is always constant, the calculation of A_k follows Equation 7.1.

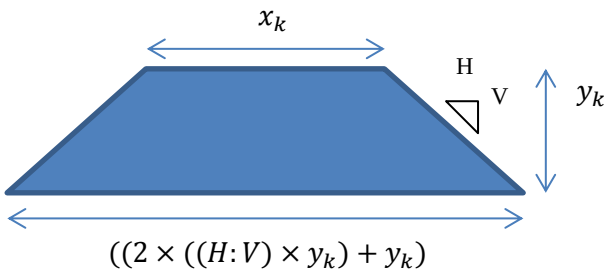

Figure 7.2: Schematic diagram of an embankment cross-section with its geometric properties.

$$A_k = 0.5 \times ((2 \times ((H:V) \times y_k) + y_k) \times {y_k}^2) \quad (7.1)$$

k may also be represented as the index of the maximum embankment height to allow the embankment costs to be computed as a function of maximum embankment height. Note that the

maximum embankment height is attributed to a protection design elevation or design discharge. To avoid confusion, let j be the index for the embankment height. Each j has information of the number of divisions (s) at each k and also the associated A_k. This information is essential in solving Equation 7.2 for the total volume (V) attributed to j. The total costs of the embankment (C_{ds}) correspond to j can then be estimated using Equation 7.3 with the assumption of 5% maintenance costs incurred every year. M is the estimated unit costs per cubic meter of the earth material, which includes the workmanship and other direct costs that can be adopted from a national estimation guideline. Other notations have been defined previously in this Section or in Chapter 4. The construction costs was assumed to occur only during the first year and the H:V to be 1:2 in accordance to a practical application of geotechnical engineering, as highlighted in Holtz (2011).

- $$V_j = (A_k \times z) \times s, \; s \in \mathbb{R} \tag{7.2}$$

$$C_{ds_j} = \left(M \times V_j\right) + \sum_{t=1}^{n_{str}} \left(\frac{1}{(1+r)^t} \times \left(\left(M \times V_j\right) \times 0.05\right)\right) \tag{7.3}$$

Channel dredging

Among the factors that contribute significantly to the costs of channel dredging are the excavation and haulage of soil. The total volumes of soil (V) that need to be handled during construction were estimated by identifying the cross-section and length of the riverbed. Figure 7.3 shows a schematic diagram of a typical river cross-section, comprising information of a current riverbed elevation and a proposed new elevation.

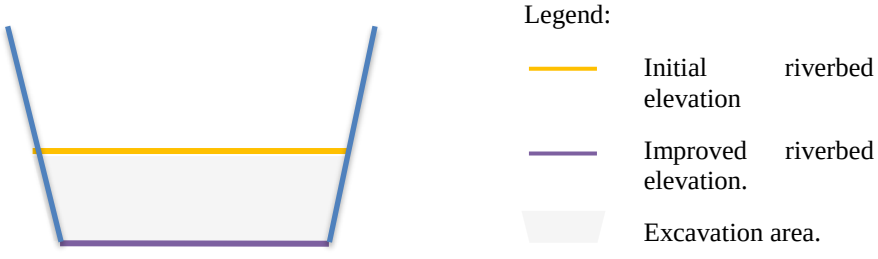

Figure 7.3: Schematic diagram of a main river channel cross-section before and after dredging.

Using a unit rate of excavation and haulage (M) and assuming the labour and other direct costs as 5% of the total costs, Equation 7.4 were adopted to obtain the total costs of the channel dredging (C_{ds_c}). The estimation also includes a yearly cost of 5% of the total costs to maintain the efficiency of the river. Other notations in the equation have been described previously. Note that additional works such as insertion of steel sheet piles, structures and amenities are excluded from the cost estimation.

$$C_{ds_c} = (M \times V_c \times 1.05) + \sum_{t=1}^{n_{str}} \left(\frac{1}{(1+r)^t} \times (M \times V_c \times 0.05) \right) \qquad (7.4)$$

Property-level protection

The property-level protection considered in this study adopts a PLP package of resistant type suggested by DEFRA (Aug 2012). An algorithm to estimate the total costs of PLP given a designed PLP extent is proposed. Two main variables were considered: total costs of equipment for a property, C_p and total number of properties to be protected, P. Using Equation 7.5, the present value for the PLP (C_{ds}) corresponds to a protection design elevation n can be estimated. i in the equation refers to the index of ground floor elevations of the properties protected with the PLP. Assuming minimal maintenance required and 5% of the total costs for the labour and fixed costs, the costs of intervention were estimated by multiplying the total number of properties and the costs per property, and the additional 5%.

$$C_{ds_n} = \sum_{t}^{n_{str}} \left(\frac{1}{(1+r)^t} \sum_{i}^{n} (C_p \times P_i) \times 1.05 \right), \quad t = \{0,20,40,80\} \qquad (7.5)$$

Embankment and Property-level protection

The costs of the combined measures of embankment and PLP can be estimated based on the costs functions of the individual measures. The algorithm was designed to handle matrix numbers as the inputs and the resulting outcomes as a Cartesian product $C_{ds_j} \times C_{ds_n}$, where C_{ds_j} is the cost for the embankment and C_{ds_n} is the cost for the property-level protection.

Flood protection costs over the appraisal period

In estimating the costs of the portfolios considered, it is important to lay out the streams of costs considered through the appraisal period. Construction costs for the embankment and the channel dredging were assumed to occur only in the first year of appraisal period, and maintenance costs to occur every year. Whilst for the PLP, DEFRA (Great Britain, Dept. for Environment, Food and Rural Affairs, Aug 2012) suggested the lifetime period of 20 years and minimum maintenance costs. This means that PLP should be replaced once every 20 years for a 100 years appraisal period, which consequently incur costs every 20 years. Table 7.2 highlights the assumptions made in relation to the type of costs and the time of occurrences. Figure 7.4 also illustrates the stream of costs of PLP over the 100 years appraisal period.

Table 7.2: Type of costs involve in each portfolio and associated occurrences

Type of measure	Type of Cost	Year of occurrence (index)	Remarks
Embankment	Investment costs	t= {0}	During the first year
	Maintenance costs	t={1,2,3…99}	Every year
Property-level protection	Investment costs	t={0,20,40,80}	In the first year in every 20 years
	Maintenance costs	-	-
Channel dredging	Investment costs	t= {0}	During the first year
	Maintenance costs	t={1,2,3…99}	Every year

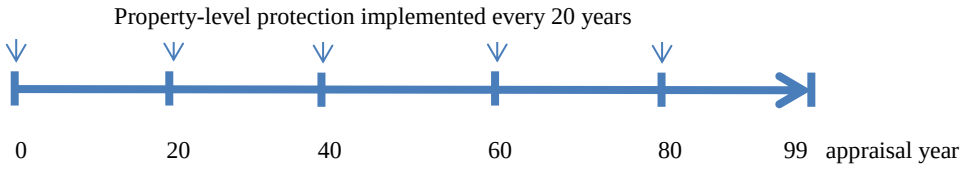

Figure 7.4: Schematic diagram of costs streams involving PLP over the appraisal period.

7.3.2 Risks function

This section provides designs risk algorithms to estimate residual risks of the base case (i.e. no intervention) and with-intervention conditions. The risk functions proposed here have the same form as the risk function presented in Section 4.2.5, but instead of adopting a simplified damage function (Section 4.2.3), the risk functions proposed in this study are built upon the developed damage calculator from Section 6.3. The damage function used here is, therefore, unique for each

considered portfolios in which the spatial influence of flood protection measures are embedded. The PDF used in the risk calculation is, on the other hand, consistent for all portfolios given the same characterisation of the flood hazard for the area. Section 5.2.2 provides explanation on approaches adopted in this study to quantify the annual risks for stationary and nonstationary conditions, considering the fitted GEV of each case (refer Section 5.4.5).

The importance of lower and upper limits of the risk integration limits have been emphasised in various places in Chapter 2 and Chapter 4. The characteristics of the damage function (i.e. from the damage-discharge relationship) and the PDF are essential to identify the lower and upper limits of the function. The lower limit of the risk integration, in this case, represents a flow discharge that prompts flood damages. It is important to identify how the interacting variables within the damage function may influence the determination of the lower limits. Table 7.3 provides associated notations of the damage function of each portfolio so as to highlight the associated variables and their possible contribution to the risk integration lower limit. The notations in the functions were specified according to the proposed damage modelling in Section 6.3. $h_w(.)$ and $V_{ds}(.)$ refers to the flood inundation level and flood overflow volume, respectively, where subscript j, c, n or nj denotes the protection design of embankment, channel modification, property-level protection or the combine protection of the embankment and property protection.

The lower limit for risk integration of the Portfolio 1 is conditioned to the protection design of the embankment. For the Portfolio 2, the lower limit is the flow discharge corresponds to the inundation level that first affects the buildings on the flood plain area. This was identified by interpolating the stage-discharge of the channel modification to obtain the lower limit for risk integration of the Portfolio 3 depends on the location of the lowest protected houses on the floodplain. The flow discharge of the lower limit was, therefore, determined by interpolating the stage-discharge relationship of the base case to obtain the flow discharge corresponds to the lowest protected buildings being flooded. The lower limit of Portfolio 4 is governed by the protection designs of both embankment and PLP, where a consecutive steps are needed to identify the flow discharge of the lower limit. First, the elevation where the protected buildings is first damaged by flood

inundation was identified. Using back-calculation, this information was then used to obtain the floodwater volume from the volume-stage relationship. The floodwater volume was further used to interpolate the flow discharge of the lower limit from the discharge-volume relationship.

Table 7.3: Important variables in damage function of each portfolio.

Portfolio	**Damage function**
Portfolio 1 (Embankment)	$D_t\left(h_{w,j}\left(V_{ds,j}(q)\right)\right)$
Portfolio 2 (Channel dredging)	$D_t\left(h_{w,c}(q)\right)$
Portfolio 3 (Property-level protection)	$D_t\left(h_{w,n}(q)\right)$
Portfolio 4 (Embankment and property-level protection)	$D_t\left(h_{w,nj}\left(V_{ds,j}(q)\right)\right)$

Further constraints of the upper limit of the risk integration are introduced by the PDF tail characteristics, hence require careful identification. By default, the upper limit is determined by the characteristic of the PDF. In the case where the upper limit may be extremely high that it is negligible, for example the ones that return a probability weighed damage of approximately zero, the upper limit may be replaced by a more sensible upper limit, which is lower than the actual upper limit.

The effects of the limits to the risk estimates will be more profound from the application of the functions. Note that the risk functions were used in the decision-making of Portfolios 1, 3b and 4, and also in the final analysis of economic performance of all Portfolios (refer Section 7.4.2).

7.3.3 Economic performance indicators

Economic appraisal of alternative portfolios leads to an identification of the most cost-effective portfolio. Although it is acknowledged that there is a variety of ways the economic appraisal can be undertaken (refer Chapter 3), this study focuses on using the well-accepted cost-benefit analysis for the decision analysis, which is consistent with what have been used in the economic appraisal of the hypothetical study in Chapter 4 and Chapter 5.

In this study, the cost-benefit analysis were applied for two objectives. The first objective is to identify an optimal decision by the application of risk-based optimization of flood protection. This is specifically to identify an optimal protection of Portfolio 1 and Portfolio 4, respectively. The second objective is to quantify the corresponding economic performance of flood protection decisions associated with the alternative portfolios in the form of NPV, BCR and IBCR.

The BCR and NPV equations from Section 5.2.3 and the IBCR (Equation 7.1 with the same notations as the ones used in Section 5.2.3) were adopted as the ultimate index for guiding the selection of the most cost-effective portfolio. Accounting the different possible condition of future underlying distribution, let T be the future predicted PDF of either stationary or nonstationary condition. The IBCR is the marginal benefit ($B_{T,2} - B_{T,1}$) of having a costlier portfolio between two competing portfolios, with the marginal costs of the portfolios ($C_{T,2} - C_{T,1}$). The returning IBCR indicates whether the costlier portfolio is justified for a higher benefit it offers. If IBCR ≥ 1, then the costlier portfolio is justified, otherwise, the least cost portfolio is preferred. Concerning more than one portfolio, the portfolios should be arranged according to an increasing order of costs. The IBCR is then quantified starting from the least cost portfolio and repeated until all portfolios have been evaluated. The one with the highest IBCR is quantitatively preferred.

$$IBCR = \left(\frac{B_{T,2} - B_{T,1}}{C_{T,2} - C_{T,1}}\right) \tag{7.1}$$

where,

$$B_T = \sum_{t=0}^{n_{str}} \frac{1}{(1+r)^t} \left(R_{t_{T,q_o}}(\mathrm{q}) - R_{t_{T,\hat{q}}}(\mathrm{q}) \right)$$

$$C_T = \sum_{t=0}^{n_{str}} \frac{1}{(1+r)^t} (\mathrm{C}_t(\hat{q}))$$

Other benefits or risk reduction measures, such as opportunities it offers or effects of flood warning may contribute to the economic performance of measures. However, these are not being considered for the fact that intangible and indirect benefit are difficult if not impossible to monetised (refer Chapter 2). Furthermore, the modelling chain proposed in Chapter 5 accounts for only direct and

tangible damage of residential buildings, hence the consistent assumption ensure the adaptability of the methodology.

7.4 Application and results

This section demonstrates the application of the proposed methodology to estimate the costs and residual risks of the considered alternative portfolios specifically for the local area in Teddington. The case study location has been presented in Section 6.4.1. The estimations of costs are presented in Section 7.4.1 and the residual risks estimations are presented in Section 7.4.2. Application of the risk-based optimization of flood protection (i.e. Portfolio 1, 3b and 4) using the configured cost and risk functions were provided in Section 7.4.3, followed by the evaluation of the economic performance of the considered portfolios in Section 7.4.4. Note that this study focuses on sensitivity of outcomes based on the different possible intervention and different condition of the underlying PDF and uncertainty range due to the natural variability is not considered. Where applicable, a discount rate of 3.5% is used to convert the costs and benefits to present values. Some configured numerical values for the costs and risk estimation were taken from the previous Chapters, which will be mentioned where applicable.

7.4.1 Costs of portfolios

This section demonstrates the costs estimations using the proposed methodology in Section 6.3.1. The stream of costs was considered yearly in accordance with the appraisal period defined in Section 6.2, i.e. $t = \{0,1,2, \dots ,99\}$. The sub-sections below explains how the costs of the considered portfolios were estimated.

Portfolio 1: Embankment

The first step in estimating embankment costs was to identify an appropriate location for the embankment, accounting the topography of the case study area. From the previous study in Chapter 6, a reasonable location has been identified and a range of embankment crest level with 3 meters as the has been established in the DEM (Section 6.4.5). The estimation steps described in Section 7.3.1

was subsequently undertaken to quantify the volume of the earth embankment required for the range of the embankment crest level considered.

Figure 7.5 shows the delineation of the ground elevation of the embankment length, having a 3 m maximum elevation level from the lowest elevation level. The x-axis represents the chainage of the considered maximum length of the embankment, which is divided into divisions of 50 m length. The y-axis represents the ground elevation level or the maximum height of the embankment considered. It is divided into layers of 0.2 m height. Equation 7.3 was then computed for the range of possible crest levels using £ 94 per cubic meter earth volume as an approximation, taken from the EA appraisal guidance (Environment Agency, 2010a).

Table 7.4 provides the input data and the computed outputs of the embankment costs estimates. Note that $j = 1$ refers to the crest elevation level index for the embankment. The total costs of the embankment as a function of flow discharge is presented in Figure 7.6, where the connection between the two were derived from the interpolation of the stage-discharge relationship (refer Section 6.4.2). The resulting metrics of cost given a range of design discharges and corresponding maximum crest levels are given in Table 7.5.

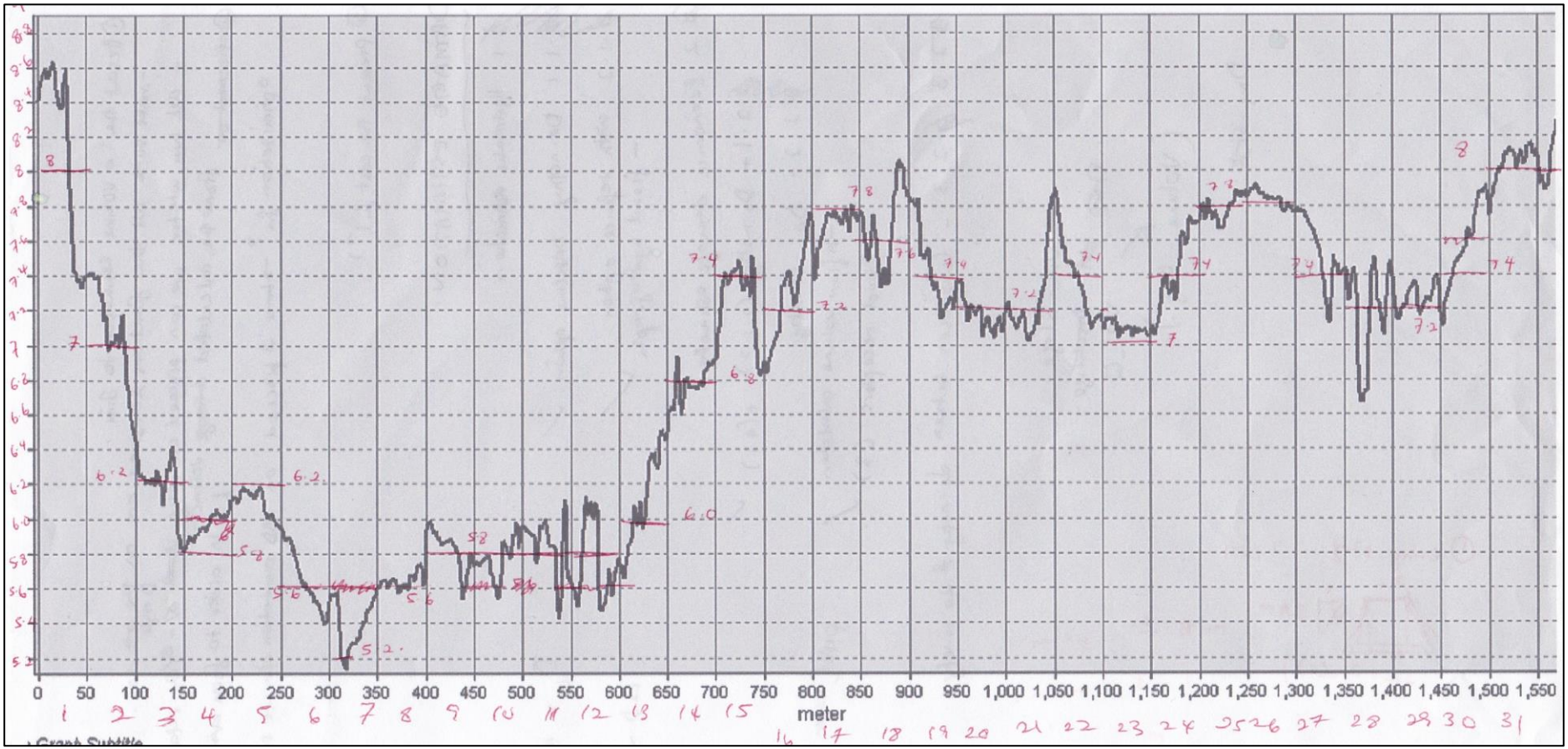

Figure 7.5: Cross-sectional length of the proposed embankment ground elevation taken from DEM. The red coloured marks are delineation of sub-sections made for the costs estimation.

Table 7.4: Summary of Portfolio 1 whole-life costs for a range of possible crest elevation.

Cest level index, j	Crest level, (m AD)	Maximum embankment crest height (m)	Volume, V_j (m^3)	Investment cost (£ in PV)	Yearly maintenance cost (£)	Maintenance (£ in PV)	Whole-life cost, (£ in PV)
1	5.6	0	0	0	0	0	0
2	5.8	0.2	66	6,204	310	8,558	14,762
3	6.0	0.4	174	16,356	819	22,563	38,919
4	6.4	0.8	714	67,116	3,356	92,587	159,703
5	7.0	1.2	2,502	235,188	11,759	324,444	559,632
6	7.4	1.6	4,476	420,744	21,037	580,420	1,001,164
7	8.0	2.0	9,468	889,992	44,500	1,227,752	2,117,744
8	8.4	2.4	14,532	1,366,008	68,300	1,884,420	3,250,429
9	8.6	3.0	17,622	1,656,468	82,823	2,285,113	3,941,581

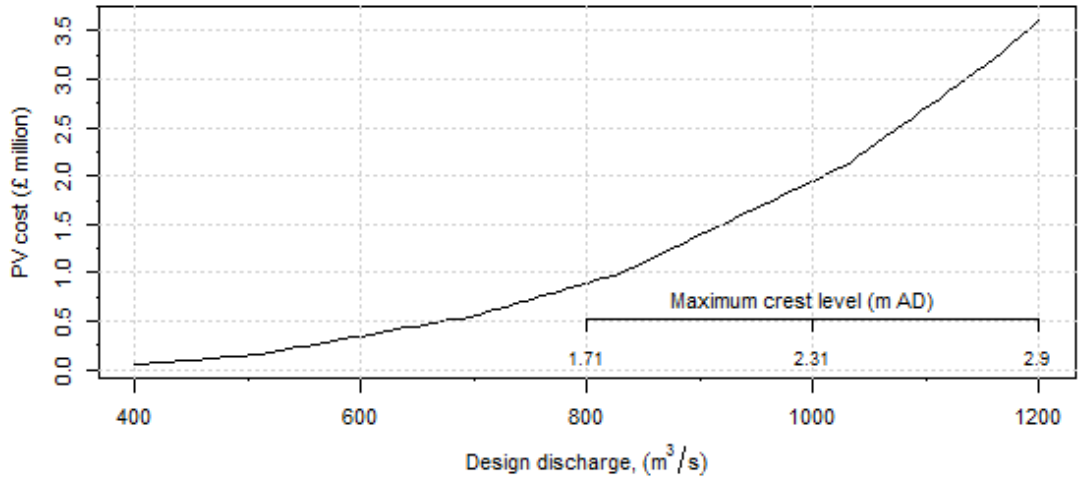

Figure 7.6: Cost-discharge relationship for embankment protection measure.

Table 7.5: Summary of Portfolio 1 whole-life costs for a range of possible design discharge.

Design discharge, (m^3/s)	Maximum embankment crest height (m)	Whole-life cost, (£ in PV)
400	0.44	51,988
500	0.77	149,662
600	1.08	349,005
700	1.40	557,491
800	1.71	896,324
900	2.01	1,389,944
1000	2.31	1,948,122
1100	2.61	2,703,917
1200	2.90	3,608,113

Portfolio 2: Channel dredging

The costs estimation of channel dredging requires information of the depth and length of the river to be dredged in determining the earth volume. In this study, the length of the river to be excavated

is approximately 800 m, identified from the delineation work in Section 6.4.2. The schematic cross-section of the riverbed before and after dredging is shown in Figure 7.7. Table 7.6 provides the estimated maintenance and total costs using an estimated cost rate of 10 £/m^3 for excavation and haulage at 5 to 10 km disposal site. The costs per unit estimates were taken from the EA (April, 2010), which extracted the costs per unit estimates from Spon.

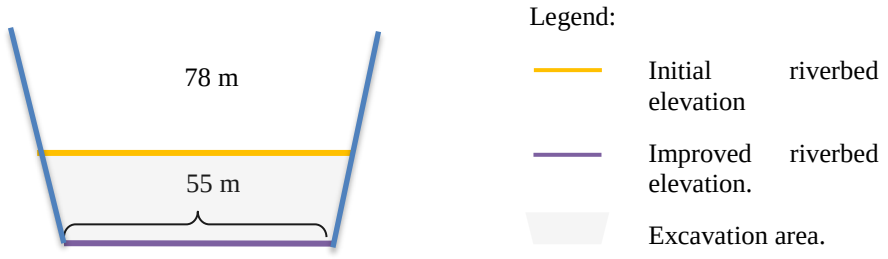

Figure 7.7: Schematic diagram of river channel cross-section with bed width before and after dredging.

Table 7.6: Summary of the whole-life costs of Portfolio 2.

Item	Description	Rate per unit, M	Total unit, V_c	Whole-life cost (£)
1.	Channel and Bank Works: Excavation and haulage (disposal at 5 – 10km)	10 £/m^3	53,200 m^3	532,000
2.	Yearly maintenance cost	-	-	27,930
2.	Maintenance costs in PV	-	-	771,520
3.	Total Cost (£ in PV)			1,330,121

Portfolio 3: Property-level protection

The costs of implementing the PLP package involve the costs of equipment required to be installed for a house and the number of houses targeted for the protection. Table 7.7 shows the list of costs estimated based on material components required for the PLP package as suggested by DEFRA (Aug 2012), classified according to lower, mid and upper costs estimates. It was assumed that the prices represent the current best estimate and can be implemented as an average value for any type of residential properties. In addition, the aggregated costs of the components include the instalment costs. The number of properties equipped with PLP of a given protection extent for a range of PLP extents considered has been identified and presented in Section 6.4.6. The costs as a function of the

PLP extents were computed by aggregating the total costs of PLP adopted at each elevation steps up to the target protection level.

Table 7.7: Costs of property-level protection resistance package components.

Components	**Cost (£)**		
	Lower	**Mid**	**Upper**
Demountable door barriers	500	700	900
Manual airbrick and vent covers	20	30	40
sewerage bung	30	40	50
toilet pan seals	60	70	80
re-pointing external walls up to 0.6m above ground level with water resistant mortar	150	200	250
silicone sealant around service and cable entry points	80	100	120
sump pump	400	500	600
waterproof external walls	200	300	400
Total cost, C_p (£)	**1,440**	**1,940**	**2,440**

Table 7.8 summarises the total costs associated with the number of properties being protected at each elevation steps, whilst Table 7.9 provides the cumulative costs associated with the range of targeted PLP extents considered. Note that the targeted PLP extent is attributed to the ground floor elevation level of the highest protected properties. Lower, mid and upper costs estimates are provided in both tables, but only the middle costs estimates were further used. For the Portfolio 3a (i.e. PLP extent corresponds to a 20-year return period of the stationary condition), the corresponding design elevation was identified using the inverse CDF from Section 5.4.1 and the stage-discharge relationship of the base case from Section 6.3.1. This returns a protection extent correspond to 6.3 m AD of ground elevation level of the highest protected properties. The design elevation was used to identify the total costs for the Portfolio 3a from Table 7.9. The Portfolio 3a of the stationary and nonstationary conditions implies the same PLP extent, although 20-year protection return period for the cases might be different.

The estimated costs as shown in Table 7.9 implies a one-off costs of implementation. For once in every 20 years of implementation over the 100 years period of appraisal, the PV costs of each considered PLP extent were computed to obtain the total PV costs of each PLP extent.. The results

are presented together with the one-off costs in Table 7.10. The table also includes the return periods of the stationary distribution associated with the targeted PLP extents. A higher PV costs can be seen for a higher protection level.

Table 7.8: Summary of property-level protection total costs at a range of ground floor elevations. Lower, middle and upper estimates of costs are included.

i	Ground floor elevation (m AD)	Number of properties with ground floor elevation i, P_i	Total costs at each elevation (£)		
			Lower	Mid	Upper
1	5.6	4	6,048	8,148	10,248
2	5.7	3	4,536	6,111	7,686
3	5.8	3	4,536	6,111	7,686
4	5.9	1	1,512	2,037	2,562
5	6	3	4,536	6,111	7,686
6	6.1	5	7,560	10,185	12,810
7	6.2	7	10,584	14,259	17,934
8	6.3	6	9,072	12,222	15,372
9	6.4	20	30,240	40,740	51,240
10	6.5	21	31,752	42,777	53,802
11	6.6	13	19,656	26,481	33,306
12	6.7	24	36,288	48,888	61,488
13	6.8	17	25,704	34,629	43,554

Table 7.9: Summary of property-level protection total costs for a range of design elevation and cumulative number of buildings protected. Lower, middle and upper estimates of costs are included.

i	PLP design elevation (m AD)	Cumulative number of properties with PLP extent i, P_i	Sum of cost corresponds to property-level protection extent, C_{ds_n} (£)		
			Lower	Mid	Upper
1	5.6	4	6,048	8,148	10,248
2	5.7	7	10,584	14,259	17,934
3	5.8	10	15,120	20,370	25,620
4	5.9	11	16,632	22,407	28,182
5	6	19	21,168	28,518	35,868
6	6.1	26	28,728	38,703	48,678
7	6.2	32	39,312	52,962	66,612
8	6.3	52	48,384	65,184	81,984
9	6.4	73	78,624	105,924	133,224
10	6.5	86	110,376	148,701	187,026
11	6.6	110	130,032	175,182	220,332
12	6.7	127	166,320	224,070	281,820
13	6.8	145	192,024	258,699	325,374

Table 7.10: Summary of Portfolio 3b whole-life costs for a range of targeted PLP extents. Only the median costs are considered.

PLP design elevation (m AD)	Design discharge (m^3/s)	Stationary distribution Return period	Cumulative number of protected properties	One-off cost (£, once every 20 years)	Whole-life cost over appraisal period (£ in PV)
5.9	352	3	11	22,407	43,601
6.1	434	7	19	38,703	75,311
6.2	475	11	26	52,962	103,057
6.3	518	18	32	65,184	126,839
6.4	569	33	52	105,924	206,114
6.5	619	62	73	148,701	289,352
6.6	670	117	86	175,182	340,881
6.7	726	242	110	224,070	436,010
6.8	790	570	127	258,699	503,393
6.9	854	1384	145	295,365	574,741

Portfolio 4: Embankment and channel modification

Costs estimation for Portfolio 4 was computed by retrieving the previously estimated costs for Portfolio 1 (i.e. embankment protection) and Portfolio 3 (i.e. property-level protection). Estimated costs were arranged to form matrixes of the same size. The resulting outcomes of the Cartesian product $C_{ds_j} \times C_{ds_n}$ then stored accordingly as presented in the 11 columns far right in Table 7.11. The first two columns of the table present the considered range of targeted PLP extent, whilst the first six rows contain the information of the selected range of embankment protection design. Note that the zero costs in the table refers to the do-nothing case. The results clearly show that a higher protection design result in a much higher whole-life cost.

7.4.2 Risk estimation of portfolios

This section presents the risk estimation of the alternative portfolios, respectively, following the explanation given in Section 7.3.2. Recall that the stationary and nonstationary future conditions considered in this study follows the PDFs of the best-fitted stationary GEV to the Thames at Kingston historical records and the best-fitted nonstationary GEV to the climate model-based future flows projections of the Thames at Kingston. The GEV parameters associated with the distributions have previously estimated in Section 5.4.1. Whilst the risk estimation of the two scenarios used different PDFs, the damage function is independent of the PDF, but conditional to the portfolios.

Table 7.11: Summary of Portfolio 4 costs for a range of targeted PLP extents based on median costs estimates.

Highest protected properties' ground elevation (m AD)	Number of protected properties		Embankment design (m^3/s)					
			N/A	400	450	500	550	600
			Highest crest level (m AD)					
			N/A	6.04	6.37	6.68	7	7.31
			Highest crest level (m)					
			0	0.44	0.61	0.77	0.93	1.08
			Cost (£ in PV)					
N/A	N/A	Cost (£ in PV)	0	51,988	101,062	149,662	243,272	349,005
5.9	11		43,601	95,589	144,663	193,263	286,873	392,606
6.1	19		75,311	127,298	176,373	224,973	318,583	424,316
6.2	26		103,057	155,044	204,119	252,719	346,329	452,062
6.3	32		126,114	178,827	227,901	276,502	370,112	475,845
6.4	52		206,114	258,101	307,176	355,776	449,386	555,119
6.5	73		289,352	341,340	390,414	439,015	532,624	638,358
6.6	86		340,881	392,868	441,942	490,543	584,153	689,886
6.7	110		436,010	487,998	537,072	585,672	679,282	785,015
6.8	127		503,393	555,381	604,455	653,056	746,666	852,399
6.9	145		547,741	626,728	675,802	724,403	818,013	923,746

It is worth to emphasise that the risk estimations of Portfolio 2 and Portfolio 3a were undertaken for fix protection designs, whilst Portfolio 1, Portfolio 3b and Portfolio 4 adopt the risk-based optimization of a range of design protection to obtain the preferred design, respectively. In the latter cases, protection designs were used together with the associated costs to obtain the total present value costs (TPVC), hence an optimal protection can be identified. The application is further demonstrated in the subsequent section.

7.4.3 Identification of an optimal protection using the risk-based optimization

This section demonstrates the application of the risk-based optimization of flood protection for Portfolio 1, Portfolio 3a and Portfolio 4, respectively. The computations were undertaken following the explanation in Section 5.2.2, but the cost and damage functions were configured in Section 7.4.1 and Section 6.5. The risk computations were targeted for a range of possible protection designs of the same magnitude as those considered earlier in the damage modelling (Section 6.5).

The lower limit of the risk function associated with each portfolio was identified through the execution of the proposed approach specified in Section 7.3.2. The upper limit, on the other hand, takes the maximum flow discharge defined in the vulnerability assessment in Chapter 6, which is

1100 m^3/s for the stationary condition (refer Section 6.4.1 for justifications) and the actual PDF's upper limit for the nonstationary condition. The following sub-sections present the quantitative outcomes in search for an optimal protection design. The results are compared between those from stationary and nonstationary conditions.

Portfolio 1: Optimization for embankment protection

Table 7.12 provides the input and output of the TPVCs of embankment designs ranging from 400 to 600 m^3/s under stationary (SE) and nonstationary (NSE) conditions. The curves of the PV risks, PV costs and TPVCs of the protection designs are depicted in Figure 7.8. For both PDFs, it is apparent that the residual risks are lower as the protection goes higher. The increase in costs of the higher protection design is insubstantial as compared to the associated reduction of risk. In comparing between the PV risks of the stationary and nonstationary conditions of the same protection design, the PV risk of the nonstationary condition is higher than that of the stationary condition for a lower protection design, but not the case when a greater protection design is considered. The reason behind this can be observed from Figure 7.9 where the annual risks of the nonstationary condition eventually decline when higher protection designs are adopted, which result in the total PV risks to drop to a lower magnitude than the total PV risks of the stationary condition. This behaviour eventually contributes to a higher rate of reduction of TPVCs over the higher protection under the nonstationary condition as compared to that under stationary condition.

Table 7.12: Summary of Portfolio 1 TPVCs and associated information associated with a range of selected design discharge. SE refers to the stationary conditions and NSE refers to the nonstationary conditions. Highlighted row shows the optimal protection design for stationary and nonstationary cases.

Design dscharge, (m^3/s)	**Return Period**	**Max crest level (m)**	**Annual risk, (£)**		**Risk, (£ in PV)**		**Cost, (£ in PV)**	**Total present value cost, $TPVC$ (£)**	
			SE	NSE	SE	NSE		SE	NSE
400	7	0.44	64,074	N/A (varies with time)	1,834,027	3,076,980	51,988	1,886,014	3,128,967
450	12	0.61	31,863		912,040	916,752	101,062	1,013,102	1,017,813
500	23	0.77	12,554		359,350	256,994	149,662	509,013	406,656
550	47	0.93	5,308		151,921	72,729	243,272	395,193	316,002
600	105	1.08	2,625		75,125	15,445	349,005	424,130	364,450

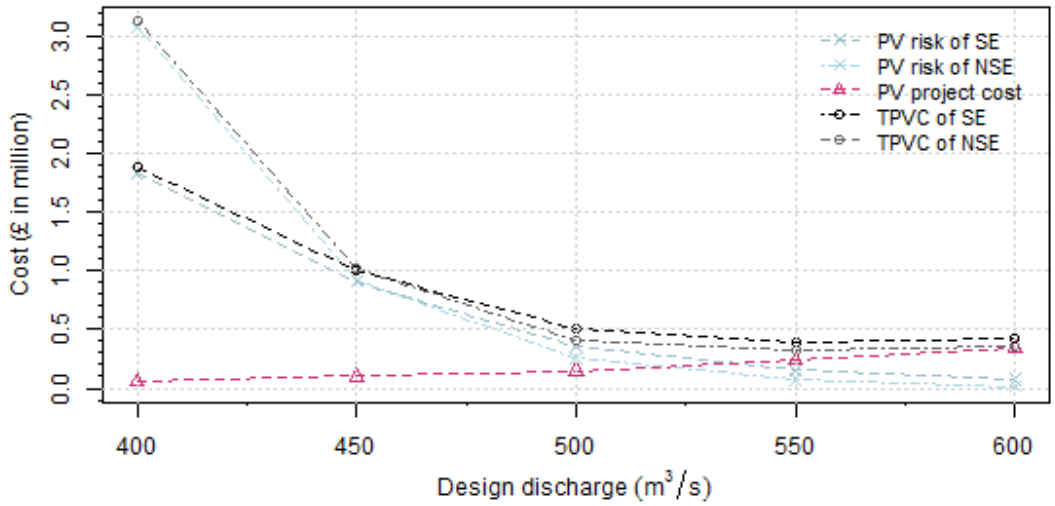

Figure 7.8: PV risk, costs and TPVC curves of Portfolio 1 for the range of design discharge.

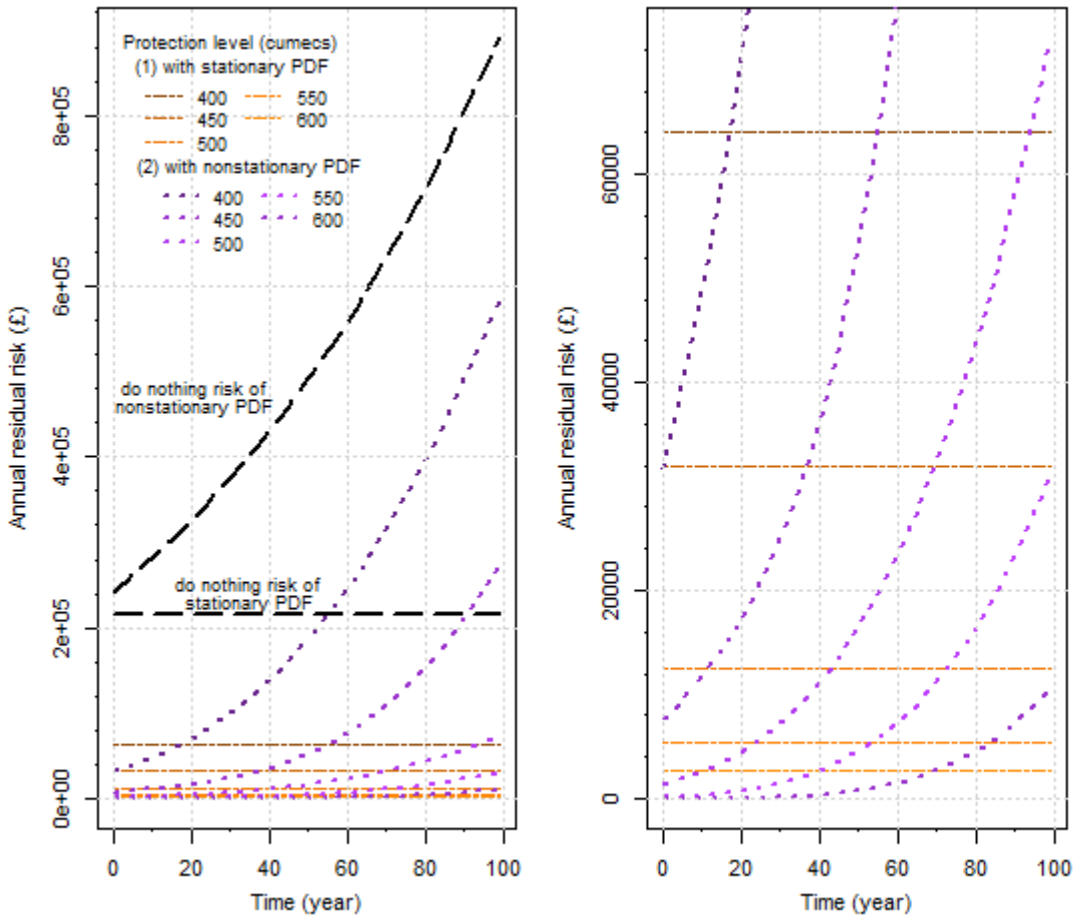

Figure 7.9: Annual risk curves from do-nothing and Portfolio 1 of the stationary and nonstationary conditions respectively as they vary through years. (a) Complete range of the expected annual risks of all scenarios, (b) Magnified range to highlight the distinct outcomes of expected annual risks from higher protection designs.

Despite the different TPVCs of stationary and nonstationary conditions of the same protection design magnitude, the optimal designs of Portfolio 1 of both cases are apparently the same, i.e. 550 m^3/s. The associated maximum crest height of this design is approximately 0.93 m, obtained through the interpolation of the stage-discharge relationship of the condition with embankment from Section 6.4.2.

Portfolio 3b: Optimized property-level protection

Table 7.13 shows the summary of the input and output in search of the optimal protection design of Portfolio 3b. The results of PV risks, PV costs and TPVCs of both cases are tabulated in Figure 7.10. The PV risks and TPVCs of the nonstationary condition are consistently higher than that of the stationary condition, indicating the small influence of the nonstationary annual risks reduction over the appraisal years to the final outcomes. The TPVCs of the stationary case return an optimal protection threshold of 117-year return period corresponds to a number of 86 building being protected. In the case of nonstationary, the resulting optimal protection result in 73 buildings to be protected.

Table 7.13: Summary of Portfolio 3b TPVCs and associated information associated with a range of selected design protection elevation. SE refers to the stationary conditions and NSE refers to the nonstationary conditions. Highlighted rows show the optimal protection designs for stationary and nonstationary cases respectively.

Highest protected properties' ground elevation (m AD)	Design discharge, m^3/s	Return period	Number of protected properties	Cost, (£ in PV)	Present value risk, (£)		Total present value cost, (£)	
					SE	NSE	SE	NSE
6.3	518	18	32	126,839	1,117,562	1,549,780	1,244,401	1,676,619
6.4	569	33	52	206,114	794,230	1,097,352	1,000,343	1,303,466
6.5	619	62	73	289,352	614,289	963,027	903,641	1,252,380
6.6	670	117	86	340,881	558,414	946,535	899,295	1,287,416
6.7	726	242	110	436,010	513,060	944,262	949,070	1,380,272
6.8	790	570	127	503,393	499,839	944,255	1,003,232	1,447,649

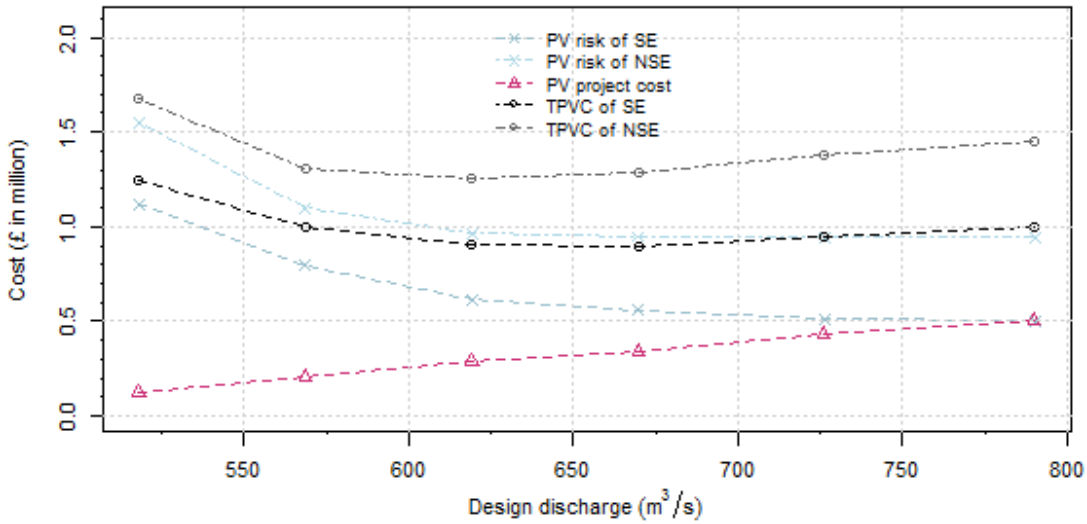

Figure 7.10: The curves of Portfolio 3b PV risk, cost and TPVC for the range of design discharge.

Portfolio 4: Optimized embankment and property-level protection

Table 7.14 shows the annual risks of the combined protections of embankment and property-level protection under the stationary condition. The annual risk declines when a higher protection design is adopted. The nonstationary annual risks are not included in the table for clarity, but the resulting PV risks of the nonstationary condition are summarised in table 7.15 along with the PV risks of the stationary condition for comparison.

Table 7.14: Summary of Portfolio 4 annual residual risk of the stationary condition.

Highest protected properties' ground elevation (m AD)	**Number of protected properties**		**Embankment design (m^3/s)**					
			N/A	400	450	500	550	600
			Highest crest level (m AD)					
			N/A	6.04	6.37	6.68	7	7.31
			Highest crest level (m)					
			0	0.44	0.61	0.77	0.93	1.08
			Residual risk (£ in annum)					
N/A	N/A	**Residual risk (£ in annum)**	214,716	64,074	31,863	12,554	5,308	2,625
5.9	11		68,873	48,112	21,033	6,260	2,042	1,027
6.1	19		55,737	42,786	20,493	6,122	1,880	944
6.2	26		45,262	37,425	19,231	5,974	1,769	891
6.3	32		39,044	32,878	17,861	5,768	1,723	874
6.4	52		27,748	21,716	13,263	4,948	1,631	866
6.5	73		21,461	15,429	8,903	4,019	1,475	816
6.6	86		19,509	13,477	6,992	3,447	1,361	766
6.7	110		17,925	11,892	5,408	2,515	1,148	670
6.8	127		17,463	11,430	4,946	2,070	1,006	604

Ground elevation of the highest protected properties (m AD)	Number of protected properties		Embankment design (m^3/s)											
			N/A		400		450		500		550		600	
			Highest crest level (m AD)											
			N/A		6.04		6.37		6.68		7		7.31	
			Maximum crest level (m)											
			0		0.44		0.61		0.77		0.93		1.08	
			Residual risk (£ in PV)											
			SE	NSE	SE	NSE	SE	NSE	SE	NSE	SE	NSE	SE	NSE
N/A	N/A	Residual risk (£ in PV)	6,151,590	10,471,502	1,834,027	3,076,979	912,040	916,751	359,350	256,993	151,921	72,729	75,125	15,445
5.9	11		1,971,383	3,563,105	1,377,139	1,858,515	602,048	206,694	179,190	278	58,449	0	29,408	0
6.1	19		1,595,372	2,610,221	1,224,692	1,541,362	586,592	196,273	175,241	173	53,812	0	27,035	0
6.2	26		1,295,540	1,911,199	1,071,222	1,261,644	550,449	179,059	171,002	109	50,625	0	25,496	0
6.3	32		1,117,562	1,549,780	941,081	1,042,389	511,238	161,207	165,093	99	49,314	0	25,016	0
6.4	52		794,230	1,097,352	621,577	601,106	379,620	104,945	141,638	93	46,697	0	24,795	0
6.5	73		614,289	963,028	441,633	466,782	254,842	56,757	115,034	86	42,227	0	23,368	0
6.6	86		558,414	946,535	385,749	450,293	200,146	41,681	98,660	83	38,951	0	21,936	0
6.7	110		513,060	944,262	340,389	448,019	154,792	39,407	72,001	78	32,871	0	19,187	0
6.8	127		499,839	944,255	327,179	448,012	141,571	39,400	59,249	77	28,806	0	17,287	0

Table 7.15: Summary of Portfolio 4 PV risks from stationary (SE) and nonstationary (NSE) cases.

It is expected that adoption of the same flood protection scheme in the stationary and nonstationary condition, respectively, will consequently lead to residual risks that is higher in nonstationary condition. As can be seen from Table 7.15, adoptions of a relatively lower protection scheme lead to a lower PV risks under the stationary condition as compared to under the nonstationary condition. However, a relatively higher combined protection design shown to yield a higher PV risks under the stationary condition as compared to the resulting PV risks under the nonstationary condition. For example, an adoption of a 0.44 m maximum embankment height and PLP to 127 residential buildings result in a higher PV risk under the nonstationary condition compared to the PV risk under the stationary case, whereas an adoption of a 0.61 m maximum embankment height and PLP to 127 residential buildings lead to a smaller PV risk under the nonstationary case as compared to the PV risk under the stationary case. The counter-intuitive findings are, nevertheless, consistent with the previous comparison of the annual risks of the stationary and nonstationary conditions.

Moreover, the Portfolio 4 is related to embankment and PLP, hence the results can be cross-checked with the results of the Portfolio 1 and Portfolio 3. For example, we can see from Figure 7.8 of Portfolio 1 that the PV risk of stationary overcome the PV risk of nonstationary for higher protection designs. The PV risk curve of the nonstationary case also starts to decrease at a much faster rate as compared to the PV risk curve of the stationary case, resulting a lower PV risk when embankment height adopted is higher than 0.61 m (i.e. corresponds to approximately 450 m^3/s). The declining rate is further aggravated when PLP is adopted in Portfolio 4, causing the PV risks to dramatically decline for the nonstationary condition. Also, under the nonstationary condition the PV risks drop to zero when 0.93 m or 1.03 m maximum embankment height is adopted (i.e. corresponds to protection designs of 550 or 600 m^3/s, respectively), indicating the significant protection for the area.

.

Ground elevation of the highest protected properties (m AD)	Number of protected properties		Embankment design (m^3/s)											
			N/A		400		450		500		550		600	
			Highest crest level (m AD)											
			N/A		6.04		6.37		6.68		7		7.31	
			MAximum crest level (m)											
			0		0.44		0.61		0.77		0.93		1.08	
			TPVC (£ in PV)											
			SE	**NSE**	**SE**	**NSE**	**SE**	**NSE**	**SE**	**NSE**	**SE**	**NSE**	**SE**	**NSE**
N/A	N/A	TPVC (£ in PV)	6,151,590	10,471,502	1,886,014	3,128,967	1,013,102	1,017,813	509,013	406,656	395,193	316,002	424,130	364,450
5.9	11		2,014,984	3,606,706	1,472,727	1,954,103	746,711	351,357	372,454	193,542	345,322	286,873	422,015	392,606
6.1	19		1,670,682	2,685,532	1,351,990	1,668,661	762,964	372,645	400,214	225,146	372,396	318,583	451,351	424,316
6.2	26		1,398,594	2,014,256	1,226,267	1,416,689	754,567	383,178	423,721	252,829	396,954	346,329	477,559	452,062
6.3	32		1,244,401	1,676,619	1,119,908	1,221,216	739,139	389,108	441,595	276,601	419,426	370,112	500,860	475,845
6.4	52		1,000,343	1,303,466	879,678	859,208	686,796	412,121	497,414	355,869	496,083	449,386	579,914	555,119
6.5	73		903,641	1,252,380	782,972	808,121	645,255	447,171	554,049	439,101	574,851	532,624	661,725	638,358
6.6	86		899,295	1,287,416	778,617	843,161	642,088	483,623	589,203	490,626	623,104	584,153	711,822	689,886
6.7	110		949,070	1,380,272	828,387	936,016	691,864	576,479	657,673	585,750	712,153	679,282	804,203	785,015
6.8	127		1,003,232	1,447,649	882,560	1,003,393	746,026	643,856	712,305	653,132	775,472	746,666	869,685	852,399

Table 7.16: Summary of Portfolio 4 TPVCs from stationary (SE) and nonstationary (NSE) conditions. The highlighted cells referring to the optimal protection of stationary and nonstationary conditions, respectively.

Resulting zero risks in Table 7.15 are the consequences of the nonstationary PDF upper limit having a smaller value that the lower limit of the damage function of Portfolio 4 annual risk calculation (refer Section 5.2.2 for illustration of the nonstationary PDF and Section 7.3.2 for the lower limit of the risk function of Portfolio 4). The results in the table indicates that the upper limit of the nonstationary PDF are smaller than the lower limit of the damage function Portfolio 4 for protection designs that are higher than the combined protection of 0.93 m maximum crest level and PLP to 11 residential buildings. For example, the computed nonstationary PDFs' upper limit returns 644 m^3/s at t=0 and 821 m^3/s at t=99, whereas a maximum 0.93 m crest level and 11 residential building being individually protected yield a 919 m^3/s lower limit regardless time. Consequently, the probability density function and the damage function in the risk estimation do not overlap, resulting the zero values.

Taking forward the quantified PV costs and PV risks, Table 7.16 compiles the resulting TPVCs of Portfolio 4 under the stationary and nonstationary conditions. It can be observed that under the stationary case, the estimated optimal protection is a combined protection of 0.93 m maximum embankment height and 11 residential buildings being individually protected. Whilst under the nonstationary case, the estimated optimal protection is a combined protection of 0.77 m maximum embankment height and 11 properties being individually protected

The PV risks and PV costs of the identified optimal designs from Portfolios 1, 3b and 4 were then brought forward to evaluate the economic performance of all portfolios. Section 7.4.4 presents the results of the economic performance of the portfolios, together with the economic performance of Portfolio 2 and Portfolio 3.

Verification of the risk computation

The previous computation of residual risks adopted a designed automated function that was built in R to expedite the numerical calculation. A readily available integration function available in R software was embedded in the function. To verify whether the designed automated function is reliable, a test was conducted by manually computing the residual risk using a conventional discrete

computational method. Comparison of the results from the different methods that use the same input data and constraints ascertains the reliability of the automated function.

Formulating risk as a cumulative result of probability-weighed damages, i.e. PWD, equation 7.7 adopted from Meyer, Priest and Kuhlicke (2012) was used to manually calculate the residual risk. $\Delta\rho$ is the probability of the interval between two consecutive exceedance probability event, in this case taken from the stationary PDF, and $\overline{D}_{ds}$ is the mean of the consequential damage of the two events. Adopting the PLP, water level was chosen as the determinant of the calculation. The water level-discharge relationship ($Q(h_w)$) was therefore interpolated using two inundation damaging events represented by h_{w_i} and $h_{w_{i+1}}$. The corresponding extreme discharges were then used together with the distribution parameters ($\boldsymbol{\theta}$) of the CDF function ($\rho(.)$) to obtain $\Delta\rho$.

$$PWD = \sum_{j=1}^{k} \overline{D}_{ds_j} \times \Delta\rho_j \tag{7.7}$$

$$\Delta\rho_j = \rho\left(\boldsymbol{\theta}, Q(h_{w_{i+1}})\right) - \rho\left(\boldsymbol{\theta}, Q(h_{w_i})\right)$$

$$\overline{D}_{ds_j} = \left(\frac{D_{ds}\left(h_{w_{i+1}}\right) - D_{ds}\left(h_{w_i}\right)}{2}\right)$$

PLP extent that protects residential buildings up to the ones located on a ground elevation level of 6.3m AD was selected to demonstrate the computation. The upper limit of the manual risk calculation was taken as 1100 m^3/s to ensure consistency with the previous computational integration. The 1100 m^3/s upper limit was then used to interpolate the corresponding maximum flood inundation elevation level through the stage-discharge relationship, returning a maximum inundation level of 7.3m AD. Subsequently, the inundation range from 6.3 to 7.3m AD was divided into equally spaced vectors. The vectors were then used to interpolate the corresponding exceedance probabilities through the associated stage-discharge relationship and CDF of the stationary condition. The consequential damages associated with the water levels were then extracted from the damage-water level relationship.

Table 7.17 summarises the resulting probability-weighed damage for the case of stationary and the inputs as previously described. The difference between the annual risk from the automated

computation (i.e. £ 39,044) and the residual risk from the manual calculation (i.e. £ 40,017) is approximately 2.4%. The discrepancy might have caused by the sub-divisions in the manual computation. However, the small percentage of discrepancy may not be significant to the final economic appraisal.

Table 7.17: Inputs and outputs of probability-weighed damage (i.e. annual risk) of adopting PLP for stationary case based on manual calculation.

	Water level, h_w	**Flood discharge, Q**	**Exceedance probability, $P(Q(h_w))$**	**Index for probability-weighed damage, j**	**Probability of the interval, $\Delta\rho$**	**Midpoint Damage, D_{ds} (£)**	**Probability-weighed damage (£)**
1	6.3	518	0.05423				
				1	0.02431	197,207	4,795
2	6.4	569	0.02992				
				2	0.01375	497,046	6,836
3	6.5	619	0.01616				
				3	0.00760	1,060,895	8,059
4	6.6	670	0.00857				
				4	0.00444	1,702,276	7,557
5	6.7	726	0.00413				
				5	0.00237	2,457,249	5,832
6	6.8	790	0.00175				
				6	0.00103	3,340,256	3,445
7	6.9	854	0.00072				
				7	0.00043	4,227,031	1,837
8	7	918	0.00029				
				8	0.00018	5,325,257	962
9	7.1	984	0.00011				
				9	0.00007	6,829,999	474
10	7.2	1051	0.00004				
				10	0.00002	8,806,948	220
11	7.3	1118	0.00001				
						$\sum_{i=1}^{n}(\Delta\rho \times \bar{D}_{ds})$:	£ 40,017

7.4.4 Economic performance of alternative portfolios

The costs and benefits are the two input variables required for computations of the economic performance. The costs were taken from Section 7.4.1 and the benefits were quantified based on the reduction of risks of each portfolio. The benefits of Portfolio 1, Portfolio 3b and Portfolio 4 were estimated using the computed risks associated with the optimal designs, respectively (refer

Section 7.4.3). For Portfolio 2 and 3a, the benefits were computed using the computed risks correspond to the associated fix designs. Metrics representing possible reduction of risk offered by each portfolio under the nonstationary and stationary conditions as compared to the do-nothing case are compiled in Table 7.18 and Table 7.19. The associated BCRs and NPVs as well as the related economic metrics are also presented in the tables. The information are arranged in accordance to the incremental costs of the portfolios, where the second far right column contains information of the portfolio with the highest costs, followed by portfolio with the least costs in the far left column. The bottom row shows the IBCRs, where the highlighted cell represents the preferred portfolio.

Table 7.18: Summary of the final economic performance of all considered portfolios under stationary condition. The highlighted row represents portfolio with the highest IBCR.

Portfolio	**(3a) Property-level protection corresponds to 1:20**	**(1) Optimized embankment**	**(4) Optimized embankment and property-level protection**	**(3b) Optimized property-level protection**	**(2) Channel dredging**
Description	32 houses individually protected	Embankment allocation with maximum crest level of 0.93 m	Embankment allocation with maximum crest level of 0.93 m and 11 houses individually protected	86 houses individually protected	1 meter dredging of main channel
Whole-life costs (£ in PV)	126,839	243,272	286,873	340,881	558,600
Risk of base case (£ in PV)	6,151,590	6,151,590	6,151,590	6,151,590	6,151,590
Risk of with-project (£ in PV)	1,117,562	151,921	58,449	558,414	3,150,456
Benefit (£ in PV)	5,034,028	5,999,669	6,093,141	5,593,176	3,001,135
NPV (£)	4,907,189	5,756,397	5,806,268	5,252,296	2,442,535
BCR	39.69	24.66	21.24	16.41	5.37
IBCR	N/A	8.29	2.14	-9.26	-11.38

Table 7.19: Summary of the final economic performance of all considered portfolios under nonstationary condition. The highlighted row represents the portfolio with the highest IBCR.

Portfolio	**3a) Property-level protection of 20 year return period**	**4) Optimized embankment and property-level protection**	**1) Optimized embankment**	**3b) Optimized property-level protection**	**2) Channel dredging**
Description	32 houses individually protected	Embankment allocation with maximum crest level of 0.77 m and 11 houses individually protected	Embankment allocation with maximum crest level of 0.93 m	73 houses protected	1 meter dredging of main channel
Whole-life costs (£ in PV)	126,839	193,263	243,272	289,352	558,600
Risk of base case (£ in PV)	10,471,502	10,471,502	10,471,502	10,471,502	10,471,502
Risk of with-project (£ in PV)	1,549,780	278	72,729	963,028	5,950,085
Benefit (£ in PV)	8,921,722	10,471,223	10,398,772	9,508,474	4,521,417
NPV (£)	8,794,883	10,277,960	10,155,500	9,219,122	3,962,817
BCR	70.34	54.18	42.75	32.86	8.09
IBCR	N/A	23.33	-1.45	-10.02	-16.29

The most cost-effective solution for both stationary and nonstationary cases, driven by the analysis of IBCR and NPV is Portfolio 4. Although the same conclusion both the stationary and nonstationary cases, the justifications behind the preferred portfolio relative to the other portfolios differ. For example, when comparing between Portfolio 1 and 4, the higher cost of Portfolio 4 as compared to the cost of Portfolio 1 under the stationary condition is justified by the relatively higher benefit from the extra protection Portfolio 4 has to offer. However, adopting Portfolio 1 under the nonstationary condition brings a higher costs but a lower benefit compared to the cost and benefit of adopting Portfolio 4 under the same nonstationary condition. Therefore, based on the analysis the higher cost from Portfolio 1 is not justified by the benefit it offers, leading to the preference of selecting Portfolio 4 over Portfolio 1 under the nonstationary condition.

The degree of protection offers in Portfolio 4 under the stationary and nonstationary condition also differ in the sense that Portfolio 4 under the stationary condition comes with a slightly higher

protection design compared to the one under the nonstationary condition. One might think that the higher protection design under the stationary condition as compared to the lower protection design under the nonstationary condition would aggravate the difference between the residual risks under the stationary and nonstationary conditions, for instance due to the expected higher probability flood events from a nonstationary distribution. Counter-intuitively, the findings from this study show that the PV residual risk of having the Portfolio 4 under the nonstationary condition (with a lower protection design) is much smaller than having the Portfolio 4 under the stationary condition (with a higher protection design). The reason behind this can be traced back when investigating the relative magnitude of the upper limit of the nonstationary PDF and the lower limit of the damage function, corresponds to the characteristic of the distributions' tail and the protection design considered, as mentioned earlier in Section 7.4.2. More discussion over the findings is presented in the subsequent section.

It is also important to acknowledge that without any intervention (i.e. the base case), the PV risk under the nonstationary condition is significantly higher than the PV risk under the stationary condition, which is in agreement with the general perception where nonstationarity will result in higher flood risk. Therefore, despite the previously estimated lower protection of Portfolio 4 under the nonstationary condition as compared that of the stationary condition, the resulting benefit of risk reduction is much higher under the nonstationary condition, leading to a higher NPV.

The analysis of the results as discussed above have look into comparing the different performance indicators, namely the residual risk, the benefit of risk reduction and the NPV, of the most preferred intervention portfolio under the stationary and nonstationary conditions, respectively. More discussions on the results in the perspective of FRM decision making are followed in the subsequent section.

On a similar note, it is worth to point out that under both stationary and nonstationary conditions, Portfolio 2 of channel dredging returns the least cost-effective solution owing to the highest long-term costs and lowest long-term benefits it offers compared to the other portfolios. The results are consistent with explanations from the EA in their publication and dissemination (refer Chapter 2).

The preference ordering as shown in Table 7.18 and Table 7.19 also highlights the rank of property-level protection amongst the other alternative measures. Such inclusion enhances the ability for stakeholders and decision makers to make a reasonable judgement and rational decisions.

7.5 Discussion and conclusion

Economic appraisal of competing flood protection measures lies at the heart of the flood risk management decision making. The risk-based approach has been widely practiced around the world, but the application of a complete risk-based approach has been proven to be challenging especially due to the characterization and derivation of flood hazard, cost and damage components. In particular, the stationary assumption may undermine the selection of the most cost effective solution in reducing flood risk and a nonstationary assumption might be more appropriate.

As a continuation from the previous chapters, the present chapter has sought to ensemble the derived damage model and the characteristics of the extreme flow distributions to estimate the corresponding flood risks. A set of flood protection portfolios is considered to illustrate a realistic decision problem with special attention to property-level protection to examine its relative performance alongside the other local flood protections. The study has explicitly incorporated the risk-based optimization of costs and benefits of the different flood protection. The two specific objectives defined for this study are achieved: (1) to investigate the performance of property-level protection when the risk-based optimization methodology is applied, and (2) the economic performance of portfolios under the nonstationary condition additional to the stationary condition.

The cost-benefit analysis of the considered portfolios shows that in terms of the IBCR, the combined protection of property-level and embankment offers the most cost-effective solution for both stationary and nonstationary conditions, despite the different preference ordering of the considered portfolios in each scenario. The results suggest that, irrespective stationary or nonstationary future conditions, instead of favouring embankment for long-term protection and property-level protection as a secondary measure, allocation of protection measures of property-level protection or combined property-level protection and embankment should be considered in the long-term investment planning. Furthermore, the application strongly promotes the use of the

risk-based optimization approach that should be tailored to a specific local area of interests before determining an optimal protection design. Standardizing a fixed protection threshold for policy guide such that suggested by DEFRA (Aug 2012) for property-level protection is prone to inappropriate investment allocation, owing to the influence of distinct characteristics of the physical system and other contributing variables.

Another interesting finding is that the estimated optimal protection of combined measures for the stationary condition returns a slightly higher protection threshold than that for nonstationary condition (embankment of 0.93m high and 11 individual properties protected as compared to embankment of 0.77m high and 11 individual properties protected), but in terms of benefit of risk reduction and project return, adaptation to the nonstationary condition is proven to be more rewarding (PV benefit of £10,471,223 as compared to £6,093,141, and NPV of £10,277,960 as compared to £5,806,268).

This study also found that the distribution tail characteristics that influence the upper limit for the risk estimation significantly influence the estimated economic performance. Furthermore, the magnitude of the protection design also influence the risk estimation. Comparison of the influence of stationary and nonstationary model on economic performance of decisions should therefore be justified through analysis of the distributions' tail characteristics and the influence of the protection designs to the upper and lower limit of the risk function.

The nonstationary model used in this study is based on the best-fitted GEV model of future flows projections of A1B climate scenario from Prudhomme et al. (2012). The use of the future flow projections as input in this exploration has expanded the research on adaptation to nonstationary flood frequency in a way that is practical to be applied in a real world options appraisal and in line with the current efforts to explore the relative implication of stationary and nonstationary model (e.g. Seidou, Ramsay and Nistor, 2012a;Rosner, Vogel and Kirshen, 2014;Salas and Obeysekera, 2014;Serinaldi and Kilsby, 2015). Moreover, the decision analysis incorporates a more realistic costs and damage functions into the cost-benefit analysis under stationary and nonstationary conditions. Using reliable costs per unit estimates and the spatially derived cost and damage

functions are useful in making an appropriate assessment. The application of the methodology is a novel approach that can be applied to assist FRM at places with strong evidence or projections of nonstationarity and at places that aims for optimal investment of local protection.

It is recognized that the present study is a pilot example and serves more as a feasibility study. Application of the developed framework to a different case study might require a refinement of the cost functions. For example, it would be worth considering expected costs from land acquisition or relevant transaction costs to better represent the costs involved. However, this depends on the problem of interests and the context of study.

The incorporation of the nonstationary model into the risk-based optimization methodology, and the consideration of the property-level protection opens other opportunities that may be worth exploring. For example, the implication of under-spending or over-spending as demonstrated in Chapter 5 can be adopted to explore the relative implication of observations-based prediction and climate model-based projections in risk estimates. As the study only focuses on the A1B scenario, implication of other scenarios might worth be explored. This study also assumes that the GEV distributions' parameters vary in accordance with time and uses the AIC to select the best model to represent the probability distribution of the extreme events for the future. However, a stabilizing trend may not be apparent or there might be different characterisation of the future change. It would also be interesting to explore the relative implication of different decision-making approaches, such as the application of bayesian analysis additional to the nonstationary and stationary models.

Chapter 8 Discussion and conclusions

Flooding is one of the most disastrous events that can affect virtually any region in the world. Historically, flood events have caused severe damages to properties and infrastructures, environmental damage and even loss of lives. At present, flood events are still very much a threat to societal prosperity. With the evidence of global warming, there have been concerns over the increase precipitation magnitude that may affect the magnitude and frequency of flood events. Whilst the case is plausibly based on theoretical explanation, the complex nature of flood generation processes has led to minimal evidence on the change of magnitude and frequency of flooding (IPCC, 2007). Furthermore, different possible representations of 'change' lead to many interpretations on the possible characterisations of change (Merz et al., 2012) that challenge analysts and flood managers. Efforts to reduce future flood risk in the most cost-effective manner irrespective of any future changes are crucial to minimize possible damaging events.

In efforts to guide long-term planning of flood risk reduction, a number of studies have used future projections from climate models and deterministic hydrological modelling to project the possible changes of extreme flows. The projected changes have been successfully adopted in the UK national guidelines to flood managers, which is given in terms of percent of change of return period (Environment Agency, 2011). Whilst the efforts are undoubtedly a great assistance to flood managers in adapting to potential future change, the prediction of change is based on a stationary assumption. Owing to the physical evidence and studies that suggest potential changes in magnitude and frequency of extreme flows due to the anthropogenic climate change (e.g. Lane, 2009;Salas and Obeysekera, 2014), there has been a strong suggestion that a nonstationary assumption should be adopted in flood frequency analysis rather than relying upon a stationary assumption (Milly et al., 2008).

Comparative studies on the effects of stationary and nonstationary assumptions mostly have focused on the consequent point estimates of design values rather than accounting for sampling

uncertainties (e.g. Seidou, Ramsay and Nistor, 2012a;Salas et al., 2013). Moreover, the focus have been on the effects of nonstationary models to design values rather than to the consequential societal benefit and decisions performance in which more meaningful insights can be offered to stakeholders and decision makers. Efforts to capture the effects of persistence and nonstationarity can be undertaken using simulation models of assumed changes (Merz et al., 2010a). Scenario analysis can also be accommodated within the simulation study to enhance understanding of the implications of contrasting possible futures (Merz et al., 2010a;Olsen, 2010)

Risk-based optimization methodology, which adopts the cost-benefit analysis approach, has been well-recognized as one of the best tools available for identifying the most cost-effective solution for a given problem. Whilst there are rigorous modelling efforts undertaken independently for the components of the risk-based optimization methodology, for example the cost and damage models are disconnectedly modelled, little attention has been paid to developing a consistent exogenous decision variable for all the risk-based optimization components. For example, studies tend to focus on evaluating flood damage as a function of water level (i.e. in unit length), which need further adjustment when adopting the holistic risk estimation with PDF as a function of discharge. Some studies also focus on modelling damage as a function of return period, which limits the use of the function in the holistic risk estimation for stationary cases. Furthermore, studies that applied the risk-based methodology tend to isolate the physical influence of flood propagation and flood measures in modelling flood vulnerability (e.g. non-existence of embankment, or using coarse resolution to predict flood extent).

Targeting a complete risk-based assessment framework that can be transferrable for case studies involving stationary and nonstationary extreme flow distributions, the aim of this study was to model extreme flows with persistence and nonstationarity, and also flood vulnerability. Section 8.1 provides short descriptions on how each of the research objectives have been accomplished, including the methodology developed, case studies and key findings. Section 8.2 summarises the overall success of the study in satisfying the research aim and highlights the overall findings and

recommendations from the modelling and case studies. The limitations and caveats of the study is revisited in Section 8.3, whilst Section 8.4 provides potential future research avenues.

8.1 Achieving the research objectives

8.1.1 Developing a risk-based optimization methodology with explicit treatment of the modelling components for a robust decision analysis framework

The first objective dealt with establishing a risk-based optimization methodology with explicit treatment of the modelling components for a rigorous decision analysis. The risk-based optimization methodology has been acknowledged as a reliable tool in cost-benefit analysis in guiding towards an optimal decision. The adoption of such method requires not only the information of the hazard profile but also the cost and damage functions related to a proposed intervention. Simplified representations of cost and damage functions are often found in studies that attempt to capture the uncertainty and sensitivity of variables of interest (e.g. Al-Futaisi and Stedinger, 1999;O'Connell et al., 2010). However, the derivation of cost and damage functions in real life application can be of a hurdle due to the extensive data requirements (e.g. Rasekh, Afshar and Afshar, 2010;Stijnen et al., 2014). Corresponding to this, studies that adopt the risk-based optimization of flood protection design often isolate the derivation of physically-based damage and cost functions (e.g. Rosner, Vogel and Kirshen, 2014).

In effort to construct reliable functions to simulate the decision-making process through the risk-based optimization methodology, this thesis has proposed two procedures for the derivation of the cost and damage functions. One is based on simplified representations of spatial characteristics alongside constant values, and the second is based on a relatively more complex influence of spatial elements. The former is referred to as a hypothetical flood risk system whilst the latter is based on near complete characteristics of a real flood risk system.

Simplified functions based on the hypothetical area were adopted to reduce the computational time whilst focusing on the uncertainty propagation due to persistence and nonstationarity, and sensitivity of economic performance to different degrees of persistence and nonstationarity. These

functions are more flexible and easier to be incorporated in the risk-based optimization for a recursive and automated computation involving thousands of simulations for uncertainty and sensitivity analysis. The development of the risk-based optimization approach of this case has been presented in Chapter 4.

The more complex derivation of damage and cost functions based on a real spatial area of flood risk system are important in efforts to capture the different spatial elements that may contribute to cost-benefit analysis. In this thesis, the derivations of the more complex functions were dedicated to compare the economic performance of different flood risk mitigation portfolios under stationary and nonstationary assumptions. Narrowing the scope of analysis to only sensitivity analysis compensated for the extra effort for the derivation of functions. The more complex derivations of the damage and costs functions were presented in Chapter 6 and 7. Irrespective the approach to derive the cost and damage functions, it was assumed that the decision makers adopt the GEV distribution in characterising the extreme flows. The computation of the risk-based optimization manipulated the lower and upper limit of the fitted GEV distribution to ensure consistency of the probabilistic estimations.

In the simulation study presented in Chapter 4 and 5, the different degree of persistence and nonstationarity only causes minor differences to the expected value of the economic performance. The range of economic performance of decisions made using the risk-based optimization in terms of the NPV were also shown to be consistently positive across all scenarios. These findings extend and confirm those of Jonkman et al. (2009a) and Rosner, Vogel and Kirshen (2014) that the application of the risk-based optimization is robust to uncertain underlying assumption about future extremes. In addition, the improvements of the approach using the asymptotic GEV distribution and associated lower and upper limit enhanced the robustness of the decision analysis for all considered possible conditions. The isolation of the return period concept in the computations and the direct use of the probability distribution for the risk estimation further extend the applicability of the approach for nonstationary cases.

8.1.2 Quantifying uncertainty propagation and sensitivity of the economic performance of alternative time-dependence strategies with partial information under persistent scenarios.

The second research objective was to capture and evaluate the uncertainty propagation of decisions made based on partial information under persistent extreme flow series and further evaluate the sensitivity of the economic performance of the alternative strategies to different degree of persistence. Persistence in extreme flows in response to the chaotic nature of the atmospheric circulation system and the possible effects of anthropogenic climate change is plausible from the theoretical point of view (Huntingford et al., 2014). Though empirical evidence is lacking, 'flood rich' and 'flood poor' periods at some places indicate that the effects of persistence have been observed (Lane, 2009). Before the implication of nonstationary to flood risk management decisions is explored, it is reasonable to test the decision analysis framework for persistent cases. The possible implication of a persistent series to decisions performance of long-term hydraulic design made based on the IID assumption has led to some simulation studies involving the generation of persistent flow series (e.g. O'Connell et al., 2010).

A decision analysis framework that simulates a risk-neutral decision makers' action in deciding upon an optimal intervention with the application of the risk-based optimization has been developed in Chapter 4. To account for the effects of finite sample size in the decision making, two alternate investment strategies were introduced; the proactive and reactive strategies. The uncertainty and sensitivity of the decisions of the respective strategies were tested under three different persistent scenarios; no correlation, moderately correlated, and highly correlated extreme flow series. All simulated series had similar mean and variance of the GEV population distribution.

The simulation-based exploration study successfully captured and analysed the uncertainty propagation in terms of the estimated optimal protection, corresponding costs, potential average damages and the resulting economic indices. The evaluation of the uncertainty propagation verified the final outcomes of economic performance of the tested strategies and persistent levels. In

addition, a cost-benefit index has been used to suggest the preferred investment strategy under the different persistent scenarios through probabilistic computation.

The simulation set-up of the study can be seen as an extension of the study demonstrated by O'Connell et al. (2010). However, instead of focusing on the average outcomes, the present study has captured the uncertainty propagation and illustrated the range of the economic performance of decisions. Moreover, the study advances the application of the cost-benefit index (Ayyub, 2014) in suggesting a preferred strategy using not only the expected value but also the variance of the simulation outcomes.

The results from the present study indicate that the proactive strategy would bring a greater long-term economic net benefit as compared to a reactive wait-and-see approach regardless the levels of persistence in the underlying process. This finding is slightly different from what was found by O'Connell et al. (2010), whereby the reactive strategy outperformed the proactive strategy in terms of the average net benefit for flow series with the highest degree of persistence. Some of the reasons for the discrepancies may be due to the distinct model representation of persistence, the parameterization of the population distribution used for the simulation of persistent series, and the cost and damage model structures.

In essence, it is believe that the present study provides reliable findings with careful parameterization of the population probability distribution based on the long-term historical records of the Thames and the physical-based model derivations. The findings from this study emphasise that the call for proactive investment to reduce adverse flood damage is advisable even when limited information of the future state is limited. Also, the small difference of the relative outcomes across the different persistent scenarios suggest a valid reason for the conventional IID assumption to still be used in the risk-based analysis although the flow series exhibit persistence variability. The quantitative findings support what have been mentioned in Hosking (1997) and Coles (2001). It is also found from this study that preference of the proactive strategy over the reactive strategy is only justified by a slight margin, suggesting the robustness and importance of the risk-based optimization in FRM decision making.

8.1.3 Quantifying uncertainty propagation and sensitivity of the economic performance of decisions with partial information under nonstationary scenarios.

The third research objective was to capture and analyse uncertainty propagation and sensitivity of the economic performance of decisions to different degree of nonstationarity when decision makers use only partial information. The work has been presented in Chapter 5. There have been strong suggestions that nonstationary probabilistic models should be used in some practical cases due to the possible exacerbation of frequency and magnitude of fluvial flooding. However, the questions on whether the stationary assumption should be discarded is still actively being debated and many simulation studies have been undertaken to understand the relative implication of stationary and nonstationary assumptions in design flood (e.g. Salas and Obeysekera, 2014;Serinaldi and Kilsby, 2015).

The simulation setup for the third objective utilize the developed risk-based optimization methodology (Section 8.1.1) to simulate a decision-making process in which alternative models of stationary and nonstationary were used. Three modules were designed, each with assigned pathways of flood risk adaptation actions (e.g. either stationary or nonstationary model selected in the decision making process) and possible actual future underlying distribution (i.e. either following the statistics of stationary or nonstationary distributions). The simulation study adopted the Monte Carlo approach to capture the uncertainty range due to the natural variability, and also used the full information of the PDF to compute the expected values. The characterization of the PDF accounted the information of the real dataset from Thames at Kingston historical flow records and also the information from the climate model projections of future flows. This has provided the advantage of having realistic underlying distributions for the study in simulating possible actual future conditions.

The results from the simulation study successfully captured the uncertainty range and the sensitivity of the economic performance under competing stationary and nonstationary model choices. From all considered actual future change, it is apparent that the use of the nonstationary model in the decision making poses larger variance of outcomes as compared to the use of the stationary model.

The relative performance of using a nonstationary model predicted from climate model projections additional to the conventional stationary model predicted from historical records was examined by comparing their percentage difference of outcomes with that of perfect information of the future (Section 5.4.5). Some specific quantitative findings indicate that adopting the nonstationary model predicted from the climate model projections in the decision making under most of the future conditions can generate a more cost-effective decisions. Nevertheless, it is found that the difference between the percentage difference of NPVs of stationary and nonstationary model choices are relatively small across the range of the actual future conditions considered. Furthermore, either stationary or nonstationary model choice in the decision making can lead to a major percentage difference of NPV when the predicted distribution deviate farther from an actual distribution.

The arguments may suggests that the more complex nonstationary model would not significantly improve our ability to prepare for the uncertain future when the risk-based optimization methodology is adopted in the decision-making process, rather the use of the simpler stationary model may be more practical to cost-effectively reduce flood risk. This echoes the strong suggestion by Serinaldi and Kilsby (2015), saying that stationary should remain the default assumption even when the evidence of nonstationarity is apparent. Nevertheless, this does not mean that nonstationary model should be discarded (Milly et al., 2015). If there is a clear evidence or reliable prediction of future change and modelling capabilities exist, comparing simulation outcomes between stationary and nonstationary models would provide valuable insights to inform flood risk management decision making in facing the uncertain future.

The simulation framework design in this study is novel in the sense that uncertainty and sensitivity analysis of economic performance of stationary and nonstationary assumptions were incorporated. Furthermore, the prediction of nonstationary model used the information from climate model future flows projections, hence ensuring the reliability of the considered future conditions for the study. The results provide compelling insights for long-term flood risk management decision making in the face of an uncertain future. It is believe that the methodological approach may assist not only decision makers, but also engineering hydrologists in understanding the relative consequences of

using either stationary or nonstationary models in a risk-based decision making against the possible future conditions.

However, it is important to note that the absolute values and percentages of the results depends on the modelling techniques adopted, the assumption on possible actual future change and the input data. This includes the observed flow records, the A1B climate scenario, assumed linear increase in the location parameter of the GEV distribution over future horizon and cost and damage model derivations. Different results might be observed when different input data and different characterisation of nonstationary GEV are used. For example, it is obvious from the presented study that the economic performance of the decisions would not only be influenced by the difference in the rate of change in the location parameters, but also from the interaction between the GEV parameters.

Therefore, adopting the framework for other case studies should account for local factors. This would ensure a more tailored analysis and realistic absolute values of the economic performance. It should be noted, however, that the physical-based damage and cost models should be kept simple to ensure that the recursive computation can run smoothly. Possible improvements of the simulation study can also be made by identifying realistic pathways of decision analysis. It is better to include decision makers' opinion to ensure that the results of the simulation study is more relevant to them.

8.1.4 Developing a systematic micro-scale vulnerability assessment framework for damage modelling concerning community-based intervention portfolios.

The fourth objective was focused on developing a systematic micro-scale vulnerability assessment framework for damage modelling. In order to test the applicability of the risk-based optimization to real flood management problem, a realistic and flexible damage function is needed to facilitate the quantitative estimates. Deriving damage models of mitigation measures relies on the assessment of the vulnerability of the area of interest, where the relationships between the flood influencing variables and the potential damages are established. It is recognized from the literature review that many damage model derivations are either focused on meso and macro scale assessment or micro-

scale assessment but with limited adaptability for continuous flood events simulation. Furthermore, with the increasing attention towards the implementation of property-level protection (PLP) as a more cost-effective solution, the influence of PLP alongside or together with the embankment to the damage model configuration is of interest.

Focusing on micro-scale assessment, this study has developed a set of novel algorithms to estimate flood damage concerning the impacts to individual buildings, with special attention to the influence of with and without property level protection. The algorithm allows vulnerability assessment to be applied for a range of possible scenarios of inundation depth and associated protection design. This indirectly has drifted away flood damage assessment from focusing only on a specific inundation scenario or on a particular extreme event. The proposed flexibility and automated computation of the vulnerability assessment has successfully facilitated the case study involving a practical application of the risk-based optimization of flood protection, specifically for the PLP and the combined protection of PLP and embankment. Moreover, the isolation of the return period concept from the approach allows subsequent flood risk assessment to be undertaken under stationary and nonstationary assumptions.

Application of the framework using spatial information of a local area downstream of Kingston gauging station and depth-damage relationship from MCM revealed that the proposed approach is capable of capturing the physical effects of the protection measures. This further suggests its adoptability for other case study that exhibit similar conceptual flood risk system. The application to the real location, however, involved adjusting some input data to impose inundation scenario to the case so as to have a clear illustration of the applicability of the methodological framework. In cases where the absolute values are of interests, verification of the results with historical flood events and their consequential damage is essential to increase the reliability of the proposed approach. Nevertheless, records of economic flood damage are subjected to uncertainty. Moreover, reliable records are hardly exist (Jongman et al., 2012). The reliability of such analysis can be improved by partial verification (e.g. Arrighi et al., 2013) or by ensuring that the input data to the modelling chain are of the best available quality.

8.1.5 Comparing the economic performance of stationary and nonstationary conditions and a number of alternative flood risk management portfolios, through a risk-based cost-benefit analysis that integrates a probability distribution and realistic damage and cost models associated with the community-based portfolios.

The fifth objective was to explore the economic performance of stationary and nonstationary assumptions through the application of the risk-based optimization associated with the vulnerability assessment of the community-based measures. Also, the economic performance of the property-level protection measures relative to the other local protection measures were also to be addressed. Whilst the flood vulnerability assessment methodological framework has proven to be flexible and tractable in Chapter 6, it is important to test whether it is applicable for practical risk-based optimization of alternative community-based measures and subsequent economic appraisal involving stationary and nonstationary assumptions.

To accomplish the objective, the study was conducted by considering four different long-term portfolios involving embankment, property-level protection, and combined measures of property level protection and embankment. Channel dredging was also considered to have an insight into the relative outcomes. The probability distributions of stationary and nonstationary were derived based on the Kingston gauged records and climate model-based projections, respectively, similar to the ones used for the previous objectives. To complete the required models for the cost-benefit analysis, the costs of the considered portfolios were first estimated using proposed cost estimation models. All the modelling components of the respective portfolios were carefully integrated and the resulting economic performance in terms of IBCR were ultimately computed.

As presented in Chapter 7, the cost-benefit analysis shows that despite the discrepancies of the portfolios ordering under stationary and nonstationary assumptions, the IBCRs of portfolios under the differing assumptions of future conditions returns similar conclusion on the preferred portfolio. The optimal combined protection of embankment and property level protection was found to be the most cost-effective option, regardless the assumption about the future condition. This suggests that property-level protection should be considered more seriously in long-term plans for reducing flood

risk, and risk-based optimization should be adopted and tailored to a specific local area of interests. The estimated optimal protection of combined measures of property level protection and embankments of the stationary condition returns a slightly higher protection threshold than that of nonstationary condition, but in terms of benefit and project return, adaptation to the nonstationary condition is more rewarding.

The study successfully extends the efforts to mainstream property-level protection alongside flood defence and other community-based protection measures (e.g. Great Britain, Dept for Environment, Food and Rural Affairs, Aug 2012;Arrighi et al., 2013;Moel, Vliet and Aerts, 2014). The damage and costs function were derived based on the spatial characteristics of a real local area, extending beyond what have been explored in existing literature on quantitative risk-based decision analysis. The study also advances the research concerning nonstationary condition by integrating the model into the risk-based analysis and through the practical application of the cost-benefit analysis. This promotes shift from the focus on the effects of nonstationary to design floods as demonstrated by some authors (e.g. Salas and Obeysekera, 2014), to the effects on economic performance of decision. The nonstationary model used in the study is based on the best-fitted GEV model of projected future flows of A1B climate scenario, representing real projected values. Similar methodology can be applied at places with strong evidence or projections of nonstationarity and at places that aim for optimal investment in local protection.

As the study was aimed more at demonstrating the concept and testing the feasibility of the methodology, application of the developed framework to a different case study might require refinement of the cost functions and/or using different projections of future scenarios or different characteristics of a nonstationary condition. It is also interesting to have an insight into the implication of under- and over-spending utilizing the developed damage and costs models, given a false assumption about the future condition. Relative implication of different decision-making approach to the decisions economic performance, such as the Bayesian analysis additional to the nonstationary and stationary flood frequency analysis may be interesting to explore.

8.2 Achieving the research aim

As mentioned in the introductory section of this chapter, the focus of the thesis was to develop and demonstrate a complete risk-based assessment framework that is flexible and can be transferrable for case studies involving persistence and nonstationary extreme flow distributions. The summary provided in Section 8.1 highlights the designed methodology for simulation and case studies as well as the rigorous modelling development that have been beneficial for addressing the research aim. Robustness as identified in Chapter 2 have been sought in this thesis through two distinct approaches; the first approach is by coupling uncertainty and sensitivity analyses whilst the second approach focuses on sensitivity analysis. The first approach adopts a moderate derivation techniques for the cost and damage models of the risk-based optimization whilst aiming to undertake thousands of recursive experiments with regard to persistence and nonstationary in effort to capture the uncertainty range, irrespective of the sensitivity of the outcomes. This means the uncertainty and sensitivity analysis are treated separately. The second approach compensates for the computational expenses of simulation runs to allow a more complex derivation of cost and damage models associated with a set of alternative portfolios, hence focusing on the sensitivity of outcomes. In particular, a more realistic damage model related to the alternative protection measures were designed in the second approach. The first approach focused on simulation studies whilst the second approach involved spatial characteristics of a real location. In both approaches, cost-benefit analysis as reviewed in Chapter 2 has been the main thrust in the decision analysis frameworks.

The first simulation study has focused on persistent series whereby a GEV-AR(1) model has been derived to generate three distinct sets of extreme flow series with unique persistent levels. The risk-based decision analysis for the persistent series were driven by the assumption of a rational decision makers' behaviour in responding to flood risk. Cost and damage functions were derived for the decision analysis.

The second simulation study addressed the influence of nonstationarity in flood risk management decision making, where a linear trend in the location parameter of GEV distribution over time was

adopted to generate annual maxima flows, representing nonstationary conditions. In particular, projections of future flows from climate models were extracted to have a realistic representation of nonstationary conditions. Using the same simulation framework as had been developed in the first simulation study, decision makers' rational behaviour in reducing flood risk via the risk-based optimization was demonstrated. The same cost and damage functions derived earlier were also used in this second round of simulation study. To realistically address the decision-making problems concerning model choice and possible future, a set of different pathways of the decision problems were selected for the exploration study. The relative outcomes related to these pathways were successfully captured and illustrated.

As discussed in Chapter 3, a micro-scale damage assessment is the most appropriate approach for a cost-benefit options appraisal. Flexible and adaptable techniques to assess flood vulnerability are vital for a complete risk-based assessment. The importance of designing a methodology for a realistic assessment of flood vulnerability to be used for the risk-based assessment of alternative options ultimately drove the subsequent work of this thesis. In accordance to the identified conceptual elements for the vulnerability assessment as reviewed in chapter 3, modelling chains related to alternative local protection measures were developed. The application of the methodology to a real location resulted in clear illustrations of the relative vulnerability of the considered alternative protections.

To illustrate the usefulness of the flood vulnerability models for the risk-based decision analysis in the context of nonstationary extreme flows, the final exploration of this thesis involved deriving spatially-driven cost functions and assembling the modelling components required for the decision analysis. The risk-based optimization was again applied for the case study. The protection measures that drove the vulnerability curves hence the damage models were all included in a set of flood risk management portfolios. The relative economic performance of the portfolios were computed and compared in the context of stationary and nonstationary conditions. In addition, the characteristic of the distribution tails were discussed in relation to the economic outcomes.

The simulations and case studies were extensive, yet manageable through a standard personal computer. This research utilized a personal computer with a processor intel-core i5 up to 2.7 GHz and 4GB ram. Software used are the CES-AES for the hydraulic modelling, Arc-GIS version 10.1 for the spatial analysis, and R version 2.15 for the statistical analysis. R also was the main software used for the most and final programming tasks. The table below provides the main research activities and the associated run times.

Research activities	**Run times**
Hypothetical study of different degree of persistence.	One to two hours
Hypothetical study of different decision pathway modules involving nonstationarity	Two to three hours
Case study of vulnerability assessment of different options.	Five to six hours
Case study of economic performance of different portfolios.	Four to five hours

The combined simulations and case studies demonstrated in this thesis has brought plenty of insights especially for flood risk managers and specialists involved in flood risk management planning. Furthermore, the developed modelling frameworks when applied should be able to extend insights into flood vulnerability and economic consequences for decision makers and stakeholders. Listed below are some of the major findings and recommendations extracted from the modelling study:

1. Concerning on the practical application of flood frequency analysis in the face of uncertain future, the study emphasised that the independent identically distributed series should remain the default assumption although persistence or nonstationarity might be expected. The influence of persistence and nonstationarity on risk-based decisions using stationary flood frequency analysis were arguably small.
2. Adaptation assessment using the climate projection as demonstrated in the thesis shows that out of 11 sets of projected future flow series, only two series fit a nonstationary model better than the stationary model; one with an estimated increase of discharge over time whilst the other one with an estimated decrease of discharge over time. This suggests that

even when the climate change scenario is force into the hydrological models to project changes in future flows, the projected change has little effects to the final decisions as compared to the observations-driven decisions. The simulation study also revealed that whilst climate model projections are useful in flood frequency analysis, observation-based decision is more cost-effective in most considered scenarios. Hence the idea to eliminate the conventional approach of adaptation to future flood risk and replace with nonstationary assumption is deemed inappropriate.

3. Although findings suggest that stationary should still remain the default assumption, if there is a clear evidence or reliable prediction of future change and modelling capabilities exist, comparing outcomes of stationary and nonstationary conditions will provide valuable insights to flood risk management decision making. This can be undertaken through simulation study and uncertainty and sensitivity analysis.
4. The application of risk-based optimization in decision making clearly contributes to the robustness of the outcomes across all considered scenarios. The results highlight that the risk-based optimization should be adopted in flood risk management decision making to ascertain a robust and cost-effective response to flood risk.
5. Based on the vulnerability assessment and the cost-benefit analysis of alternative engineering interventions for local protection, it is evident that long-term protection by channel dredging alone provides little protection from the less frequent flood events and in the case study ranked last as an option. Moreover, it is evident from the study that property-level protection serves well as a complement protection to flood defence regardless stationary and nonstationary future conditions. The findings support the many efforts to mainstream property-level protection in long-term planning of risk reduction.

8.3 Limitations and caveats

The methodological development and the application demonstrated in this thesis have carefully selected the modelling techniques and data sources for reliable and realistic outcomes of the exploration study. However, several limitations and caveats have been identified as discussed

through chapters 4, 5, 6 and 7. It is worth reiterating the sources of limitations and caveats that may limits the findings to a certain extent:

1) The analysis of persistent series was limited to the autoregressive lag 1 model coupled with the GEV distribution (i.e. GEV-AR(1)).

2) The parameterization of the GEV-AR(1) model and the base case of the simulation and real case study throughout the thesis is the Thames at Kingston annual maxima flow records.

3) The nonstationary condition for the case study is from one particular climate model projections of A1B climate scenario.

4) Scenarios of possible future change are restricted to increasing flow rate over time. Time was chosen as the covariate to the location parameters of the GEV distribution, whilst other parameters are assumed to be constant over time.

5) The configuration of the cost and damage models and the associated constants values were based on practice reported in the literature and Environmental Agency documentation, but contain inevitable limitations.

6) Indirect contribution to flood damage were excluded from the analysis.

7) Inundation scenarios and the consequential flood damage could not be empirically verified with data from real floods.

8) The assumptions on decision makers' behaviour and preferred model choice in responding to flood risk were not verified empirically.

9) Protection measures were assumed to be completely reliable over the period of appraisal and only functional failure was considered.

10) Economic and social systems were assumed to be static over time. For example, the population density was assumed to be constant over time and no significant socio economic development on the case study area was considered

8.4 Potential further research

1. Other forms of nonstationary over the appraisal period, such as step change or log-scale of GEV distribution can be considered in the decision analysis. The characterization should, however, be justified according to evidence from historical or reliable studies of future projections.
2. Adaptation assessment using similar decision analysis framework as have been presented in the thesis may be applied to other climate projections. Parametric modelling of stationary and nonstationary conditions should in this case be included, accounting for the practical application of risk-based decision making.
3. Although the simulation-based adaptation assessment using the climate model projection seems to suggest that the conventional approach of using observations is still relevant, other approaches such as the Bayesian analysis using combined information from the climate projection and observations may be considered in the decision analysis and the outcomes may be compared to understand the implications.
4. As the presented simulation and case studies were focused on the risk-based optimization of flood protection, comparison of the outcomes from these studies and outcomes from a fixed protection allocation scenario might be interesting.
5. Other sources that contribute significantly to costs and damage function derivation, such as indirect sources, might be incorporated. However, this is highly depends on the problem of interest and the required detail of the study.
6. Other alternative measures of community-based protection, or combination of them, may be included in the vulnerability assessment and the cost-benefit analysis of stationary and nonstationary conditions. Different period of appraisal according to their realistic lifespan might also be considered.

Papers presented by the candidate

Rehan, B. and Hall, J.W (2014) Flood risk management decision analysis with finite historical records and highly variable climate effects. Vulnerability, Uncertainty, and Risk: American Society of Civil Engineers (ASCE). pp. 2867-2879. doi: 10.1061/9780784413609.289

Rehan, B. and Hall, J.W (2016) Uncertainty and sensitivity analysis of flood risk management decisions based on stationary and nonstationary model choices. *To be presented at Flood Risk 2016.* France.

References

Ailliot, P., Thompson, C. and Thomson, P. (2011) Mixed methods for fitting the GEV distribution. *Water Resources Research,* 47, pp. W05551.

Al-Futaisi, A. and Stedinger, J.R. (1999) Hydrologic and economic uncertainties and flood-risk project design. *Journal of Water Resources Planning and Management-ASCE,* 125 (6).

Allan, R.P. and Soden, B.J. (2008) Atmospheric warming and the amplification of precipitation extremes. *Science,* 321 (5895), pp. 1481-1484.

Apel, H., Thieken, A.H., Merz, B. and Blöschl, G. (2004) Flood risk assessment and associated uncertainty. *Natural Hazards and Earth System Sciences,* 4, pp. 295-308.

Apel, H., Aronica, G.T., Kreibich, H. and Thieken, A.H. (2009) Flood risk analyses-how detailed do we need to be? *Natural Hazards,* 49 (1), pp. 79-98.

Arcement, J.G.J. and Schneider, V.R. (1989) *Guide for Selecting Manning's Roughness Coefficients for Natural Channels and Flood Plains.* 1st ed., United States: U.S. Geological Survey Water-supply (USGS).

Arnell, N. (1996) *Global warming, river flows and water resources.* Chichester: Wiley.

Arrighi, C., Brugioni, M., Castelli, F., Franceschini, S. and Mazzanti, B. (2013) Urban micro-scale flood risk estimation with parsimonious hydraulic modelling and census data. *Natural Hazards and Earth System Sciences,* 13 (5), pp. 1375-1391.

Arroyave, J.A.V. and Crosato, A. (2010) Effects of river floodplain lowering and vegetation cover. *Proceedings of the Institution of Civil Engineers-Water Management,* 163 (9), pp. 457-467.

Asquith, W.H. (2012) *lmomco---L-moments, trimmed L-moments, L-comoments, censored L-moments, and many distributions.* R package version 1.7.2 ed., Texas Tech University, Lubbock, Texas.

Ayyub, B.M. (2014) *Risk analysis in engineering and economics.* 2nd ed., London: Chapman & Hall/CRC.

Beaulieu, C., Chen, J. and Sarmiento, J.L. (2012) Change-point analysis as a tool to detect abrupt climate variations. *Philosophical Transactions of the Royal Society A-Mathematical Physical and Engineering Sciences,* 370 (1962).

Bell, V.A. et al. (2012) How might climate change affect river flows across the Thames Basin? An area-wide analysis using the UKCP09 Regional Climate Model ensemble. *Journal of Hydrology,* 442, pp. 89-104.

Boettle, M. et al. (2011) About the influence of elevation model quality and small-scale damage functions on flood damage estimation. *Natural Hazards and Earth System Sciences,* 11 (12), pp. 3327-3334.

Boniphace, E.R. and Willems, P. (2011) Impact of dependence in river flow data on flood frequency analysis based on regression in quantile plots: Analysis and solutions. *Water Resources Research,* 47, pp. W12537.

Broekx, S. et al. (2011) Designing a long-term flood risk management plan for the Scheldt estuary using a risk-based approach. *Natural Hazards,* 57 (2), pp. 245-266.

Cai, Y. (2011) Multi-variate time-series simulation. *Journal of Time Series Analysis,* 32 (5), pp. 566-579.

Castellarin, A. and Pistocchi, A. (2012) An analysis of change in alpine annual maximum discharges: implications for the selection of design discharges. *Hydrological Processes,* 26 (10), pp. 1517-1526.

Centre for Ecology and Hydrology (2014) *National river flow archive: 39001 - Thames at kingston.* [Online] Available from: http://www.ceh.ac.uk/data/nrfa/data/peakflow.html?39001 [Accessed 2012]

Chan, N.H. (2010) *Time series: applications to finance with R and S-Plus.* 2nd ed., Hoboken, N.J.: Wiley.

Chartered Institution of Water and Environmental Management (2014) Floods and dredging - a reality check. [Online]. *Chartered Institution of Water and Environmental Management (CIWEM), Februari 2014*. Available from: http://www.ciwem.org/media/1035043/floods_and_dredging_-_a_reality_check.pdf [Accessed 2014]

Chen, Z. and Grasby, S.E. (2009) Impact of decadal and century-scale oscillations on hydroclimate trend analyses. *Journal of Hydrology,* 365 (1-2), pp. 122-133.

Coles, S. (2001) *An introduction to statistical modeling of extreme values.* London: London : Springer.

Condon, L.E., Gangopadhyay, S. and Pruitt, T. (2015) Climate change and non-stationary flood risk for the upper Truckee River basin. *Hydrology and Earth System Sciences.,* 19, pp. 159-175.

Cryer, J.D. and Chan, K. (2008) *Time series analysis: with applications in R.* New York, NY: Springer.

Dankers, R. and Feyen, L. (2009) Flood hazard in Europe in an ensemble of regional climate scenarios. *Journal of Geophysical Research-Atmospheres,* 114.

Dawson, R., Hall, J.W. and Bates, P.D. (2005) Quantified Analysis of the Probability of Flooding in the Thames Estuary underImaginable Worst-case Sea Level Rise Scenarios. *Water Resources Development,* 21 (4).

Dawson, R.J. et al. (2011) Assessing the effectiveness of non-structural flood management measures in the Thames Estuary under conditions of socio-economic and environmental change. *Global Environmental Change,* 21 (2), pp. 628-646.

De Kok, J. and Grossmann, M. (2010) Large-scale assessment of flood risk and the effects of mitigation measures along the Elbe River. *Natural Hazards,* 52 (1), pp. 143-166.

De Moel, H., Asselman, N.E.M. and Aerts, J.C.J.H. (2012) Uncertainty and sensitivity analysis of coastal flood damage estimates in the west of the Netherlands. *Natural Hazards and Earth System Sciences,* 12 (4), pp. 1045-1058.

De Wrachien, D., Mambretti, S. and Schultz, B. (2011) Flood management and risk assessment in flood-prone areas: measures and solutions. *Irrigation and Drainage,* 60 (2), pp. 229-240.

Dessai, S. and Hulme, M. (2007) Assessing the robustness of adaptation decisions to climate change uncertainties: A case study on water resources management in the East of England. *Global Environmental Change,* 17 (1), pp. 59-72.

Di Baldassarre, G. (2012) *Floods in a Changing Climate: Inundation Modelling.* Cambridge: Cambridge University Press.

Di Baldassarre, G., Laio, F. and Montanari, A. (2009) Design flood estimation using model selection criteria. *Physics and Chemistry of the Earth, Parts A/B/C,* 34 (10–12), pp. 606-611.

Dunsmore, S.J. (1997) River Thames Flood Hydrology Design Curves. *Water and Environment Journal,* 11 (1), pp. 67-71.

Dutta, D., Herath, S. and Musiake, K. (2003) A mathematical model for flood loss estimation. *Journal of Hydrology,* 277 (1–2), pp. 24-49.

Dutta, D. et al. (2013) Storage-based approaches to build floodplain inundation modelling capability in river system models for water resources planning and accounting. *Journal of Hydrology,* 504, pp. 12-28.

El Adlouni, S., Bobee, B. and Ouarda, T.B.M.J. (2008) On the tails of extreme event distributions in hydrology. *Journal of Hydrology,* 355 (1-4), pp. 16-33.

El Adlouni, S. et al. (2007) Generalized maximum likelihood estimators for the nonstationary generalized extreme value model. *Water Resources Research,* 43 (3), pp. W03410.

Environment Agency (2010) *Flood risk management estimating guide - update 2010.* Worthing, West Sussex, United Kingdom: Environmental Agency.

ESRI (2012) *ArcGIS 10.2.* [computer program] ESRI.

European Environment Agency (2011) *Disasters in Europe: more frequent and causing more damage.* [Online]. Available from: http://www.eea.europa.eu/highlights/natural-hazards-and-technological-accidents [Accessed 2014]

European Union (2007) *Directive 2007/60/EC of the European parliament and of the council, Official Journal of the European Union*. 23 October 2007, [Online]. Available from: http://www.envir.ee/sites/default/files/flooddirective.pdf [Accessed 2014].

Feyen, L. et al. (2012) Fluvial flood risk in Europe in present and future climates. *Climatic Change,* 112 (1).

Gethering, W. and Puckett, K. (2013) *Design for climate change.* 1st ed., London: Riba.

Gilleland, E. and Katz, R.W. (2011) New software to analyze how extremes change over time. *Eos, Transactions American Geophysical Union,* 92 (2), pp. 13-14.

Goldman, D. (1997) Estimating expected annual damage for levee retrofits. *Journal of Water Resources Planning and Management-ASCE,* 123 (2).

Great Britain, Environment Agency (2010) *Flood and coastal erosion risk management appraisal guidance.* [Online]. Available from: https://www.gov.uk/government/publications/flood-and-coastal-erosion-risk-management-appraisal-guidance [Accessed 2013]

Great Britain, Environment Agency (April 2010) *Lower Thames Flood Risk Management Strategy: Phase 4 Technical Report.* Almondsbury, Bristol: Environment Agency.

Great Britain, Environment Agency (August 2010) *Lower Thames Flood Risk Management Study: Strategy Appraisal Report.* Almondsbury, Bristol: Environment Agency.

Great Britain, Environment Agency (2011) *Adapting to climate change. Advice for flood and coastal erosion risk management authorities.* [Online]. Available from: https://www.gov.uk/government/publications/adapting-to-climate-change-for-risk-management-authorities [Accessed 2014]

Great Britain, HM Treasury (2011) *The Green Book: Appraisal and evaluation in Central Government.* [Online]. Available from: http://www.gov.uk/government/uploads/system/uploads/attachment_data/file/220541/green_book_complete.pdf https://www.gov.uk/government/uploads/system/uploads/attachment_data/file/220541/green_book_complete.pdf[Accessed 2012].

Great Britain, Department for Environment, Food and Rural Affairs (2012) *Establishing the cost-effectiveness of property flood protection: Final report: FD2657.* [Online] Available from: http://randd.defra.gov.uk/Default.aspx?Module=More&Location=None&ProjectID=18119 [Accessed 2013]

Great Britain, Department for Environment, Food and Rural Affairs (n.d.) *Flood and coastal resilience partnership funding - an introductory guide.* [Online]. Available from: http://archive.defra.gov.uk/environment/flooding/funding/documents/flood-coastal-resilience-intro-guide.pdf [Accessed 2014]

Great Britain, Environment Agency (n.d.) *Floodwalls and flood embankments.* [Online]. Available from: http://evidence.environment-agency.gov.uk/FCERM/Libraries/Fluvial_Documents/Fluvial_Design_Guide_-_Chapter_9.sflb.ashx [Accessed 2012].

Great Britain, Environment Agency (December 2014) *Effectiveness of additional dredging: part of the 20 year flood action plan.* [Online]. Available from: https://www.gov.uk/government/uploads/system/uploads/attachment_data/file/392471/The_effectiveness_of_dredging_elsewhere.pdf [Accessed 2015].

Great Britain, Environment Agency Geomatics (2014) *LiDAR data.* [Online] Available from: https://www.geomatics-group.co.uk/geomatics/contactus.aspx. [Accessed 2014]

Great Britain, Environment Agency (May 2011) *River Tame Flood Risk Management Strategy.* Sapphire East, Solihull: Environmental Agency, United Kingdom.

Hall, J.W. et al. (2003a) Integrated Flood Risk Management in England and Wales. *Natural Hazards Review,* 4 (3), pp. 126.

Hall, J.W. et al. (2003b) A methodology for national-scale flood risk assessment. *Proceedings of the Institution of Civil Engineers: Water and Maritime Engineering,* 156 (3), pp. 235-247.

Hall, J.W. and Penning-Rowsell, E.C (2011) Setting the scene for flood risk manangement. In G. Pender and H. Faulkner (eds.). *Flood risk science and management.* Oxford: Wiley-Blackwell.

Hall, J.W. (2014) Flood Risk Management: Decision Making Under Uncertainty. In (K. Beven and J. Hall (eds). *Applied uncertainty analysis for flood risk management*. London. Imperial College Press, pp. 3-24.

Hall, J.W. and Solomatine, D. (2008) A framework for uncertainty analysis in flood risk management decisions. *International Journal of River Basin Management,* 6 (2), pp. 85-98.

Hallegatte, S. (2010) Uncertainties in the Cost-Benefit Analysis of Adaptation Measures, and Consequences for Decision Making. *Climate: Global Change and Local Adaptation,* , pp. 169-192.

Hallegatte, S. et al. (2012) *Policy research working paper: Investment Decision Making Under Deep Uncertainty. Application to climate change.* The World Bank. [Online]. Available from: http://econ.worldbank.org [Accessed in 2014]

Hamill, L. (2011) *Understanding hydraulics.* 3rd ed. Basingstoke: Palgrave Macmillan.

Hannaford, J.and Hall, J.W. (2012) Flood Risk in the UK: Evidence of Change and Management Response. In: Z. Kundzewicz (ed.). *Changes in Flood Risk in Europe*. Wallingford, Oxfordshire: International Association of Hydrological Sciences (IAHS) Press and Centre for Ecology and Hydrology, pp. 344-361.

Hannaford, J. and Marsh, T.J. (2008) High-flow and flood trends in a network of undisturbed catchments in the UK. *International Journal of Climatology,* 28 (10), pp. 1325-1338.

Harvey, H., Hall, J.W. and Peppe, R. (2012) Computational decision analysis for flood risk management in an uncertain future. *Journal of Hydroinformatics,* 14 (3).

Harvey, H., Hall, J.W. and Peppé, R. (2009) Outline of a framework for systematic decision analysis in flood risk management. In Anderssen, R.S., R.D. Braddock and L.T.H. Newham (eds.). *18th World IMACS Congress and MODSIM09 International Congress on Modelling and Simulation*. Modelling and Simulation Society of Australia and New Zealand and International Association for Mathematics and Computers in Simulation, July 2009, pp. 2377-2383.

Heidari, A. (2009) Structural master plan of flood mitigation measures. *Natural Hazards and Earth System Sciences,* 9 (1), pp. 61-75.

Hine, D. and Hall, J.W. (2010) Information gap analysis of flood model uncertainties and regional frequency analysis. *Water Resources Research,* 46.

Hirsch, R.M. (2011) A Perspective on Nonstationarity and Water Management. *Journal of the American Water Resources Association,* 47 (3), pp. 436-446.

Holtz, R.D., Kovacs, W.D. and Sheahan, T.C. (2011) *An introduction to geotechnical engineering.* 2nd ed., London: Pearson.

Horritt, M.S. and Bates, P.D. (2002) Evaluation of 1D and 2D numerical models for predicting river flood inundation. *Journal of Hydrology,* 268 (1–4), pp. 87-99.

Hosking, J.R.M. (1997) *Regional frequency analysis: an approach based on L-moments.* Cambridge: Cambridge University Press.

Hosking, J.R.M. (1990) L-Moments: Analysis and Estimation of Distributions Using Linear Combinations of Order Statistics. *Journal of the Royal Statistical Society. Series B (Methodological),* 52 (1), pp. 105-124.

HR Wallingford (2001) *Conveyance and Afflux Estimation System (CES-AES).* [computer program]. HR Wallingford/JBA.

Hsu, W., Tseng, C., Chiang, W. and Chen, C. (2012) Risk and uncertainty analysis in the planning stages of a risk decision-making process. *Natural Hazards,* 61 (3), pp. 1355-1365.

Hundecha, Y. and Merz, B. (2012) Exploring the relationship between changes in climate and floods using a model-based analysis. *Water Resources Research,* 48.

Huntingford, C. et al. (2014) Potential influences on the United Kingdom's floods of winter 2013/14. *Nature Climate Change,* 4 (9), pp. 769-777.

IPCC (2007) Climate Change 2007: The Physical Science Basis. In: Solomon, S., et al. (eds.). *Contribution of Working Group I to the Fourth Assessment Report of the Intergovernmental Panel on Climate Change,* Cambridge;New York: Cambridge University Press.

IPCC (2012) Managing the Risks of Extreme Events and Disasters to Advance Climate Change Adaptation. In: Field, C.B., et al. (eds.). *A Special Report of Working Groups I and II of the Intergovernmental Panel on Climate Change.* Cambridge;New York: Cambridge University Press.

Irandoust, S. and Biswas, A.K. (2012) *Floods in Asia: Lessons to be learned from Thailand.* Available from: http://www.nationmultimedia.com/opinion/Floods-in-Asia-Lessons-to-be-learned-from-Thailand-30174413.html [Accessed 2015].

Jongman, B. et al. (2012) Comparative flood damage model assessment: towards a European approach. *Natural Hazards and Earth System Sciences,* 12 (12), pp. 3733-3752.

Jonkman, S.N. et al. (2009) Risk-based design of flood defence systems: a preliminary analysis of the optimal protection level for the New Orleans metropolitan area. *Journal of Flood Risk Management,* 2 (3), pp. 170-181.

Kapnick, S. and Hall, A. (2012) Causes of recent changes in western North American snowpack. *Climate Dynamics,* 38 (9-10), pp. 1885-1899.

Katz, R.W. (2013) Statistical methods for nonstationary extremes. In A. AghaKouchak D. Easterling K. Hsu S. Schubert and S. Sorooshian (eds.), *Extremes in a changing climate: Detection, analysis and uncertainty.* Dordrecht: Springer Netherlands, pp. 15-37.

Katz, R.W., Parlange, M.B. and Naveau, P. (2002) Statistics of extremes in hydrology. *Advances in Water Resources,* 25 (8-12), pp. 1287-1304.

Kay, A.L. and Jones, D.A. (2012a) Transient changes in flood frequency and timing in Britain under potential projections of climate change. *International Journal of Climatology,* 32 (4).

Kay, A.L. and Jones, R.G. (2012b) Comparison of the use of alternative UKCP09 products for modelling the impacts of climate change on flood frequency. *Climatic Change,* 114 (2), pp. 211-230.

Kebede, A.S. and Nicholls, R.J. (2012) Exposure and vulnerability to climate extremes: population and asset exposure to coastal flooding in Dar es Salaam, Tanzania. *Regional Environmental Change,* 12 (1), pp. 81-94.

Keskitalo, E.C.H. (2013) Introduction. Local organisation to address flood risks: possibilities for adaptation to climate change. In E.C.H. Keskitalo (ed.), *Climate change and flood risk management: adaptation and extreme events at the local level.* Cheltenham: Edward Elgar, pp. 1-34.

Khaliq, M.N. et al. (2006) Frequency analysis of a sequence of dependent and/or non-stationary hydro-meteorological observations: A review. *Journal of Hydrology,* 329 (3-4), pp. 534-552.

Kilsby, C.G. et al. (2007) A daily weather generator for use in climate change studies. *Environmental Modelling & Software,* 22 (12), pp. 1705-1719.

Kind, J. (2010) Cost-benefit analysis for flood protection standards in the Netherlands. In *Floods and Economics: appraising, prioritising and financing flood risk management measures and instruments, Working Group F on Floods, Thematic Workshop,* Ghent, Belgium, 25-26 October 2010 [Online] Available from: www.vliz.be/imisdocs/publications/92/235392.pdf [Accessed in 2013]

Klijn, F. et al. (2009) *Flood risk assessment and flood risk management: An introduction and guidance based on experiences and findings of FLOODsite.* [Online]. Available from: http://www.floodsite.net/html/partner_area/project_docs/T29_09_01_Guidance_Screen_Version_D29_1_v2_0_P02.pdf [Accessed in 2013].

Knight, D.W. et al. (eds.) (2010) *Practical Channel Hydraulics; Roughness, Conveyance and Afflux.* London: Taylor & Francis Group.

Konrad A. S. (2013) *Climate change in Asia.* [Online]. Available from: http://ejap.org/environmental-issues-in-asia/natural-disasters-asia.html [Accessed in 2014]

Kourgialas, N.N. and Karatzas, G.P. (2013) A hydro-economic modelling framework for flood damage estimation and the role of riparian vegetation. *Hydrological Processes,* 27 (4), pp. 515-531.

Koutsoyiannis, D. and Montanari, A. (2015) Negligent killing of scientific concepts: the stationarity case. *Hydrological Sciences Journal,* 60 (7-8), pp. 1174-1183.

Koutsoyiannis, D. and Montanari, A. (2007) Statistical analysis of hydroclimatic time series: Uncertainty and insights. *Water Resources Research,* 43 (5), pp. W05429.

Kron, W. (2005) Flood Risk = Hazard • Values • Vulnerability. *Water International,* 30 (1), pp. 58-68.

Kuiry, S., Sen, D. and Bates, P. (2010) Coupled 1D–Quasi-2D Flood Inundation Model with Unstructured Grids. *Journal of Hydraulic Engineering,* 136 (8), pp. 493-506.

Kumar, R. and Chatterjee, C. (2005) Regional flood frequency analysis using L-moments for North Brahmaputra region of India. *Journal of Hydrologic Engineering,* 10 (1), pp. 1-7.

Kundzewicz, Z.W. (2012) *Changes in flood risk in Europe.* Wallingford, Oxfordshire: International Association of Hydrological Sciences (IAHS) Press and Centre for Ecology and Hydrology.

Kundzewicz, Z.W. et al. (2005) Trend detection in river flow series: 1. Annual maximum flow. *Hydrological Sciences Journal,* 50 (5), pp. 797-810.

Kundzewicz, Z.W., Hirabayashi, Y. and Kanae, S. (2010) River Floods in the Changing Climate-Observations and Projections. *Water Resources Management,* 24 (11), pp. 2633-2646.

Kundzewicz, Z.W. and Robson, A.J. (2004) Change detection in hydrological records - a review of the methodology. *Hydrological Sciences Journal,* 49 (1), pp. 7-19.

Kundzewicz, Z.W., et al. (eds.) (2013) Flood risk and climate change: global and regional perspectives. *Hydrological Sciences Journal,* 59 (1), pp. 1-28.

Lane, S.N. (2009) Flood risk periods, flood poor periods and the need to look beyond instrumental records. [Online]. In: *Geophysical Research Abstracts*: *EGU General Assembly 2009,* Austria April 2009, Vol. 11. Available from: http://meetingorganizer.copernicus.org/EGU2009/EGU2009-13743.pdf [Accessed in 2013]

Leclerc, M. and Ouarda, T.B.M.J. (2007) Non-stationary regional flood frequency analysis at ungauged sites. *Journal of Hydrology,* 343 (3-4), pp. 254-265.

Linde, A.H.T. et al. (2010) Simulating low-probability peak discharges for the Rhine basin using resampled climate modeling data. *Water Resources Research,* 46, pp. W03512.

Long, G., et al. (eds.) (2011) Performance based inspection of flood defence infrastructure: Integrating visual inspection and quantitative survey measurements. [Online]. Flood risk management research consortium (FRMRC) Research report SWP4.2. Available from: https://web.sbe.hw.ac.uk/frmrc/downloads/Performance%20based%20inspection%20of%20flood%20defence%20infrastructure.pdf [Accessed in 2013]

Madsen, H., et al. (eds.) (2013) *A review of applied methods in Europe for flood frequency analysis in a changing environment.* [Online] Centre for ecology and hydrology on behalf of European cooperation in science and technology (COST). Available from: http://nora.nerc.ac.uk/501751/. [Accessed in 2014]

Maidment, D.R. (1993) *Handbook of hydrology.* New York;London: McGraw Hill.

Malamud, B.D.and Turcotte, D.L. (2013) Time series: analysis and modelling. In: J. Wainwright and M. Mulligan (eds.) *Environmental modelling: Finding simplicity in complexity*, 2nd ed., West Sussex: John Wiley & Sons, pp. 27-43.

Marsh, T. and Harvey, C.L. (2012) The Thames flood series: a lack of trend in flood magnitude and a decline in maximum levels. *Hydrology Research,* 43 (3), pp. 203-214.

Martins, E.S. and Stedinger, J.R. (2000) Generalized maximum-likelihood generalized extreme-value quantile estimators for hydrologic data. *Water Resources Research,* 36 (3), pp. 737-744.

Mason, B. (2006) *Community disaster resilience: A summary of the March 20, 2006 workshop of the disasters roundtable.* Washington, D.C.: National Academies Press (NAP).

Mason, D.C., Schumann, G. and Bates, P.D. (2011) Data utilization in flood inundation modelling. In: G. Pender and H. Faulkner (eds.), *Flood risk science and management,* Oxford: Wiley-Blackwell.

Matalas, N.C. and Olsen, J.R. (2000) Analysis of Trends and Persistence in Hydrologic Records. In: Y.Y Haimes, D.A. Moser and E.Z. Stakhiv (eds.), *Risk-based decisionmaking in water resources IX,* US: American Society of Civil Engineers (ASCE), pp. 61-76.

Mays, L.W. (2011) *Water resources engineering.* 2nd ed., Hoboken, N.J.: Wiley.

Mens, M.J.P. et al. (2011) The meaning of system robustness for flood risk management. *Environmental Science & Policy,* 14 (8), pp. 1121-1131.

Merz, S.B. et al. (2010a) Fluvial flood risk management in a changing world. *Natural Hazards and Earth System Sciences,* 10 (3), pp. 509.

Merz, B. et al. (2014) Floods and climate: emerging perspectives for flood risk assessment and management. *Natural Hazards and Earth System Sciences,* 14 (7), pp. 1921-1942.

Merz, B. et al. (2010b) Review article 'Assessment of economic flood damage'. *Natural Hazards and Earth System Sciences,* 10 (8), pp. 1697-1724.

Merz, B. and Thieken, A. (2009) Flood risk curves and uncertainty bounds. *Natural Hazards,* 51 (3), pp. 437-458.

Merz, B. et al. (2012) HESS Opinions 'More efforts and scientific rigour are needed to attribute trends in flood time series'. *Hydrology and Earth System Sciences,* 16 (5), pp. 1379-1387.

Messner, F., et al. (eds.) (2007) *Evaluating flood damages: guidance and recommendations on principles and methods.* [Online]. Sixth Framework Programme for European Research and Technological Development (2002-2006). Available from: http://www.floodsite.net/html/partner_area/project_docs/T09_06_01_Flood_damage_guidelines_D9_1_v2_2_p44.pdf [Accessed in 2012]

Meyer, V. et al. (2013) Review article: Assessing the costs of natural hazards - state of the art and knowledge gaps. *Natural Hazards and Earth System Sciences,* 13 (5), pp. 1351-1373.

Meyer, V., Priest, S. and Kuhlicke, C. (2012) Economic evaluation of structural and non-structural flood risk management measures: examples from the Mulde River. *Natural Hazards,* 62 (2).

Michael, S. (2011) *Cost-benefit analysis: a practical guide.* London: Thomas Telford.

Milly, P.C.D. et al. (2008) Climate change: Stationarity is dead: Whither water management? *Science,* 319 (5863), pp. 573-574.

Milly, P.C.D. et al. (2015) On Critiques of 'Stationarity is Dead: Whither Water Management?' *Water Resources Research,* 51 (9), pp. 7785-7789.

Mkhandi, S.H., Kachroo, R.K. and Guo, S.L. (1996) Uncertainty analysis of flood quantile estimates with reference to Tanzania. *Journal of Hydrology,* 185 (1-4), pp. 317-333.

Moel, H., Vliet, M.V. and Aerts, J.C.J.H. (2014) Evaluating the effect of flood damage-reducing measures: a case study of the unembanked area of Rotterdam, the Netherlands. *Regional Environmental Change,* 14 (3), pp. 895-908.

Molua, E.L. (2012) Climate extremes, location vulnerability and private costs of property protection in Southwestern Cameroon. *Mitigation and Adaptation Strategies for Global Change,* 17 (3), pp. 293-310.

Moody, P. and Brown, C. (2013) Robustness indicators for evaluation under climate change: Application to the upper Great Lakes. *Water Resources Research,* 49 (6), pp. 3576-3588.

Mun, J. (2006) *Modeling risk: applying Monte Carlo simulation, real options analysis, forecasting, and optimization techniques.* Hoboken, N.J.: Wiley; Chichester: John Wiley distributor.

O'Connell, P.E. et al. (2010) Evaluating strategies for adaptation investment in a highly variable climate. In: *British Hydrological Society Third International Symposium.* Newcastle 2010. [Obtained a copy from one of the authors]

O'Connell, P.E. and O'Donnell, G. (2014) Towards modelling flood protection investment as a coupled human and natural system. *Hydrology and Earth System Sciences,* 18 (1), pp. 155-171.

Olsen, J.R. (2010) Current methods for water resource planning. In: J.R. Olsen K. Julie and W. Reagan (eds.), *Workshop on Nonstationarity, Hydrologic Frequency Analysis and Water Management*, US: Colorado Water Institute Information, Series No. 109, pp. 40-42.

Olsen, J.R. et al. (1999) Climate variability and flood frequency estimation for the Upper Mississippi and Lower Missouri Rivers. *Journal of the American Water Resources Association,* 35 (6).

Olsen, J.R. (2006) Climate change and floodplain management in the United States. *Climatic Change,* 76 (3-4), pp. 407-426.

Palma, W. and Zevallos, M. (2011) Fitting non-Gaussian persistent data. *Applied Stochastic Models in Business and Industry,* 27 (1), pp. 23-36.

Penning-Rowsell, E.C., et al. (eds.) (2010) *The benefits of flood and coastal risk management: a handbook of assessment techniques - 2010.* London: Flood Hazard Research Centre (FRHC), Middlesex University.

Penning-Rowsell, E.C. (2014) A realistic assessment of fluvial and coastal flood risk in England and Wales. *Transactions of the Institute of British Geographers,* 40 (1), pp. 44-61.

Penning-Rowsell, E.C. et al. (2013) A threatened world city: the benefits of protecting London from the sea. *Natural Hazards,* 66 (3), pp. 1383-1404.

Press, W.H. (2007) *Numerical recipes: the art of scientific computing.* 3rd ed., Cambridge: Cambridge University Press.

Priest, S.J., Parker, D.J. and Tapsell, S.M. (2011) Modelling the potential damage-reducing benefits of flood warnings using European cases. *Environmental Hazards-Human and Policy Dimensions,* 10 (2), pp. 101-120.

Prosdocimi, I., Kjeldsen, T.R. and Svensson, C. (2014) Non-stationarity in annual and seasonal series of peak flow and precipitation in the UK. *Natural Hazards and Earth System Sciences,* 14 (5), pp. 1125-1144.

Prudhomme, C. et al. (2012) *Future flows climate data. NERC Environmental Information Data Centre.*

Ranger, N. et al. (September 2010) *Adaptation in the UK: a decision-making process.* [Online] Grantham Research Institute on Climate Change and the Environment, Centre for Climate Change Economics and Policy. Available from: http://www.cccep.ac.uk/wp-content/uploads/2015/09/PB-Ranger-adaptation-UK.pdf [Accessed in 2014].

Rao, A.R. (2000) *Flood frequency analysis.* Boca Raton;London: CRC Press.

Rasekh, A., Afshar, A. and Afshar, M.H. (2010) Risk-Cost Optimization of Hydraulic Structures: Methodology and Case Study. *Water Resources Management,* 24 (11), pp. 2833-2851.

Reed, D.W., et al. (eds.) (1999) Statistical procedures for flood frequency estimation. In *Flood estimation handbook (FEH).* United Kingdom: Centre for Ecology and Hydrology (CEH), 3, pp. 225.

Reynard, N.S., et al. (eds.) (2009) *Regionalised impacts of climate change on flood flows.* London: Department for Environment, Food and Rural Affairs (DEFRA).

Rosner, A., Vogel, R.M. and Kirshen, P.H. (2014) A risk-based approach to flood management decisions in a nonstationary world. *Water Resources Research,* 50 (3), pp. 1928-1942.

Rosqvist, T. et al. (2013) Event tree analysis for flood protection—An exploratory study in Finland. *Reliability Engineering & System Safety,* 112 (0), pp. 1-7.

Salas, J.D. et al. (2013) Quantifying the Uncertainty of Return Period and Risk in Hydrologic Design. *Journal of Hydrologic Engineering,* 18 (5), pp. 518-526.

Salas, J.D. and Obeysekera, J. (2014) Revisiting the Concepts of Return Period and Risk for Nonstationary Hydrologic Extreme Events. *Journal of Hydrologic Engineering,* 19 (3), pp. 554-568.

Samuelson, W. (2012) *Managerial economics. 7th* ed., Hoboken, NJ: John Wiley & Sons.

Sayers, P., et al. (eds.) (2013) *Flood risk mangement: A strategic approach.* Paris: UNESCO.

Sayers, P.B., Hall, J.W. and Meadowcroft, I.C. (2002) Towards risk-based flood hazard management in the UK. *Proceedings of the Institution of Civil Engineers-Civil Engineering,* 150, pp. 36-42.

Sayers, P. (2012) *Flood risk: planning, design and management of flood defence infrastructure.* London: ICE Publishing.

Schanze, J. (2006) Flood risk management - A basic framework. In: J. Schanze, E. Zemen, J. Marsalek (eds.). *Flood Risk Management: Hazards, Vulnerability and Mitigation Measures, NATO Science Series,* 60, pp. 1-20.

Seidou, O., Ramsay, A. and Nistor, I. (2012a) Climate change impacts on extreme floods II: improving flood future peaks simulation using non-stationary frequency analysis. *Natural Hazards,* 60 (2), pp. 715-72

Seidou, O., Ramsay, A. and Nistor, I. (2012b) Climate change impacts on extreme floods I: combining imperfect deterministic simulations and non-stationary frequency analysis. *Natural Hazards,* 61 (2), pp. 647-659.

Serinaldi, F. (2015) Dismissing return periods! *Stochastic Environmental Research and Risk Assessment,* 29 (4), pp. 1179-1189.

Serinaldi, F. and Kilsby, C.G. (2015) Stationarity is undead: Uncertainty dominates the distribution of extremes. *Advances in Water Resources,* 77 (0), pp. 17-36.

Sherwood, J.M. (1993) *Estimation of peak-frequency relations, flood hydrographs, and volume-duration-frequency relations of ungauged small urban streams in Ohio.* [Online] United States Geological Survey (USGS) Water-Supply Paper 2432. Available from: http://pubs.usgs.gov/wsp/2432/report.pdf [Accessed in 2012].

Speijker, L.J.P. et al. (2000) Optimal maintenance decisions for dikes. *Probability in the Engineering and Informational Sciences,* 14, pp. 101-121.

Stahl, K. et al. (2010) Streamflow trends in Europe: evidence from a dataset of near-natural catchments. *Hydrology and Earth System Sciences,* 14 (12), pp. 2367-2382.

Stedinger, J.R. and Griffis, V.W. (2011) Getting from here to where? Flood frequency analysis and climate. *Journal of the American Water Resources Association,* 47 (3), pp. 506-513.

Stijnen, J.W. et al. (2014) The technical and financial sustainability of the Dutch polder approach. *Journal of Flood Risk Management,* 7 (1), pp. 3-15.

Strupczewski, W.G. et al. (2011) On the tails of distributions of annual peak flow. *Hydrology Research,* 42 (2-3).

Su, H. and Tung, Y. (2013) Incorporating uncertainty of distribution parameters due to sampling errors in flood-damage-reduction project evaluation. *Water Resources Research,* 49 (3), pp. 1680-1692.

Thurston, N., Finlinson, B. and Breakspear, R. (June 2008) *Developing the evidence base for flood resistance and resilience: Summary Report.* [Online] Joint DEFRA/EA Flood and Coastal Erosion Risk Management R&D Programme. Available from: http://evidence.environment-agency.gov.uk/FCERM/Libraries/FCERM_Project_Documents/FD2607_7322_TRP_pdf.sflb.ashx [Accessed in 2014]

Tijms, H.C. (2012) *Understanding probability.* Cambridge: Cambridge University Press.

Tsvetanov, T.G. and Shah, F.A. (2013) The economic value of delaying adaptation to sea-level rise: An application to coastal properties in Connecticut. *Climatic Change,* 121 (2), pp. 177-193.

Tung, Y.K. and Yen, B.C. (2005) *Hydrosystems Engineering Uncertainty Analysis.* N.Y., USA: McGraw-Hill.

Tung, Y.K. (2005) Flood defense systems design by risk-based approaches. *Water International,* 30 (1).

Twigger-Ross, C., Brooks, K., Papadopoulou, L., Orr, P., Sadauskis, R., Coke, A., Simcock, N., Stirling, A. and Walker, G. (2015) *Community resilience to climate change: an evidence review.* York: Joseph Rowntree Foundation.

UNESCO (2005) Concepts in Probability, Statistics and Stochastic Modelling. *Water Resources Systems Planning and Management.* UNESCO, pp. 169.

Viglione, A. et al. (2012) Extreme rainstorms: Comparing regional envelope curves to stochastically generated events. *Water Resources Research,* 48, pp. W01509.

Waage, M. (2010) Nonstationarity water planning methods. In: J.R. Olsen K. Julie and W. Reagan (eds.), *Workshop on Nonstationarity, Hydrologic Frequency Analysis and Water Management,* US: Colorado Water Institute Information, Series No. 109, pp. 40-42.

Wainwright, J. and Mulligan, M. (2013) *Environmental modelling: finding simplicity in complexity.* Oxford: Wiley-Blackwell.

Walker, W.E., Haasnoot, M. and Kwakkel, J.H. (2013) Adapt or Perish: A Review of Planning Approaches for Adaptation under Deep Uncertainty. *Sustainability,* 5 (3), pp. 955-979.

Ward, M.N. et al. (2013) Reservoir performance and dynamic management under plausible assumptions of future climate over seasons to decades. *Climatic Change,* 118 (2), pp. 307-320.

Ward, P.J., H.de Moel and Aerts, J.C.J.H. (2011) How are flood risk estimates affected by the choice of return-periods? *Natural Hazards and Earth System Sciences,* 11 (12), pp. 3181.

Ward, P.J. et al. (2014) Including climate change projections in probabilistic flood risk assessment. *Journal of Flood Risk Management,* 7 (2), pp. 141-151.

Ward, R.C. (2000) *Principles of hydrology.* 4th ed. London: McGraw-Hill.

Watsham, T.J. (1997) *Quantitative methods in finance.* London: International Thomson Business Press.

WMO/GWP (2008) Urban Flood Risk Management - A tool for Integrated Flood Management. Technical Document No. 11, Flood Management Tools Series [Online]. *Associated Programme on Flood Management.* Available from: http://www.apfm.info/publications/tools/Tool_06_Urban_Flood_Risk_Management.pdf [Accessed in 2011]

Woodward, M. (2012) *The use of Real Options and multi-objective optimisation in flood risk management.* PhD, University of Exeter.

Wright, N.G. and Hargreaves, D.M. (2013) Environmental applications of computational fluid dynamics. In: J. Wainwright and M. Mulligan (eds.), *Environmental modelling: Finding simplicity in complexity.* 2nd ed. John Wiley & Sons, pp. 91-110.

Yu, C. et al. (2012) A GIS-supported impact assessment of the hierarchical flood-defense systems on the plain areas of the Taihu Basin, China. *International Journal of Geographical Information Science*, 26 (4), pp. 643-665.

Zhou, Q. et al. (2012) Framework for economic pluvial flood risk assessment considering climate change effects and adaptation benefits. *Journal of Hydrology*, 414, pp. 539-549.